THE UNIVERSITY
of EDINBURGH

Effect of administration of selective progesterone receptor modulators (SPRMs) on uterine and endometrial morphology

Lucy Harriet Ravenscroft Whitaker

Thesis for the degree of Doctor of Medicine

The University of Edinburgh

2017

Table of Contents

Declaration

In accordance with the requirements of the University of Edinburgh, I hereby declare that the studies undertaken in this thesis were the unaided work of the author, except where due acknowledgement is made.

All work described herein has not previously been submitted or accepted for another degree or professional qualification.

Lucy Harriet Ravenscroft Whitaker
July 2017

Abstract

Introduction: The human menstrual cycle is regulated by sex-steroid hormones, including oestrogen (E), progesterone (P4) and androgens which act by ligand binding to their cognate receptors. Perturbation of the complex series of events governing the menstrual cycle may lead to heavy menstrual bleeding (HMB). This is a common debilitating condition and often associated with uterine fibroids. There remains an unmet need for effective, long-term medical treatment so women avoid surgery and preserve their fertility.

Selective progesterone receptor modulators (SPRMs, e.g. ulipristal acetate, UPA) are synthetic ligands that bind the progesterone receptor (PR). Many SPRMs have been developed but only mifepristone (for the management of unwanted pregnancy) and UPA are in current clinical use. UPA is licensed for the intermittent treatment of symptomatic fibroids. SPRMs have potential utility for treatment of HMB as administration rapidly induces amenorrhoea but the mechanisms by which this is achieved are unknown.

SPRM administration results in unique endometrial morphological changes (progesterone receptor modulator-associated endometrial changes; PAEC). Despite endometrial unopposed estradiol exposure these morphological changes do not appear to be associated with malignancy or pre-malignancy risk. Indeed endometrial cell proliferation appears reduced despite relative progesterone-antagonism.

Based upon findings with other SPRMs it was hypothesised that: (i) administration of UPA would have an endometrial specific effect upon the reproductive tract, with regard to alteration in morphology, localisation of sex steroid receptors (SSR) and cell proliferation.; (ii) administration of UPA would impact upon progesterone-regulated (P-regulated) genes in the endometrium.

Methods: The data presented within this thesis are derived from biopsies obtained at hysterectomy from the endometrium, fallopian tubes and cervices of women with symptomatic fibroids administered UPA for 8-15 weeks. Samples were obtained for histological assessment, immunohistochemistry and RNA extraction for subsequent quantitative RT-qPCR of sex-steroid receptors (SSR) and proliferation markers. In addition key P-regulated genes within the endometrium were investigated by RT-qPCR and selected protein expression. To further interrogate the anti-proliferative effect, RNA

was extracted from "paired" endometrial biopsies from the same woman in the proliferative phase of the menstrual cycle and following subsequent treatment with UPA for at least eight weeks and microarray gene analyses undertaken.

Results: Morphological alteration of the endometrium with UPA administration was consistent with previously published data, but with a higher prevalence than previously described. There was a striking alteration in expression and localization of SSRs, particularly PR and androgen receptor (AR), and alteration of many P-regulated genes, consistent with UPA acting with low progesteroneagonism within the endometrium. There was no alteration of SSR expression within the cervix and proliferation was unchanged. Fallopian tube morphology and SSR expression was consistent with proliferative phase but cell proliferation was reduced following UPA administration, consistent with secretory phase levels.

Microarray analyses identified multiple transcripts altered relative to proliferative phase, with *GREM2* the most significantly down-regulated gene and *MUC1* one of the most significantly upregulated genes. Consistent with low levels of mitotic figures and cell proliferation, the most down regulated KEGG pathway was the cell cycle. Multiple elements within this were subsequently validated (RT-qPCR) and included key regulators of all elements of the mitotic cell cycle, many of which were novel to those previously described following administration of another SPRM, mifepristone.

In summary the novel data presented in this thesis considerably extend the data available to date concerning the actions of the SPRM, UPA, on the female reproductive tract, and increases knowledge regarding a compound with promising utility for the management of the debilitating complaint of HMB.

Lay summary

Heavy periods are a common problem for women of child-bearing age and impact significantly on quality of life. A common cause of heavy periods is fibroids (non-cancerous tumours of the muscle layer of the womb). Current medical treatments often fail and many women eventually undergo surgical removal of the uterus (hysterectomy). Ulipristal acetate (UPA) is a new tablet treatment for fibroids which reduces bleeding but how it works is unknown.

The menstrual cycle of women is regulated by two key hormones oestrogen and progesterone. These are known as sex-steroids and act by binding to receptors. These receptors frequently occur in the endometrium (lining of the womb) but can also be found elsewhere in the body, including in the fallopian and tube and cervix. UPA acts by binding with the receptor for progesterone.

Our early work suggested that UPA reduces the replication of cells in the endometrium but we don't know exactly how this happens, nor which cell type in the endometrium is most significantly affected. The endometrial cells look different when seen under a microscope compared to untreated women but so far there has been no evidence that women taking UPA have an increased risk of cancer of the endometrium. We also do not know what the effect of treatment with UPA has upon the fallopian tube and cervix.

The work presented in this thesis has examined the effect of UPA on the appearance of cells in the endometrium, fallopian tube and cervix, and whether there was an alteration in the appearance of cells and a change in the number and location of the receptors for key sex-steroid hormones. This was done using samples taken from the womb of women with heavy periods and fibroids after hysterectomy. Some of these had had treatment with UPA before their operation. Other samples of endometrium were obtained in the gynaecology clinic from women before and after treatment with UPA. The effect of treatment with UPA on levels of genes regulated by progesterone in the endometrium was also investigated. Finally in order to try and further understand how UPA treatment reduces cell replication in the lining of the womb endometrial samples from women before and after UPA treatment were compared.

I found that treatment with UPA changes the appearance of the endometrium. This is in

keeping with other people's findings. New data presented here describes how the patterns of sex-steroid receptors were altered and genes controlled by progesterone were also altered. I found that cervix samples from women treated with UPA were unaltered, and that the fallopian tubes from these women looked similar to those of women in the first half of their menstrual cycle, but had a lower level of cell replication.

In keeping with our earlier findings I found samples from women taking UPA had a lower level of cell replication in the lining of the womb than before they started treatment. New data generated during my studies revealed that genes involved in cell replication were also altered. Many of these have not been demonstrated before with other medications similar to UPA.

In summary, the findings presented in this thesis extend the knowledge base about the effects of UPA on the lining of the womb, fallopian tubes and cervix. This is important as UPA appears to be an effective treatment for women with heavy periods and fibroids.

Acknowledgements

I would like to thank my supervisors, Professors Hilary Critchley and Alistair Williams for their support, encouragement and advice throughout my MD. These last two years have been a hugely rewarding experience, and they have my utmost gratitude for the opportunity to have learned so much from them – I could not have asked for better supervisors or a more welcoming lab group.

To Hilary, I cannot express sincere enough thanks: for her support in my studies, her patient education of me in clinical trials and research methodology and for her unfailing guidance, support and encouragement through fellowship applications and my aspirations in a future career in academic gynaecology. For her tolerance of my woeful inability to spell or grasp of basic grammar. In addition for her clinical training and for steadfastly providing a role model to aspire to, as a clinician, surgeon, scientist, trialist and mentor.

To Alistair, for his endless patience in indoctrinating me into the dark arts of pathology, advice, tolerance and steadfast support.

I am incredibly grateful to Dr Alison Murray for her limitless patience in teaching PCR and immunohistochemistry, and her tremendous help in the gestation of our Human Reproduction paper. In addition her tireless advice, be it scientific or life, this thesis would not have been possible without her. To all the other members of the HODC group: Moira, Kate, Hazel and Reena for their patience, assistance and help, particularly when deadlines were looming or keeping my cells alive. They have been hugely fun to work with and have helped maintain my sanity and my thanks for being such a welcoming group. To Sheila Milne for help in grant and manuscript preparation and Ronnie Grant for his assistance with figure preparation. To Jackie Maybin for her assistance with research application and manuscript preparation and advice. To Mike Miller and Lynsey Bowell for the guidance with immunohistochemistry and image capture. To Dr Kevin Robertson for his advice regarding the micro array and power calculation. I would like to express my thanks to Professor Philippa Saunders for her invaluable advice and support, and to the rest of her group (in particular Dr Pete Sanderson) for their additional advice regarding immunohistochemistry. I am also hugely grateful to Professor Andrew Horne, for his fallopian tubes, advice and support, particularly with

our endless Cochrane review, and for being the first person to encourage me down an academic path.
To Catherine Murray and Sharon McPherson, our clinical research nurses, I am profoundly thankful for their help in sourcing patient samples and information, and assistance with the DexFEM and UCON clinical trials and teaching me the reality of the coal face of a clinical trial.

I would like to thank the countless patients who so graciously volunteered and donated in support of medical research, in particular the women who gave repeated pipelles biopsies for chapter 5. I remain in awe of them and am profoundly grateful. This MD would have been impossible without them.

I would like to thanks my friends and colleagues in the QMRI, SCRH and St John's Hospital, in particular Dr Kirsty Munro and Dr Sarah Murray, for finding me patients and trial participants, support with the clinical trials and helping me to maintain my sanity.

Finally, and perhaps most of all, I would like to thank my family. There have been difficult times over the last 2 years for all of us, and they remain unswerving in their support and love, even if my father still looks hugely uncomfortable when I talk about periods with such enthusiasm.

LHRW June 2017

List of Abbreviations

11β-HSD	11-βhydroxysteroid dehydrogenase
17β-HSD	17-βhydroxysteroid dehydrogenase
ACOG	American Congress of Obstetricians and Gynecologists
AMH	anti-Mullerian hormone
ANAPC4	anaphase-promoting complex subunit 4
ANOVA	Analysis of variance
AP1	activator protein 1
AR	androgen receptor
ATBP5	ATP synthase, H+ transporting, mitochondrial F1 complex, beta polypeptide
AUB	abnormal uterine bleeding
AUB-L	abnormal uterine bleeding of leiomyoma (fibroid) origin
BCL	B-cell CLL/lymphoma
BMI	body mass index
BMP2	bone morphogenetic protein 2
BRCA1	breast cancer 1
BSA	bovine serum albumin
BW	bond wash
CBG	cortisol binding globulin
CCNA1	cyclin A1
CCNA2	cyclin A2
CCNB1	cyclin B1
CCNB2	cyclin B2
CCNE2	cyclin E2
CDC20	cell division cycle 20
CDC25A	cell division cycle 25A
CDC7	cell division cycle 7
CDK1	cyclin-dependent kinase 1
CDKN	cyclin-dependant kinase inhibitor
CHEK2	checkpoint kinase 2
CHI	Community Health Index
CIN	cervical intraepithelial neoplasia
COCP	combined oral contraceptive pill

COUP-TFII	nuclear receptor subfamily 2 group F member 2
COX-2	cyclooxygenase
CT	computed tomography
CV	coefficient of variation
DAB	3, 3'-Diaminobenzidine
DBD	DNA binding domain
DEG	differentially expressed
DHEA	dihydroepiandrostenedione
DNA	deoxyribonucleic acid
E2	oestradiol
E2F2	E2F transcription factor 2
EDTA	Ethylenediaminetetraacetic acid
ELISA	enzyme-linked immunosorbent assay
ER	oestrogen receptor
ERK	extracellular signal–regulated kinases
ERα	oestrogen receptor alpha
ERβ	oestrogen receptor beta
ES	early secretory
ESPL1	extra Spindle Pole Bodies Like 1
ESR1	oestrogen receptor 1
ESRES	East of Scotland Research Ethics Service
FDA	Food and Drug Administration
FEMME	A randomised trial of treating fibroids with either embolisation or myomectomy to measure the effect on quality of life among women wishing to avoid hysterectomy (the FEMME study): study protocol for a randomised controlled trial
FFPE	formalin-fixed paraffin-embedded
FGF	fibroblast growth factor
FGFR	fibroblast growth factor receptor
FIGO	Fédération International de Gynécologie et d'Obstétrique
FKBP51	FK506 binding protein 5 (FKBP5)
FKBP52	FK506 binding protein 4, 59kDa (FKBP4)
FOXM1	forkhead box M1
FOXO1	forkhead box O1

FSH	follicle stimulating hormone
FT	fallopian tubes
G_1	Gap 1 (pre-synthesis)
G_2	Gap 2 (pre-mitosis)
GADD45A	growth arrest and DNA damage inducible alpha
GnRH	gonadotrophin-releasing hormone
GO	Gene Ontology
GOPD	gynaecology out-patients department
GR	glucorticoid receptor
GREM2	gremlin 2
H&E	haematoylin and eosin
H_2O_2	hydrogen peroxide
HAND2	heart and neural crest derivatives expressed 2
HIC-5	hypermethylated in cancer-5
HMB	heavy menstrual bleeding
HOXA10	homeobox A10
HPO	hypothalamic, pituitary and ovarian axis
HRE	hormone response elements
HSP	heat shock protein
IGFBP-1	insulin-like growth factor binding protein 1
IgG	immunoglobulin G
IHC	immunohistochemistry
IHH	indian hedgehog
IL-10	interleukin-10
IL-13	interleukin-13
IL-15	interleukin 15
IL-17	interleukin-17
IL-8	interleukin-8
IMB	intermenstrual bleeding
IUCD	intrauterine contraceptive device
J867	asoprisnil
KEGG	Kyoto Encyclopedia of genes and Genome
KLF-15	Kruppel-like factor 15
KLF-4	Kruppel-like factor 4

KLF-9	Kruppel-like factor 9
LBD	ligand binding domain
LDL	low-density lipoprotein
LH	luteinising hormone
LMP	last menstrual period
LNG-IUS	levonorgestrel-releasing intrauterine system
LNG-IUS	levnorgestrel releasing intrauterine system
LS	late secretory
M	mitosis
MAD2L1	mitotic Arrest Deficient-Like 1
MAPK	mitogen-activated protein kinases
MDG	Menstrual Disorders Group
miRNA	micro-RNA
MMP	matrix metalloproteinase
MMT	3-(4,5-dimethylthiazol-2-yl)-2,5-diphenyltetrazolium bromide
MR	mineralocorticoid receptor
MRgFUS	MR-guided focused ultrasound
MRI	magnetic resonance imaging
mRNA	messenger ribonucleic acid
MS	mid secretory
MUC1	mucin 1, cell surface associated
MYC	v-myc myelocytoamtosis viral oncogene homolog (avian)
NcoR	nuclear co-receptors
NF-κB	nuclear factor-κB
NHS	normal horse serum
NICE	National Institute for Health and Care Excellence
P4	progesterone
PA	progesterone antagonist
PAEC	progesterone receptor modulator endometrial associated changes
PAI	plasminogen activator inhibitor
PCNA	proliferating cell nuclear antigen
PCR	polymerase chain reaction
PH3	phospho Histone 3
POP	progeserone-only contraceptive pill

PR	progesterone receptor
PRA	progesterone receptor A isoform
PRB	progesterone receptor B isoform
PRE	progesterone response element
PRL	prolactin
PRM	progesterone receptor modulators
PTCH1	transmembrane receptor patched-1
PTEN	phosphatase and tensin homologue
PTTG1	pituitary Tumor-Transforming 1
Rb	retinoblastoma
RCOG	Royal College of Obstetricians and Gynaecologists
RCT	randomised controlled trial
REC	Research Ethics Committee
RIN	RNA integrity number
RNA POL2	RNA polymerase 2
RNA-Seq	RNA-Sequencing
RT-qPCR	Quantitative reverse transcription polymerase chain reaction
RU-486	mifepristone
S	synthesis (DNA-synthesis)
SBG	sex hormone binding globulin
SCJ	squamo-columnar junction
SDHA	succinate dehydrogenase
SEE-FIM	Protocol for Sectioning and Extensively Examining the FIMbriated End
SEM	standard error of the mean
SERM	selective oestrogen receptor modulator
SLC13A5	sodium dependant citrate co-transporter 13A5
SMO	smoothened
SMRT	silencing mediator of retinoic acid and thyroid hormone receptor
SP1	specificity protein 1
SPRM	selective progesterone receptor modulator
SRC	steroid receptor co-activator
Src kinase	proto-oncogene tyrosine-protein kinase Src
SRY	sex-determining region Y

SSR	sex-steroid receptors
STAT	signal transducer and activator of transcription
STI	sexually transmitted infections
TBST	tris-buffered saline with tween
TGFβ	transforming growth factor-beta
TGF-β	Transforming growth factor-beta
t-PA	tissue plasminogen activator
UAE	uterine artery embolization
UCON	Ulipristal acetate versus conventional management of heavy menstrual bleeding (HMB; including uterine fibroids): a randomised controlled trial and exploration of mechanism of action
UPA	ulipristal acetate
u-PA	urokinase plasminogen activator
USS	ultrasound scan
Wnt	wingless-type MMTV integration site
ZK 230211	lonaprisan
ZK 89299	onapristone

Chapter Contents

List of figures

List of tables

Chapter 1

Chapter 2

Chapter 3

Chapter 1.

Introduction

In humans the female reproductive system comprises the hypothalamic, pituitary and ovarian axis (HPO axis) and the reproductive tract (fallopian tubes, uterus, cervix and vagina). The principle functions of this system are to produce an ovum, enable its fertilisation and implantation, and allow growth and safe delivery of the foetus into the external world. In the absence of pregnancy, the functional layer of the endometrium is shed. This is followed by subsequent rapid proliferation and remodelling in anticipation of implantation of another potential blastocyst. This process of cyclical development, differentiation and shedding of the endometrium is termed the menstrual cycle. The average length of the cycle in the female human is 28 days. Hence the shedding of the endometrium is termed menses, the plural of the Latin word for month, mensis.

1.1 Why women menstruate

Menstruation is not a ubiquitous process to all female animals. Whilst all female placental mammals have a uterine lining that is receptive at fertile time-points, menstruation is predominantly limited to primates, elephant shrews and several species of bat (Martin 2007). In all other species, where there is no outward menstruation, oestrus cycles are followed by 'covert menstruation' in which the receptive endometrium is completely reabsorbed (Strassmann 1996). The benefits of one system over another remain incompletely understood. Previous hypotheses included that the energy expenditure of maintaining the endometrium outweighed shedding and rebuilding (Strassmann 1996) or that it was an evolutionary defence against sperm carried pathogens (Finn 1996). Current thinking is that menstruation is a consequence of decidualisation. This is the process of conversion of endometrial stromal cells into specialised decidual cells that have the capacity to sustain an embryo. In menstruating species decidualisation occurs prior to fertilisation, in contrast, non-menstruating mammals decidualise only at the point of implantation. Decidualisation is thought to confer evolutionary benefits through facilitating placental invasion of healthy embryos, enabling an element of embryo selection by the uterus in menstruating species (Finn 1998).

1.2 Physiology of the menstrual cycle

Menstrual cycle physiology may be considered at different levels; hypothalamic, pituitary, ovarian and endometrial (Figure 1.1).

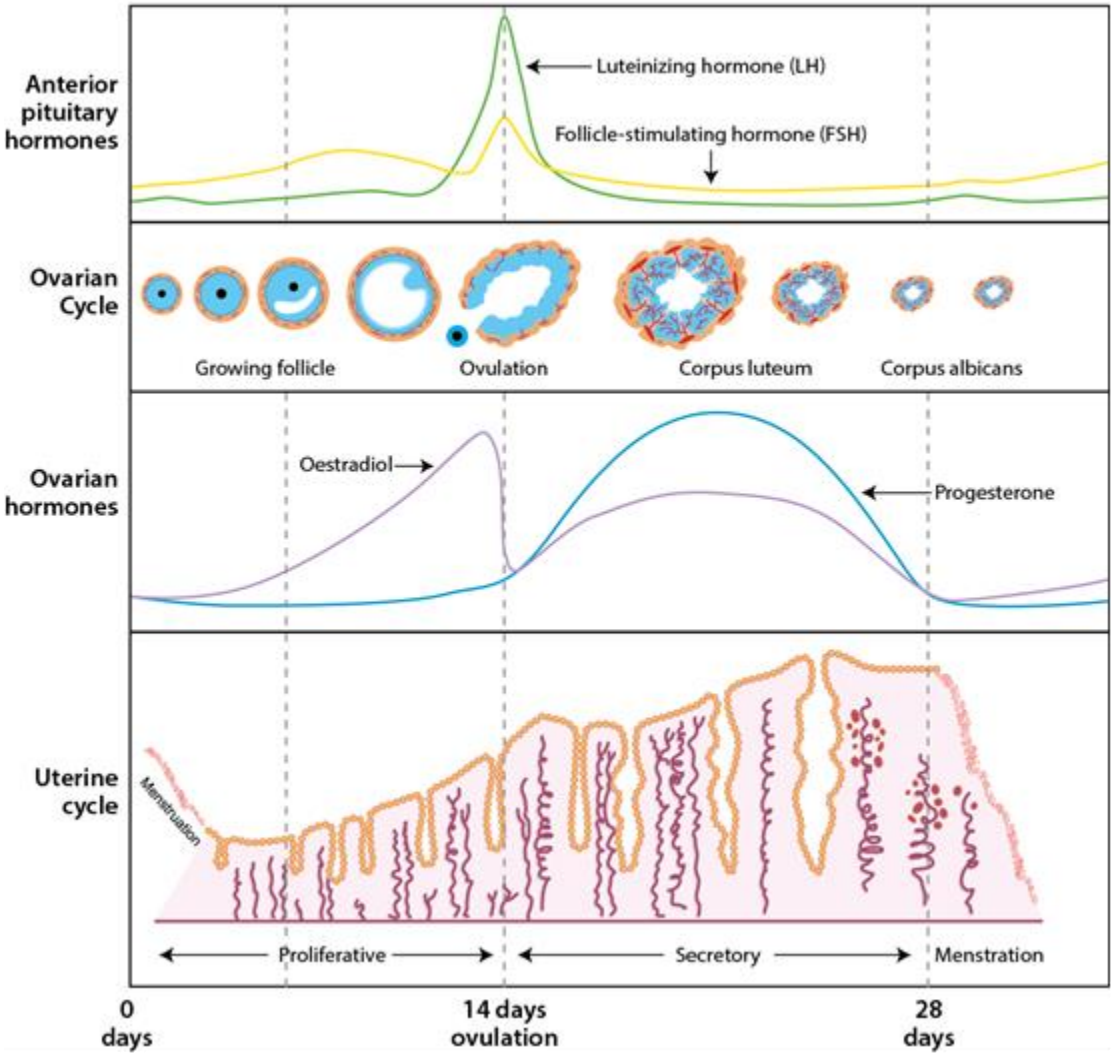

Figure 1.1 The menstrual cycle

Schematic representation of pituitary and ovarian hormones and response of the ovary and endometrium across the menstrual cycle

This is a draft of a figure from the chapter 'The menstrual cycle' that has been accepted for publication by Oxford University Press in the forthcoming book Oxford Textbook of Obstetrics and Gyanecology (chapter by Lucy Whitaker, Karolina Skorupskaite, Jacqueline A Maybin and Hilary O D Critchley), edited by William Ledger due for publication in 2017.

Communication between the hypothalamus, pituitary and target organs of the reproductive tract is determined by a combination of peptide and steroid hormones to regulate menstruation. The predominant hormones of the menstrual cycle are gonadotrophin-releasing hormone (GnRH), follicle stimulating hormone (FSH), luteinising hormone (LH), oestrogen (predominantly oestradiol, (E2)) and progesterone (P4). Function of this endocrine system is affected by the stage of reproductive life.

1.2.1 Hypothalamic-pituitary regulation of ovarian function

Regulation of the menstrual cycle begins with the hypothalamus and GnRH (Figure 1.2). GnRH is produced and released by axonal transport from the hypothalamus into the capillaries of the hypophyseal portal system for delivery to the anterior pituitary gland, where it stimulates the synthesis and secretion of LH and FSH from the gonadotrophs.

GnRH is secreted in a pulsatile manner. In the normal cycling woman GnRH pulses are of low amplitude, but increase in their frequency during the follicular phase, to a frequency of every 60 minutes during late follicular phase. High GnRH pulse frequency favours LH release, thus LH release is predominant over FSH in the late follicular phase. In contrast the luteal phase is characterised by high amplitude and low frequency (approximately every 216 minutes) of pulsatile GnRH secretion. Low GnRH pulsatility stimulates FSH secretion, which is dominant over LH in the luteal and early follicular phase necessary for follicular development (Figure 1.1-2). LH stimulates androgen production, the hormonal precursor for E2, by binding to theca cells in the ovary; FSH promotes follicular growth, activates aromatase and induces expression of LH receptors on the granulosa cell in preparation to respond to the pre-ovulatory LH surge (Messinis, Messini et al. 2014). Kisspeptin, a hypothalamic neuropeptide, is now recognised as key regulator of pulsatile GnRH secretion (Figure 1.2) (Skorupskaite, George et al. 2014).

During the menstrual cycle GnRH and gonadotropin activity is highly regulated by ovarian feedback loops. In the follicular phase, oestrogen exerts negative feedback at the level of hypothalamus to suppress LH and FSH secretion. However in the late follicular phase, by yet unclear mechanisms negative oestrogen feedback switches to positive oestrogen feedback, culminating in the pre-ovulatory LH surge (and to a lesser extent a rise in FSH) necessary for ovulation.

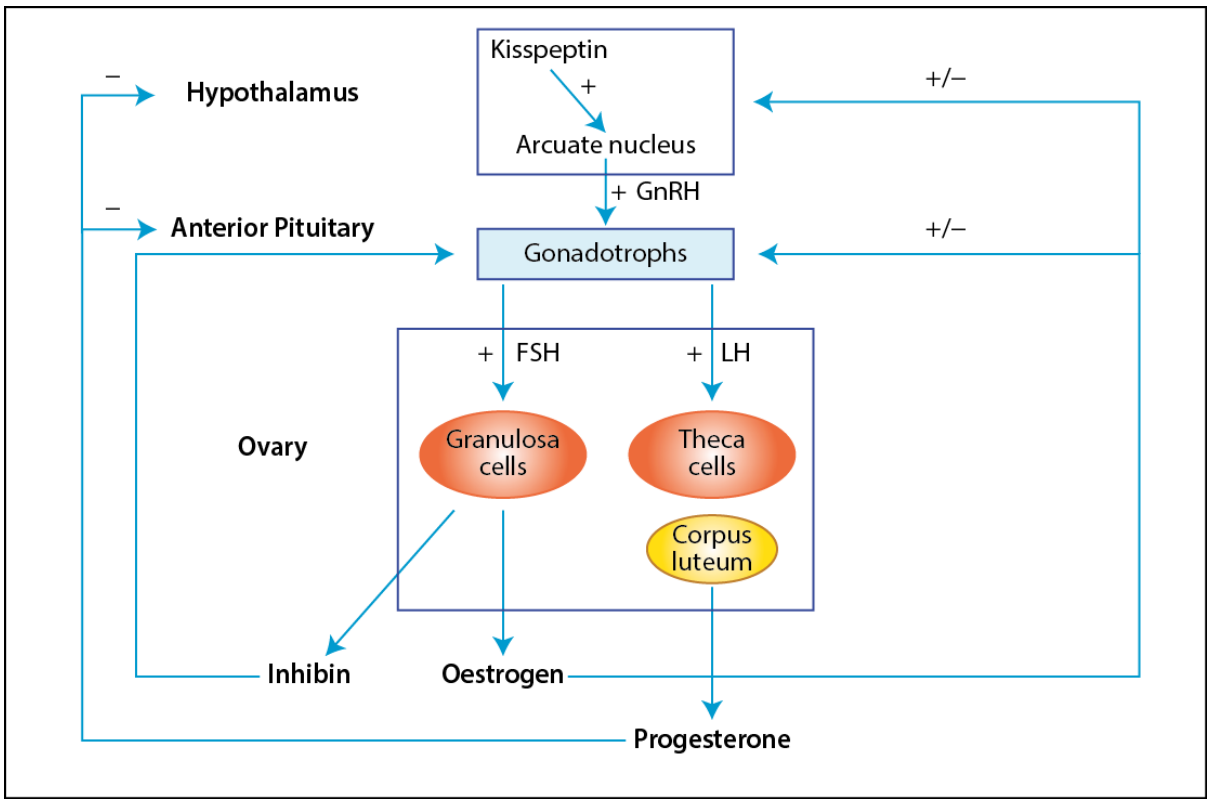

Figure 1.2 Regulation of the menstrual cycle

Release of gonadotrophin-releasing hormone (GnRH) from the hypothalamus signals to the anterior pituitary. This in turn results in follicle stimulating hormone (FSH) and luteinising hormone (LH) secretion from the gonadotrophs. These stimulate the ovary to produce oestradiol and progesterone which regulate endometrial function.

GnRH and gonadotropin signalling is tightly regulated by negative and positive gonadal-steroid loops and is further regulated by other hypothalamic neuropeptides (such as kisspepetin).

This is a draft of a figure from the chapter 'The menstrual cycle' that has been accepted for publication by Oxford University Press in the forthcoming book Oxford Textbook of Obstetrics and Gyanecology (chapter by Lucy Whitaker, Karolina Skorupskaite, Jacqueline A Maybin and Hilary O D Critchley), edited by William Ledger due for publication in 2017.

Following ovulation progesterone from the corpus luteum mediates negative feedback to slow down GnRH pulse frequency and subsequently LH secretion. With demise of the corpus luteum in the absence of pregnancy, gonadal steroid secretion declines, and progesterone withdrawal results in menstruation and stimulation of FSH secretion in response to a loss of negative sex-steroid feedback (Critchley, Kelly et al. 2001).

1.2.2 Ovarian function

Ovarian function within the menstrual cycle can be broadly divided into the follicular phase, ovulation, luteal phase and finally the luteal-follicular transition.

Follicular phase

Throughout ovarian life the oocytes reside within follicles. At any time point in the reproductive years there are follicles at different developmental stages within the ovary (Binelli and Murphy 2010, Rimon-Dahari, Yerushalmi-Heinemann et al. 2016).

Initially, primary oocytes develop in primordial follicles, consisting of a primary oocyte surrounded by a single flattened layer of granulosa cells. At the beginning of each menstrual cycle, a cohort of primordial follicles transition into primary follicles, before developing into larger pre-antral follicles. At this stage, the zona pellucida develops between the oocyte and granulosa cells and surrounding stromal cells differentiate to form the theca. Subsequently, the follicles enlarge, developing a fluid-filled cavity termed the antrum. As well as producing E2, pre-antral and early antral follicles produce anti-Mullerian hormone (AMH), which appears to have an inhibitory action on the growth of nearby primordial follicles, thus preventing their activation (Eppig 2001, Binelli and Murphy 2010, Rimon-Dahari, Yerushalmi-Heinemann et al. 2016).

As the follicles grow they acquire FSH and LH receptors and become increasingly gonadotrophin dependent, with antral follicles completely dependent on FSH for granulosa cell proliferation and LH for theca cell sex steroidogenesis. The largest follicle in the cohort is termed the dominant follicle, with all other growing follicles undergoing atresia. The dominant follicle produces E2, resulting in a rapid rise in serum E2 concentration and consequent reduction in FSH and LH levels by negative feedback at the hypothalamus. This dominant follicle matures into a pre-ovulatory follicle and expresses LH receptors on both granulosa and theca cells. There is a short period of positive feedback in the late follicular phase whereby increasing E2 levels result in a

surge of LH. The pre-ovulatory follicle responds to this surge by undergoing ovulation (Eppig 2001, Rimon-Dahari, Yerushalmi-Heinemann et al. 2016).

Ovulation

Following the LH surge, and just prior to ovulation the oocyte responds to its hormonal environment and re-enters meiosis. The granulosa cells decrease E2 secretion as a result of decreased sensitivity to FSH and progesterone production is initiated. The rise in LH and FSH causes an increase in antral blood flow and the increased vascularity and local secretion of prostaglandins causes an increase in size of the follicle, distending the surface of the ovary. Proteolytic enzymes are synthesised in the theca and activated by prostaglandins, causing degradation of the distended follicular wall followed by rupture of the follicle capsule and ejection of the oocyte. This occurs on around day 14 of the menstrual cycle (Rimon-Dahari, Yerushalmi-Heinemann et al. 2016). Under the influence oestrogens prior to ovulation, increased tubal motility and elevated activity of the densely ciliated fimbriae allows approximation of the aperture of the distal fallopian tube to the ovary (Pauerstein and Eddy 1979). This promotes passage of the expelled oocyte into the tube to be met by the ascending spermatozoa, if present. If fertilisation occurs, meiosis is completed (Rimon-Dahari, Yerushalmi-Heinemann et al. 2016).

Luteal phase

Following ovulation the walls of the ovarian follicle collapse. Under the influence of LH both the theca and the granulosa cells proliferate and the latter develop into luteal cells. There is an influx of lipid droplets and lutein, which gives the corpus luteum its characteristic yellow appearance. The E2 and P4 secreted by the luteal cells negatively feedback to the anterior pituitary and levels of FSH and LH decrease. The corpus luteum is reliant on LH for P4 production and luteolysis occurs in the absence of pregnancy as the mature corpus luteum becomes less sensitive to the remaining circulating LH. Demise of the corpus luteum begins at around day 24 and the corpus luteum is replaced by whitish scar tissue, the corpus albicans. Over subsequent cycles it is replaced by connective tissue, then absorbed (Smith and Meidan 2014, Rimon-Dahari, Yerushalmi-Heinemann et al. 2016).

Luteal- Follicular transition

As the corpus luteum degenerates, circulating concentrations of E2 and P4 rapidly decrease. As a result, FSH and LH plasma concentrations rise and a fresh group of follicles are recruited whilst progesterone withdrawal (P-withdrawal) initiates menses (Critchley, Kelly et al. 2001, Eppig 2001).

1.2.3 Endometrial response to ovarian stimulus

The endometrium consists of glandular epithelial cells surrounded by stromal fibroblasts, overlaid by a layer of luminal epithelium. There is a small leucocyte population and occasional lymphoid follicles may be observed. The endometrium is separated into two functionally separate layers overlying the myometrium: the basal layer and the functional layer (Mutter and Ferenczy 2001). The basal layer is preserved but the functional layer is shed each cycle. The constituent cells may express receptors for the sex steroids E2, P4 and androgens, as well as the glucocorticoid hormone, cortisol (McDonald, Henderson et al. 2006, Critchley and Saunders 2009). The relative expression and localisation of receptors varies with stage of cycle and is described in detail in **Chapter 3** (**3.1.3.1**). The endometrium has a complex blood supply predominantly arising from the radial branches of the uterine artery with some collateral supply from the ovarian vessels. There are both short and straight arteries which supply the basal layer and longer, spiral vessels supplying the whole of the endometrium. The spiral vessels connect with the venous system though capillary networks and direct arterio-venous communications (Girling and Rogers 2009). In addition to the vasculature there is a lymphatic system, predominantly limited to the basal layer of the endometrium (Girling and Rogers 2012).

The endometrial component of the menstrual cycle is divided into proliferative, secretory and menstrual phases, broadly corresponding to the follicular, luteal and luteal-follicular transition phases of the ovarian cycle. The classical histological description of the cycling endometrium dates from the 1950s (Noyes, Hertig et al. 1950) but for research purposes dating may be more robustly determined utilising histological features combined with date of reported last menstrual period (LMP) and measurement of serum E2 and P4 (Talbi, Hamilton et al. 2006).

Proliferative phase

Following menstruation the exposed basal layer of the endometrium proliferates rapidly under the influence of rising circulating E2 levels. Glands increase in number and in length (Figure 1.3A). Initially glandular cells are cuboidal and the glands themselves are small but become columnar in appearance with pseudo-stratification of nuclei. There are numerous mitotic figures and no evidence of mucous secretion or vacuolation (Figure 1.3E). The stroma is compact, with scanty cytoplasm and frequent mitotic figures. Angiogenesis commences with elongation of the spiral arteries. As a result of proliferation of both glandular and stromal cells the thickness of the endometrium increases from around 2mm in the post-menstrual phase to around 14mm just prior to ovulation (Noyes, Hertig et al. 1950, Mutter and Ferenczy 2001).

Secretory phase

Following ovulation there is an initial interval phase (Day 14-15) as P4 levels start to rise and then the characteristic appearances of the progesterone dominated secretory phase start to appear. These continue to develop until approximately 48 hours after P-withdrawal (due to demise of corpus luteum). The hallmarks of the secretory phase are glandular secretion and stromal cell differentiation (decidualisation). The secretory phase can be broadly subdivided in early-, mid- and late-secretory changes, though these phases are continuous and some areas of the endometrium may develop at a different rate to other regions.

<u>Early secretory (Day 16-18)</u>

Following ovulation, secretion of progesterone from the corpus luteum rapidly inhibits proliferation. The endometrial glands begin to assume a more tortuous appearance, and acquire increased secretion of glycoproteins, evident as sub-nuclear vacuolation (Figure 1.3B&F). Glandular nuclei move to the centre of cells and mitosis is supressed. Subnuclear vacuolation is most obvious in the mid zone of the functional layer initially but extends throughout the functional layer, with maximal expression by day 18. In the early secretory phase the stroma is indistinguishable from that of the proliferative phase. The endometrial spiral arterioles undergo remodelling to become increasingly coiled in anticipation of interaction with invading trophoblast if fertilization has occured (Noyes, Hertig et al. 1950, Mutter and Ferenczy 2001).

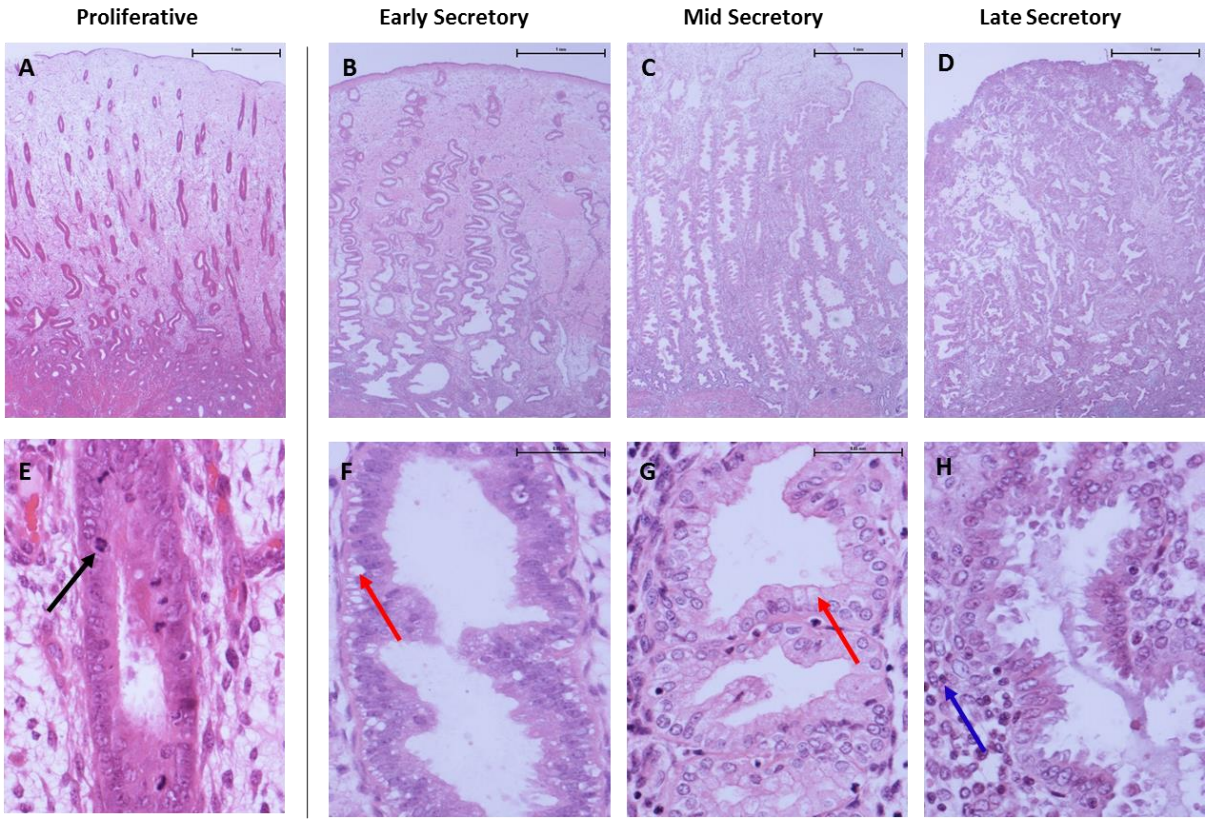

Figure 1.3 Histological changes of the endometrium across the menstrual cycle
Representative H&E images of full thickness endometrial biopsies (lumen to endometrial/myometrial interface) obtained at the time of hysterectomy from women in the proliferative (A&E), early secretory (B&F), mid secretory (C&G) and late secretory (D&H) phase of the menstrual cycle. In proliferative phase glands are cuboidal and mitotic figures present (E,↑). In early secretory phase glands appear more tortuous (B) and sub-nuclear vacuolation occurs (F, ↑). By mid secretory phase the vacuoles have migrated past the nuclei to the apical surface of the glandular cells (G, ↑) and begin to discharge into the lumen. The glands overall have a more serrated appearance (C). By late secretory phase the vacuoles have all discharges and the stroma has a decidualised appearance (H, ↑).
Scale bars 1000µm low magnification, 50µm high magnification

Mid secretory (Day 19-23)

The glands appear more tortuous, with a serrated appearance when transected along the long axis (Figure 1.3C). Basal vacuoles within the glands progressively push past the nucleus, and thus the nuclei appeared to be basally located (Figure 1.3G). The vacuoles discharge into the lumen of the glands, resulting in dilatation of the glands with proteinaceous material. The peak of secretion coincides with anticipated time of implantation of a blastocyst. Gland secretion is more marked in the basal layer compared to the functional layer of the endometrium. There is stromal oedema as a result of increased capillary permeability and predecidual transformation begins around day 22 of the menstrual cycle. Adjacent to vessels the stromal fibroblasts begin to convert from spindle shaped cells into plumper, epithelial-like cells with enlarged nuclei and increased cytoplasm (i.e. decidulaisation). Vascular changes include endothelial cell proliferation and coiling of the spiral arterioles (Noyes, Hertig et al. 1950, Koji, Chedid et al. 1994, Mutter and Ferenczy 2001).

Late secretory (Day 24-28)

There is reduction in secretory activity of the glands and serration is more pronounced (Figure 1.3D&H). The glands become more tightly packed. Decidual change is more pronounced and extends from the surface to the deeper stroma (Figure 1.3H). Occasional mitotic bodies may appear on day 27. There is an influx of leucocytes beginning on day 24 and by day 26 a neutrophil populate predominates. Just prior to menstruation apoptosis is observed within glands, small fibrin thrombi are present in the arterioles and there is extravasation of red blood cells (Noyes, Hertig et al. 1950, Koji, Chedid et al. 1994, Mutter and Ferenczy 2001).

Menstruation

In the absence of pregnancy the corpus luteum regresses, resulting in a rapid decrease in circulating E2 and P4. It is P-withdrawal that initiates menstruation (Figure 1.4), resulting in a local inflammatory response within the endometrium, characterised by cytokine release and leucocyte infiltration with consequent oedema, which culminates in the shedding of the functional layer with preservation of the basal region. The basal layer has an exposed, raw mucosal surface that requires efficient repair (Critchley, Kelly et al. 2001, Maybin and Critchley 2015).

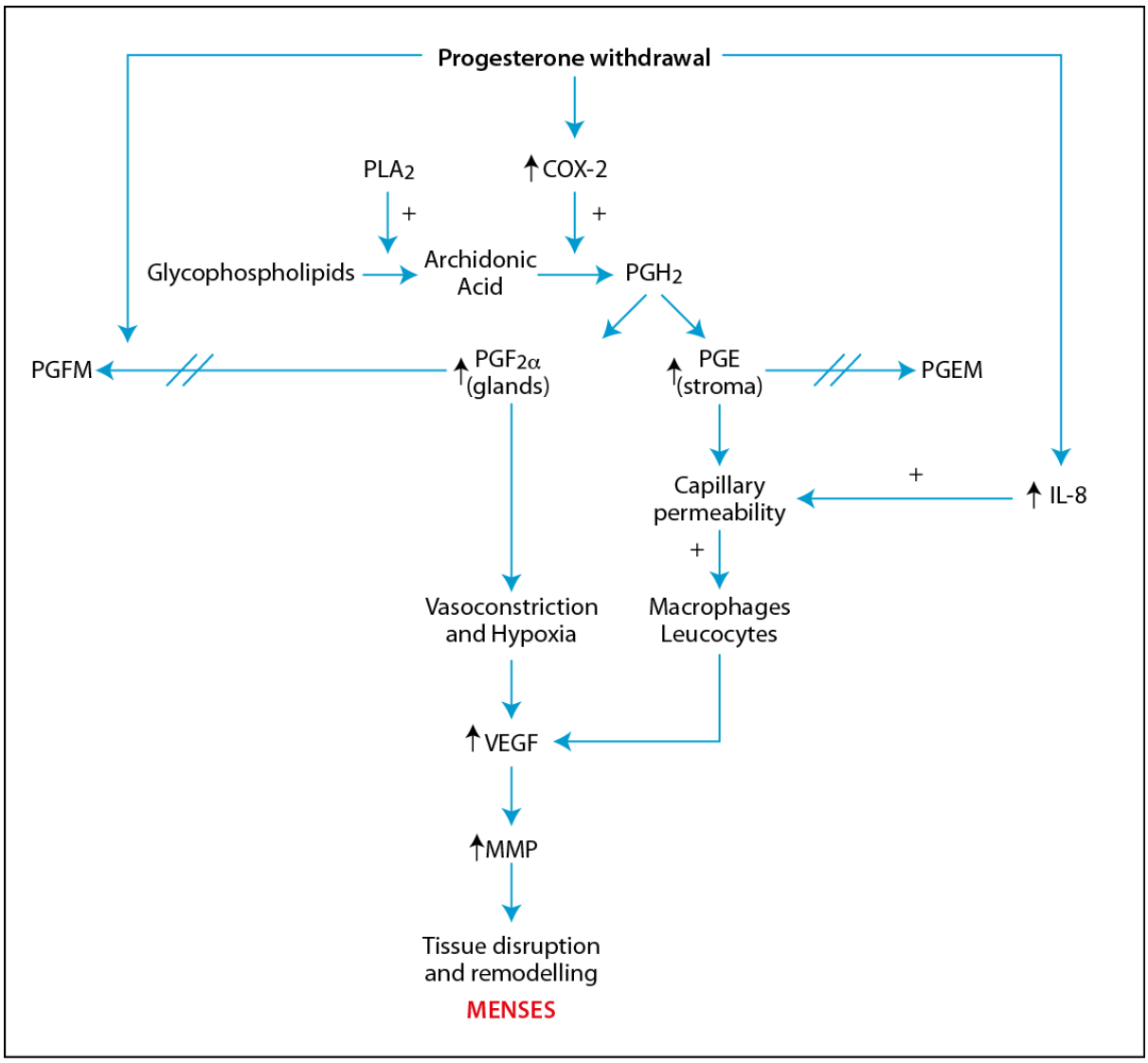

Figure 1.4 Progesterone withdrawal activates inflammatory pathways resulting in menstruation

Following demise of the corpus luteum, progesterone withdrawal in the late secretory phase increases local prostaglandin production and inhibits breakdown of active prostaglandins, resulting in a cascade of inflammation at menses.
Local increase in prostaglandins results in an influx of leucocytes, vasoconstriction of spiral arterioles and resultant hypoxia. The culmination of this process is the shedding of the functional layer of endometrium.
COX-2 cyclo-oxygenase; PLA_2 phospholipase A2; PGH_2 prostaglandin H2; PGF_2 prostaglandin F2 alpha; PGFM prostaglandin F2 alpha metabolites; PGE prostaglandin E; PGEM prostaglandin E metabolites; VGEF vascular endothelial growth factor; MMP matrix metalloproteinases; IL-8 interleukin-8

This is a draft of a figure from the chapter 'The menstrual cycle' that has been accepted for publication by Oxford University Press in the forthcoming book Oxford Textbook of Obstetrics and Gyanecology (chapter by Lucy Whitaker, Karolina Skorupskaite, Jacqueline A Maybin and Hilary O D Critchley), edited by William Ledger due for publication in 2017.

Inflammatory mediators generated within the endometrium upon withdrawal of progesterone include matrix metalloproteinases (MMPs), prostaglandins, cyclooxygenase (COX-2), and interleukin-8 (IL-8) (Figure 1.4). Leukocyte traffic is initially neutrophil dominated, which contain high levels of MMPs and may activate tissue MMPs, playing a critical role in the induction of endometrial shedding (Marbaix, Kokorine et al. 1996). Macrophage numbers also increase, contributing to cytokine production, local remodelling of the endometrium and removal of debris. Tight regulation of localised "physiological" inflammation is critical to secure satisfactory onward endometrial repair and prevent excessive bleeding at menses (Jabbour, Kelly et al. 2006, Maybin and Critchley 2015).

An intact endometrial coagulation system is necessary for efficient cessation of menstruation. Endometrial blood vessel injury initiates immediate activation and aggregation of platelets with activation of both the intrinsic and extrinsic coagulation cascade, ultimately leading to the formation of a stable fibrin clot to seal previously bleeding vessels (Maybin and Critchley 2015). In parallel the fibronolytic pathway is activated, whereby there is conversion of plasminogen to active plasmin, promoting the degradation of fibrin deposits. Tissue plasminogen activator (t-PA) and urokinase plasminogen activator (u-PA) drive the production of plasmin. In contrast, plasminogen activator inhibitor (PAI) inhibits fibrinolytic activity. The human endometrium contains t-PA and u-PA, as well as PAI and the u-PA receptor (Gleeson, Devitt et al. 1993, Nordengren, Pilka et al. 2004). Tight regulation to balance coagulation and fibrinolysis is necessary for normal menstruation.

During menstruation, damaged vasculature at the shed surface leads to bleeding. The volume of blood lost is influenced by the viscosity of blood and the radius and length of the blood vessels, and of these, vessel radius is the dominant contributory factor (Maybin, Critchley et al. 2011). Therefore, the endometrium has evolved specialised spiral arterioles that have the ability to undergo intense vasoconstriction during the late secretory and menstrual phases to limit blood loss. Experiments in the non-human primate, the rhesus macaque, suggest that this vasoconstriction is so forceful that the luminal portion of the endometrium becomes hypoxic (Markee 1940). There is increasing evidence that this hypoxia may trigger a cellular protective response that increases local repair factors and drives blood vessel and tissue regeneration (Maybin, Battersby et al. 2011, Maybin, Hirani et al. 2011, Maybin and Critchley 2015).

1.3 Abnormal uterine bleeding

Chronic abnormal uterine bleeding (AUB) is defined as 'bleeding from the uterine corpus that is abnormal in volume, regularity and/or timing that has been present for the majority of the last 6 months' (Fraser, Critchley et al. 2011, Munro, Critchley et al. 2011). Abnormality for volume, frequency, regularity and duration were defined as outwith accepted 5-95th percentiles by the Menstrual Disorders Group (MDG) of the Fédération International de Gynécologie et d'Obstétrique (FIGO) (Fraser, Critchley et al. 2011). In addition to these definitions of normality, underlying aetiologies were categorised in a structured fashion, covered by the pneumonic PALM-COEIN (Figure 1.5) (Munro, Critchley et al. 2011). PALM reflects the structural causes, including polyp, adenomyosis, leiomyoma and malignancy. COEIN represents the non-structural causes such as coagulopathies, ovulatory dysfunction, endometrial, iatrogenic and not yet classified which includes aetiologies such as chronic endometritis and vascular malformations.

1.3.1 AUB and fibroids

Uterine fibroids (leiomyoma) are benign tumours of the myometrium. They are common, whilst overall incidence varies widely (217-3745 cases per 100 000 woman years), and by the age of fifty around 70% of Caucasian women and more than 80% of women of Afro-Caribbean descent will have a least one fibroid (Baird, Dunson et al. 2003, Stewart, Cookson et al. 2017). The relationship between AUB and uterine fibroids still remains incompletely understood. Between 50 and 70% of women with fibroids are asymptomatic (Stewart, Laughlin-Tommaso et al. 2016) but fibroids are highly prevalent in women presenting with AUB. In addition those with fibroids may present with pressure symptoms and infertility.

Previous suggested theories for leiomyoma-dependant AUB (AUB-L) include an increased endometrial surface area and the presence of engorged and fragile vasculature in the peri-fibroid environment (Munro 2012). The resultant increase in vascular flow seen with these enlarged vessels may overwhelm platelet action (Stewart and Nowak 1996). However the effect of fibroids on endometrial function is now thought to represent a field change,, where endometrial function is altered throughout the entire uterine cavity, rather than limited only to the endometrial regions overlying the fibroids(s), and knowledge is increasing about the complex cellular and molecular changes found in association with fibroids.

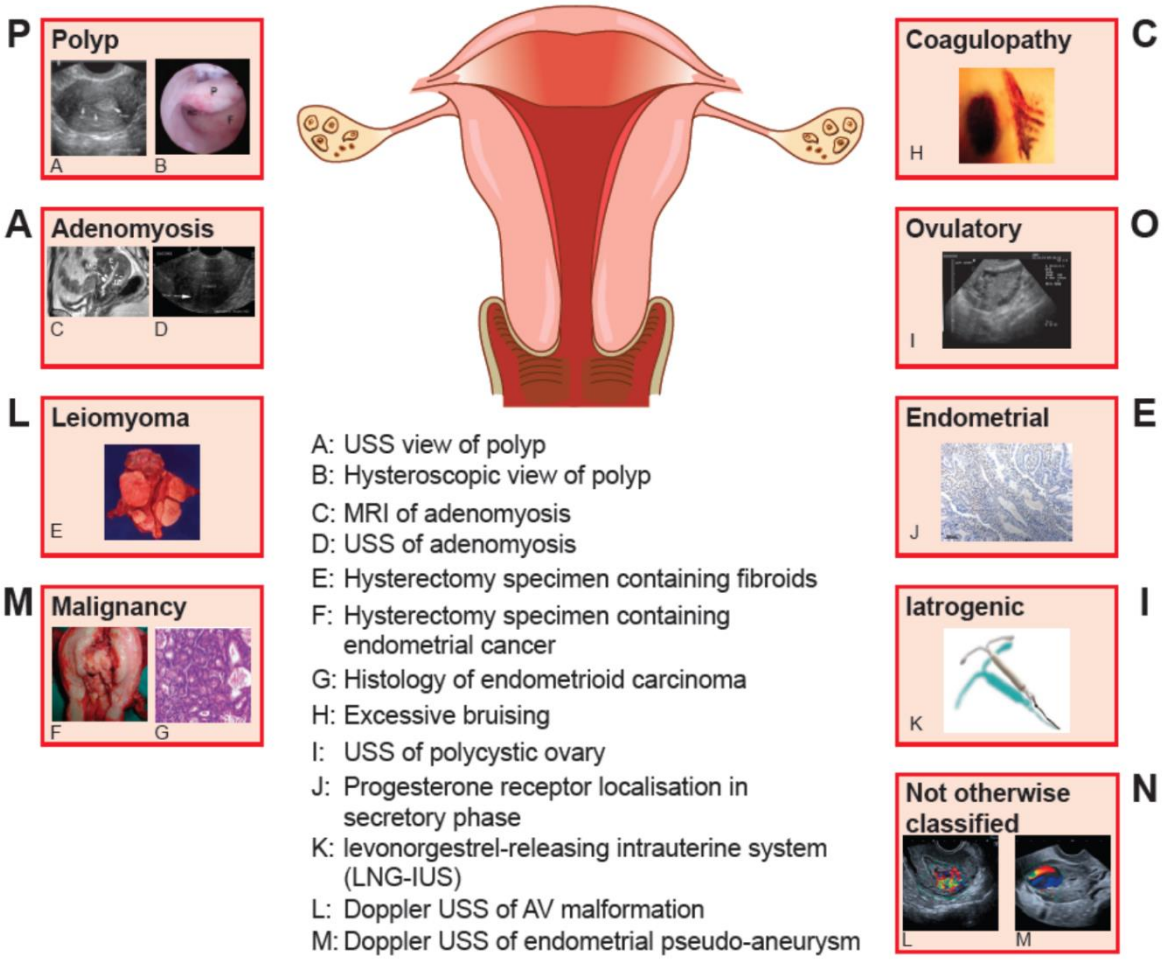

Figure 1.5 FIGO classification of causes of abnormal uterine bleeding (AUB); 'PALM COEIN'

A structured approach to the causes of AUB. PALM represents structural causes including polyps, adenomyosis, leiomyoma (fibroids) and malignancy. COEIN reflects non-structural causes including coagulopathy, ovulatory, endometrial, iatrogenic and not otherwise classified causes such as endometritis and vascular malformations.

Reproduced from Whitaker and Critchley 2016. Abnormal uterine bleeding

https://doi.org/10.1016/j.bpobgyn.2015.11.012

Alteration in angiogenesis, vasoactive substrates and growth factors as well as alteration in coagulation are now all thought to contribute to AUB in the context of fibroids (Stewart and Nowak 1996).

Plasminogen modulators have been demonstrated to be altered in the presence of fibroid and this may impact upon haemostasis and repair within the endometrium (Stewart and Nowak 1996). Transforming growth factor-beta (TGF-β3) levels are increased in the endometrium in women with fibroids and is associated with reduced levels of plasminogen-activator inhibitor-1 (PAI-1), thrombomodulin and antithrombin III, both in vivo and in endometrial stromal cells treated in vitro with TGF-β3 (Sinclair, Mastroyannis et al. 2011).

As descried in section **1.2** menstruation and endometrial repair is an inflammatory event. Alterations in blood plasma levels of circulating interleukin (IL) -13, IL-17 and IL-10 have been reported in women with fibroids (Wegienka, Baird et al. 2013) but it is unknown how this impacts upon immune function and inflammation within the endometrium.

1.3.2 Management of AUB and fibroids: the unmet clinical need

AUB, encompassing heavy menstrual bleeding (HMB) is a common disorder, affecting 14-25% of women of reproductive age (Shapley, Jordan et al. 2004, Fraser, Langham et al. 2009). HMB may have a profound negative impact on multiple aspects of an individual's life (Bitzer, Heikinheimo et al. 2015) and this is reflected in the definition of HMB utilised by both the ACOG and RCOG. Rather than the objective measurement of >80ml per cycle, they prefer the patient centred definition of heavy menstrual bleeding (HMB) as articulated in the National Institute for Health and Care Excellence 2007 Clinical Guideline: 'excessive menstrual blood loss which interferes with a woman's physical, social, emotional and/or material quality of life' (NICE 2007).

In addition to the direct impact on the woman and her family, there are significant costs both to the economy and the health service. A study conducted in the USA reported that financial losses of >$2000 per patient per annum due to home management costs and work absence (Frick, Clark et al. 2009). In the USA, where the burden of AUB-L is higher, the annual economic burden of fibroids is estimated to be between $5.9 billion and $34.4

billion (Cardozo, Clark et al. 2012). In the UK each year, over 800 000 women seek help for AUB (NICE 2007) and it is the 4th most common reason for referral to UK gynaecological services (RCOG 2012).

There remains a paucity of high quality evidence from randomised-controlled trials for the treatment of AUB-L (Gliklich, Leavy et al. 2011). Alongside amelioration of bleeding, existing treatment options need to address fertility desire, impact of pressure symptoms, any other AUB contributors and co-morbidities (Table 1.1). For some, particularly in the peri-menopausal phase with amenorrhoea and regression of fibroid size imminent, a conservative approach (incorporating oral iron replacement if indicated) may be an acceptable treatment approach. For others either medical or surgical treatment may be necessary (Whitaker and Critchley 2016).

In the absence of pressure symptoms, an oversized cavity or leiomyoma related infertility the standard treatments of levonorgestrel-releasing intrauterine system (LNG-IUS), anti-fibrinolytics, non-steroidal anti-inflammatories (e.g. mefenamic acid) or systemic progestin's may be sufficient (NICE 2007). However these may have limited utility in the AUB-L phenotype compared with other causes of HMB. Whilst there is evidence of efficacy with the LNG-IUS in AUB-L (Maruo, Ohara et al. 2007), the risk of expulsion is higher (Sangkomkamhang, Lumbiganon et al. 2013). Dissatisfaction with oral treatment has been demonstrated to be higher than LNG-IUS (Gupta, Daniels et al. 2015) and unscheduled bleeding is common with progestin treatment, irrespective of mode of administration, which may limit acceptability (Bitzer, Heikinheimo et al. 2015).

Other medical treatments include selective progesterone receptor modulators (SPRMS) and GnRH analogues. SPRMs are discussed in depth in section **1.4**. GnRH analogues are effective at reducing both menstrual bleeding and the size of fibroids but side effects and impact upon bone density limit longer-term utility. Furthermore rebound of symptoms is rapid on cessation (Moroni, Martins et al. 2015). GnRH agonists often have utility as a short-term treatment prior to surgery but there is good evidence that the SPRM ulipristal acetate (UPA) is better tolerated in those women pre-surgery without loss of efficacy (Donnez, Tomaszewski et al. 2012).

Table 1.1 Symptom-based approach for management of abnormal uterine bleeding in the context of uterine fibroids

Symptoms			
	AUB only	AUB with pressure symptoms; family complete and no desire to retain fertility	AUB symptoms and fertility preservation/subfertility
No cavity distortion	LNG-IUS Tranexamic acid Mefenamic acid UPA GnRH analogue P	UPA GnRH analogue	Tranexamic acid Mefenamic acid UPA (short course) GnRH analogue (short course)
	UAE EA Hysterectomy	UAE (MRgFUS) Myomectomy Hysterectomy	Myomectomy UAE (evidence here needed) (MRgFUS)
Cavity distortion	Tranexamic acid Mefenamic acid UPA GnRH analogue P4	UPA GnRH analogue	Tranexamic acid Mefenamic acid UPA (short course) GnRH analogue (short course)
	TCRF UAE Hysterectomy	UAE Myomectomy Hysterectomy	TCRF Myomectomy UAE (evidence here needed)

Medical treatment
Surgical treatment

LNG-IUS	Levonorgestrel-releasing -intrauterine system
UPA	Ulipristal acetate
GnRH analogue	Gonadotrophin-releasing hormone analogue
P4	Systemic progestogens • Medroxyprogesterone acetate • Norethisterone • Depo-Medroxyprogesterone acetate
EA	Endometrial ablation
UAE	Uterine artery embolisation
(MRgFUS)	MR-guided focused ultrasound – predominantly experimental at present
TCRF	Transcervical resection of fibroid

There is no robust evidence for alternative therapies such as herbal remedies or acupuncture for the treatment of fibroids (Zhang, Peng et al. 2010, Liu, Yang et al. 2013), and trials of selective ER modulators (SERMs) and aromatase inhibitors have remained disappointing (Stewart, Laughlin-Tommaso et al. 2016). Other options include uterine artery embolization (UAE) (Moss and Christie 2016), MR-guided focused ultrasound (MRgFUS) (Quinn, Vedelago et al. 2014), a technique that is not widely available and with a small evidence base, and surgical options such as myomectomy, endometrial ablation (in the absence of cavity distortion) and hysterectomy. The latter two are fertility ending procedures. For those wishing to preserve fertility there is as yet insufficient evidence for recommendation of either UAE or myomectomy over the other, though the anticipated outputs of the FEMME study (McPherson, Manyonda et al. 2014) will hopefully provide robust evidence for impact on symptoms and other qualitative measures between these two treatment modalities. Hysterectomy is a definitive treatment. Surgery is often challenging, with high potential blood losses and risk of ureteric injury due to anatomical distortion in the pelvis, and with increasing obesity the complexity of surgery is compounded.

There remains conflict about which treatment strategy results in the highest patient satisfaction. The recent RCOG National HMB audit found higher patient satisfaction with surgical intervention (RCOG 2014) and hysterectomy remains the most cost-effective beyond 5 years (Roberts, Tsourapas et al. 2011). This led to the RCOG postulating that those with more severe symptoms may benefit from an earlier recourse to surgery (RCOG 2014). In contrast, a recent Cochrane review, whilst acknowledging that surgical intervention was more effective than medical treatment in reducing menstrual bleeding at one year, did not find conclusive evidence of a difference in satisfaction between the LNG-IUS and surgery. Furthermore they highlighted the risk of serious complication following hysterectomy and thus recommended that women should continue to consider less radical treatment options as a first line treatment strategy (Marjoribanks, Lethaby et al. 2016).

A recent national audit in England and Wales (RCOG HMB audit) reported that at 1-year post referral only a third of women (including those managed with surgery) were ‘satisfied’ (or better) at the prospect of current menstrual symptoms continuing, as currently experienced, for the next 5 years (RCOG 2014). Despite existing medical treatments available, in the USA thousands of UAEs, approximately 30, 000

myomectomies, and 200,000 hysterectomies are performed annually for symptomatic fibroids (Bulun 2013). Indeed in North America the lifetime risk of hysterectomy is 45%, of which only 8% are performed for cancer (Merrill 2008). Of all surgical treatments performed specifically for fibroids, nearly three-quarters are hysterectomies (Borah, Laughlin-Tommaso et al. 2016), reflecting dissatisfaction with existing alternative treatment modalities.

While there may be relief from HMB during pregnancy and lactation, and an end to the problem at menopause, women affected will tend to suffer the adverse impacts of AUB over what should be the prime years of their lives. Women are increasingly deferring child bearing – over half of all UK-born babies are to women in their 4th and 5th decade of life (Haines 2016). As the incidence of fibroids rises with age, those affected by AUB-L increasingly are likely to wish to preserve their fertility and as such there remains an unmet need for effective but fertility sparing treatments. A class of compounds with potential utility are the SPRMs.

1.4 The Selective Progesterone Receptor Modulators (SPRMs)

Progesterone was first isolated in 1934 (Allen and Wintersteiner 1934) and synthetic progestins have long been used for both hormonal manipulation and contraception. Since the discovery of the progesterone receptor (PR) (Sherman, Corvol et al. 1970), the clinical utility of a PR antagonist has long been appreciated but the discovery of the first SPRM mifepristone (RU-486) occurred during the search for a potent glucorticoid receptor (GR) ligand (Gagne, Pons et al. 1985). Studies in mice and non-human primates (NHP) demonstrated potent anti-progestogenic effects and an anti-proliferative effect upon the endometrium (Cullingford and Pollard 1988, Chwalisz, Brenner et al. 2000). Since the development of mifepristone, multiple other synthetic ligands have been derived (Figure 1.6). Early SPRMs were derived from testosterone (Mifepristone, asoprisnil, Lonaprisan and onapristone) or progesterone (ulipristal acetate; UPA and telapristone) and have a bulky C11 side chain (Petit-Topin, Fay et al. 2014).

Mifepristone was considered to be a relatively pure progesterone anatagonist (P-antagonist), as determined by the McPhail test.

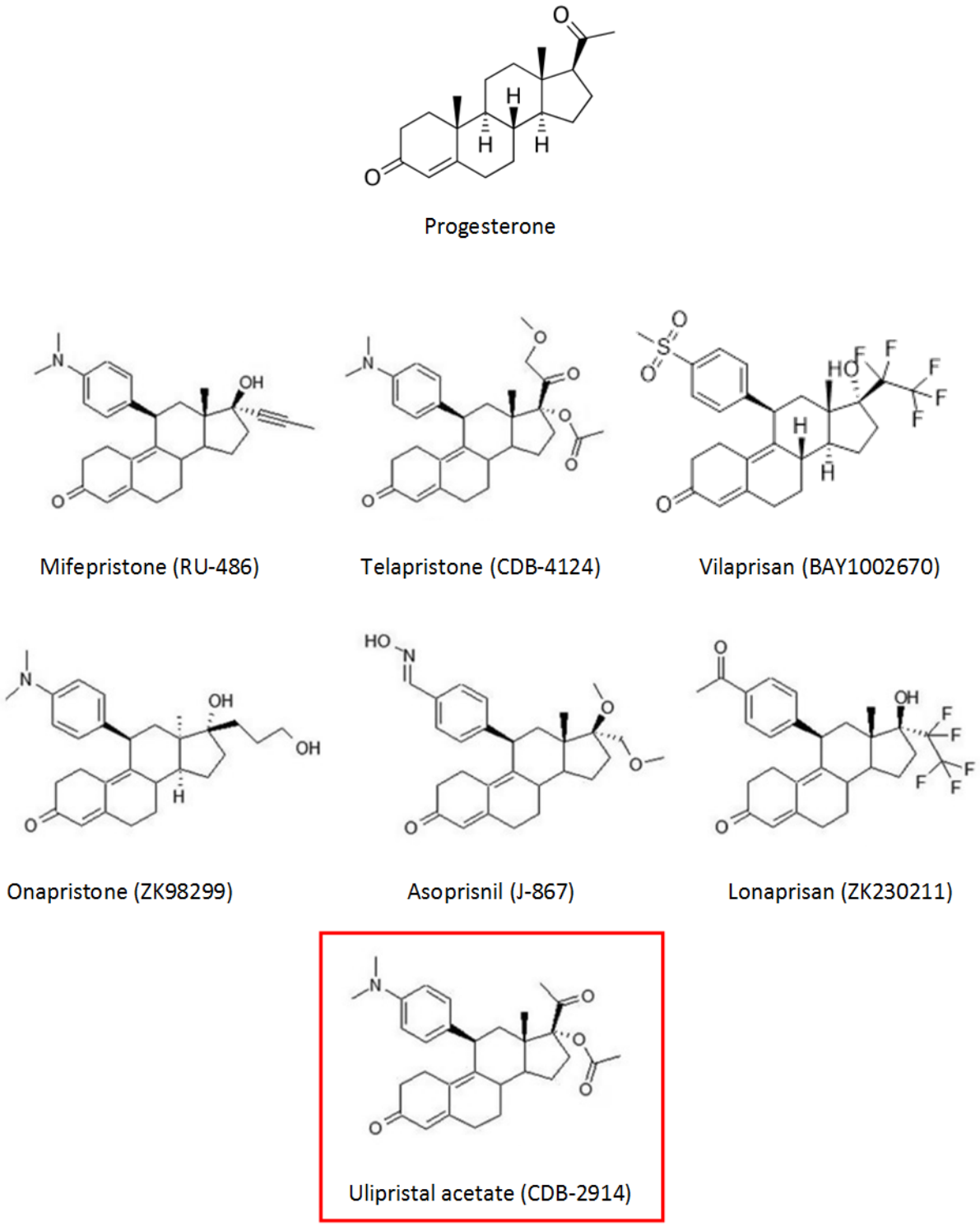

Figure 1.6 Structure of common SPRMs

Chemical structure of some SPRMs utilised in clinical trials. Only mifepristone and ulipristal acetate are currently licensed for clinical use although vilaprisan is currently under investigation in an ongoing phase III trial

This was the standard test for determining the PR agonist/antagonist activity of compound, in which E-primed immature rabbits are administered a compound and the effect upon endometrial development assessed (McPhail 1934). Utilising the McPhail test many of these demonstrate potent P-antagonism, in particular lonaprisan, onapristone, mifepristone and ZK137316 (Elger, Bartley et al. 2000) and has been supported by gene profiling (Afhuppe, Sommer et al. 2009). Ulipristal acetate (UPA) has also been demonstrated to be a highly potent P-antagonist (Spitz and Chwalisz 2000, Petit-Topin, Fay et al. 2014). Others, such as asoprisnil display more mixed antagonism and agonism, and were initially referred to as mesoprogestins (Elger, Bartley et al. 2000). Given this, and the subsequent appreciation that all class members may demonstrate both cell and tissue mixed antagonism and agonism (Smith and O'Malley 2004), many consider all these compounds to be classified as selective progesterone receptor modulators (SPRMs).

This change in nomenclature has also had some political origins. Mifepristone and other early SPRMs were referred to as progesterone antagonist (PAs). In keeping with an anti-progesterone effect it was demonstrated that mifepristone and other PAs had the ability to interrupt pregnancy (Ulmann and Silvestre 1994). This potential as an abortifacient had political ramifications (Ulmann 2000) and in 1989, a year after the licensing of mifepristone for termination of pregnancy, it was withdrawn temporarily from the market following political pressure (Dorozynski 1997). 'Political chemistry' continued elsewhere, restricting development of SPRMs, irrespective of intended use (Hodgen 1991). Indeed it was only in 2000 that it become available in the United States for the management of unwanted pregnancy (Gottlieb 2000). The use of the term SPRM was in part adopted to distinguish from compounds that had the ability to interrupt pregnancy (Elger, Bartley et al. 2000), though mifepristone is frequently described as an SPRM and administration of UPA is both effective as an emergency contraceptive (Glasier 2014) and embryotoxic in some animal studies (Tarantal, Hendrickx et al. 1996).

Irrespective of PR-ligand studied, they have all been shown to have similar affinity for the PR, and bind both PR isoforms (Chabbert-Buffet, Meduri et al. 2005, Bouchard, Chabbert-Buffet et al. 2011). The degree of antagonism/agonism is thought to be determined by the relative recruitment of co-regulators (Smith and O'Malley 2004). Some SPRMs have affinity for other steroid receptors, most notably mifepristone for GR, whilst UPA is highly selective for the PR and has significantly reduced GR binding

compared to mifepristone and almost negligible ER, androgen receptor (AR) and mineralocorticoid receptor (MR) binding (Wolf, Hsiu et al. 1989, Attardi, Burgenson et al. 2004, Petit-Topin, Fay et al. 2014). This is similar to the receptor binding of asoprisnil (Schubert, Elger et al. 2005).

SPRMs have been considered for use in pituitary adenomas, breast disease and several cancers (Whitaker, Williams et al. 2014) but the key role that progesterone plays in reproductive physiology has resulted in many potential applications of SPRMs within gynaecology. At present in the UK only mifepristone and UPA are licensed for use within gynaecological practice.

Mifepristone is licensed for the termination of pregnancy. In addition it may have utility in the management of miscarriage and in some countries is used for induction of labour (Chabbert-Buffet, Meduri et al. 2005). A 30mg dose of UPA is utilised for emergency contraception. It acts predominantly by inhibition of ovulation (Brache, Cochon et al. 2013). It is at least as effective as levonorgestrel and has a longer effective window of use. Both mifepristone and UPA have been evaluated as long-term contraceptives and have shown promising efficacy and acceptability (Lakha, Ho et al. 2007, Brache, Sitruk-Ware et al. 2012) but neither have been taken forward at present into clinical use. Phase II studies of the use of SPRMs in endometriosis have demonstrated positive results (Kettel, Murphy et al. 1998, Chwalisz, Perez et al. 2005). SPRMs have been used anecdotally with great effect for adenomyosis but an appropriately designed and powered randomised controlled trial (RCT) for this indication has yet to be performed.

The main area of current utility in gynaecology is in the management of symptomatic fibroids. The SPRMs mifepristone, asoprisnil and ulipristal acetate (UPA) have all been shown to be effective at reducing fibroid size and affording control of bleeding compared to placebo but no one agent is more effective than another (Murji, Whitaker et al. 2017). Asoprisnil has not been proceeded beyond phase III studies. Multiple clinical trials and a meta-analysis have demonstrated efficacy of mifepristone in reducing fibroid size and controlling uterine bleeding (Shen, Hua et al. 2013) but long-term use of mifepristone has been hampered by concerns regarding endometrial safety, the negative connotations of its use as an abortificant and glucorticoid side effects. Further compounds are under development, most notably Vilaprisan which is in phase III studies at present and has had encouraging phase I results published (Wagenfeld, Bone et al. 2013, Schutt, Kaiser

et al. 2016) and phase II results presented at international meetings (Singh, Ren et al. 2017).

At present UPA is the only licensed SPRM for intermittent management of symptomatic fibroids and is now recommended as first line treatment by NICE for those with fibroids >3cm and anaemia (NICE 2016). This recommendation is based upon the "PEARL" studies, which demonstrated effective and rapid control of bleeding with over 90% of women achieving amenorrhoea, and significant reduction in fibroid size. Crucially there was also non-inferiority to a GnRH analogue in reduction in fibroid size, and reduced side effects (Donnez, Tomaszewski et al. 2012). In addition, repeated cycles demonstrated ongoing reduction in fibroid size and added reassurance regarding endometrial safety (Donnez, Vazquez et al. 2014, Donnez, Hudecek et al. 2015, Fauser, Donnez et al. 2017). Regrowth of fibroids is slower on cessation of UPA compared with a GnRH analogue and this may reflect the differing mechanism of volume reduction as UPA significantly increases apoptosis in leiomyoma cells (Horak, Mara et al. 2012). Indeed in the first two PEARL studies some women chose not to proceed to hysterectomy as previously planned, as they had ongoing amelioration of symptoms despite cessation of treatment (Donnez, Tatarchuk et al. 2012, Donnez, Tomaszewski et al. 2012). This has also been demonstrated by other groups reflecting 'real world' use (Fernandez, Schmidt et al. 2017). Maintenance of circulating E2 at a mid-follicular level is likely responsible for the favourable side effect profile compared to GnRH analogues, and provides reassurance regarding bone safety, critical for a long-term medical option. Finally there have been successful pregnancies in women following UPA treatment, demonstrating that they may be an effective fertility preserving treatment (Luyckx, Squifflet et al. 2014) and in some women they have been a useful adjunct in reversing subfertility by correcting distortion of the uterine cavity (de la Fuente, Borras et al. 2016, Murad 2016).

Whilst a small proportion of women administered UPA do not achieve fibroid shrinkage or control of uterine bleeding, for the vast majority it does represent an effective and acceptable, and critically, fertility preserving medical option for the management of symptomatic fibroids. However despite demonstration of efficacy, reassurance regarding safety and the subsequent adoption into standard clinical practice there remains many unknowns with regard to effects upon the endometrium and other components of the reproductive tract.

1.5 Hypothesis

Based upon the information currently available from other studies of SPRMs it is hypothesised that:

1. SPRM administration has an endometrial specific effect upon the epithelium of the human reproductive tract

2. SPRM administration impacts upon progesterone-regulated genes in the human endometrium

3. SPRM administration has an anti-proliferative effect within the epithelium of the human reproductive tract

1.6 Aims

<u>Aim 1</u> To describe the impact of SPRM administration upon steroid receptor expression and localisation in the epithelium of the human female reproductive tract

Research questions:

- Is there a morphological effect of UPA administration on the endometrium, fallopian tube and cervix?
- Is there alteration in sex-steroid receptor mRNA levels in the endometrium and fallopian tube?
- Is there alteration in sex-steroid receptor protein expression and localisation in the endometrium, fallopian tube and cervix?
- Is the effect endometrial specific?

<u>Aim 2</u> To study the impact of SPRM administration on progesterone-regulated genes in the human endometrium

Research questions

- What is the impact upon known endometrial P-regulated gene transcription?
- Is there alteration in protein localisation of P-regulated genes under investigation?
- Does the presence of co-existing endometriosis alter response of endometrial P-regulated genes?
- Does administration of SPRM, UPA alter clearance of PTEN null glands in the endometrium?

<u>Aim 3</u> To study the mechanisms whereby SPRM administration reduces cell proliferation in the epithelium of the human female reproductive tract.

Research Questions

- Is there reduction in cell proliferation in the fallopian tube and cervix following UPA administration?
- What candidate genes are implicated in the anti-proliferative effect within the endometrium?
- Is there alteration in mRNA levels and protein expression in the endometrial cell cycle?

Chapter 2.
Materials and Methods

2.1 Reproductive Tract Tissue Resource

2.1.1 Tissue governance

Tissue resources are carefully regulated to provide an adequate research resource in which participants have their rights and confidentiality carefully protected.

The Critchley Female Reproductive Tract Tissue Resource forms part of the Lothian NRS BioResource led by Professor David Harrison (the Designated Individual for tissue). This was approved by East of Scotland Research Ethics Service (ESRES; 15/ES/0094; 14th July 2015).

The Female Reproductive Tract Tissue Resource contains samples from previous studies now jointly covered under Research Ethics Committee (REC) approval 16/ES/0007 (previously 10/S1402/59) and current active studies:

- 07/S1103/20. Mechanisms Involved in Endometrial Repair and Regeneration
- 12/SS/0238 Mechanism of Action of PRMs (Progesterone Receptor Modulators)
- 14/LO/1602 Ulipristal acetate versus conventional management of heavy menstrual bleeding (HMB; including uterine fibroids): a randomised controlled trial and exploration of mechanism of action: 'UCON'

Samples utilised in this doctoral thesis from The Female Reproductive Tract Tissue Resource REC approval include samples from superseded REC approvals (Table 2.1).

Table 2.1. Updated REC approved studies for tissue collection

REC	Study Name
05/S1103/14	Local Cortisol Regulation in the Ovary and Uterus
05/S1103/32	Regulators of Vascular Function in the Female Reproductive Tract
2001/6/5	Local mediators in menstruation
1994/6/17	The Role of Steroid Hormones in Benign Gynaecological Conditions

2.1.2 Reproductive Tract Tissue Resource participation

Eligible women are aged from 18 years and have benign gynaecological conditions. Participants are recruited from NHS Lothian attending gynaecology services including outpatient clinics, preadmission services, Day Surgery units and in patient wards

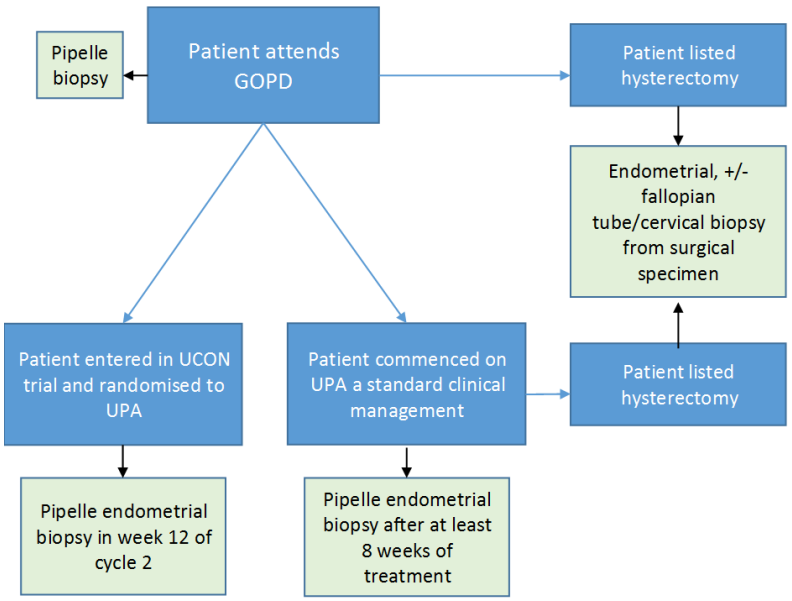

Figure 2.1 Schematic of potential tissue sample collection points

GOPD: gynaecology out-patients department, UPA: Ulipristal acetate, UCON: Ulipristal acetate versus conventional management of heavy menstrual bleeding (HMB; including uterine fibroids): a randomised controlled trial and exploration of mechanism of action. Randomised clinical trial. Subjects allocated to UPA have 3, 12 weeks courses of treatment each separated by four weeks off treatment.

Table 2.2 Information collected from female reproductive tract "tissue bank" resource participants

Age	
Menstrual Cycle and Bleeding pattern	LMP, Cycle, menses duration, HMB (subjective) intermenstrual bleeding Pain
Medication	Contraceptives (COCP, POP, parental, LNG-IUS, IUCD & ECP) GnRH analogue use Sex hormones and their modulators SPRMs (and bleeding control when on treatment) Corticosteroids and NSAIDs Tranexamic acid Other regular medications
Clinical presentation	HMB, pain, endometriosis, other clinical presentation Fibroids, polyps, ovarian pathology
Previous gynaecology & obstetric history	Ablation/UAE, other gynaecological surgery Infertility, ectopic pregnancy Previous or previous pelvic infection/STI Parity, mode of delivery
Pathology	Previous pathology reports & report linked to research sample collection
Imaging	USS/MRI/CT
Clinical comments	Findings at the time of surgery
Obesity status	Height, weight & body mass index (BMI)
Tobacco smoking history	Current, previous, never

(Figure 2.1). Other clinical departments involved are Pathology, Clinical laboratory services and Operating Theatres. Potential participants are identified by the clinical research staff in collaboration with clinical colleagues. They are provided with a participant information sheet and given the opportunity to discuss studies with research staff. If they wish to take part a consent form is then signed, copies are filed in the clinical notes, kept by the clinical research team and given to the participant.

Following consent each participant is allocated a unique participant and laboratory number, tissue samples are allocated an additional sample number. Any subsequent participation re-uses the participation and laboratory number but receives separate sample numbers.

Samples collected include: endometrium, 'full thickness' endometrium/myometrial biopsy, cervix, fallopian tubes and venous blood. 'Full thickness' endometrial biopsies are biopsies transecting from the lumen of the uterine cavity, through the full thickness of the endometrium (encompassing the functional and basal layer) through to the underlying myometrium. Samples are either: fixed in formalin, collected in RNA later and frozen, fresh frozen, placed in culture medium, placed in medium for use in animal models (eg xenograft studies with appropriate Home Office approval), venous whole blood and centrifuged serum/plasma. Further detail about tissue collection, processing and storage can be found in section **2.2**.

Demographic and clinical data are collected (table 2.2). All identifiable features (Name, date of birth, Hospital and Community Health Index (CHI) number) are removed prior to releasing information to researchers to ensure anonymity is protected. Data are stored on a secure University of Edinburgh computer and with NHS Lothian Caldicott Guardianship approval (CG/DF/1437).

2.2 Tissue Collection

Participants were consented under the appropriate ethics as outlined in **2.1**. In addition to tissue, a venous blood sample was collected to assist with menstrual cycle staging.

2.2.1 Endometrium

2.2.1.1 Endometrial biopsies, full thickness

'Full thickness' endometrial biopsies were collected at the time of surgery from women with uterine fibroids treated with Ulipristal acetate (UPA; 5mg oral once daily) for up to 15 weeks prior to hysterectomy. 'Full thickness' endometrial biopsies are biopsies span the lumen of the uterine cavity, through the full thickness of the endometrium (encompassing the functional and basal layer) through to the underlying myometrium (Figure 2.2).

After surgical removal, the uterus was taken promptly to the local pathology laboratory in an unfixed state. The specimen was orientated with the use of a probe inserted through the external os of the cervix to fundus of the cavity. The uterus was then opened along the plane of the probe utilising a long bladed knife. Tissue blocks for research were removed encompassing full thickness endometrium and underlying myometrium. These samples were placed in cassette for orientation and immersed in in 4% neutral-buffered formalin overnight at 4°C followed by storage in 70% ethanol. They were subsequent embedded in paraffin wax for sectioning prior to haematoylin and eosin (H&E) and immunohistochemical staining. In addition endometrial samples were removed and immersed in RNAlater (Ambion, Texas, USA) at 4°C overnight and then flash frozen at −80°C for RNA extraction. The remainder of the uterine specimen was then placed in an adequate volume of formalin for overnight fixation and sampled the subsequent day for routine diagnostic assessment.

Control proliferative and secretory endometrium from women with HMB/fibroids was obtained from endometrial tissue archives (REC approval: 10/S1402/59) and processed in the manner described above. All controls were not on hormonal treatment at the time of biopsy.

2.2.1.2 Endometrial biopsies

"Paired" (described below) endometrial biopsies were obtained from women with fibroids treated with UPA 5mg daily with ethical approval and written informed consent. Samples were obtained using a pipelle biopsy sampler (Pipelle de Cornier Mark II, Laboratoire CCD, France). This was inserted into the uterus through the cervical os, typically in the outpatient setting. When the fundus was reached the inner tube was

pulled back to create a suction. Endometrial tissue was then aspirated from the uterine cavity as the sampler was rotated and slowly withdrawn.

Biopsies were divided into equivalent portions and i) immersed in RNAlater, or ii) fixed in 4% neutral-buffered formalin and processed as previously described. In addition a sample was sent for standard clinical histological assessment.

The index endometrial biopsy was taken prior to treatment with UPA, staged as described in section **2.3**. A follow-up sample was taken whilst on treatment after the 10th week of UPA administration. Additional paired samples were obtained as part of the mechanistic arm of the UCON trial. In this multicentre randomised clinical trial (REC approval: 14/LO/1602, EudraCT: 2014-003408-65) women with HMB were randomized to treatment with either levonorgestrel-releasing intra uterine system or UPA. The UPA was prescribed in a different regime to the current UK license. In short women received treatment for three twelve-week cycles, each separated by four weeks off treatment. Subjects did not require to have a withdrawal bleed between each treatment cycle. The lead site, Edinburgh, had an embedded exploratory "mechanistic" arm: 20 of the subjects allocated to UPA underwent magnetic resonance imaging (MRI) scan at three time points (prior to commencing treatment and in the final week of cycle two and three). In addition they underwent endometrial biopsy in the final week of treatment cycle two.

In addition to these "paired" samples, unpaired samples from women with symptomatic fibroids in either the proliferative or secretory phase of the menstrual cycle, or following UPA administration were also obtained for use as independent controls in certain experiments.

2.2.2 Fallopian Tube

Fallopian tube biopsies were collected with ethical approval and written informed consent. They were taken from women who had their fallopian tubes removed at the time of hysterectomy (n=6) following treatment with UPA (5mg daily) for up to 15 weeks prior to surgery. Samples for RNA extraction were collected from the ampulla (B) and following formalin fixation longitudinal samples encompassing fimbrae (A) and ampulla (B) and processed as previously described. This approach for sampling the fallopian tube

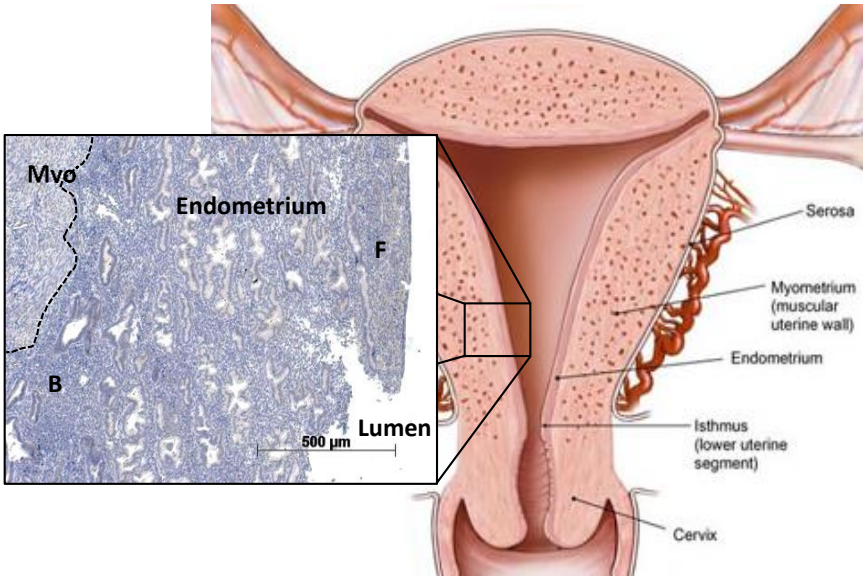

Figure 2.2 Endometrial/myometrial junction in full-thickness human endometrial biopsies

Photomicrograph represents haematoxylin-stained, 'full-thickness' human endometrial tissue from luminal epithelium (right-most in photomicrograph), through functional and basal endometrial layers to endometrial/myometrial junction (left-most in photomicrograph). B: basal layer, F functional layer *µm = micrometre, myo = myometrium; diagram of uterus adapted from MediVisuals Inc.* (© 2007).

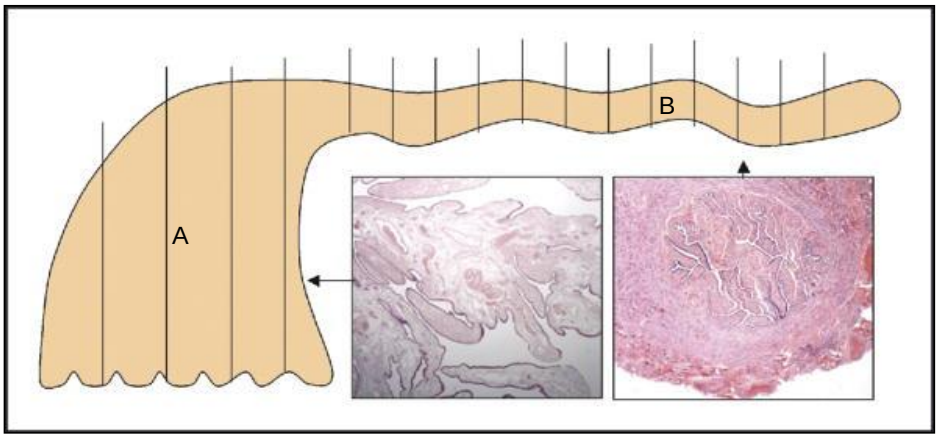

Figure 2.3 The SEE-FIM protocol for analysis of the fallopian tube in prophylactic salpingo-oophorectomies.

This varies from the conventional approaches by longitudinal sectioning of the fimbria (A) to maximize exposure of this epithelium (lower left) in addition to the proximal tube (lower right) (B). Adapted from Crum, Drapkin et al. 2007

for histological assessment is from the widely accepted SEE-FIM protocol (Crum, Drapkin et al. 2007) (Figure 2.3).

Control sample fallopian tube biopsies from women in proliferative and secretory phase were obtained from fallopian tube tissue archives (n=8 and 8). These consisted of biopsies (2–3 cm) from the ampullary region of the fallopian tube collected from participants at the time of hysterectomy for benign gynaecological conditions. Cycle phase was determined as described in section **2.3**. Biopsies were divided into equivalent portions and i) immersed in RNAlater, or ii) fixed in 4% neutral-buffered formalin and processed as previously described.

2.2.3 Cervical biopsies

Cervical biopsies were collected with ethical approval and written informed consent. Cervical biopsies were taken from women who had had their cervix removed at the time of hysterectomy (n=8) following treatment with UPA (5mg daily) for up to 12 weeks prior to surgery. The cervix was opened *en bloc* at the time of opening the uterus. Following fixation overnight in formalin full thickness biopsies taken which included the endocervical canal, transformation zone and ectocervix. Control proliferative (n=4) and secretory (n=5) cervical biopsies from hysterectomy specimens from women with HMB/fibroids were obtained from cervical tissue archives. These women had previously donated endometrium at the time of their hysterectomy (REC approval: 10/S1402/59) facilitating staging as outlined in section **2.3**.

2.3 Tissue dating

2.3.2 Progesterone and oestradiol assay

For the majority of women a blood serum sample was obtained to determine circulating progesterone (P4) and oestradiol (E2) levels at the time of tissue collection. A whole blood venous sample was take on the same day as tissue collection, centrifuged and the serum frozen prior to quantification.

A notable exception to this were the nine subjects undergoing hysterectomy following up to 12 week of UPA under REC approval 12/SS/0238.

2.3.2.1 Progesterone assay

The progesterone ELISA was performed by coating 96-well plates (Greiner Bio-One GmbH, Germany) with 100µl of goat anti mouse IgG (Jackson ImmunoResearch Inc, USA) per well at a dilution of 1:500 in ELISA coating buffer (100mM Na Bicarbonate, pH 9.6) covered and incubated in a fridge at 4oC overnight. Before use the plates were washed 3 times with wash buffer 0.05M Tris/HCl + 0.05% Tween 20, pH 7.4 (Tween® 20, Sigma-Aldrich, USA). Standards, samples and controls (20µl per well) were added to each well, followed by 80µl of Progesterone 3 - HRP conjugate (Astra Biotech GmbH, Germany) at 1:20,000 in assay buffer (PBS pH 7.4 containing 0.1 %BSA and 250 ng/ml Cortisol), followed by 50 µl of monoclonal progesterone Ab (Meridian Life Sciences, Memphis, USA) 1:100,000 in assay buffer. Plates were incubated at room temperature for 2 hr on a microtitre plate shaker (IKA®, Schuttler MTS4, IKA Labortechnik, Germany), washed 5 times with assay wash buffer and 120µl of substrate solution (3,3,5,5-Tetramethylbenzidine, Millipore Corporation, USA) added to each well. Plates were incubated at room temperature without shaking in the dark. After 20 min, the reaction was stopped by adding 80µl of 2N H_2SO_4 solution (Sigma-Aldrich Company Ltd., UK). Finally, plates were read on a plate reader at 450nm.

Standard curves were prepared with a total of 8 different concentrations (16, 8, 4, 2, 1, 0.5, 0.25 0 ng/ml). Samples, standards and controls were included in duplicate. Inter- and intra-assay CV were calculated from two controls of low and high P4 in duplicate in each of eight assays. The inter-assay CV for low and high pools respectively were 11.4 and 9.1% the intra-assay CV were 8.9 and 5.6%. The lower limit of detection was calculated at 0.1 ng/ml. Cross-reaction with other steroids was: oestrone: 0.17%, oestradiol: 0.28%, oestriol: 0.18%, dehydroepiandrosterone: 0.02%, testosterone: 0.36%, dihydrotestosterone: 0.15%, 17α-hydroxyprogesterone: 2.9%, androstenedione: 0.14%, 11-deoxycortisol: 0.46%, corticosterone: 0.18%, cortisone: 0.04% and cortisol: 0.04%. Results were converted into nmol/l by multiplying the ng/ml result by 3.18.

2.3.2.2 Oestradiol assay

Oestradiol was performed on a Roche Cobas E411 immunoassay analyser (Roche Diagnostics, Burgess Hill, UK) using the manufacturer's kits and controls according to their instructions. The lower limit of detection is reported at 18.4 pmol/l. The limit of quantitation is 91.8 pmol/L Within assay %CV was found to be <5% across the

measurable range and between batch CV 6.5% and 5.7% for the low and high quality control material respectively.

2.3.2 Menstrual Cycle staging

Endometrial biopsies were dated according to the three following criteria:

1. Histological appearance: as assessed by consultant pathologist (Professor Alistair Williams), based on criteria described by Noyes *et al* (Noyes, Hertig et al. 1950).
2. Last menstrual period (LMP): as reported by patient.
3. Serum progesterone and oestradiol concentrations: measured from serum samples collected from patients at the time of their endometrial biopsy.

The histological assessment of the control samples was undertaken blinded to LMP/cycle information and the serum P4 and E2 levels. For samples of UPA treated women cycle staging was not undertaken as the majority of treated women are expected to be anovulatory. However these women still underwent a histological assessment and this information was given to the pathologist in keeping with standard clinical practice.

2.4 Sample Characteristics

Samples were collected under the following REC approvals (as outlined in section **2.1.1**) and a corresponding code is indicated in the description of sample characteristics (Table 2.3).

2.4.1 Full thickness endometrial biopsies

Table 2.4 contains sample details of full thickness endometrial biopsies obtained at the time of hysterectomy as described in section **2.2.1.1**, from women exposed to UPA for up to 15 weeks. Samples for serum P4 and E2 levels were not obtained for many of these women. Table 2.5 contains sample details of proliferative and secretory biopsies obtained at the time of hysterectomy utilised as controls.

2.4.2 Endometrial biopsies

Table 2.6 contains sample details of endometrial biopsies obtained in the outpatient clinics from women exposed to UPA for up to 15 weeks. Many of the samples were 'paired': a baseline sample was taken prior to commencing UPA. A further biopsy was obtained from the same patient after at least 8 weeks of treatment. One sample was taken

8 days after completion of treatment. That individual had not had a withdrawal bleed from cessation of treatment at the time of biopsy. Samples from the "UCON mechanistic study" had their biopsy collected in the final week of their second cycle of UPA treatment (see **2.2.1.2**). Table 2.7 contains sample details of proliferative and secretory controls biopsies obtained in outpatient clinics.

2.4.3 Fallopian Tube biopsies

Table 2.8 contains sample details of fallopian tubes biopsies obtained at the time of hysterectomy from women exposed to UPA for up to 12 weeks, previously described in section **2.4.1**. Table 2.9 contains samples of details of fallopian tubes from proliferative and secretory menstrual cycle phase. Additional participant information was available from subjects who had co-consented to the reproductive tract tissue resource; RECs: 10/S1402/59 (B); 07/S1103/29 (D); 05/S1103/14 (F).

All specimens (UPA exposed and controls) had an H&E stained tissue section reviewed by a pathologist. All biopsies had wholly benign features.

2.4.4 Cervical biopsies

Table 2.10 contains sample details of cervical biopsies obtained at the time of hysterectomy from women exposed to UPA for up to 12 weeks, previously described in section **2.4.1**. Table 2.11 contains samples of details of control cervical biopsies from proliferative and secretory menstrual cycle phases.

All specimens (UPA exposed and controls) had an H&E stained tissue section reviewed by a pathologist. All had wholly benign features.

Table 2.3 REC approvals for tissue collection

REC	Study Name	Code
16/ES/0007	Female Reproductive Tissue Resource	A
10/S1402/59	Female Reproductive Tissue Resource	B
12/SS/0238	Mechanism of Action of PRMs (Progesterone Receptor Modulators)	C
07/S1103/29	Mechanisms Involved in Endometrial Repair	D
14/LO/1602	Ulipristal acetate versus conventional management of heavy menstrual bleeding (HMB; including uterine fibroids): a randomised controlled trial and exploration of mechanism of action: 'UCON'	E
05/S1103/14	Local Cortisol Regulation in the Ovary and Uterus	F
05/S1103/32	Regulators of Vascular Function in the Female Reproductive Tract	G
2001/6/5	Local mediators in menstruation	H
1994/6/17	The Role of Steroid Hormones in Benign Gynaecological Conditions	I
04/S1103/20	Expression profiling of trophoblast from women with intra- and extra-uterine pregnancies to reveal candidate genes as markers for ectopic pregnancy	J
10/S1102/40	Improving women's health and pregnancy outcome: understanding the aetiology of ectopic pregnancy	K

Table 2.4 Sample characteristics of "full thickness" endometrial biopsies from women administered UPA

Pt No	REC	Date of collection	S No	SC No	Age	BMI	Parity	HMB	Fib	Endo	Duration of Rx	Days off Rx	Bleeding control	E2	P4	Histology	RIN
5746	C	02/05/2013	1600	CP1231E	46	27.5	2+1	Yes	Yes	No	64	2	Amenorrhoea			PAEC	8.7
5747	C	13/05/2013	1609	CP1232E	39	33.1	1+1	Yes	Yes	No	76	0	Amenorrhoea			PAEC	8.7
5748	C	17/05/2013	1605	CP1233E	49	26.5	1+1	Yes	Yes	No	76	2	Amenorrhoea			PAEC	8.7
5749	C	27/05/2013	1608	CP1234E	45	21.3	0+0	Yes	Yes	Yes	81	0	HMB unchanged			PAEC	8.8
5750	C	09/08/2013	1607	CP1235E	48	28.4	3+3	Yes	Yes	No*	63	1	Amenorrhoea			PAEC	9.1
5751	C	09/08/2013	1601	CP1236E	43	32.6	1+1	Yes	Yes	Yes	83	0	Amenorrhoea			PAEC	7.7
5752	C	19/09/2013	1602	CP1237E	47	31.8	1+0	Yes	Yes	Yes	75	1	Lighter with IMB			PAEC	9.2
5753	C	14/10/2013	1603	CP1238E	45	33.7	2+0	Yes	Yes	Yes*	84	0	Amenorrhoea			PAEC	8.7
5754	C	09/12/2013	1604	CP1239E	39	29.1	0+0	Yes	Yes	No	102[1]	0	Amenorrhoea			PAEC	8.6
5779	B	13/10/2014	1660	CT1264E	48	26.1	0+0	Yes	Yes	No	103[1]	1	Amenorrhoea	NS	NS	PAEC	NA
8520	B	29/02/2016	1937	CT1916E2	48	27.2	0+0	Yes	Yes	Yes	72	1	Constant	444	7.1	PAEC	NA
5819	A	18/04/2016	2052	CT1690E	33	29.1	1+4	Yes	Yes	No	87	5	Lighter	549	0.3	P	NA
5780	B	08/12/2014	1661	CT1265E	48	34.9	3+0	Yes	Yes	No	67	0	Lighter	NS	NS	P	NA
5793	B	10/09/2015	1675	CT1278E	48	35.4	2+1	Yes	Yes	Yes	78	2	Lighter with IMB	400	35.7	S	NA
8028	B	12/05/2014	1544	CT1392E	48	36.8	2+0	Yes	Yes	Yes*	63	0	Amenorrhoea	113	0.3	S	NA
7973	C	20/01/2014	1606	CP1337E	42	24.7	2+0	Yes	Yes	No	80	1	Lighter	NS	NS	PAEC	NA
8087	A	17/08/2015	1906	CT1450E	46	28.1	0+1	Yes	Yes	No	94	0	Constant bleeding	473	1	PAEC	NA

UPA: Ulipristal acetate, Pt No: participant number, REC: Research ethics committee (approval), S No: sample number, SC No: Study code number, BMI: Body mass index, HMB: Heavy menstrual bleeding, Fib: Fibroids, Endo: Endometriosis, Rx: treatment, E2: oestradiol, P: progesterone, RIN: RNA integrity number, IMB: intermenstrual bleeding

PAEC: progesterone receptor modulator endometrial associated changes P: Proliferative S: Secretory

*: subject had adenomyosis

[1]: Operation deferred, UPA treatment course extended to day of surgery

Table 2.5a Sample characteristics of "full thickness" endometrial biopsies from proliferative phase of the menstrual cycle

Pt No	REC	Date of collection	S No	SC No	Age	BMI	Parity	HMB	Fib	Endo	LMP	Cycle	E2	P4	Histology	RIN
5053	I	24/07/2001	254	118	35	NS	3+0	Yes	Yes	No	15/07/2001	7/28-31	311	1.4	P	NA
5323	I	03/06/2003	425	154	45	NS	3+0	Yes	No	No	18/05/2003	5-7/28-32	107	0.94	P	NA
5406	I	12/09/2005	547	268	49	21.0	0+0	No	Yes	No	30/08/2005	7/26-28	908.69	6.94	P	NA
5412	G	30/11/2005	602	2	48	NS	2+0	Yes	Yes	No*	17/11/2005	7/26-30	324.83	1.98	P	NA
5492	F	22/05/2006	634	220	43	NS	0+0	Yes	Yes	No	16/05/2006	10/28-32	67	3.72	P	NA
5575	G	18/02/2008	856	CB242E	44	NS	0+0	Yes	Yes	No	10/02/2008	7-8/26-28	474	4.04	P	NA
5578	G	17/03/2008	860	CB245E	43	NS	2+2	Yes	Yes	No	03/03/2008	7/24-26	1410	2.45	P	NA
5582	F	02/06/2008	863	CA248E	44	NS	0+0	Yes	Yes	No	27/05/2008	8-12/25-30	88	1.24	P	NA
5621	F	17/02/2009	883	CA385E	44	NS	2+1	Yes	Yes	No	10/02/2009	5-6/28-32	971	4.49	P	8.7
5670	D	15/11/2010	1133	CH454E	47	34.9	1+0	Yes	Yes	No*	05/11/2010	5/28-30	5.1	1.4	P	7.9
5685	D	24/03/2011	1144	CH469E	44	26.6	4+3	Yes	Yes	No	15/03/2011	7/25-30	497	<3	P	8.4
7115	I	25/09/2003	461	171	44	NS	2+2	Yes	No	No	12/09/2003	5/26-30	921	7.89	P	NA
7195	I	07/09/2004	514	187	40	NS	3+0	Yes	Yes	No	27/08/2004	5/28	667.03	10.86	P	9.4
7593	G	28/08/2009	1025	CB563E	51	19.4	1+0	Yes	Yes	Yes*	16/08/2009	8-9/24-28	1682	5.97	P	NA
7750	D	21/03/2011	1271	CH1028E	40	29.1	3+0	Yes	Yes	No	11/03/2011	10/22-28	762	<3	P	8.9
7782	B	09/08/2011	1297	CT1060E	47	27.7	3+1	Yes	Yes	No*	17/07/2011	5-6/21-28	320	3.6	P	9.5

Pt No: Participant number, REC: Research ethics committee (approval), S No: sample number, SC No: Study code number, BMI: Body mass index,
HMB: Heavy menstrual bleeding, Fib: Fibroids, Endo: Endometriosis, LMP: Last menstrual period, E2: oestradiol, P4: progesterone, RIN: RNA integrity number, NS: Not stated
P: Proliferative
*: sample had adenomyosis

Table 2.5b Sample characteristics of "full thickness" endometrial biopsies from secretory phase of the menstrual cycle

Pt No	REC	Date of collection	S No	SC No	Age	BMI	Parity	HMB	Fib	Endo	LMP	Cycle	E2	P4	Histology	RIN
7820	B	17/11/2011	1328	CT1098E	46	24.6	3+0	Yes	Yes	No	01/11/2011	6-9/28	396	31.4	ES	NA
5005	I	05/04/2001	213	109	33	NS	3+0	Yes	Yes	Yes	15/03/2001	5-8/28	412	29.3	MS	NA
5212	I	13/05/2002	352	138	44	NS	3+0	Yes	Yes	No	02/05/2002	6-7/21-28	8.25	12.62	MS	NA
5690	D	07/03/2011	1149	CH474E	39	30.0	3+1	No	Yes	No*	08/02/2011	2-7/25-30	323	38.6	MS	8.6
7152	I	19/02/2004	487	179	35	NS	2+0	Yes	Yes	No	30/01/2004	3-4/28	722	59.94	MS	NA
7187	H	17/08/2004	509	250	43	NS	1+1	No	Yes	No*	26/07/2004	3-4/24-25	428	50.63	MS	NA
7218	I	22/11/2004	523	194	43	NS	1+0	Yes	No	No	02/11/2004	3-6/28	853	101	MS	NA
7695	D	27/10/2010	1188	CH973E	39	19.9	1+0	Yes	Yes	No	27/09/2010	10-14/21-26	78.6	21.4	MS	8.9
7725	D	07/03/2011	1252	CH1003E	47	28.2	0+0	Yes	Yes	No	14/02/2011	7/28	228	45.7	MS	8.5
7759	D	13/05/2011	1277	CH1037E	50	25.8	1+1	Yes	Yes	No	22/04/2011	7-10/21-24	77.4	21.1	MS	9.2
7764	D	17/05/2011	1280	CH1042E	43	21.1	3+1	Yes	Yes	No*	30/04/2011	7-10/21-28	272	27.2	MS	9.4
7783	B	08/08/2011	1298	CT1061E	45	27.5	2+0	Yes	Yes	Yes*	21/07/2011	5-7/28	530	28	MS	9.0
7853	B	16/02/2012	1412	CT1131E	52	27.4	2+1	Yes	Yes	Yes*	30/01/2012	5-7/21-28	359	22.4	MS	9.3
7839	B	26/01/2012	1348	CT1117E	42	22.1	1+0	Yes	Yes	No	03/01/2012	6/22	396	35.9	MS	8.9
7760	D	16/05/2011	1278	CH1038E	37	25.3	2+1	Yes	Yes	No*	20/04/2011	11-19/23-30	262	14	LS	NA
5743	B	03/09/2012	1390	CT1227E	47	25.3	1+2	Yes	Yes	No	04/08/2012	10-12/28	132	6.4	LS	9.4
8508	B	14/09/2015	1676	CT1905E2	46	28.9	3+1	Yes	Yes	No*	NS	3-7/28-31	259	17.2	LS	9.5

Pt No: Participant number, REC: Research ethics committee (approval), S No: sample number, SC No: Study code number, BMI: Body mass index,
HMB: Heavy menstrual bleeding, Fib: Fibroids, Endo: Endometriosis, LMP: Last menstrual period, E2: oestradiol, P4: progesterone, RIN: RNA integrity number,
NS: Not stated
ES: Early secretory MS: Mid secretory S: Late
*: sample had adenomyosis

Table 2.6 Sample characteristics of endometrial biopsies from women administered UPA

Pt No	REC	Date of collection	S No	Study code No	Age	BMI	Parity	HMB	Fib	Endo	Duration of Rx	Days off Rx	Bleeding control	E2	P4	Histology	RIN
5777	A	08/03/2016	1938	CT1262E3+	52	29.6	1+2	Yes	Yes	No	81	0	Amenorrhoea	55	5.2	Inactive with no atypia#	7.6
5785	E	27/04/2016	1958	CU1270E3+	44	34.6	3+0	Yes	No	No	78[1]	0	Amenorrhoea	303	15.7	Secretory (some non-physiological)	9.0
5790	E	22/01/2016	1684	CU1275E+	40	NS	3+0	Yes	No	No	79[1]	0	Unchanged	NS	NS	Mildly disordered proliferative	9.6
5795	A	03/05/2016	1960	CT1280E2+	47	22.9	2+1	Yes	Yes	No	77	8[2]	Amenorrhoea	359	0.2	PAEC	8.4
5805	E	18/10/2016	1812	CU1289E2	48	22.0	2+1	Yes	Yes	No	81[1]	0	Amenorrhoea	1665	0.5	Inactive with no atypia#	8.8
5817	A	21/07/2016	1988	CT1691E2+	48	22.7	2+0	Yes	Yes	No	80	0	Amenorrhoea	1491	1.7	PAEC	9.1
7886	A	19/05/2016	1964	CT1162E3+	46	21.3	0+0	Yes	Yes	No	60	0	Amenorrhoea	319	0.5	Inactive with no atypia#	9.4
8002	A	16/03/2016	1942	CT1366E3+	51	20.9	1+1	Yes	Yes	Yes	66	0	Amenorrhoea	819	21.8	Disordered proliferative#	7.5
8045	A	02/06/2016	2062	CT1409E3+	47	42.7	5+2	Yes	Yes	No	76	0	Amenorrhoea	72	0.2	PAEC	NA
8097	A	29/03/2016	1951	CT1460E2+	41	29.0	0+1	Yes	Yes	No	70	0	Amenorrhoea	149	2.7	Inadequate#	7.5
8100	A	24/03/2016	1949	CT1463E2+	49	46.4	2+0	Yes	Yes	No	82	0	Amenorrhoea	60	3.4	Consistent with UPA#	7.9
8117	A	18/07/2016	1985	CT1480E2	40	32.3	2+0	Yes	Yes	No	77	0	Lighter	317	50.3	PAEC	9.2
8122	A	07/07/2016	1981	CT1485E2+	41	28.0	1+1	Yes	Yes	No	69	0	Amenorrhoea	305	0.2	PAEC	NA
8123	A	05/07/2016	1980	CT1486E2+	41	39.9	3+1	Yes	Yes	Yes	75	0	Amenorrhoea	162	0.2	PAEC	9.2
8124	A	18/07/2016	1986	CT1487E2+	49	30.5	1+1	Yes	Yes	No	81	0	Amenorrhoea	97	0.2	Consistent with UPA#	NA
8126	E	09/11/2016	1867	CU1489E2+	45	30.4	0+1	Yes	Yes	No	81[1]	0	Amenorrhoea	114	<0.2	PAEC	9.2
8130	A	20/07/2016	1987	CT1493E2+	44	33.2	0+0	Yes	Yes	No	70	0	Amenorrhoea	137	4.8	PAEC	NA
8506	E	12/08/2016	1807	CU1903E3+	41	23.5	3+0	Yes	No	No	82[1]	0	Lighter	237	1.6	Proliferative	9.1
8522	A	14/03/2016	1941	CT1929E2+	46	38.6	0+3	Yes	Yes	No	80	0	Lighter	302	3.6	PAEC	8
9046	E	24/08/2016	1993	CU1676E2+	44	30.1	5+0	Yes	No	No	80[1]	0	Amenorrhoea	432	<0.2	Inadequate#	NA
9055	A	02/06/2016	2063	CT1685E2+	47	NS	0+9	Yes	Yes	Yes	79	0	Lighter	135	0.2	PAEC	7.5

Pt No: participant number REC: Research ethics committee (approval) BMI: Body mass index HMB: Heavy menstrual bleeding Fib: Fibroids Endo: Endometriosis Rx: treatment
LMP: Last menstrual period E2: oestradiol P4: progesterone, RIN: RNA integrity number, NS: Not stated PAEC: progesterone receptor modulator endometrial associated changes
+: sample has a paired control sample *: sample had adenomyosis
#: Minimal tissue in biopsy or fragmented sample. Sufficient tissue may be available to exclude malignancy but may be insufficient to assess for features of PAEC or to unequivocally state PAEC as diagnosis
[1]: sample from UCON subject – pipelles taken in final week of second 12 week cycle of treatment
[2]: sample taken 8 days after stopping UPA. Patient remained amenorrhoeic at the time of biopsy

Table 2.7 Sample characteristics of endometrial biopsies from proliferative and secretory phase of the menstrual cycle

Pt No	REC	Date of collection	Sample No	Study code No	Age	BMI	Parity	HMB	Fib	Endo	LMP	Cycle	E2	P4	Histology	RIN
5706	B	02/06/2011	1354	CT490E	46	24.0	0+0	Yes	Yes	No	24/05/2011	7/26-28	714	<3	P	7.7
5777	B	23/11/2015	1678	CT1262E2^{+}	52	29.6	1+2	Yes	Yes	No	05/11/2015	7/24-29	145	0.4	P	8.6
5785	B	28/07/2015	1673	CT1270E2^{+}	44	34.6	3+0	Yes	No	No	06/07/2015	5-6/26-27	331	3.6	P	9.6
5790	B	12/05/2015	1671	CT1275E^{+}	39	26.8	3+0	Yes	Yes	No	29/04/2015	5-16/28-31	477	21.7	P	9.1
5795	B	07/01/2016	1679	CT1280E^{+}	46	22.9	2+1	Yes	Yes	No	14/12/2015	8/21-25	522	4.7	P	8.1
7694	D	26/10/2010	1187	CH972E	51	25.3	0+0	Yes	Yes	No	14/10/2010	4/28	12.5	3.4	P	9.4
7718	D	16/12/2010	994	CH996E	42	20.9	2+0	Yes	Yes	No	09/12/2010	5-6/28-32	672	<3	P	9.0
7720	D	13/01/2011	996	CH998E	49	19.9	2+0	Yes	Yes	No	05/01/2011	5/28	142	<3	P	8.3
7811	B	06/10/2011	1318	CT1089E	38	28.7	2+1	Yes	Yes	No	20/09/2011	7-10/28	171	5.7	P	8.5
7835	B	02/02/2012	1343	CT1113E	44	23.2	2+0	Yes	Yes	No	21/01/2012	5-6/28	1272	<3	P	9.3
7886	B	25/02/2016	1935	CT1162E2^{+}	46	21.3	0+0	Yes	Yes	No	18/02/2016	6-14/28-46	104	5.1	P	8.2
8097	B	29/10/2015	1916	CT1460E^{+}	40	28.9	0+1	Yes	Yes	No	20/10/2015	3-8/21-28	224	2.5	P	7.7
8100	B	26/11/2015	1920	CT1463E^{+}	48	46.4	2+0	Yes	Yes	No	NS	10/14-21	229	3.1	P	8.3
8131	A	23/06/2016	1976	CT1494E	47	25.6	2+0	Yes	Yes	No	15/06/2016	7/14	1376	0.8	P	9.5
8506	B	24/11/2015	1917	CT1903E2^{+}	41	23.8	3+1	Yes	No	No	13/11/2015	5/28-29	430	1.3	P	10.0
8522	B	14/12/2015	1724	CT1929E^{+}	46	38.6	0+3	Yes	Yes	No	25/11/2015	4-8/35-43	312	8.5	P	8.3
9046	B	17/09/2015	2027	CT1676E^{+}	43	31.4	5+0	Yes	No	No	09/09/2015	7-14/21	213	0	P	NA
9055	B	03/12/2015	2036	CT1685E^{+}	47	25.9	1+1	Yes	Yes	Yes	18/11/2015	7-10/21	207	4.5	P	10.0
8085	A	23/7/2015	1904	CT1448E	46	32.7	1+0	Yes	No	No	13/07/2015	5-7/26-30	199	1.8	P	9.2
5817	A	13/04/2016	2053	CT1691E^{+}	48	22.3	2+0	Yes	Yes	No	NS	NS	145	0.4	DP	NA
8002	B	14/12/2015	1723	CT1366E2^{+}	51	20.9	1+1	Yes	Yes	Yes	05/11/2015	10/21-28	731	27.2	DP	NA
8122	A	21/04/2016	1953	CT1485E^{+}	41	28.0	1+1	Yes	Yes	No	07/04/2016	5/21	444	62.9	ES	NA
7840	B	19/01/2012	1349	CT1118E	49	25.9	2+0	Yes	Yes	No	28/12/2011	5-7/14-28	418	14.8	MS	9.5
8045	A	10/03/2016	2050	CT1409E2^{+}	46	42.7	5+2	Yes	Yes	No	25/02/2016	5-7/21-28	361	28.8	MS	NA
8124	A	21/04/2016	1955	CT1487E^{+}	49	30.5	1+1	Yes	Yes	No	04/04/2016	3-5/28	129	7.4	LS	NA
8130	A	05/05/2016	1963	CT1493E^{+}	44	33.1	0+0	Yes	Yes	No	NS	8-9/28	170	4.6	LS	NA
8123	A	21/04/2016	1954	CT1486E^{+}	41	39.1	3+1	Yes	Yes	Yes	17/04/2016	7/42-29	135	0.2	M	NA

Pt No: Participant number REC: Research ethics committee (approval) BMI: Body mass index HMB: Heavy menstrual bleeding Fib: Fibroids Endo: Endometriosis LMP: Last menstrual period E2: oestradiol P4: progesterone, RIN: RNA integrity number, NS: Not stated P: Proliferative DP: Disordered proliferative ES: Early secretory MS: Mid secretory LS: Late secretory M menstrual^{+}: sample has a paired UPA treated sample *: sample had adenomyosis

Table 2.8 Sample characteristics of fallopian tube biopsies from women administered UPA

Pt No	REC	Date of collection	Sample No	Study code No	Age	BMI	HMB	Fib	Endo	Duration UPA	E2	P4	Endometrial Histology	Staging	Use
5746	C	02/05/2013	118	CP1231FR	46	27.5	Yes	Yes	No	64	NO	NO	PAEC	N/A	PCR/IHC
5747	C	13/05/2013	119	CP1232FR	39	33.1	Yes	Yes	No	76	NO	NO	PAEC	N/A	PCR/IHC
5748	C	17/05/2013	116	CP1233FL	49	26.5	Yes	Yes	No	76	NO	NO	PAEC	N/A	PCR/IHC
5750	C	09/08/2013	112	CP1235FR	48	28.4	Yes	Yes	No*	63	NO	NO	PAEC	N/A	PCR/IHC
5751	C	09/08/2013	113	CP1236FL	43	32.6	Yes	Yes	Yes	83	NO	NO	PAEC	N/A	PCR/IHC
5754	C	09/12/2013	123	CP1239FL	39	29.1	Yes	Yes	No	102[1]	NO	NO	PAEC	N/A	PCR/IHC

UPA: Ulipristal acetate Pt No: participant No REC: Research ethics committee (approval) BMI: Body mass index HMB: Heavy menstrual bleeding Fib: Fibroids Endo: Endometriosis E2: oestradiol P4: progesterone PAEC: progesterone receptor modulator endometrial associated changes.
*: subject had adenomyosis [1]: Operation deferred, UPA treatment course extended to day of surgery
All Fallopian tubes had benign appearance under routine H&E clinical pathology review

Table 2.9 Sample characteristics of fallopian tube biopsies from proliferative and secretory phase of the menstrual cycle

Pt No	REC	Date of collection	Sample No	Study code No	Age	BMI	HMB	Fib	Endo	LMP	Cycle	E2	P4	Endometrial Histology	Use
7482	J	29/04/2008	68	276	42	NS	Yes	Yes	No	20/4/08	7-10/21-24	503	5	P	PCR/IHC
5621	J, F	17/02/2009	85	385	44	NS	Yes	Yes	No	10/2/09	5-6/2-32	971	4	P	IHC
7568	J, F	29/05/2009	75	538	44	NS	Yes	Yes	No	15/5/09	3/28	513	4	P	PCR/IHC
7680	J, F	31/08/2010	162	748	36	35	Yes	No	No	24/8/10	7/28	248	<3	P	PCR/IHC
3137	K	03/05/2011	314	875	NS	NS	NS	NS	NS	29/4/11	10/14-28	160	<3	P	PCR/IHC
3161	K, B	19/07/2011	325	892	46	37	Yes	No	No*	13/7/11	5-10/21-28	335	<3	P	IHC
3171	K	22/09/2011	338	2009	NS	NS	NS	NS	NS	12/9/11	12/14-21	311	<3	P	PCR
5734	K, B	13/02/2012	345	1218	41	32	Yes	No	No	2/2/12	5/21	400	<3	P	PCR
3149	K	17/05/2011	317	878	NS	NS	NS	NS	NS	29/4/11	7-10/21-28	222	24	E/MS	PCR
7498	J, D	15/07/2008	70	292	41	NS	Yes	Yes	No	23/6/08	5/21-23	532	34	MS	IHC
6316	J	16/01/2009	100	611	43	NS	Yes	Yes	Yes*	24/12/08	7/14-21	357	18	MS	IHC
7567	J, F	27/05/2009	74	537	43	NS	Yes	Yes	No*	4/5/09	10/22-25	494	49	MS	PCR/IHC
7641	J, D	14/04/2010	158	771	38	34	Yes	Yes	No*	4/4/10	5-7/14-21	691	246	MS	PCR/IHC
7672	J, F	09/08/2010	160	740	47	27	Yes	Yes	No*	22/7/10	5-6/28	410	70	MS	PCR/IHC
7678	J, F	23/08/2010	161	746	48	29	Yes	Yes	No	29/6/10	6-10/28-69	598	<3	MS	PCR/IHC
3123	K, B	28/07/2011	327	894	36	25	No	No	Yes*	7/7/11	4-5/28-31	563	59	MS	PCR

REC: Research ethics committee (approval) BMI: Body mass index HMB: Heavy menstrual bleeding Fib: Fibroids Endo: Endometriosis LMP: Last menstrual period E2: oestradiol P4: progesterone NS: Not stated P: Proliferative ES: Early secretory MS: Mid secretory *: sample had adenomyosis
All Fallopian tubes had benign appearance under routine H&E clinical pathology review

Table 2.10 Sample characteristics of cervical biopsies from women administered UPA

Participant No	REC	Date of collection	Sample No	Study code No	Age	BMI	Parity	HMB	Fib	Endo	Smear History	Duration UPA	E2	P4	Endometrial Histology
5746	C	02/05/2013	9	CP1231C	46	27.5	2+1	Yes	Yes	No	Normal	64	No	No	PAEC
5747	C	13/05/2013	10	CP1232C	39	33.1	1+1	Yes	Yes	No	Normal	76	No	No	PAEC
5748	C	13/05/2013	2	CP1233C	49	26.5	1+1	Yes	Yes	No	Normal	76	No	No	PAEC
5749	C	27/05/2013	8	CP1234C	45	21.3	0+0	Yes	Yes	Yes	Normal	81	No	No	PAEC
5750	C	09/08/2013	1	CP1235C	48	28.4	3+3	Yes	Yes	No*	Normal	63	No	No	PAEC
5751	C	09/08/2013	7	CP1236C	43	32.6	1+1	Yes	Yes	Yes	Normal	83	No	No	PAEC
5753	C	07/10/2013	3	CP1238C	45	33.7	2+0	Yes	Yes	Yes*	Normal	84	No	No	PAEC
7973	C	20/01/2014	4	CP1337C	42	24.7	2+0	Yes	Yes	No	Negative^	80	No	No	PAEC

UPA: Ulipristal acetate, REC: Research ethics committee (approval) BMI: Body mass index HMB: Heavy menstrual bleeding Fib: Fibroids Endo: Endometriosis. E2: oestradiol P4: progesterone, PAEC: progesterone receptor modulator endometrial associated changes.
Negative^: This participant had moderate dyskaryosis on smear in 2005. She underwent LLETZ which revealed CIN2. Subsequent smears were all normal
All cervixes had benign appearance under routine H&E clinical pathology review

Table 2.11 Sample characteristics of cervical biopsies from proliferative and secretory phase of the menstrual cycle

Participant No	REC	Date of collection	Sample No	Study code No	Age	BMI	Parity	HMB	Fib	Endo	Smear History	LMP	Cycle	E2	P4	Endometrial Histology
5053	I	24/07/2001	UB19964/05	118	35	NS	3+0	Yes	No	No	Normal	15/07/2001	7/28-31	311	1.4	P
5406	I	12/09/2005	UB11030/03	268	49	21	0+0	No	Yes	No	Normal	30/08/2005	7/26-28	908.69	6.94	P
5323	I	03/06/2003	UB14651/01	154	45	NS	3+0	Yes	No	No	Normal	18/05/2003	5-7/28-32	107	0.94	P
7115	I	25/09/2003	UB19713/03	171	44	NS	2+2	Yes	No	No	Normal	12/09/2003	5/26-30	921	7.89	P
7152	I	19/02/2004	UB25854/04	179	35	NS	2+0	Yes	Yes	No	Normal	30/01/2004	3-4/28	722	59.94	MS
7187	H	17/08/2004	UB4056/04	250	43	NS	1+1	No	Yes	No	Normal	26/07/2004	3-4/24-25	428	50.63	MS
7218	I	22/11/2004	UB6748/01	194	43	NS	1+0	Yes	No	No	Normal	02/11/2004	3-6/28	852.79	100.95	MS
5212	I	13/05/2002	UB18031/04	138	44	NS	3+0	Yes	Yes	No	Normal	02/05/2002	6-7/21-28	8.25	12.62	MS
5005	I	05/04/2001	UB9523/02	109	33	NS	3+0	Yes	Yes	Yes	Normal	15/03/2001	5-8/28	412	29.3	MS

REC: Research ethics committee (approval) BMI: Body mass index HMB: Heavy menstrual bleeding Fib: Fibroids Endo: Endometriosis LMP: Last menstrual period E2: oestradiol P4: progesterone NS: Not stated P: Proliferative MS Mid secretory. All cervixes had benign appearance under routine H&E clinical pathology review

2.5 RNA extraction and quantitative reverse transcription polymerase chain reaction (RT-qPCR)

Polymerase chain reaction (PCR) is a molecular biology technique to amplify a single or few copies of DNA across several orders of magnitude. Genes of interest in RNA samples can be assessed by reverse transcriptase of the mRNA to create complementary DNA (cDNA).Through repeat heating and cooling (thermal cycling) in the presence of a heat-stable DNA polymerase (typically Taq polymerase), selected specific regions of cDNA are amplified. A reporter dye emits fluorescence during the amplification of the target sequences in real time. This is then detected and quantified.

Amplification of cDNA are determined by specific forward and reverse primers to the sequence of interest and a corresponding probe which anneals between the two primers. When using the Taqman system, (Taq polymerase) it is the displacement of the probe from the cDNA by the primer that results in emission of fluorescence by the reporter dye at the 5' end of the probe.

All RT-qPCR reactions described in this thesis are using the Taqman system.

2.5.1 RNA extraction and cDNA preparation

Total RNA was isolated from endometrial and fallopian samples using Qiagen RNAeasy mini kit as per the manufacturers protocol (Qiagen, Manchester UK) with tissue homogenisation with a TissueLyser (Qiagen, Manchester UK). Concentration was determined using NanoDrop 1000 spectrophotometer V3.7 (Thermo Fisher Scientific, USA) and stored at -80°C.

Endometrial RNA samples for gene microarray had their quality assessed. These was performed using the Agilent RNA 6000 nano kit in conjunction with Agilent 2100 Bioanalyser system with 2100 Expert analysis software (Agilent Technologies, UK). In summary samples of mRNA are loaded into gel matrix in a chip containing a set of interconnected micro channels. These separate nucleic acid fragments based on their size as they are driven through the channels electroporetically. This allows visualisation of the 18S and 28S rRNA (ribosomal RNA) fluorescence peaks. The ratio of 28S to 18S fluorescence peaks allows the calculation of an RNA integrity number (RIN), which if

below 7.5, is indicative of RNA degradation (Figure 2.4). Some additional samples also had RIN previously determined and are indicated in Table 2.4-7.

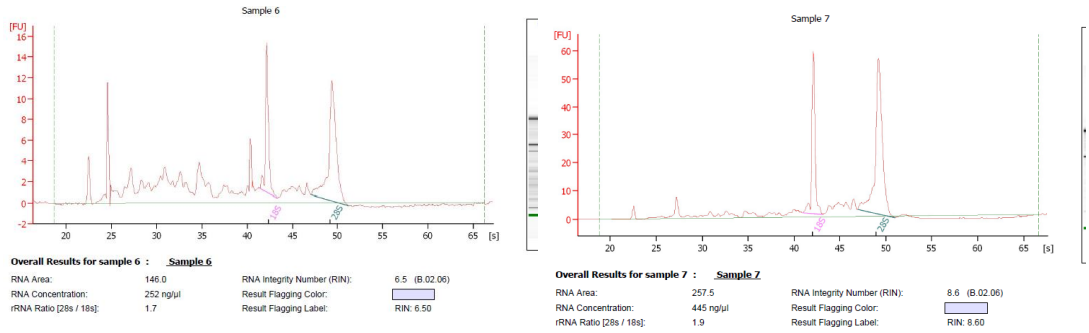

Figure 2.4 Agilent assessment of RNA quality

Sample 6 has a higher degree of RNA degradation whereas sample 7 has less fragmentation. Sample 7 is of better quality to use for subsequent PCR and micro array (RIN 6.5 and 8.6 respectively).

cDNA was prepared according to manufactures protocol using either Superscript Vilo cDNA kit (Invitrogen, Paisley UK) or iScript cDNA Synthesis Kit (Bio-Rad Laboratories, USA). For all cDNA reactions 100ng RNA template was used and 2 control samples prepared omitting either reverse transcriptase or RNA to detect contaminating genomic DNA or contamination of the cDNA preparation mix respectively.

Following mixing of the samples, an incubation programme was run on a Bioer GenePro PCR Cycler (Hangzhou Bioer Ltd., Binjiang, China) for either 20 minutes at 25°C, 60 minutes at 42°C and 5 minutes at 95°C (Superscript Vilo reaction) or 5 minutes at 25°C, 30 minutes at 42°C and 5 minutes at 85°C (iscript reaction). cDNA samples were stored at -20°C until required.

2.5.2. Primers and probes

Gene specific primers were designed using the online Universal Probe Assay (Roche Diagnostics, USA) and synthesised by Eurofins Genomics (Germany) (Table 2.12).

18s and Indian Hedgehog (IHH) primers were bought as pre-validated sets (Applied Biosystems, UK) and used according to the manufacturer's protocol. All other primers were validated before use. This involved setting up a standard curve using cDNA of endometrium at serial dilutions to demonstrate optimal efficiency of the PCR primers

used. In summary RT-qPCR of serial 2-fold dilution of cDNA (1/2 to 1/64) produced from a pooled set of RNA samples. Log[RNA] was plotted against ΔC_q values to determine the slope of the line through the x, y coordinates. All primer/probe sets designed for use in this thesis yielded absolute slope values of <0.1.

Validation of primers was performed on secretory endometrium with the exception of cell cycle genes (*CCNA1, CCNE2, CDC25A, CDK1, CCNB2, CCNA2, CCNB1, E2F2, CDC7, MYC, CHEK2* and *PCNA*) which were validated on proliferative endometrium. Proliferative endometrium was chosen for validation of these these cell cycle primers as expression of mRNAs was low in secretory phase. This prevented meaningful extended dilution of the inputted cDNA and efficacy of the reaction could not be assessed. With the use of proliferative endometrium these primers all validated at an acceptable level of efficiency.

Probes were obtained from the Universal Probe Library (Roche Diagnostics, USA). Choice of probe was determined by primer design by the Universal Probe assay (Roche Diagnostics, USA).

2.5.3 Quantitative reverse transcription polymerase chain reaction (RT-qPCR)

RT-qPCR was performed in triplicate reactions in 384 well plates (STARLAB, Germany). 10µl reactions containing 5µl Express qPCR Supermix (Thermo Fisher Scientific, USA), 0.1ul (200nM) each of the reverse and forward primer and 0.1ul (100nM) of probe (UPL, Roche, UK), 3.7µl nuclease free water and 1µl of cDNA were placed in each well. Secretory endometrium was used as a normalising control.

Additional controls were provided by

- **Blank (No RNA):** The RNA is exchanged for H_2O at the time of making cDNA. This determines if there is contamination in the mix used to make cDNA. As there will be no cDNA made it should give no value in real time PCR.
- **–RT**: Reverse transcriptase omitted at time of cDNA preparation. This is to detect contaminating genomic DNA.
- **H20:** A sample of the water used to formulate the mix for PCR reactions. This is to exclude contamination of the water used to prepare the mix for PCR reactions.

These 3 controls were checked against each gene used.

PCR conditions were 95°C for 2 minutes, plus 40 cycles of 95°C for 15 sec and 60°C for 60 sec using ABI Prism 7900 Fast PCR instrument (Applied Biosystems; Thermo Fisher Scientific, USA).

Data from RT-qPCR experiments were analysed by the $\Delta\Delta C_q$ (quantification cycle) method, as described by Applied Biosystems. Target mRNA-derived cDNA levels are normalised to cDNA loading for each sample using the internal controls described prior (*18S/SHDA* and *ATP5B,* table 2.14), and then related to an internal control. Relevant statistical analyses were performed using GraphPad 7.0 and are described in the corresponding chapters.

PCR results were not further validated by either gel electrophoresis of the PCR product or sequencing of the PCR product.

Table 2.12 Primers and Roche probes used for PCR reactions

Target Gene	Full name	Forward primer	Reverse primer	Roche probe
ATBP5	Human ATP synthase, H+ transporting, mitochondrial F1 complex, beta polypeptide	agaggtcccatcaaaaccaa	tcctgctcaacactcatttcc	50
SDHA	succinate dehydrogenase	tccactacatgacggagcag	ccatcttcagttctgctaaacg	70
18S	18s	Pre validated set	Pre validated set	NA
PR	Human progesterone receptor	tttaagagggcaatggaagg	cggattttatcaacgatgcag	11
PRB	Human progesterone receptor B	aatgggctgtaccgagaggt	tctcagtccctcgctgagtt	45
AR	Homo sapiens androgen receptor	gctgatcataggcctctctc	tgccctgaaagcagtcctct	14
ESR1	Human oestrogen receptor 1	aaccagtgcaccattgataaaa	tcctcttcggtcttttcgtatc	68
FKBP51	Homo sapiens FK506 binding protein 5 (FKBP5)	ggatatacgccaacatgttcaa	ccattgctttattggcctct	15
FKBP52	Homo sapiens FK506 binding protein 4, 59kDa (FKBP4)	cccgggagaagaagctctat	aggaagcctctgccttgg	30
FOXO1	Homo sapiens forkhead box O1	aagggtgacagcaacagctc	ttccttcattctgcacacga	11
HAND2	Homo sapiens heart and neural crest derivatives expressed 2	tcaagaagaccgacgtgaaa	gttgctgctcactgtgcttt	35
BCL6	B-cell CLL/lymphoma 6	tctgcgtcatgcttgtgtta	caacgcggtaatgcagttta	76
KLF-4	Homo sapiens Kruppel-like factor 4 (gut)	gggagaagacactgcgtca	ggaagcactgggggaagt	52
KLF-9	Homo sapiens Kruppel-like factor 9	ctccgaaaagaggcacaagt	cgggagaacttttaaggcagt	76
KLF-15	Homo sapiens Kruppel-like factor 15	caaaagcagccacctcaag	tcagagcgcgagaacctc	64
IGFBP-1	Homo sapiens insulin-like growth factor binding protein 1	aatggattttatcacagcagacag	ggtagacgcaccagcagagt	58
IL-15	Homo sapiens interleukin 15 (IL15), transcript variant 1	cagatagccagcccatacaag	ggctatggcaaggggttt	46
IHH	Human indian hedgehog	Pre validated set		NA
HOXA10	Homo sapiens homeobox A10 (HOXA10), transcript variant 1	ccttccgagagcagcaaa	ttggctgcgttttcacct	61
COUP-TFII	Human nuclear receptor subfamily 2 group F member 2	ccatagtcctgttcacctcaga	aatctcgtcggctggttg	36
BMP2	Human bone morphogenetic protein 2	cggactgcggtctcctaa	ggaagcagcaacgctagaag	49
PRL	Human prolactin	caaaggatcgccatggaa	cacaggagcaggtttgacac	18
GREM2	gremlin 2, DAN family BMP antagonist (GREM2)	cagggaaagcttccagaaca	cagggaaagcttccagaaca	8
MUC1	Human mucin 1, cell surface associated	cctgcctgaatctgttctgc	catgaccagaacccgtaaca	77
FOXM1	Homo sapiens forkhead box M1	actttaagcacattgccaagc	cgtgcagggaaaggttgt	11
CCNA1	Cyclin A1 (CCNA1), transcript variant 1	aaatgggcagtacaggagga	ccacagtcagggagtgcttt	78
CCNE2	Homo sapiens cyclin E2 (CCNE2)	gccattgattcattagagttcca	aaatactgtcccactccaaacc	74
CDC25A	cell division cycle 25A (CDC25A), transcript variant 1,	catggactccaggagggtaa	cactgctatctctttcatttgagg	34
CDK1	Cyclin-dependent kinase 1 (CDK1), transcript variant 1,	tggatctgaagaaatacttggattcta	caatcccctgtaggatttgg	79
CCNB2	Homo sapiens cyclin B2 (CCNB2)	tggaaaagttggctccaaag	tcagaaaaagcttggcagaga	7
CCNA2	Cyclin A2 (CCNA2)	ggtactgaagtccgggaacc	gaagatccttaaggggtgcaa	84
CCNB1	Homo sapiens cyclin B1 (CCNB1)	catggtgcactttcctcctt	aggtaatgttgtagagttggtgtcc	18
E2F2	E2F transcription factor 2 (E2F2),	aggggaagtgcatcagagtg	gcgaagtgtcataccgagtct	23
CDC7	cell division cycle 7 (CDC7), transcript variant 1,	tgctatgcaacagataaagtttgtag	tcctggtgtacctgcccta	62
MYC	Homo sapiens v-myc myelocytoamtosis viral oncogene homolog (avian) (MYC)	tttttcgggtagtggaaaacc	ttcctgttggtgaagctaacg	75
PCNA	Human proliferating cell nuclear antigen	gaggcactcaaggacctcat	agtccatgctctgcaggttt	3

2.6 Candidate antibody Immunohistochemistry

Immunohistochemistry (IHC) refers to the process of selectively imaging antigens (e.g. proteins) in cells of a tissue section by exploiting the principle of antibodies binding specifically to antigens (epitope). Detection can either be direct with a labelled primary antibody to the antigen of interest, or an indirect approach with an unlabeled specific primary antibody to the antigen. Following binding a secondary, labelled antibody is applied. This secondary antibody is typically conjugated either with fluorescent or enzyme reporter to permit visualization.

2.6.1 Sectioning and slide rehydration

Tissue samples were obtained as outlined in section **2.2**. The samples were formalin fixed for 24 hours then paraffin embedded (FFPE) as tissue blocks. Sections of 5µm thickness were cut by microtome (Leica RM2235, Germany), mounted on coated glass slides (1mm; Surgipath, Germany) and dried overnight in an oven at 50°C. Slide de-waxing was performed by immersion in xylene twice for five minutes each time followed by rehydration in alcohol of reducing concentrations (x5 immersions).

2.6.2 Antigen retrieval and primary antibody

Antigen retrieval was performed in a Decloaking Chamber™ Pro (Biocare Medical, USA) by boiling at 125°C for 30 seconds then reducing the temperature to 90°C for 10 seconds in either 0.01 M citrate buffer (pH 6) or 10 mM Tris, 1 mM EDTA and 0.05% Tween-20 buffer (pH9) (Table 2.13). The slides were then cooled and rinsed in water for 5 minutes. Endogenous peroxidase was inactivated by incubation of the slides in a solution of 3% H_2O_2/methanol (Sigma-Aldrich Ltd, Dorset UK; Thermo Fisher Scientific Ltd.) for 30 minutes. The slides were then washed in tris-buffered saline with tween (TBST) twice for 5 minutes.

1:5 normal horse serum (NHS) with 5% bovine serum albumin (BSA) was applied for 30 minutes to block non-specific protein binding. 200Ul of primary antibody was then applied at the optimised concentration in 1:5 NHS with 5%BSA (Table 2.13) and incubated overnight in a humidified chamber at 4°C. Appropriate matched weight/concentration IgG was applied as a negative control and incubated overnight in the same fashion. Control immunoglobulins were from the same species in which the primary monoclonal antibodies were raised or the immunoglobulin fraction of serum

from non-immunised animals in which polyclonal antibodies were raised in place of the primary antibodies (Table 2.14).

2.6.2 Secondary antibody and 3, 3'-Diaminobenzidine (DAB) Immunohistochemistry

The subsequent day the slides were washed with TBST x2 then incubated with the appropriate ImmPRESS Ig reagent (see Table 2.15) for 30 minutes. Following two subsequent TBST washes DAB was applied (diluted 1 drop in 1ml of its supplied buffer; ImmPACT DAB, Vector laboratories, UK). Oxidisation of DAB by peroxidase enzymes yields a brown precipitate, indicating the presence of antibody-antigen complex - 'positive immunoreactivity'. The development of brown staining monitored under a microscope. The reaction was stopped by immersion in tap water.

2.6.3 Dehydration, counterstain and mounting

The slides were then counterstained with Harris haematoxylin, briefly rinsed in 1% acid alcohol (70% ethanol containing 1% concentrated hydrochloric acid) and immersed in Scott's tap water (distilled water with 20 g/L sodium bicarbonate, 3.5 g/L magnesium sulphate) for 25 seconds, followed by dehydration through graded alcohols. Finally they were immersed in xylene for 10 minutes and mounted with glass coverslips using Pertex (Histolab Products AB, Gothenburg, Sweden).

2.6.4 Exceptions to IHC protocol

Three IHC experiments were performed in a different fashion to the methods outlined above:

Immuno-localisation of the progesterone receptor (PR) in the cervix, immuno-localisation of the oestrogen alpha receptor (ERα) in the endometrium and immuno-localisation of the putative progesterone marker B-cell lymphoma (BCL6) in the endometrium.

2.6.4.1 Immuno-localisation of CDC25A in the endometrium and PR in the cervix

Slides were dewaxed, rehydrated, and antigen retrieval and inactivation of endogenous peroxidase performed as above. Prior to protein block an avidin and biotin block (Vector, USA) were performed sequentially for 15 minutes each with TBST washes in between. The protein block then primary antibody was applied as above then incubated overnight.

The following day the slides were washed in TBST and a secondary antibody applied (horse anti mouse with biotin conjugate, Vector BA2000) for 30 minutes. Following TBST wash, an avidin/biotinylated enzyme complex (ABC, Vector USA) was applied for 30 minutes. The slides were then washed further in TBST prior to DAB enzyme for antibody localisation. Slides were counterstained, dehydrated and mounted as outlined in section **2.6.3.**

2.6.4.2 Immuno-localisation of ERα in the endometrium

ERα IHC was performed using an automated IHC staining system (Leica Bond-Max immunostainer, Leica Microsystems, UK). In summary slides were dewaxed and rehydrated then underwent citrate antigen retrieval as described in section **2.6.1/2**. They were then inserted into slide chambers, inserted into the bond and underwent the following sequence of treatments:

1. Bond wash (BW; Tris Buffered Saline (Fischer, USA with added Tween 20)); (10 minutes)
2. Peroxide block* (5 minutes) → BW (10mins)
3. Primary antibody (60 minutes) → BW (10mins)
4. Post primary* (15 minutes) → BW (10mins)
5. Polymer* (15 minutes) → BW (10mins)
6. Deionised water* rinse
7. DAB* (10 minutes) → Deionised water* rinse
8. Haematoxylin (5 minutes) → Deionised water* rinse
9. Dehydrated and mounted by hand as described in 2.6.3

All reagents marked * are from Leica Bond Polymer Refine detection kit. (DS 9800)

2.6.4.3 Immuno-localisation of BCL6 in the endometrium

BCL6 IHC was performed using an automated IHC staining system (Leica Bond III immunostainer, Leica Microsystems, UK). In summary slides were dewaxed and rehydrated as described in **2.6.1** then following insertion into slide chambers, inserted into the Bond instrument. They then underwent antigen retrieval in ER2 (a Leica Bond proprietary antigen retrieval solution pH 9; AR9640, Leica UK) for 20 minutes at 100° C then and underwent the following sequence of treatments:

1. Bond wash (BW; AR9590, Leica UK) (10 minutes)
2. Peroxide block* (5 minutes) → BW (10mins)
3. Primary antibody (15 minutes) → BW (10mins)

4. Post primary* (8 minutes) → BW (6mins)
5. Polymer* (8 minutes) → BW (4mins)
6. Deionised water* rinse
7. DAB* (10 minutes) → Deionised water* rinse
8. Haemtoxylin (5 minutes) → Deionised water* rinse
9. Dehydrated and mounted by hand as described in 2.6.3

All reagents marked * are from Leica Bond Polymer Refine detection kit. (DS 9800)

2.6.5 Image capture and analysis

Slides were viewed with a Provis AX70 (Olympus Optical, UK) and photographs taken with a fitted Canon DS6031 camera (Cannon Amsterdam). In addition the majority of slides were scanned using a slide scanner (Axio scan.Z1; Zeiss, Germany). Scanned images were annotated using Zen Blue software. All slides were reviewed by both LHRW and ARWW.

2.6.5.1 Histoscoring

In certain immunohistochemical reactions, tissues staining was either clearly absent or present and so was not further quantified. In selected others a semi-quantitative histoscoring strategy was employed to determine immunohistochemical staining intensity and localisation.

In 'full thickness' (section **2.2.1.1**) endometrial tissue sections the tissue was divided into the following cellular compartments: surface epithelium (if present), glandular epithelium and stroma. In endometrial tissue sections derived using a pipelles biopsy sampler, tissue was divided in to glandular epithelium and stroma. Fallopian tube and cervical biopsies were not semi quantified.

A histoscore of 0 – 300 was determined by multiplying a staining intensity grade of 0 – 3 (where 0 = no staining, 1 = weak staining, 2 = moderate staining and 3 = strong staining) by an estimation of the percentage of tissue staining positive within each cellular compartment (to the nearest 10%). All histoscoring was performed separately by two individuals, blinded to stage of cycle or treatment allocation and protein of interest. The mean and standard error of mean (SEM) were calculated.

Statistical analysis was performed using Graphpad prism software (Graphpad, USA). Data were subjected to the D'Agostino-Pearson omnibus normality test. Data with a Guassian distribution had a one-way ANOVA applied to determine difference between groups. For non-parametric data Kruskal-Wallis test was used to determine differences between sample groups. If statistical significance was found post-hoc tests were applied (unpaired t-test or and Mann-Whitney test depending on distribution). $p < 0.05$ was considered to be statistically significant.

This semi-quantitative histoscoring strategy is a standard method, and has been used in several previous studies (Aasmundstad, Haugen et al. 1992, Wang, Critchley et al. 1998, Critchley, Osei et al. 2006). Scores obtained with this method have been found comparable to those obtained by a computerised image analysis system, with a strong correlation found between the two methods (Wang *et al.*, 1998).

Table 2.13 Antibodies and antigen retrieval used for immunohistochemistry

Endometrial full thickness biopsy

Protein	Supplier	Reference	Antibody type	Host	Retrieval buffer	ImmPRESS™ kit	Dilution (normal horse serum	Negative control (table 2.14)
PR	Dako	A0098	Polyclonal	Rabbit	Citrate	Rabbit MP-7401	1:200	1
PRB	Cell Signalling	3157S	Monoclonal	Rabbit	Citrate	Rabbit MP-7401	1:800	1
AR	Spring Bioscientific	M4070	Monoclonal	Rabbit	Citrate	Rabbit MP-7401	1:200	1
ERα	Vector	VP-E614	Monoclonal	Mouse	Citrate	N/A: see **2.6.4.2**	1:5000	2
FKBP51	Abcam	ab2901	Polyclonal	Rabbit	TRIS	Rabbit MP-7401	1:1000	1
FKBP52	Proteintech Europe	10655-1-AP	Polyclonal	Rabbit	TRIS	Rabbit MP-7401	1:600	1
FOXO	Cell Signalling	2880	Monoclonal	Rabbit	Citrate	Rabbit MP-7401	1:250	1
HAND-2	Santa Cruz	SC9409	Polyclonal	Goat	Citrate	Goat MP-7405	1:200	4
BCL6	Novacastra	NCL-L-Bcl-6-564	Monoclonal	Mouse	ER2	N/A: see **2.6.4.3**	1:100	2
PTEN	Dako	M3627	Monoclonal	Mouse	Citrate	Mouse MP-7402	1:750	2
CDC25A	Abcam	Ab2357	Monoclonal	Mouse	Citrate	N/A: see **2.6.4.1**	1:100	3
Endometrial biopsy								
PTEN	Dako	M3627	Monoclonal	Mouse	Citrate	Mouse MP-7402	1:400	2
Ki67	Novacastra	NCL-Ki67-MM1	Monoclonal	Mouse	Citrate	Mouse MP-7402	1:500	2
Fallopian tube								
PR	Dako	A0098	Polyclonal	Rabbit	Citrate	Rabbit MP-7401	1:100	1
PRB	Cell Signalling	3157S	Monoclonal	Rabbit	Citrate	Rabbit MP-7401	1:800	1
AR	Spring Bioscientific	M4070	Monoclonal	Rabbit	Citrate	Rabbit MP-7401	1:500	1
ERα	Vector	VP-E614	Monoclonal	Mouse	Citrate	Mouse MP-7402	1:150	2
Ki67	Novacastra	NCL-Ki67-MM1	Monoclonal	Mouse	Citrate	Mouse MP-7402	1:500	2
Cervix								
PR	Novacastra	NCL-PCR-312	Monoclonal	Mouse	Citrate	N/A: see **2.6.4.1**	1:800	2
PRB	Cell Signalling	3157S	Monoclonal	Rabbit	Citrate	Rabbit MP-7401	1:400	1
AR	Abcam	ab74272	Polyclonal	Rabbit	Citrate	Rabbit MP-7401	1:200	1
ERα	Vector	VP-E614	Monoclonal	Mouse	Citrate	Mouse MP-7402	1:100	2

Table 2.14 Control Antibodies used for immunohistochemistry

Protein	Supplier	Reference	Antibody type	Concentration	Ref No (table 2.13)
Rabbit Ig fraction	Dako	X0903	Polyclonal	20g/L	1
Mouse IgG1	Sigma-Aldrich	M7894	Monoclonal	5mg/ml	2
Mouse IgG2	Sigma-Aldrich	M5409	Monoclonal	200ug/ml	3
Goat IgG	Santa Cruz	SC-2080	Polyclonal	500ug/ml	4

Chapter 3.

The impact of selective progesterone receptor modulator (SPRM), ulipristal acetate (UPA), administration on morphology and sex-steroid receptor expression in the human female reproductive tract

3.1 Background

The composite parts of the female reproductive tract have common embryological derivatives yet have highly specialised individual function depending on the region. All elements express sex-steroids receptors which regulate their activity.

3.1.1 Embryological development of the reproductive tract

In vertebrates the urogenital system, consisting of the kidneys, gonads, urinary and reproductive tracts, develop from the mesoderm. The reproductive tracts develop from the mesonephric (Wolffian) and paramesonephric (Müllerian) ducts. The female phenotype is the default developmental outcome of the reproductive tract. Only in the presence of testicular influences (*SRY*, anti-Müllerian hormone (AMH), testosterone and insulin-like 3) does a male phenotype develop with differentiation of the mesonephric duct. In the absence of these factors the mesonephric ducts regress to leave vestigial structures only, namely the ovarian appendix and Gartner's duct. The Müllerian ducts develop into the female reproductive tract. This comprises of the urogenital sinus, sexual duct (upper vagina, cervix, uterine corpus and fallopian tubes) and the ovaries. External genitalia derive from the genital tubercle, fold and swellings (Table 3.1).

The female sexual duct arises from the paramesonephric ducts (Figure 3.1). These appear between days 44-48 of gestation and develop as longitudinal invaginations of the coelomic mesothelium along the mesonephric ridge lateral to the mesonephric ducts. Under the influence on *Wnt4* (produced by the mesonephros) these invaginations extend towards the mesonephric ducts (Kobayashi, Shawlot et al. 2004) and once associated, the tips form a proliferative centre (Figure 3.1A). Under the influence of *Wnt9*, this primitive uterovaginal canal migrates caudally towards the urogenital sinus. On contact with the terminal end of the uterovaginal canal it forms Müller's tubercle. Posterior to this the urogenital sinus thickens to form the vaginal epithelial plate. This cannulates cranially from the caudal end to produce the lumen of the vagina (Figure 3.1B) (Carlson 2008).

Once the paramesonephric ducts contact the urogenital sinus they fuse to develop a true lumen, which cranially opens into the coelomic cavity. Fusion progresses cranially up to the future uterine tubes which themselves remain un-fused and sequentially become the

A

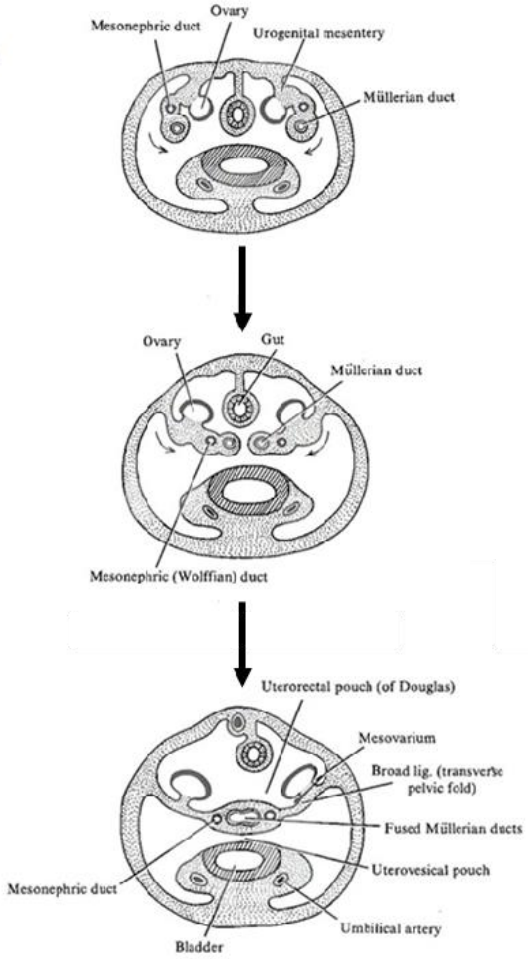
Mesonephric duct
Ovary
Urogenital mesentery
Müllerian duct
Ovary
Gut
Müllerian duct
Mesonephric (Wolffian) duct
Uterorectal pouch (of Douglas)
Mesovarium
Broad lig. (transverse pelvic fold)
Fused Müllerian ducts
Uterovesical pouch
Mesonephric duct
Umbilical artery
Bladder

B

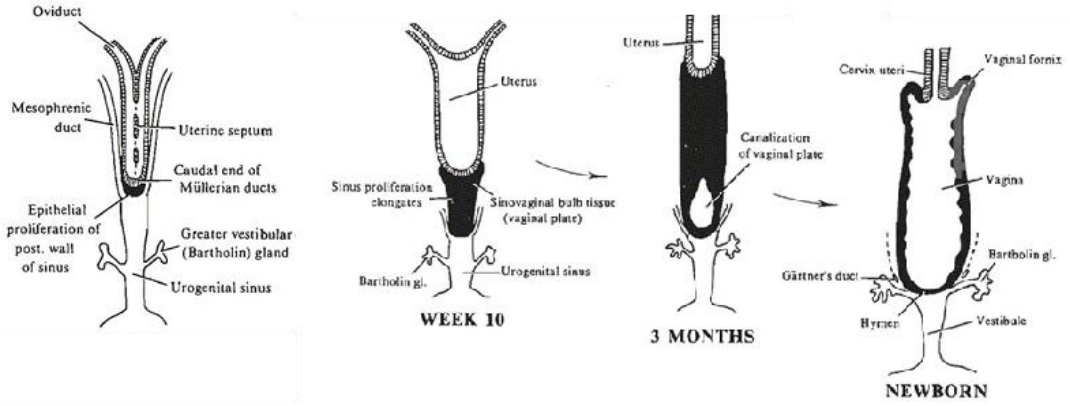
Oviduct
Mesophrenic duct
Uterine septum
Caudal end of Müllerian ducts
Epithelial proliferation of post. wall of sinus
Greater vestibular (Bartholin) gland
Urogenital sinus
Uterus
Sinus proliferation elongates
Sinovaginal bulb tissue (vaginal plate)
Bartholin gl.
Urogenital sinus
WEEK 10
Uterus
Canalization of vaginal plate
3 MONTHS
Cervix uteri
Vaginal fornix
Vagina
Bartholin gl.
Gärtner's duct
Hymen
Vestibule
NEWBORN

C

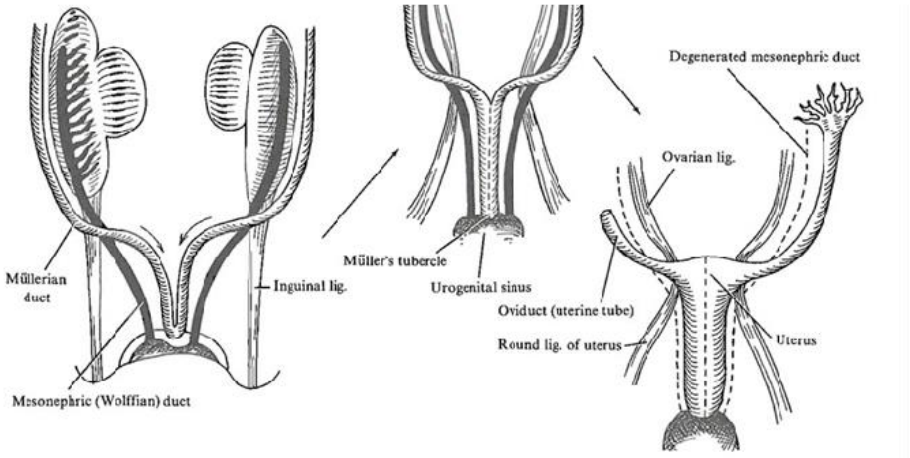
Müllerian duct
Inguinal lig.
Mesonephric (Wolffian) duct
Müller's tubercle
Urogenital sinus
Degenerated mesonephric duct
Ovarian lig.
Oviduct (uterine tube)
Round lig. of uterus
Uterus

Figure 3.1 Embryological development of the female reproductive tract

A Migration of the mesonephric and Müllerian duct with subsequent fusion in the midline. **B** Caudal protrusion of the fused Müllerian ducts towards the urogenital sinus with development of the sinovaginal plate at the distal end of the Müllerian duct. Subsequent canulisation of the vaginal plate to form the vagina. **C** Fusion of the Müllerian duct to form the uterus with sparing of the uterine tubes (subsequent fallopian tube).

Adapted from Pansky B (1982). Differentiation of The Female Genital Tracts: Uterus, Vagina, Auxiliary Glands, Mesenteries. In: Review of Medical Embryology Prentice Hall (Macmillan USA)

Table 3.1. Embryological origins of the female reproductive tract

Indifferent structure	**Female derivative**
Genital ridge	Ovary
Primordial germ cells	Ova
Sex cords	Follicular (granulosa cells)
Mesonephric tubules	Oöphoron, paroöphoron
Mesonephric (Wolffian) ducts	Appendix of the ovary, Gartner's duct
Paramesonephric (Müllerian) ducts	Uterine tube
	Uterus
	Upper vagina
Definitive urogenital sinus (lower part)	Lower vagina
	Vaginal vestibule
Genital tubercle	Clitoris
Genital folds	Labia minora
Genital swellings	Labia majora

fallopian tubes. The lower fused caudal element forms the single median uterovaginal primordium which gives rise to the epithelium and glands of the uterus. The adjacent mesenchyme is the progenitor of the endometrial stroma and myometrium (Figure 3.1C).

Correct differentiation of the Müllerian duct is dependent on a complex system of *Hox* and *Wnt* genes. A series of homeobox (*Hox*) genes are present in the epithelium of the human reproductive tract and are critical for the segmental patterning that develops in the reproductive tract. Hoxa9 is expressed at high levels in the uterine ducts that subsequently develop in the fallopian tubes. Hoxa10 is expressed in the developing uterus and Hoxa11 in the primordia of the lower uterine segment and cervix. Hoxa13 is expressed in the ecto-cervix and upper vagina (Figure 3.2) (Du and Taylor 2004). Hoxa10 in particular plays a role in the determination of correct tissue boundaries (Mullen and Behringer 2014). The actions of *Wnt4* and *Wnt9* have been described above, differentiation is further modified by *Wnt7a* which is critical for uterine and fallopian tube development and expressed throughout the Müllerian duct. Expression continues after birth in the uterus and fallopian tube and appears necessary for the maintenance of expression of Hoxa10 and Hoxa11 (Mullen and Behringer 2014).

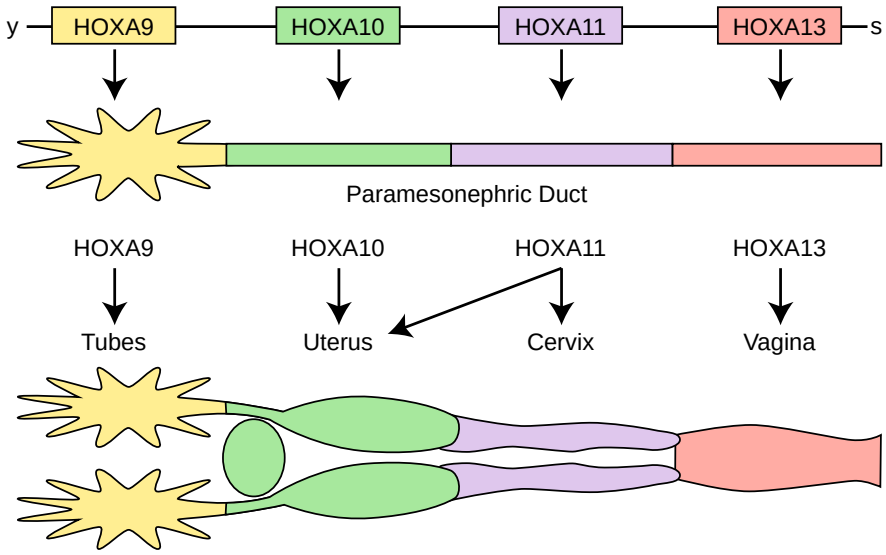

Figure 3.2 Homeobox (Hoxa) gene expression in the female reproductive tract

There is differentiation of *HOX* genes in the reproductive tract. These have a critical role in the regional differentiation of the developing reproductive tract and *Hoxa10* and *Hoxa11* expression persist in adult life.

Adapted from and redrawn: Du, H. and H. S. Taylor (2004). Molecular regulation of mullerian development by Hox genes. Ann N Y Acad Sci **1034**: 152-165.

3.1.2 Normal histology of the human female reproductive tract

3.1.2.1 Endometrium

The endometrium is derived *in utero* from the median uterovaginal primordium (epithelium and glands) and the adjacent mesenchyme (endometrial stroma) as described in section **3.1.1**. Following maturation of the HPO axis and the onset of puberty, the cyclical changes reflective of the menstrual cycle establish. The effects of the menstrual cycle upon the morphology of the endometrium have already been described in chapter 1 (section **1.2.3**) but are briefly summarised below:

Proliferative phase

Following menstruation the exposed basal layer of the endometrium proliferates rapidly under the influence of systemic rising oestradiol (E2) concentrations. Concurrently the glandular cells within the endometrium expand: in the early proliferative phase the glandular cells are initially cuboidal and the glands themselves are small. By the late proliferative phase the glands are tortuous and the individual epithelial cells appear columnar. There is brisk proliferation and mitotic figures are observed in both epithelial and stroma. The stroma is compact throughout the proliferative phase and angiogenesis commences with elongation of the spiral arteries (Noyes, Hertig et al. 1950, Mutter and Ferenczy 2001).

Secretory phase

The morphological changes associated with progesterone (P4) exposure develop between ovulation and approximately 48 hours after P-withdrawal (due to demise of the corpus luteum). Following ovulation, proliferation is inhibited by P4 secretion from the corpus luteum. Glandular nuclei move to the centre of cells and mitosis is supressed. The endometrial glands become more tortuous and acquire increased secretion of glycoproteins, evident as sub-nuclear vacuolation (feature of the early secretory phase). These vacuoles are then discharged into the lumen of glands in the mid secretory phase. The endometrial spiral arterioles undergo remodelling to become increasingly coiled (Noyes, Hertig et al. 1950, Mutter and Ferenczy 2001, Girling and Rogers 2009).

Menstrual phase

In the absence of pregnancy the corpus luteum regresses, resulting in a rapid decrease in circulating P4 and E2. It is P-withdrawal that initiates menstruation. Localised inflammation within the endometrium occurs, characterised by infiltration of leucocytes, cytokine release with resultant oedema, activation of matrix metalloproteinases (MMPs)

and lysis of the extracellular matrix. This culminates in the shedding of the upper two-thirds of the endometrium (the functional layer). The lower third of the endometrium (basal layer) remains in situ but has an exposed, raw mucosal surface that requires efficient repair (Maybin and Critchley 2015).

3.1.2.2 Fallopian tube

The fallopian tubes (FT) develop bilaterally from the uterine tube *in utero* as described in section **3.1.1**. Macroscopically the FT connect the posterior superior fundus of the uterine cavity with the peritoneal cavity, adjacent to their corresponding ipsilateral ovary. The FT are typically 8-12cm long and 0.5-1.2cm in diameter. They have an over-lying double layer of peritoneum; the mesosalpinx which connects to the broad ligament and are also connected to the uterine cornua by the utero-ovarian ligament. They have 4 distinct segments, the interstitium (lying within the myometrium), the isthmus, the ampulla and the infundibulum with protruding fimbriae (Figure 3.3A).

Microscopically the lumen of the tube is lined with a mucosal layer consisting of a single layer cells comprising of both ciliated columnar cells and non-ciliated secretory cells, with overlying stroma. Ciliated cells are most abundant in the infundibulum and the ampulla. The secretory cells produce the tubal fluid essential for the nutrition of the fertilised ovum as it proceeds towards the uterine cavity. There is marked folding of the mucosa, 'plica', which is most evident within the ampulla, which merges into the fimbriae. Overlying the stroma is a muscular layer, consisting of 3 layers of smooth muscle. The outermost layer is the serosa, formed from the visceral peritoneum (Figure 3.3B).

Recognition of a distinct oviductal cycle in women was first described in 1928 (Novak and Everett 1928). Under the influence of oestrogen in the proliferative phase of the menstrual cycle, both the number of ciliated cells and the activity of the cilia are increased. Furthermore the secretory cells increase their height and secretory activity, peaking at ovulation, with egress of height following discharge of their contents into the lumen of the tube (Pauerstein and Eddy 1979). Increased circulating P4 is associated with atrophy and deciliation (Donnez, Casanas-Roux et al. 1985).

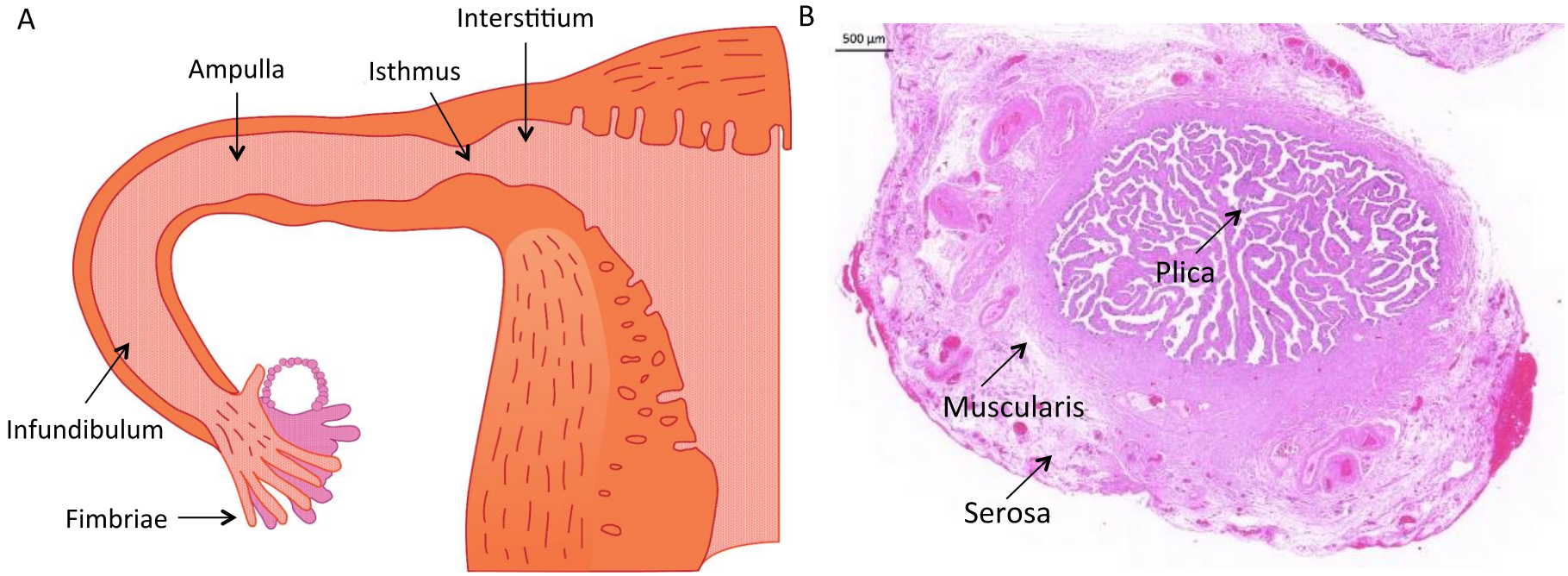

Figure 3.3 Anatomy of the human fallopian tube

A Regions of the fallopian tube
B Low power representative H&E image of ampullary region of the fallopian tube

3.1.3.3 Cervix

The cervix develops from the caudal end of the fused Müllerian ducts (as described in section **3.1.2)** and represents the inferior aspect of the uterus. It is continuous at its superior margin with the uterine corpus, and at its inferior margins with the vaginal epithelium. The cervix itself also protrudes slightly into the vaginal lumen. In adult life it measures approximately 2.5cm in diameter and 3cm in length. It is a fibro-muscular organ, lined with a mucous membrane and has 3 distinct regions – the ectocervix, the endocervix and the dividing squamo-columnar junction (SCJ) the latter of which has an adjacent region of squamous metaplasia, referred to as the transformational zone (Figure 3.4A). The epithelial surfaces overlie a predominantly fibrous stroma with some smooth muscle fibres. Through the centre of the cervix is a lumen connecting the vagina to the uterus: the endocervical canal, the vaginal opening termed the external os and opening into the uterine cavity the internal os. Though the cervix comprises of different epithelial types, they all arise from the Müllerian ducts (Reich and Fritsch 2014).

The ectocervix is the region protruding into the vagina and covered with non-keratinised stratified squamous epithelium (Figure 3.4A & B). Cells are stratified and have 3 layers; superficial, intermediate and parabasal/basal (Figure 3.4B). The latter is the most active with occasional mitotic activity seen, and all layers have altered levels of glycogen depending on the availability of oestrogen.

The endocervix is the tissue adjacent to the endocervical canal and is lined with simple glandular epithelium with branching crypts into the underlying stroma (Figure 3.4A & C). These cells are mucous producing and are tall and cylindrical. Occasional ciliated cells are seen, typically close to the internal os. The nucleus is typically adjacent to the basement membrane but can be displaced during active mucous secretion and pushed towards the centre of the cell. In the absences of inflammation or pre-malignancy/malignancy mitosis is rare. The SCJ between the ecto- and endocervix is an abrupt transition (Figure 3.4D) but laterally evidence of squamous metaplasia can usually be demonstrated with immature squamous epithelium overlying endocervical crypts. The location of the SCJ varies during the phase of a woman's reproductive life and can be altered by exogenous hormonal treatment. Squamous metaplasia is maximal under high oestrogenic stimulus, such as early pregnancy and when using the COCP. At menopause the SCJ recedes into the endocervical canal.

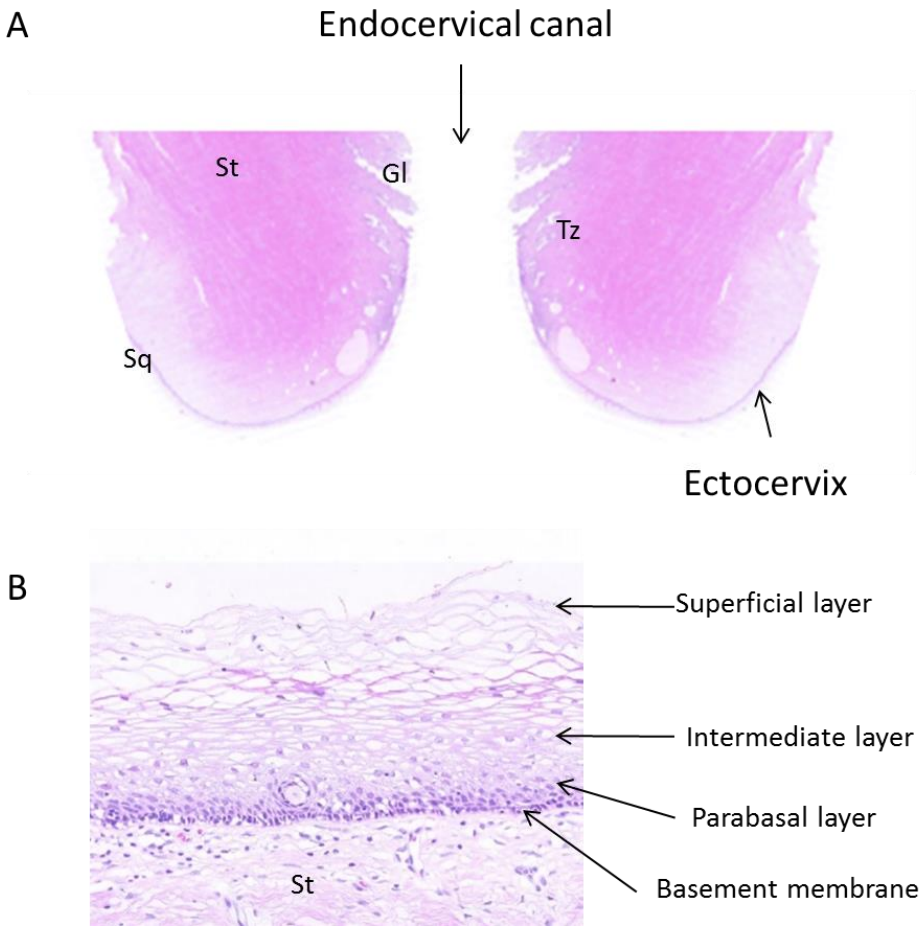

Figure 3.4 Anatomy and histology of the human cervix

A Low power microscopic images demonstrating ectocervical squamous epithelium (Sq), endocervical glandular epithelium (Gl) and the underlying stroma (St). The transformation zone (Tz) separates the true glandular and squamous epithelium which meet at the squamo-columnar junction.
B Squamous epithelium **C** Glandular epithelium **D** Transformation zone

3.1.3 Sex-steroid receptor expression in the human reproductive tract

Steroid hormones are synthesised from cholesterol, derived from circulating low-density lipoprotein (LDL) or intracellular cholesterol esters (Figure 3.5). They all have the same basic ring structure comprising of 17 carbon atoms with different numbers of carbon side-chains. Glucocorticoids, aldosterone and progesterone (P4) all have 21 carbon atoms, testosterone and other androgens have 19 and oestrogens have 18. They circulate either in free form, or protein bound, typically to sex hormone binding globulin (SHBG), cortisol binding globulin (CBG) and albumin.

The predominant forms of oestrogen are oestrone (E1), oestradiol (E2) and oestriol (E3). The predominant forms of androgens are testosterone, androstenedione and dihydroepiandrostenedione (DHEA). In the female human the ovary is the predominant source of circulating oestrogen and progesterone, though there is some peripheral conversion of oestrogen from circulating androgens in adipose and breast tissue, the liver and adrenals. Androgens are synthesised in the adrenals and ovary, and are also peripherally converted from the less potent androgens, androstenedione and DHEA.

The sex-steroids receptors act as ligand-activated transcription factors. The sex-steroid receptors comprise of the progesterone receptor (PR), the oestrogen receptor (ER) and the androgen receptor (AR). PR has two isoforms (PRA and PRB) (Wang, Critchley et al. 1998) and ER has an alpha and beta sub types (ERα and ERβ) (Kuiper, Enmark et al. 1996).

These receptors all have a similar structure: a DNA-binding domain that contains 2 zinc finger motifs, a hinge domain and a domain responsible for ligand binding (Figure 3.6). Ligand selectivity is determined by sequence differences within the ligand-binding domains. Following ligand binding the receptors undergo a conformational change. ER is situated in the nucleus but PR and AR are located in the cytoplasm in their unbound forms, complexed with a heat shock protein (HSP). Following ligand binding they undergo a conformational change that causes HSP to dissociate, revealing a nuclear translocation signal that initiates translocation of the hormone-receptor complex to the nucleus.

Once in the nucleus they typically form either homodimers or heterodimers with the hormone response element, typically based in the promoter region of target genes.

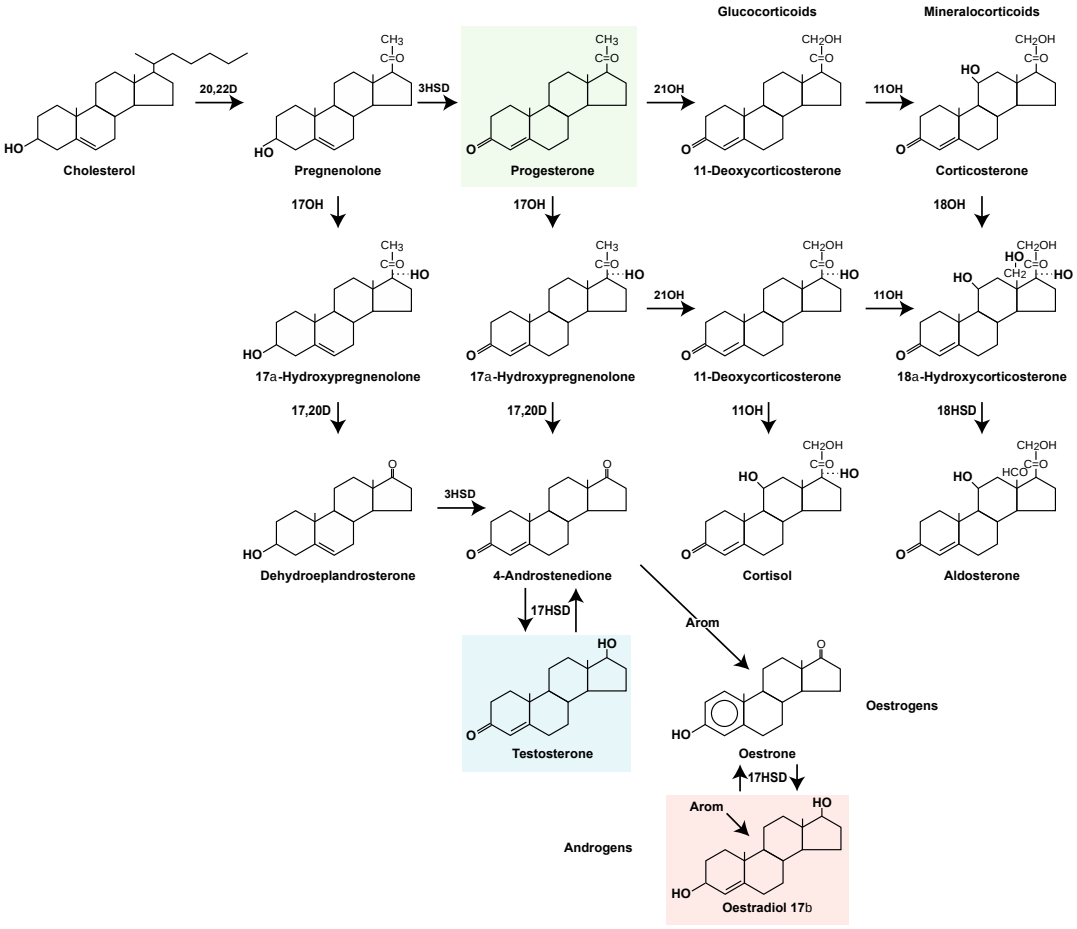

Figure 3.5 Synthesis of sex-steroids from cholesterol
Cholesterol is the precursor of all steroid hormones; it is oxidized to pregnenolone and then converted into progesterone by oxidation and a keto/enol tautomerization; other steroid hormones are derived from progesterone such as mineralocorticoids, cortisol, androstenedione and subsequently androgens and oestrogens

Transcriptional activity is further modified by the recruitment of additional co-regulatory proteins that may either increase (co-activators) or decrease (co-repressors) transcription (Critchley and Saunders 2009, Wagenfeld, Saunders et al. 2016).

The activity of the sex-steroids is thus dependent on the availability of the unbound ligand, its cognate receptor and co-regulatory proteins. The transcriptional endpoints of sex-steroid receptors (SSR) binding are altered by the cell type in which it is located.

3.1.3.1 Endometrium

The presence of SSR in endometrium and their variation across the menstrual cycle has been extensively described.

Progesterone receptor (PR)

PR encompasses both the A and B subunit. There is no specific antibody to the A subunit. Both expression and localisation of total PR varies across the menstrual cycle. One of the most comprehensive descriptions was published by Lessey *et al* in 1988 following semi-quantitative immunohistochemical analysis of endometrial biopsies obtained at the time of hysterectomy from 33 normally cycling women (Lessey, Killam et al. 1988). Samples were dated according to Noyes criteria (Noyes, Hertig et al. 1950) and split into 5 categories; menses, early proliferative, late proliferative, early secretory and late secretory. Epithelial expression was low at the time of menses and rose throughout the proliferative phase. Following ovulation, expression rapidly fell and remained low up to and including menstruation. Stromal expression was moderate at the time of menses, and rose throughout the cycle, peaking in the early secretory phase. It then fell, with its nadir at menstruation (Lessey, Killam et al. 1988). A relatively similar pattern was demonstrated by Snijders et al, the exception being that Snijders further categorised the secretory women into early-, middle- and late-secretory phase, thus demonstrating the maximal epithelial expression to be in the early secretory phase. He also separately assessed the functional and basal compartments illustrating relatively similar patterns in both layers across the cycle (Snijders, de Goeij et al. 1992). A further assessment of PR expression with a separate ovulatory category but summation of both functional and basal immunopositivity suggested that ovulation was the point of maximal expression prior to decline in levels (Wang, Critchley et al. 1998, Mote, Balleine et al. 1999).

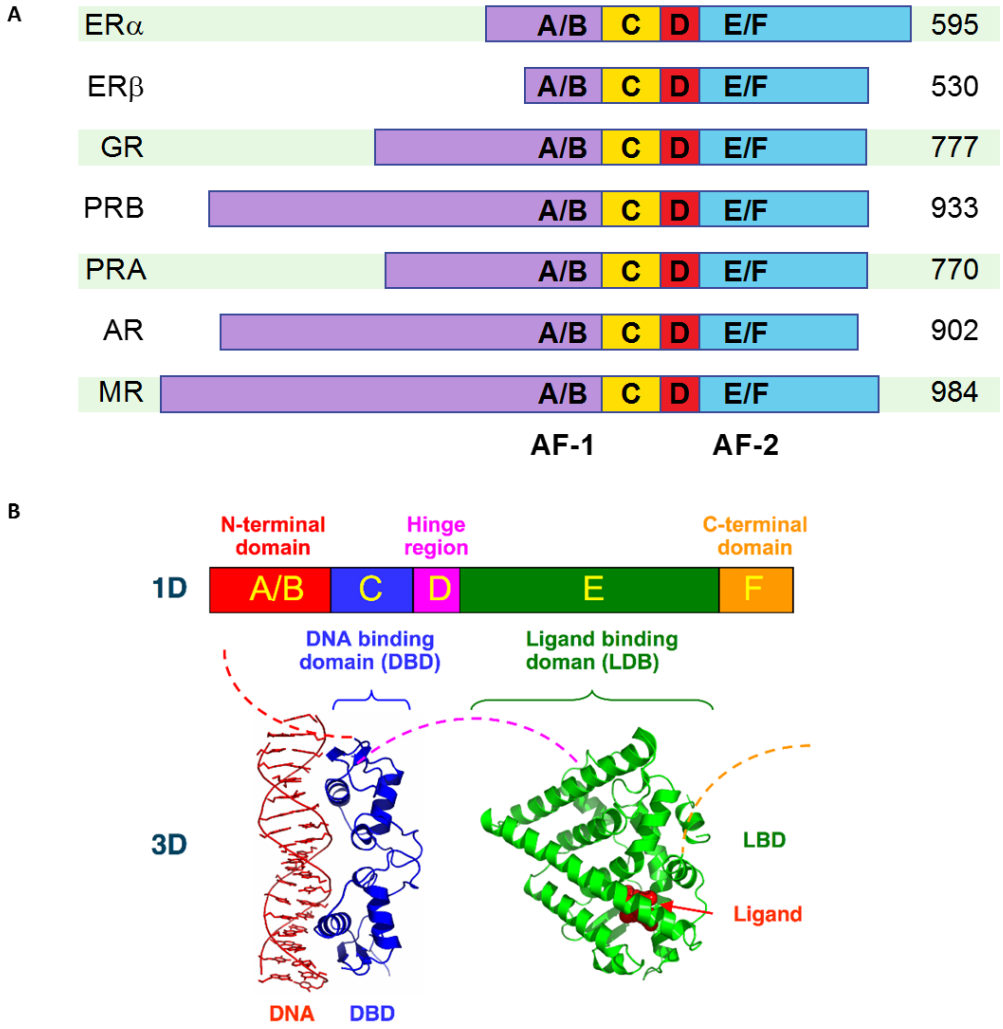

Figure 3.6 Structure of sex-steroid receptors

A Protein structure, number of amino acids and **B** 3D representation of the sex steroid receptor superfamily.

All family members share a common structural arrangement:
A/B: N-terminal regulatory domain, contains the activation function AF-1
C: DNA binding domain (DBD) which contains 2 zinc fingers which bind to DNA – hormone response elements (HRE)
D: Hinge region
E: Ligand binding domain (LBD), contains the activation function AF-2
F: C-terminal regulatory domain

3.6A Adapted and redrawn from Critchley *et al* Repro Sci 2009
3.6B Reproduced form wikipedia. https://en.wikipedia.org/wiki/Nuclear_receptor (Accessed 8th March 2017)

PRB

PRB is maximally expressed in the mid-proliferative phase in both epithelium and stroma. Whilst levels subsequently fall, there is a brief increase of stromal expression in the early-secretory phase, with epithelial expression lowest in the late secretory phase and epithelial expression lowest at the time of menstruation (Wang, Critchley et al. 1998, Mote, Balleine et al. 1999). Through subtractive inference, it is thought that PRA is the dominant subtype in the early secretory phase (Wang, Critchley et al. 1998, Brosens, Hayashi et al. 1999), particularly in the basal layer of the endometrium (Snijders, de Goeij et al. 1992).

Oestrogen receptor alpha (ERα)

Lessey *et al* have previously described expression of ERα with epithelial expression rising through proliferative phase and waning rapidly in secretory with levels lowest at the time of menstruation. Stromal expression mirrors that of epithelial, with the exception that secretory levels fall less quickly (Lessey, Killam et al. 1988). This was in contrast to Snijders (Snijders, de Goeij et al. 1992) who demonstrated that epithelial ER expression remained relatively high in early secretory phase prior to very low levels in the mid secretory phase. The degree of reduction of expression between early and mid-secretory phase was higher in the functional layer compared with basal endometrium. Snijders furthermore found that stromal expression was lowest in early secretory phase with a further small rise in the mid-secretory phase – reflecting circulating E2 levels (Snijders, de Goeij et al. 1992).

The α and β subunits have been separately assessed. Both are expressed in the in glands and stroma. In the functional layer ERα reduces in both epithelial and stroma cells in the secretory phase, whereas ERβ declines only in the epithelial cells. Basal expression of both is unchanged by stage of cycle (Critchley, Brenner et al. 2001). ERα up regulates PR (Chauchereau, Savouret et al. 1992, Brosens, Tullet et al. 2004) and mediates proliferation (Jabbour, Kelly et al. 2006). The role of ERβ in the human endometrium is not fully elucidated (Critchley and Saunders 2009) but likely plays a role in attenuating ERα mediated response to oestrogen (Hapangama, Kamal et al. 2015).

Androgen Receptor (AR)

AR is expressed in the endometrium but expression is predominantly limited to the stroma (Slayden, Nayak et al. 2001, Marshall, Lowrey et al. 2011, Whitaker, Murray et al.

2017). Basal expression is relatively constant but expression in the functional layer rises from proliferative phase levels to maximal expression in the early secretory stage, with minimal expression in late secretory. Glandular expression is minimal (Slayden, Nayak et al. 2001), and only occasional positive epithelial cells are observed following P-withdrawal (Critchley and Saunders 2009).

Cyclical alterations in sex-steroid receptors are summarised in Table 3.2.

Table 3.2 Summary of sex-steroid receptor expression in human endometrium

Sex-steroid receptor	Phase of cycle			
	Proliferative		Secretory	
	Glands	Stroma	Glands	Stroma
PR	Present	Present	Reduced	Present
PRB	Present	Present	Reduced	Markedly reduced
ERα	Present	Present	Reduced	Reduced
ERβ	Present	Present	Reduced	Present
AR	Absent	Present	Occasional LS	Maximal ES

ES: early secretory LS: Late secretory

3.1.3.2 Fallopian tube

Both PR and ER are present in the fallopian tube (Pollow, Inthraphuvasak et al. 1981). Epithelial PR are present throughout the menstrual cycle (Amso, Crow et al. 1994). PR and PRB are present in both the fimbriae and the ampulla, the PRB:PR ratio is higher in the ampullary region compared to the fimbrial region (Briton-Jones, Lok et al. 2005). Both PR and PRB are maximally down regulated in the secretory phase of the menstrual cycle (Horne, King et al. 2009). ER are maximal mid cycle with epithelial expression in both the ampulla and the fimbriae (Amso, Crow et al. 1994), but another study demonstrated that ERα does not alter significantly across the menstrual cycle (Horne, King et al. 2009). AR are present in fallopian tubes but are not significantly altered by phase of menstrual cycle (Horne, King et al. 2009).

There are both similarities and differences in the effects of progesterone and oestrogen within the fallopian tube and the endometrium. In both tissues E2 stimulates cell proliferation and up regulates the PR. However within the fallopian tube P4 acts solely

as an oestrogen antagonist, and it is E2 that is responsible for epithelial hypertrophy, secretion, and ciliogenesis. This is in contrast to endometrium where P4 is responsible not only for antagonism of E2 action, but also stimulates cell differentiation, vascular proliferation and remodelling and decidualisation (Brenner and Slayden 1994).

3.1.3.3 Cervix

PR is expressed within the uterine cervix. Glandular epithelium expresses PR, and levels are relatively unchanged by stage of menstrual cycle (Lin 1984, Cano, Serra et al. 1990), though a non-significant rise can be detected in late proliferative phase (Snijders, de Goeij et al. 1992). There is disagreement as to whether squamous epithelium expresses PR with some studies demonstrating presence (Lin 1984, Ackerman, Summerfield et al. 2016), with no effect of cycle phase (Lin 1984), and others demonstrating either total absence (Cano, Serra et al. 1990) or expression limited to the secretory phase (Nikolaou, Koumoundourou et al. 2014). PR is present in the cervical stroma but evidence is conflicting as to whether there is no cycle change in expression (Cano, Serra et al. 1990) or is increased in proliferative phase compared with secretory phase of the menstrual cycle (Lin 1984). PRB is also expressed within the stroma of the cervix (Winkler, Kemp et al. 2002), but limited evidence is available regarding other localization or change throughout the menstrual cycle. ERα is present in both the ecto and endocervix, with ectocervical expression down regulated in secretory phase and weak stromal staining (Cano, Serra et al. 1990, Nikolaou, Koumoundourou et al. 2014). Endocervical expression is either down regulated in secretory phase (Cano, Serra et al. 1990) or unaltered by stage of cycle (Snijders, de Goeij et al. 1992). AR is present in both the squamous epithelium and stroma of the human cervix (Noel, Bucella et al. 2008). Some small studies have indicated presence in the endocervix (van der Kwast, Dommerholt et al. 1994) but there are no data published regarding effect of cycle stage of protein expression.

3.1.4 Known effects of SPRMS on human reproductive tissue

3.1.4.1 Endometrial morphology; Progesterone receptor modulator-associated endometrial changes (PAEC)

SPRMs have an unusual effect upon the morphology of the endometrium. Initial clinical trials of long-term SPRM administration found increases in both endometrial thickness and rates of hyperplasia, typically simple in nature (Murphy, Kettel et al. 1995, Eisinger,

Meldrum et al. 2003, Levens, Potlog-Nahari et al. 2008, Bagaria, Suneja et al. 2009). This finding was felt not to be unexpected due to the likely endometrial impact of unopposed oestrogen (Murphy, Kettel et al. 1995). As greater experience of the histological effects of SPRMs accumulated, histological findings were increasingly described as non-physiological secretory changes (Chwalisz, Larsen et al. 2007, Engman, Granberg et al. 2009).

In 2006 a meeting was called in Bethesda, USA. Stakeholders from industry, the Food and Drug Administration (FDA) and researchers were present and recognition of the difficulties posed to pathologists acknowledged, particularly given that the findings did not appear to easily match established diagnostic entities. Prior to the meeting slides from 84 women receiving SPRMs (mifepristone, ulipristal acetate, asoprisnil and JNJ-17072341) were given to a panel of 7 expert pathologists who were blinded to treatment (Mutter, Bergeron et al. 2008). There was agreement that some of the samples reviewed represented normal cycling variations and benign pathologies such as polyps and endometritis. Equally the expert pathology group concurred that some represented disordered proliferative and there were no overtly pre-malignant malignant cases. Finally there was a group that did not fit into any existing standard diagnostic group.

The common theme of these unusual histological features was the co-existence within a single sample of individual histological features that are not seen in normal cycling endometrium and are usually attributed to either changes associated with hormone diminution, or stimulation with exogenous sex-steroids. These included inactive or apoptotic glands alongside intact stroma. Ciliated tubal metaplasia (an oestrogen-associated event) was present in inactive or secretory endometrium. Individual glands had unusual combinations of mitotic activity (albeit low) alongside apoptotic degeneration or secretory change. Cystic dilatation was present but glands were only weakly mitotic and often had associated apoptosis. Within the stroma unusual appearances of the vasculature were observed including widely disseminated thick-walled vessels (the degree of dispersion implying association with an endometrial polyp was unlikely) and delicate but prominent anastomosing capillary networks in a 'chicken-wire' pattern. Furthermore, stromal vessels were occasional ectatic but never demonstrated fibrin thrombi (a feature of unopposed oestrogen). These changes were summarised into a new histological entity referred to as progesterone receptor modulator-associated endometrial changes (PAEC) (Mutter, Bergeron et al. 2008).

The features of PAEC have been further refined and a pathologists guide has been produced by Gedeon Richter (https://www.hpra.ie/docs/default-source/3rd-party-documents/educational-materials/esmya_pathologist-guide-sept-2015.pdf?sfvrsn=2 2015, Gedeon Richter, Hungary) who manufacture the only SPRM licensed for clinical use in UK and Europe. They are generally split into four categories of features.

1. Endometrial gland architectural irregularity and cystic dilatation
    a. Scattered cystic ducts intermixed with small tubular or tortuous glands. Some show significant cystic dilatation.
    b. Glands are occasionally crowded but this is limited to microscopic foci.
2. Inactive glandular epithelium
    a. Glands are lined with a single layer of cuboidal or low columnar cells that do not have nuclear stratification.
    b. Occasional ciliated metaplasia can be observed.
    c. Infrequent mitoses are present.
3. Non-physiological secretory appearance
   Glands are tortuous or coiled (thereby resembling secretory phase) but have poorly developed secretory activity.
    a. Low levels of mitosis with occasional apoptosis.
    b. Focal cytoplasmic vacuolations.
    c. Surface apocrine-type secretory changes, the lamina of cysts often contains a watery secretion.
4. Glands are irregular distributed in densely cellular stroma without pre-decidual change.
    a. Glands are often widely dispersed in columns of dense stroma.
    b. Abnormal vasculature present: ‘chicken wire’ capillaries, thick-walled arterioles, ectatic thin-walled vessels.

Table 3.3 Features differentiating between PAEC, unopposed oestrogen exposure and complex hyperplasia

Feature	PAEC	Unopposed oestrogen effect	Complex endometrial hyperplasia
Gland architecture			
Cystic dilatation	Usually present	Present	Absent/focal/widespread
Disordered architecture	Focal	Focal	Diffuse
Complex architecture	Absent	Focal	Diffuse
Budding into stroma	Absent	May be present	Present
Luminal papillation	Absent	May be present	Present
Gland crowding	Absent	Focally present*	Present
Gland – stroma ratio	Unchanged	Unchanged/focally present*	Increased
Glandular epithelium			
Cell type	Flat cuboidal	Tall columnar	Tall columnar
Stratification of nuclei	Absent	Present	Present
Mitoses	Infrequent	Usually frequent	Frequent
Cytoplasmic vacuolation	Common	Uncommon	Uncommon
Nuclear size	Small, ovoid	Small or medium	Large, rounded
Nuclear shape	Ovoid	Ovoid or rounded	Rounded
Nucleoli	Usually absent	Usually present	Present
Nuclear atypia	Absent	Absent	May be present
Squamous metaplasia	Absent	Occasional	Frequent
Stroma			
Stromal density	Compact, moderately cellular	Abundant, may be densely cellular/oedematous	Usually densely cellular
Foam cells	Absent	Infrequent	Present
Stromal breakdown	Absent	Present	Present
Intravascular fibrin	Absent	Present	Present

*present in disordered proliferative pattern

Adapted from Esmya® (ulipristal acetate): Pathologist's guide PRM-Associated Endometrial Changes (PAEC) (Gedeon Richter, UK 2015)

The key features for distinguishing PAEC from proliferative endometrium or hyperplasia are low mitotic activity, abortive sub nuclear vacuoles, apoptosis and absence of stromal breakdown and glandular crowding (Williams, Bergeron et al. 2012). Other elements help to distinguish from unopposed oestrogen effects and complex endometrial hyperplasia (Table 3.3).

Amongst women administered SPRMs, rates of PAEC vary. In the largest clinical trials of UPA administration, around 78% of women treated with UPA for 3 months demonstrated non-physiological changes after treatment, but these rapidly regress to levels comparable to placebo group on cessation of treatment (Donnez, Tatarchuk et al. 2012, Donnez, Tomaszewski et al. 2012, Williams, Bergeron et al. 2012). Limited numbers of randomised clinical trials published subsequent to the guidelines on the diagnosis of PAEC have specifically reported on rates of PAEC. One study examining mifepristone reported specific PAEC rates of 24.5% (Carbonell, Acosta et al. 2013) and other additional studies examining UPA found a rate of 7% (Segal, Zarek et al. 2014), 10% (Nieman, Blocker et al. 2011) and 48% (Brache, Sitruk-Ware et al. 2012). Studies not specifically mentioning PAEC either report non-physiological secretory changes of 88% [mifepristone; (Engman, Granberg et al. 2009)] and 43-58% [asoprisnil; (Chwalisz, Larsen et al. 2007)] or continue to report simple hyperplasia 25-63% [mifepristone; (Bagaria, Suneja et al. 2009, Prasad, Varun et al. 2013)]. The reason for such variation is unclear but may be influenced by either the duration of treatment, choice of agent, time of sampling relative to treatment schedule, familiarity of the reporting pathologist or method of sampling.

3.1.4.2 Known effects of SPRMs on sex-steroid receptor expression in the endometrium

As described in chapter 1, SPRMS have high affinity for PR (Attardi, Burgenson et al. 2004), but do not bind ER (Wolf, Hsiu et al. 1989) or AR (Slayden and Brenner 2004).

Knowledge regarding the effect of SPRMs on the reproductive tract has been derived both from clinical trials in humans and from studies in the non-human primate (NHP).
Old world primates naturally menstruate. The rhesus macaque has a naturally occurring 28 day cycle and an anatomically similar uterus with structures analogous to the fundus, corpus and isthmus (Brenner and Slayden 2012). Arising from the uterus are the

oviducts which are equivalent to the fallopian tubes (Brenner and Slayden 2012). The isthmus leads into the cervix, the anatomy of which varies between primates; in the rhesus macaque there is a colliculum which obstructs the canal (Demers, Macdonald et al. 1972). The endometrium is separated into 4 zones, corresponding to those observed in women. The upper 2 zones contain the luminal epithelium and straight necked glands. These are functional, and undergo secretory transformation and are supplied by spiral arteries. Zone III contains branched glands which terminate in zone IV, adjacent to the myometrium (Brenner and Slayden 2012). PR and ER are both expressed in the endometrium of naturally cycling animals (Brenner, West et al. 1990).

The major contribution of this non-human primate model has been due to the ability to exclude hormonal fluctuations that naturally occur in both animals and women. Ovariectomy with subsequent sequential administration of oestradiol and progesterone as subcutaneous implants simulates the human proliferative and secretory phases, and removal of the progesterone implant (analogous to P-withdrawal following demise of the corpus luteum) initiates menstruation (Brenner and Slayden 2012). Uniformity of hormone exposure allows generation of precise experimental data with a decreased number of animals. PR and ER are expressed in an analogous fashion to naturally cycling humans (Critchley, Brenner et al. 2001, Slayden, Nayak et al. 2001) and AR expression is also observed (Brenner, McClellan et al. 1991, Adesanya-Famuyiwa, Zhou et al. 1999, Critchley, Brenner et al. 2001).

Endometrium

In the NHP mifepristone resulted in strong epithelial and stromal immunoreactivity of PR. This was in contrast to secretory phase where there was slight stromal immunolocalisation only. In proliferative phase both stromal and epithelial immunopositivity was present (Slayden and Brenner 1994). This was replicated with the SPRM ZK 230211 (lonaprisan) (Slayden and Brenner 2004). Treatment with the SPRM ZK 137316 also resulted in dense epithelial and stromal immunoreactivity in the functional layers, but stromal immunoreactivity was minimal within the basal layer (Slayden, Zelinski-Wooten et al. 1998). The previous studies had not differentiated between the two regions. There are no NHP studies regarding the impact upon of SPRMS on PRB expression and localisation. In human studies where mifepristone was administered, epithelial and stromal PR immunopositivity was similar to the proliferative phase (Narvekar, Cameron et al. 2004). The SPRM asoprisnil also increased

epithelial expression of PR compared with secretory phase, and in contrast to mifepristone, abrogated stromal expression (Wilkens, Male et al. 2013). Neither of these studies commented on the effects on PRB immunopositivity and localisation but a separate study has demonstrated in human endometrium a pattern of glandular immunopositivity with relative stromal sparing following administration of mifepristone (Sun, Christow et al. 2003).

Endometrial ER expression is altered by administration of SPRMs. In the NHP, treatment with mifepristone resulted in moderate epithelial and stromal staining in proliferative phase, minimal immunopositivity in both cellular types in secretory phase, with strong immunopositivity in both glandular and stromal cells following mifepristone administration (Slayden and Brenner 1994). As with PR, the effect on ER expression following mifepristone was replicated with the SPRM ZK 230211 (Slayden and Brenner 2004). The SPRM ZK 137316 also resulted in dense epithelial and stromal immunoreactivity, and this was present in both functional and basal layers (Slayden, Zelinski-Wooten et al. 1998). In human studies mifepristone administration resulted in an immunolocalisation that phenocopied proliferative phase (Narvekar, Cameron et al. 2004).

AR immunoreactivity in the NHP was limited to the stroma in both functional and basal layers in proliferative and secretory phases. Administration of the SPRMs mifepristone, ZK 137316 and ZK 2302111 increased stromal immunoreactivity markedly. Mifepristone was the most significant up regulator of AR immunopositivity. Strikingly, all three SPRMs markedly increased epithelial immunopositivity, most noticeably with mifepristone, though this increase was relatively limited to the functional layer. The exception to this was ZK 137316, which resulted in significant up regulation of AR expression epithelial cells in the basal layer as well (Slayden, Nayak et al. 2001). In women treated *in vivo* with the SPRM mifepristone a similar effect upon stromal and epithelial AR expression was noted with significant up regulation at either low dose (2mg) treatment for 30 days, or a single dose of 200mg (Slayden, Nayak et al. 2001). Samples were collected by suction catheter and so tissue examined was likely to be predominantly from the functional layer.

In summary administration of SPRMs other than UPA impacted both upon SSR expression and localisation in the endometrium of NHP and humans. The most striking

effect upon SSR localisation was upon PR and AR expression, but differs depending on SPRM studied. ER expression was increased, without alteration of localisation. The effects are summarised in Table 3.4

Fallopian tube

Much of the data of the effect of SPRMs on the fallopian tube is limited to reports utilising the NHP models. Mifepristone administration is associated with ciliation and secretory epithelium morphologically, similar to proliferative phase. Epithelial and stromal PR & ER expression were similar to proliferative phase. In the secretory phase immunopositivity was limited to the stroma (Slayden and Brenner 1994). This was consistent with blockade by mifepristone of progesterone action within the oviduct. Of note epithelial PR positivity was not present in all nuclei, both in the proliferative phase and in mifepristone treated animals. Compared to secretory phase, ZK 137316 administration results in a prevention of deciliated and non-secretory appearance in a dose dependent fashion, again suggestive of blockade of progesterone, but the impact upon SSR were not assessed (Slayden, Zelinski-Wooten et al. 1998).

In human studies one study demonstrated that mifepristone increased PR concentration in both epithelial and stromal cells relative to secretory phase. Proliferative phase was not assessed. This effect was limited to the ampullary region, with no significant alteration in expression noted in the isthmic portion. Utilising western blot, it was demonstrated that both PR and PRB were altered with mifepristone administration and that PRB had a greater increase following treatment with mifepristone (Christow, Sun et al. 2002). A separate study also demonstrated an increase relative to secretory phase, in both epithelial and stromal immunopositivity of PRB following mifepristone, and that this was evident both in the ampulla and the isthmus (Sun, Christow et al. 2003). Mifepristone increased ER epithelial expression but not in the stroma. In contrast to PR, this alteration in expression was more marked at the isthmic region compared with ampulla (Christow, Sun et al. 2002).

The proliferative phase was not assessed in the human studies, and so direct comparison between immunopositivity of PR in human tissue in proliferative phase and following SPRM administration cannot be commented upon, thus conclusions regarding tissue specificity effects rely upon the NHP studies described above. These data would suggest that it is only relative to secretory phase that tissue morphology and SSR expression are

altered, suggesting within the fallopian tube it is a non-competitive anti-oestrogen effect that is observed. This is in contrast to the endometrium, and thus suggests an endometrial specific effect.

Cervix

Much of the existing literature on the cervical effects of SPRMs are in respect to the use of mifepristone in the context of management of unintended pregnancy (in conjunction with misoprostol), and as a cervical ripening agent for the induction of labour. In the setting of pregnancy in animal models, administration of mifepristone results in an influx of macrophages (Kirby, Heuerman et al. 2016) and decreased collagen content (Yellon, Dobyns et al. 2013).

Oral administration of SPRMs to the non-pregnant cervix does result in altered functionality. Cervical dilation is increased following mifepristone treatment (Gupta and Johnson 1990, Bokström and Norström 1995). *In vitro* treatment increases collagen synthesis (Bokström and Norström 1995), and abrogates P-agonist-induced PR and PRB down-regulation (Ackerman, Summerfield et al. 2016)

3.1.4.3 Known effects of Ulipristal acetate (UPA)

Studies of the effect of UPA on the endometrium in NHP models show similar patterns of immunolocalisation of PR and ER as in proliferative phase (secretory was not assessed) (Brenner, Slayden et al. 2010). Both PR and ER were strongly expressed in epithelial and stromal cells in both groups. Studies in NHP demonstrate strong epithelial immunopositivity of AR following treatment with UPA, in contrast to proliferative phase when immunopositivity was limited to the stroma only (Brenner, Slayden et al. 2010). Studies on the effects of UPA on SSR expression in human endometrium have been limited to conference abstracts only prior to the publication of data from this thesis (Murray, Williams et al. 2014). These demonstrated a similar pattern of immunolocalisation of PR as the effect of asoprisnil with no reported data within the abstract upon the localisation of ER and AR. The effects on SSR expression and localisation following administration both UPA and other SPRMS to date are summarised in Table 3.4.

Table 3.4 Summary of known effects of SPRMs on sex steroid receptor expression and localisation in the endometrium of the non-human primate (rhesus macaque) and human

SPRM	Model	Protein expression and localisation								Reference
		PR		PRB		ERα		AR		
		G	S	G	S	G	S	G	S	
Mifepristone	NHP	++	++	NK	NK	++	++	++*	++	(Slayden and Brenner 1994, Slayden, Nayak et al. 2001)
	Human	++	++	NK	NK	++	++	++	++	(Slayden, Nayak et al. 2001, Narvekar, Cameron et al. 2004)
ZK137316	NHP	++	++	NK	NK	++	++	++#	++	(Slayden, Zelinski-Wooten et al. 1998, Slayden, Nayak et al. 2001)
	Human	NK	NK	NK	NK	NK	NK	NK	NK	
ZK230211	NHP	++	++	NK	NK	++	++	++*	++	(Slayden, Nayak et al. 2001, Slayden and Brenner 2004)
	Human	++	++	NK	NK	+	+	++*	++	(Heikinheimo, Vani et al. 2007)
Asoprisnil	NHP	NK	NK	NK	NK	NK	NK	NK	NK	
	Human	++	-	++	-	NK	NK	NK	NK	(Sun, Christow et al. 2003, Wilkens, Male et al. 2013)
UPA	NHP	++	++	NK	NK	++	++	++	++	(Brenner, Slayden et al. 2010)
	Human	NK	NK	NK	NK	NK	NK	NK	NK	

PR: Progesterone receptor, PRB: Progesterone receptor B, ERα: Oestrogen receptor alpha, AR: Androgen receptor, G: Gland, S: Stroma, NHP: Non-human primate, NK: not known

++ Strong immunopositivity + light immunopositivity +/- infrequent immunopositivity

*Minimal/absent immunopositivity in basal layer

++#: ++ in functional layer, + in basal layer

Studies of the effects of UPA on the human fallopian tube are limited to *in vitro* treatment with UPA. Ciliary beat frequency was reduced and PR/PRB mRNA levels increased in a dose-dependent fashion but effect on protein expression and localisation was not assessed (Li, Liao et al. 2014).

A separate group of researchers also using an *in* vitro treatment system demonstrated no alteration in ampullary morphology following treatment with UPA, although baseline cycle stage was not stated. They demonstrated increase in ampullary PR and ERα epithelial immunolocalisation following UPA treatment. They also observed an increase in stromal PR immunopositivity but ERα was unchanged (Yuan, Zhao et al. 2015).

There appear to be no published studies regarding the impact of UPA on cervical morphology and SSR expression.

3.2 Hypothesis

Whilst the effects of UPA on endometrial histological morphology are well recognised, incidence varies highly and impact upon the morphology of the human fallopian tube and cervix is unknown. There is almost negligible published literature on the effects of UPA on SSR expression and localisation in human reproductive tract tissue. The majority of the published literature is limited to NHP studies or *in vitro* studies. Other SPRMs demonstrate profound effects upon SSRs within the endometrium but descriptions have been limited and are occasionally contradictory. Within the fallopian tube, the effects of other class members in NHP models demonstrate alteration relative to secretory phase only and within the cervix the very limited data suggests blockade of P-mediated effects only. This suggests a possible endometrial specific effect upon localisation and expression.

Hypothesis: SPRM administration has an endometrial specific effect upon the epithelium of the human reproductive tract

3.3 Aim

To describe the impact of SPRM administration upon steroid receptor expression and localisation in the epithelium of the human female reproductive tract

- Is there a morphological effect of UPA administration on the endometrium, fallopian tube and cervix?
- Is there alteration in sex-steroid receptor mRNA levels in the endometrium and fallopian tube?
- Is there alteration in sex-steroid receptor protein expression and localisation in the endometrium, fallopian tube and cervix?
- Is the effect endometrial specific?

3.4 Materials and methods

Nine women with symptomatic fibroids underwent hysterectomy following treatment with Ulipristal acetate (UPA) 5mg orally once daily for up to 15 weeks prior to surgery (minimum nine weeks of treatment). They had given informed consent and the study had REC approval (12/SS/0238; section **2.1.1**). At the time of surgery, biopsies were collected from the endometrium and fallopian tube/cervix if removed concurrently. Samples were processed as previously described (section **2.2**) and tissue taken for RNA extraction for RT-qPCR and formalin fixation prior to immunohistochemistry. Corresponding control biopsies from women with symptomatic fibroids in proliferative and secretory phase of cycle were obtained from tissue archives (section **2.1.1**). Subjects were well characterised (section **2.4.1 Table 2.3-5, Table 2.10-13**).

RNA was extracted, quality checked and cDNA produced prior to performing RT-qPCR for *PR, PRB, AR* and *ERα* (as previously described; section **2.5**) of the endometrium (n=9 in each group) and fallopian tubes (n=6). Endometrial PCR was performed by AA Murray and not repeated by LHRW due to scarcity of RNA from these valuable samples, but ΔΔCT transformation of raw data, statistical analysis and figures were all performed by LHRW. FFPE sections were cut for H&E staining and immunolocalisation of PR, PRB, AR and ERα performed (section **2.6, Table 2.13-2.14**). This was performed on the endometrium (n=6-9), fallopian tube (n=6) and cervix (n = 8 UPA, 4 proliferative and 5 secretory). ERβ was not assessed in any tissue types.

Statistical analysis of RT-qPCR results was performed using Graphpad prism software (Graphpad, USA). Data were subjected to the D'Agostino-Pearson omnibus normality test. Data with a Guassian distribution had a one-way ANOVA applied to determine difference between groups. For non-parametric data Kruskal-Wallis test was used to determine differences between sample groups. Results are presented as ±SEM. $p < 0.05$ was considered to be statistically significant. Following ANOVA/Kruskal-Wallis test post-hoc testing was performed if appropriate using Tukey's or Dunn's multiple comparison.

3.5 Results

3.5.1 Effect of UPA administration on endometrial morphology and sex-steroid receptor expression

3.5.1.1 Endometrial morphology is altered by administration of UPA and causes characteristic changes

Administration of UPA impacted upon endometrial morphology (Figure 3.7 & 3.8). All subjects demonstrated features of PAEC although the degree of cystic dilatation was more marked in some (Figure 3.7D, E F, & I) than others (Figure 3.7A & G). There was evidence of focal gland crowding (Figure 3.7A, D, H & 3.8A; 1.), irregular scattering (Figure 3.7A, D, F & I) and architectural irregularity: along with cystic dilatation the evidence of tortuosity associated with the gland dilatation (Figure 3.7C & I, 3.8B; 2.).

The glands often appeared relatively inactive: they were lined with a single layer of cuboidal cells without nuclear stratification (Figure 3.8C & D; 3.). Occasional ciliated metaplasia was seen (Figure 3.8E; 4.). Many glands displayed a non-physiological secretory appearance and whilst they were coiled or tortuous (thus resembling secretory phase) they had poorly developed secretory activity, i.e. mitoses were observed, albeit infrequently (Figure 3.8F; 5.) and apoptosis was occasionally present (Figure 3.8G; 6.). Surface apocrine-type secretory changes were often observed with characteristic 'blebbing' at the luminal surface of the gland (Figure 3.8G; 7.). Some cells exhibited cytoplasmic vacuolation but this was infrequent (Figure 3.8C; 8.). The dilated glands were filled with fluid (Figure 3.8E & G; 9.). Macroscopically this fluid was watery in appearance at the time of endometrial sampling. The stroma was predominantly densely packed (Figure 3.7B, C, E-G, 3.8C-G; 10) and there was no evidence of pre-decidual change.

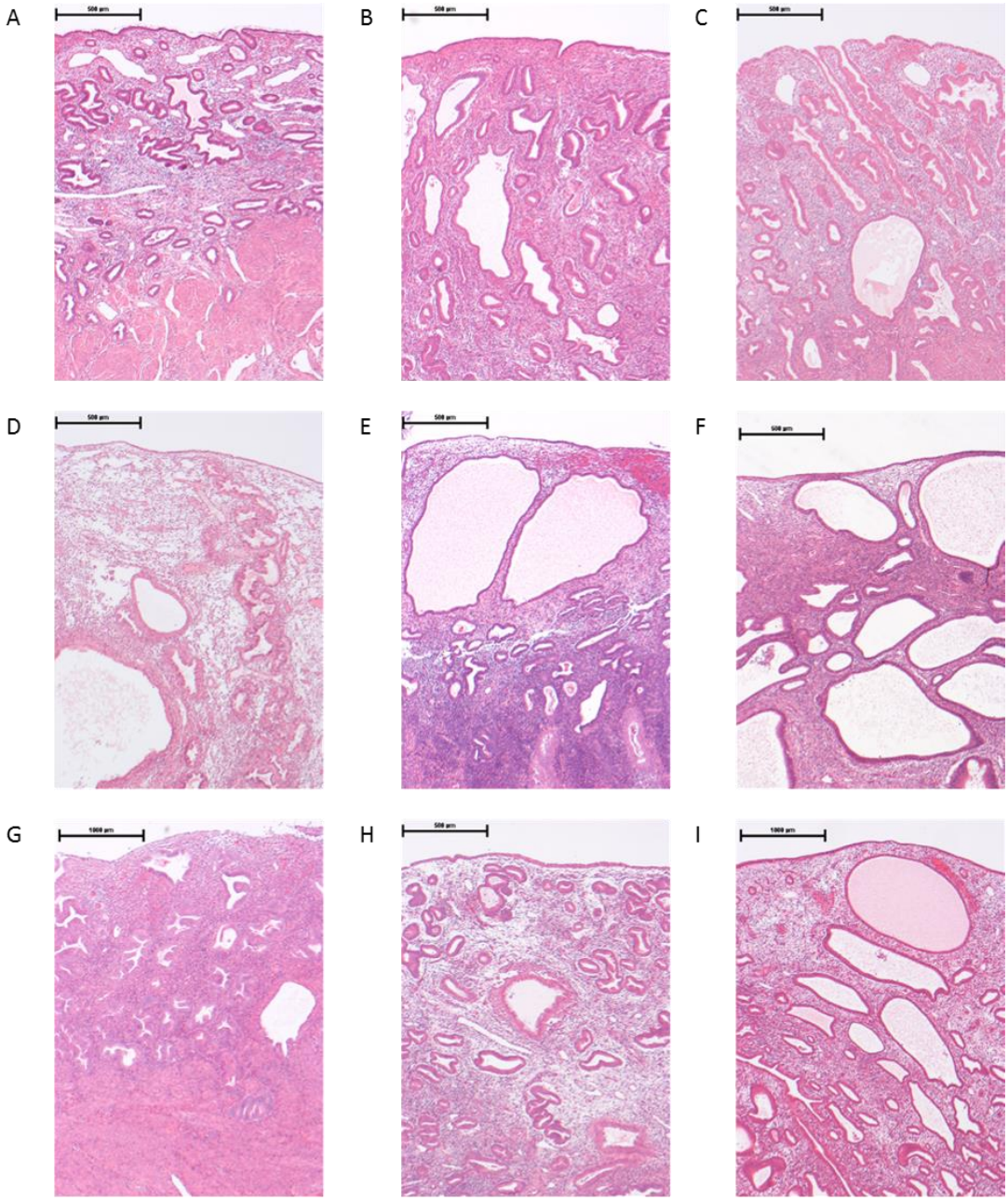

Figure 3.7 Treatment with selective progesterone receptor modulator, ulipristal acetate (UPA) results in altered endometrial histology

Representative H&E images of 9 full thickness endometrial biopsies. All subjects demonstrate progesterone receptor associated endometrial changes (PAEC). The degree of cystic dilatation is variable with some subjects demonstrating more cystic dilatation (E/F/I) than other subjects (A/G).

A Subject CP1231, B Subject CP1232, C Subject CP1233, D Subject CP1234, E Subject CP1235, F Subject CP1236, G Subject CP1237, H Subject CP1238, I Subject CP1239.

Scale bars 500µm

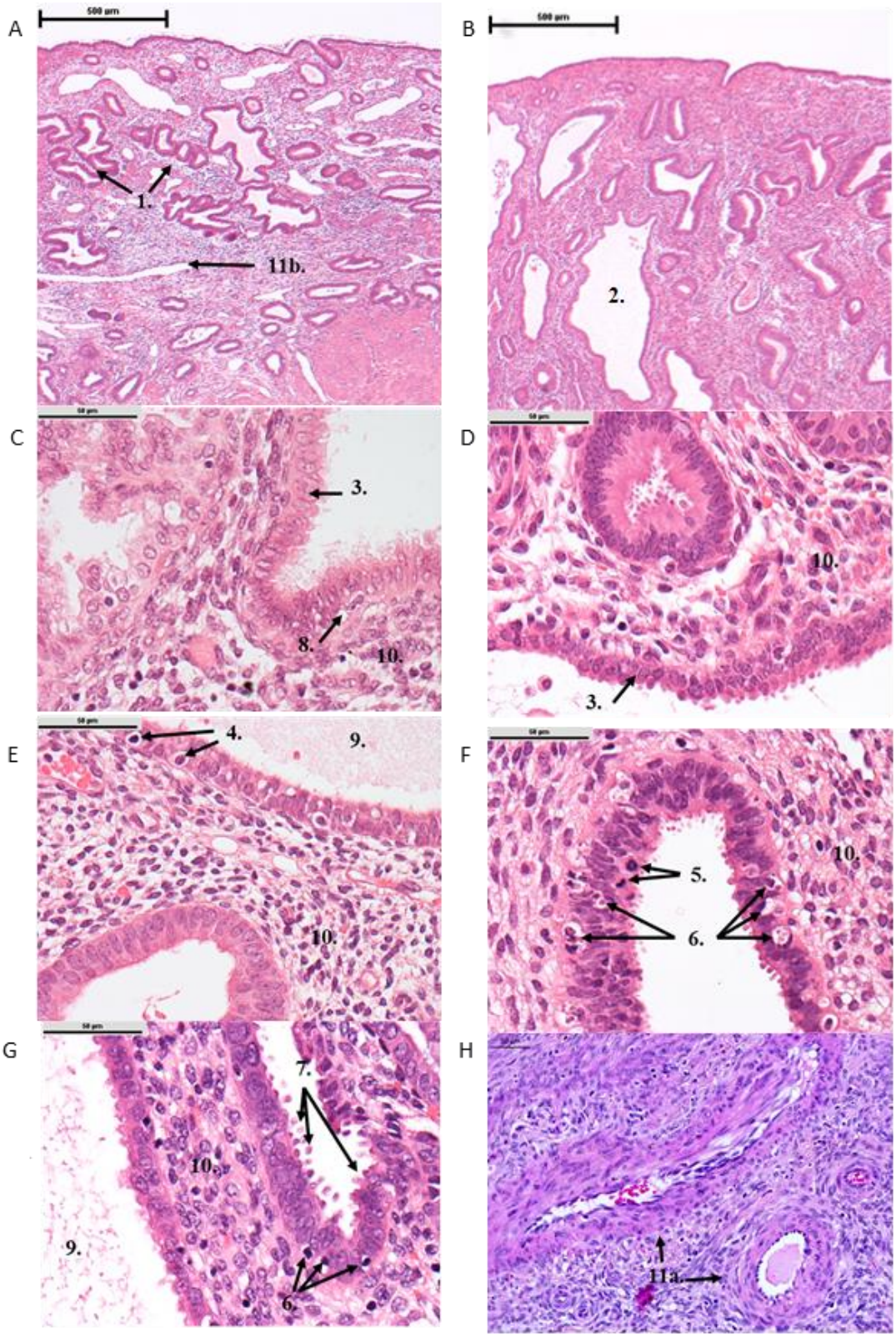
A
500 µm
1.
11b.
B
500 µm
2.
C
3.
8.
10.
D
10.
3.
E
4.
9.
10.
F
10.
5.
6.
G
7.
10.
9.
6.
H
11a.

Figure 3.8 Treatment with selective progesterone receptor modulator, ulipristal acetate (UPA), results in specific features of progesterone receptor modulator associated endometrial changes (PAEC)

Representative H&E images of full thickness (endometrial lumen to endometrial-myometrial junction) endometrial biopsies obtained at the time of hysterectomy from women treated with UPA for up to 15 weeks. Feature of PAEC are present:

Endometrial glands demonstrate focal crowding (1; within image A) and extensive cystic dilation with a tortuous appearance to glands (2; within image B).

Glandular epithelium appears inactive with low cuboidal, non-stratified epithelial cells (3; within image C & D). There is evidence of ciliated metaplasia (4; within image E). Mitoses are present but low in number (5; within image F) and apoptosis is occasionally observed (6; within images F & G). There is evidence of non-physiological secretory differentiation with surface apocrine-type secretory changes (7; within image G) and occasional cytoplasmic vacuolation (8; within image C). Watery secretions may be observed in the lumen of glands (9; within image E & G). Glands are irregularly scattered (image A) and stroma is densely packed (10; within image C-G) with a non-decidualised appearance.

Abnormal vasculature may be observed with both thick-walled arterioles (11a; within image H) and ectatic thin-walled vessels (11b; within image A).

Scale bars 500µm low power, 50µm high power

Key

1. Focal crowding
2. Dilated and tortuous glands
3. Low cuboidal, non-stratified epithelial cells
4. Ciliated metaplasia
5. Infrequent mitoses
6. Apoptosis
7. Surface apocrine-type secretory changes
8. Cytoplasmic vacuolation
9. Watery secretions
10. Densely cellular stroma
11. Abnormal vasculature
    a. Thick-walled vessels
    b. Ectatic thin-walled vessels

A Subject CP1231, B/D Subject CP1232, C Subject CP1234, E Subject CP1233, F Subject C1236, G/H Subject CP1235

Occasional unusual vasculature could be observed but was not ubiquitous. Some arterioles showed a thickened muscularis (Figure 3.8H; 11a.), and observed in only 3 subjects (CP1235; Figure 3.7E & 3.8H, CP1236; Figure 3.7F and CP1238; Figure 3.7H). Others had a thin walled, ectatic appearance (Figure 3.8A, 11b.). Overall the majority of the vasculature was normal.

The degree of cystic dilatation did not correspond to duration of treatment or bleeding control (table 2.4). The subject who had increased bleeding had occasional significant cystic dilatation (CP1234; Figure 3.7D). Of the 2 subjects who had irregular spotting one had evidence of dilated cysts (CP1232; Figure 3.7B) and the other had less widespread cystic dilatation (CP1237; Figure 3.7G).

All subjects had 2 or more biopsies obtained. One sample was obtained from the fresh specimen as described in section **2.2.1.1** and the second following the overnight fixation of residual uterine specimen for standard diagnostic assessment. The later were initially reported by general pathologists and one was described as normal secretory (CP1231) and another as normal proliferative (CP1232). However following expert pathology review, (Professor ARW Williams) it was concluded that all biopsies (both research and standard diagnostic) demonstrated features of PAEC.

No subjects had evidence of hyperplasia, neoplasia, polyps or infection.

3.5.1.2 Treatment with UPA increased relative mRNAs levels encoded by sex-steroid hormone receptors

UPA increased relative *PR* and *PRB* mRNA levels in the endometrium significantly compared to secretory phase endometrium but these was not significantly different to proliferative phase samples (Figure 3.9A, B). Relative concentrations of *PR* and *PRB* mRNAs were significantly lower in secretory endometrium compared to proliferative tissue. Relative *AR* mRNA levels in UPA-treated samples were significantly increased compared to both proliferative and secretory phase samples. *AR* mRNA levels were not significantly different between proliferative and secretory phase samples (Figure 3.9C). Relative levels of *ESR1* (ERα) mRNA were significantly higher in UPA-treated samples and proliferative phase than in secretory phase. There was no significant difference in *ESR1* concentration between proliferative phase and UPA treated samples (Figure 3.9D).

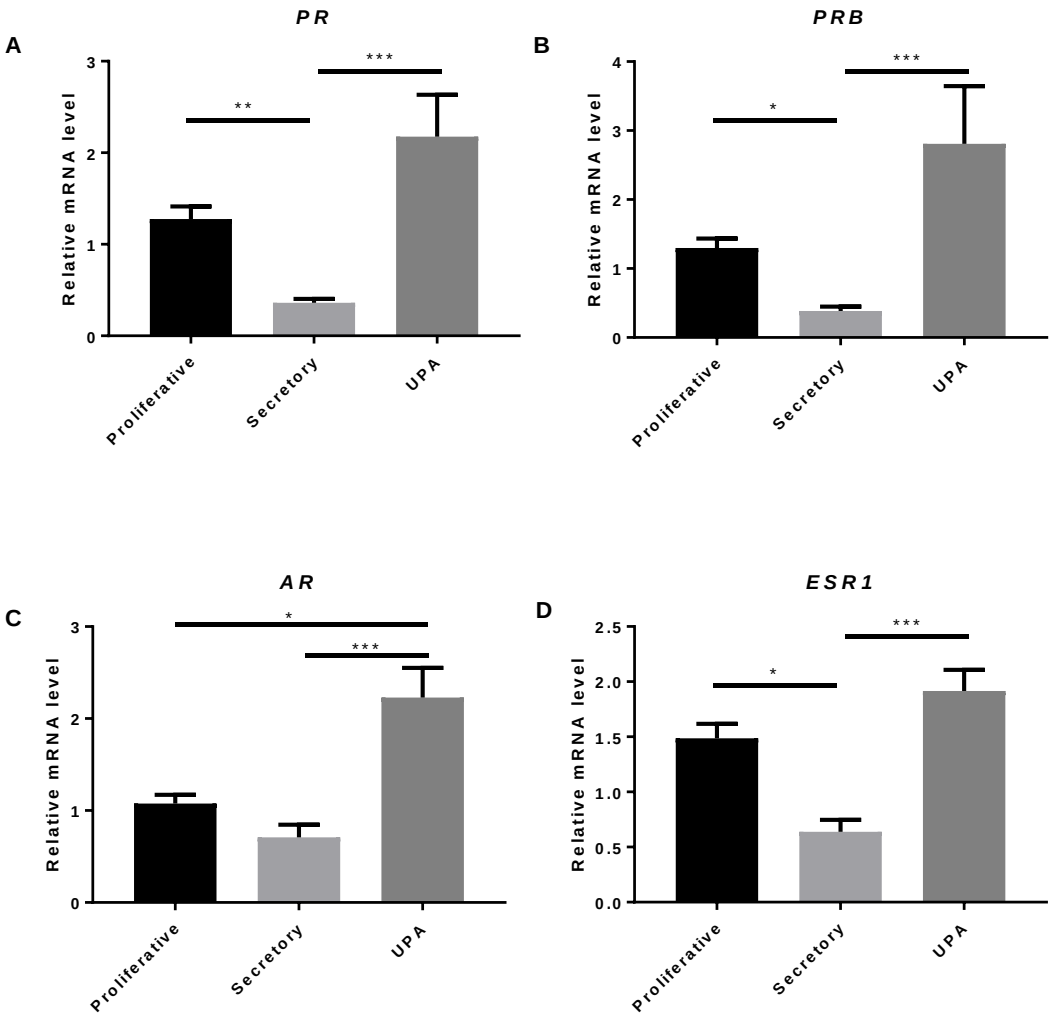

Figure 3.9 Treatment with selective progesterone receptor modulator, ulipristal acetate (UPA), increased the concentration of mRNAs encoding sex-steroid receptors in tissue extracts from human endometrium as determined by RT-qRT-PCR

Relative mRNA levels of progesterone receptor (*PR*; A Kruskal-Wallis p <0.0001), *PRB* (B Kruskal-Wallis p = 0.0001), androgen receptor (*AR*; C Kruskal-Wallis p = 0.0001) and oestrogen receptor S1 (*ESR1*; D Kruskal-Wallis p = 0.0004) from woman with fibroids during proliferative and secretory stages after UPA administration. n=9 for each group. * *P*<0.05, ** p<0.01, ***p<0.001. Bars +/- SEM.

3.5.1.3 Immunoexpression of endometrial sex steroid receptors is altered by UPA administration.

In agreement with previous studies (Lessey et al., 1988; Wang et al., 1998) intense immuno-positive staining for PR (with antibody recognising both isoforms) was detected in cell nuclei in both glandular epithelial cells and stromal fibroblasts in proliferative endometrium (Figure 3.10A & D). Intensity was reduced in epithelial cell nuclei in the secretory phase with minimal immunopositive staining. Within the stroma immunopositive staining appeared strong (Figure 3.10B & E). UPA-treated endometrium showed a pattern of PR immunopositive staining characterised by intense staining of nuclei in glandular epithelium and weak/negligible immunoexpression in stromal fibroblasts in both functional and basal layers (Figure 3.10C & F). This pattern did not phenocopy either proliferative or secretory endometrium (Figure 3.10D & E).

These results of localisation alteration were mirrored by results obtained using a PRB-specific antibody (Figure 3.11), although strong immunopositivity appeared less frequently in the stromal nuclei of secretory endometrium (Figure 3.11E) and the epithelial cells of UPA exposed endometrium (Figure 3.11F) compared with proliferative endometrium (3.11D) or PR immunopositivity (Figure 3.10).

Consistent with previous findings in our group (Marshall et al., 2011), immunopositive staining for AR was detected in nuclei of stromal fibroblasts in proliferative endometrium (Figure 3.12A & D). Occasional AR positive epithelial cells were detected in secretory phase (Figure 3.12E), coincident with a reduction in staining intensity in stromal cells. Immunostaining of UPA-treated endometrial sections revealed a unique pattern characterised by intense immunopositive staining of cell nuclei in both epithelial cells and stromal fibroblasts (Figure 3.12C & F). Immunopositive stromal and epithelial nuclei were observed in the full thickness of the endometrium (Figure 3.12C), including within the basal layer up to the myometrial interface (Figure 3.12F).

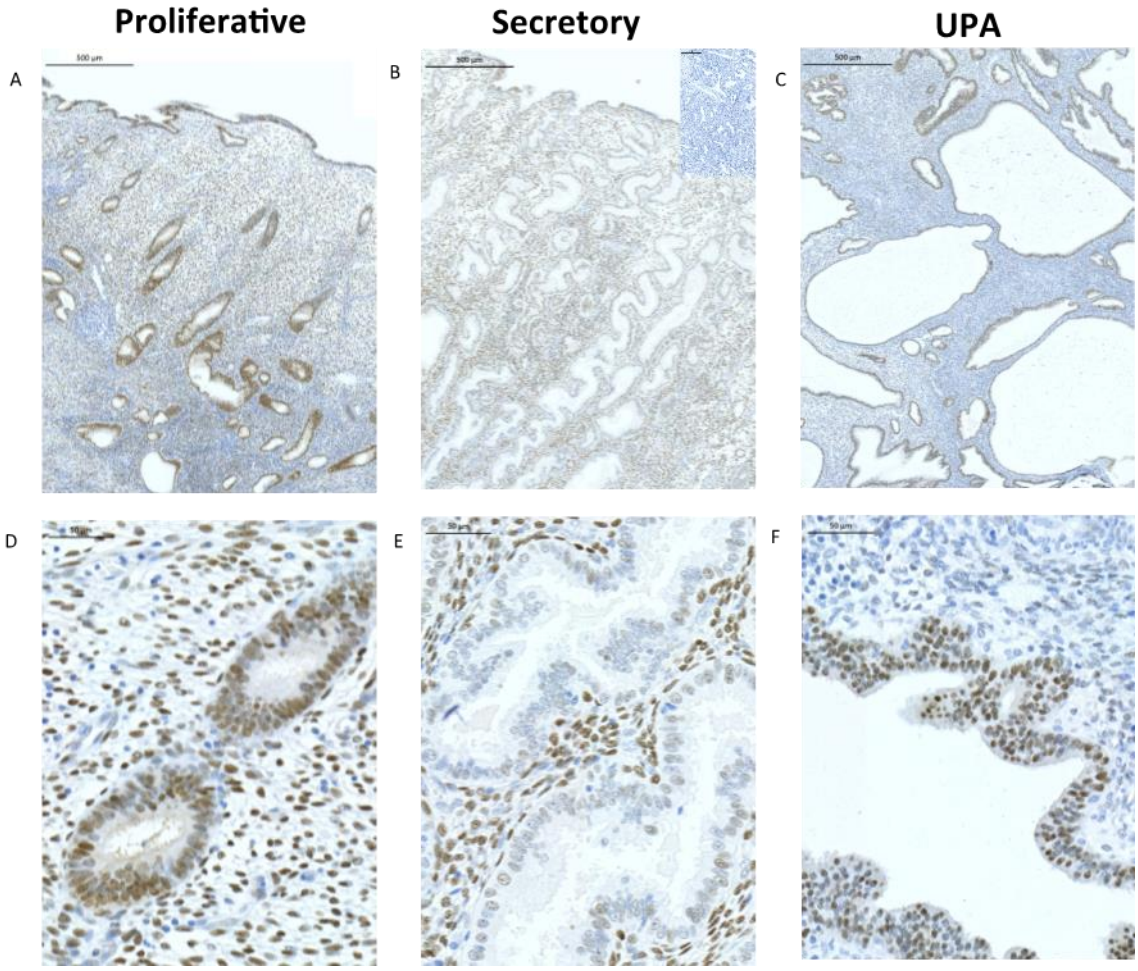

Figure 3.10 Administration of selective progesterone receptor modulator, ulipristal acetate (UPA), modulates progesterone receptor (PR) localisation

Representative low- (A-C) and high-power (D-F) immuno-localisation of PR in endometrium from woman with fibroids during proliferative (A&D) and secretory stages (B&E) after UPA administration (C&F). Samples from UPA-treated women displayed intense immunopositive (+ = positive and - = negative) glandular nuclei with only a few immunopositive cells in the stroma, a result in contrast with proliferative phase (G+S+) or secretory phase (G-S+). Lower power (scale bar = 500µm) and high power magnification (scale bar = 50 µm); G: Glands, S: Stroma. Negative controls shown as inserts on secretory endometrium.

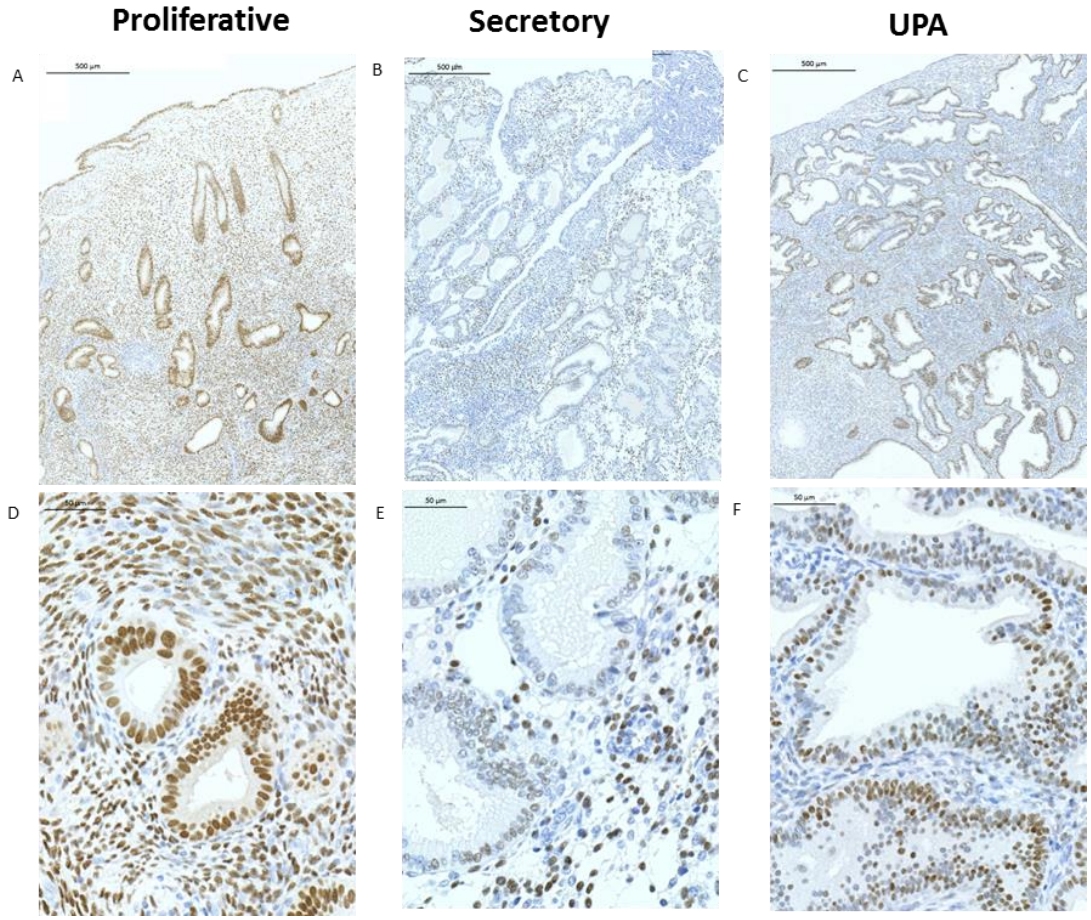

Figure 3.11 Administration of selective progesterone receptor modulator, ulipristal acetate (UPA), modulates PRB receptor localisation

Representative low- (A-C) and high-power (D-F) immuno-localisation of PRB in endometrium from woman with fibroids during proliferative (A&D) and secretory stages (B&E) and after UPA administration (C&F). Samples from UPA-treated women displayed intense immunopositive (+ = positive and - = negative) glandular nuclei with only a few immunopositive cells in the stroma, a result in contrast with proliferative phase (G+S+) or secretory phase (G-S+). Lower power (scale bar = 500µm) and high power magnification (scale bar = 50 µm); G: Glands, S: Stroma. Negative controls shown as inserts on secretory endometrium.

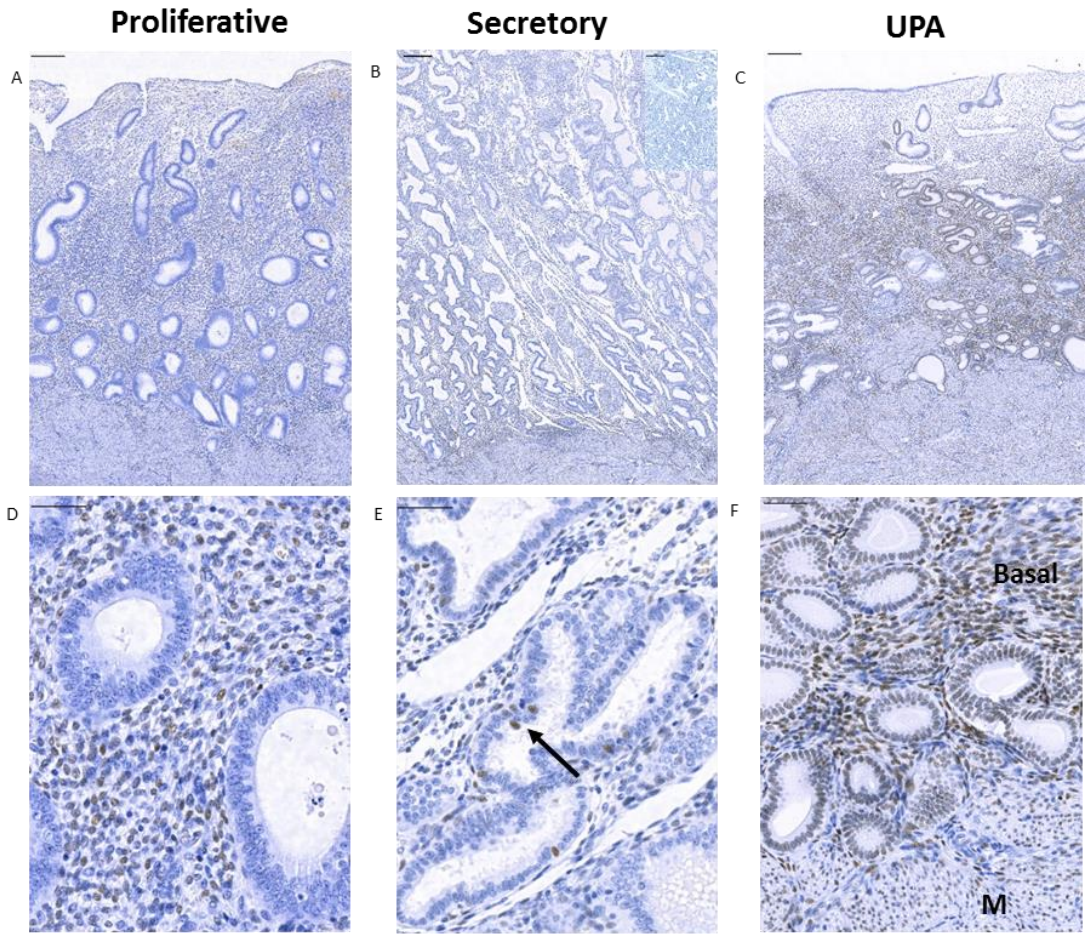

Figure 3.12 Administration of selective progesterone receptor modulator, ulipristal acetate (UPA), modulates androgen receptor (AR) localisation

Representative low- (A-C) and high-power (D-F) immuno-localisation of AR in endometrium from woman with fibroids during proliferative (A&D) and secretory stages (B&E) and after UPA administration (C&F). Samples from UPA-treated women (C & F) displayed intense immunopositive (+ = positive and - = negative) glandular and stroma nuclei, a result in contrast with proliferative phase (D; G-S+) or secretory phase (E; occasional G+, arrowed, and light S+). AR immuno-positive glandular nuclei were present in both the functional and basal endometrium (F; basal) and were observed at the myometrial interface (M). Lower power (scale bar = 500µm) and high power magnification (scale bar = 50 µm); G: Glands, S: Stroma. Negative controls shown as inserts on secretory endometrium.

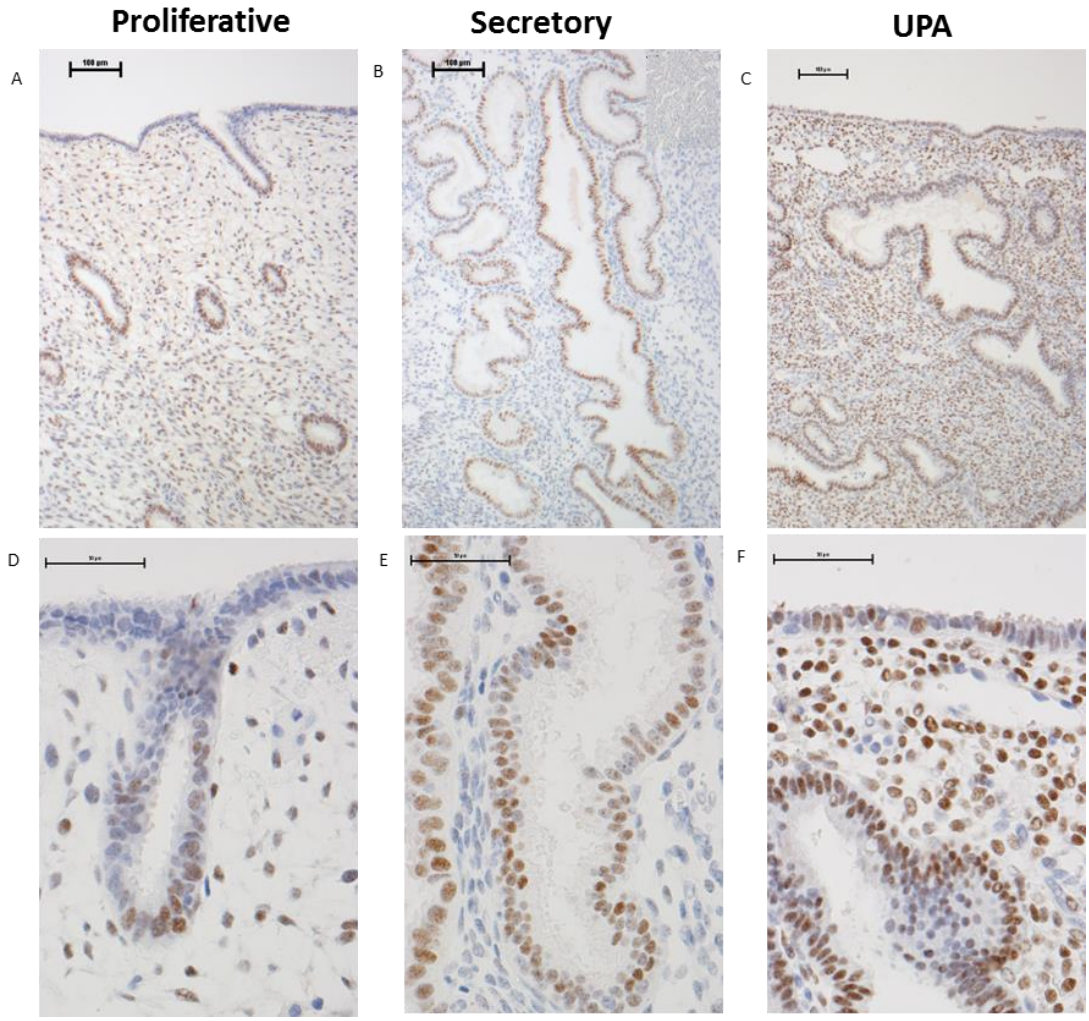

Figure 3.13 Administration of selective progesterone receptor modulator, ulipristal acetate (UPA), modulates oestrogen receptor alpha (ERα) receptor localisation

Representative low- (A-C) and high-power (D-F) immuno-localisation of ERα in endometrium from woman with fibroids during proliferative (A&D) and secretory stages (B&E) and after UPA administration (C&F). Samples from UPA-treated women (C & F) displayed intense immunopositive (+ = positive and - = negative) glandular and stroma nuclei, a result in contrast with proliferative phase (G+S+) or secretory phase (G+S-). The secretory sample shown is from early secretory, hence the maintenance of glandular immunopositivity.
Lower power (scale bar = 500µm) and high power magnification (scale bar = 50 µm); G: Glands, S: Stroma. Negative controls shown as inserts on secretory endometrium.

The expression profile of ESR1 (ERα) protein differed between proliferative and secretory endometrium with reduced immunoexpression detected in secretory phase tissue in stromal fibroblasts (Figure 3.13A & C, B & E). In the example shown epithelial ERα immunopositivity is maintained (Figure 3.13B &E), this sample is from early secretory phase. As expected, in samples from mid- and late-secretory, the epithelial immunopositivity was lost (data not shown). ERα immunoexpression in UPA-treated endometrium mirrored that of proliferative endometrium and appeared more intense in degree of staining (Figure 3.13C & F).

3.5.1.4 Summary of impact of UPA on sex-steroid receptor expression and localisation in the endometrium

The results of the effect of UPA upon sex-steroid receptors in the endometrium are summarised in Table 3.5.

Table 3.5 Impact of UPA administration on endometrial sex-steroid mRNA levels and protein expression and localisation

SSR	Relative mRNA level	Protein expression and localisation					
		Proliferative		Secretory		UPA	
		G	S	G	S	G	S
PR	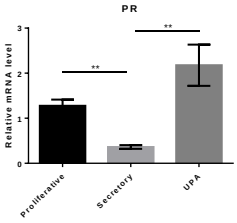	++	++	-	++	+++	-
PRB	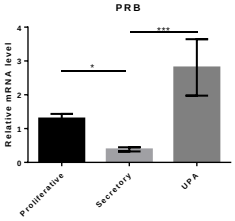	++	++	-	++	++	-
AR	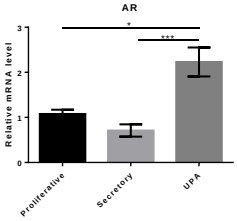	-	++	+/-	+	++	+++
ERα	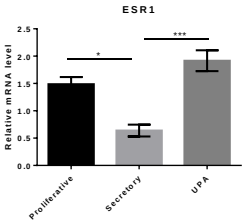	++	+	+/-	+/-	++	++

SSR: sex steroid receptor, G: glandular epithelium; S: stroma PR progesterone receptor; PRB: progesterone receptor B; AR: androgen receptor; ERα: oestrogen receptor alpha.

* p <0.05, ** p <0.01, *** p <0.001

+++ Dense immunopositivity, ++ moderate immunopositivity + light immunopositivity +/- infrequent immunopositivity – absent immunopositivity

3.5.2 Effect of UPA administration upon fallopian tube morphology and sex-steroid receptor expression

3.5.2.1 UPA administration did not alter fallopian tube morphology compared to proliferative phase

At low magnification fallopian tubes from women in proliferative phase (Figure 3.14A) or secretory phase (Figure 3.14B) of the menstrual cycle or following UPA administration (Figure 3.14C) were indistinguishable. At higher magnification in proliferative phase ampullary nuclei in epithelial cells were pseudostratified (Figure 3.14E&I, *) and the luminal aspect of cells demonstrated multiple ciliations (arrowed). In contrast nuclei in secretory phase were stratified, and more cuboidal in morphology with minimal cytoplasm (Figure 3.14F&J). Cilia appeared rarely, though the frequency varied between subjects. Epithelium from women administered UPA demonstrated multiple ciliations and a pseudostratified appearance (Figure 3.14G&K), resembling proliferative phase (Figure 3.14E&I). Fimbria from women administered UPA demonstrated ciliation and some pseudostratification (Figure 3.14H&L).

3.5.2.2 Administration of UPA modulated relative mRNA levels of PR and ERα in the fallopian tube relative to secretory but not proliferative phase

UPA increased fallopian tube PR and ERα relative mRNA levels compared with secretory phase ($p < 0.05$; Figure 3.15A & D). There was no statistical difference between UPA and secretory phase relative mRNA levels of PRB or AR (Figure 3.15B & C). There was no statistical difference between proliferative phase relative mRNA levels of either PR, PRB, AR or ERα and UPA exposed fallopian tubes (Figure 3.15). There was a generalised trend towards reduced secretory levels of PR, PRB and ERα compared to proliferative phase but this did not achieve statistical significance (Figure 3.15A, B &D).

3.5.2.3 Administration of UPA increased expression of PR and ERα but did not alter localisation.

PR nuclear immunopositivity was observed in the ampullary glandular epithelium of proliferative phase, secretory and UPA exposed fallopian tubes (Figure 3.16A-C & E-G). The intensity of immunopositivity appeared most dense in UPA exposed fallopian tubes (Figure 3.16G), appeared slightly less intense in proliferative phase (Figure 3.16E) and

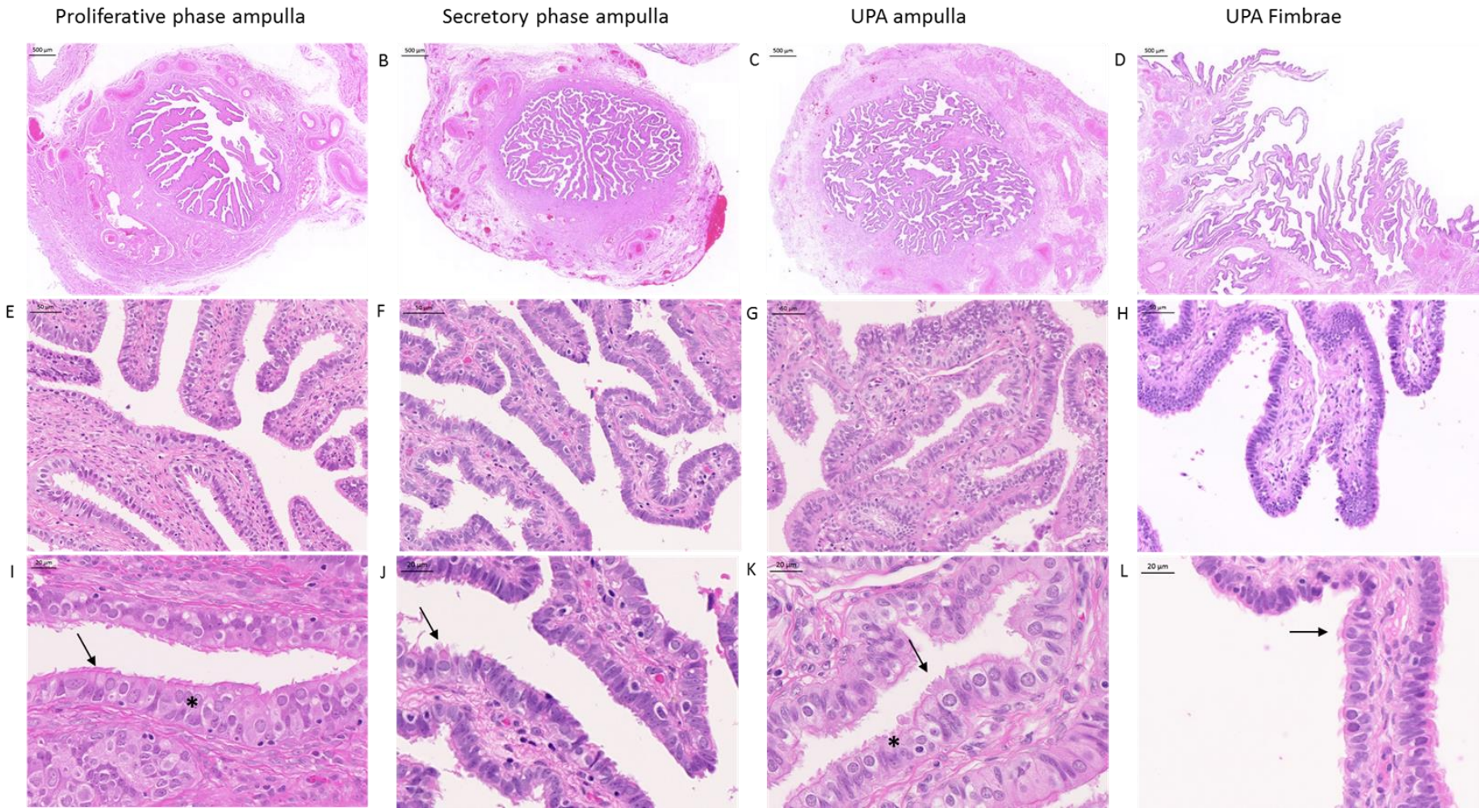
Proliferative phase ampulla
Secretory phase ampulla
UPA ampulla
UPA Fimbrae
A
B
C
D
E
F
G
H
I
J
K
L
500 µm
50 µm
40 µm
20 µm

Figure 3.14 Administration of selective progesterone receptor modulator, ulipristal acetate (UPA) results in fallopian tube ampullary epithelial histology that resembles that from women in proliferative phase

Representative H&E images from the ampullary region of the fallopian tube from women in the proliferative (A, E, I) and secretory (B, F, J) phase of the menstrual cycle, and following administration of UPA (C&D, G&H, K&L).

Nuclei in proliferative phase are pseudostratified (E&I,*) with multiple ciliations (↑). Nuclei in secretory phase are stratified, and more cuboidal in morphology with minimal cytoplasm (F&J). Cilia are appeared rare though frequency varied between subjects. Epithelium from women administered UPA demonstrate multiple ciliations and a pseudostratified appearance (G&K), resembling proliferative phase (E&I). Fimbriae from women administered UPA demonstrated occasional cilation (↑) and some pseudostratification (H&L).

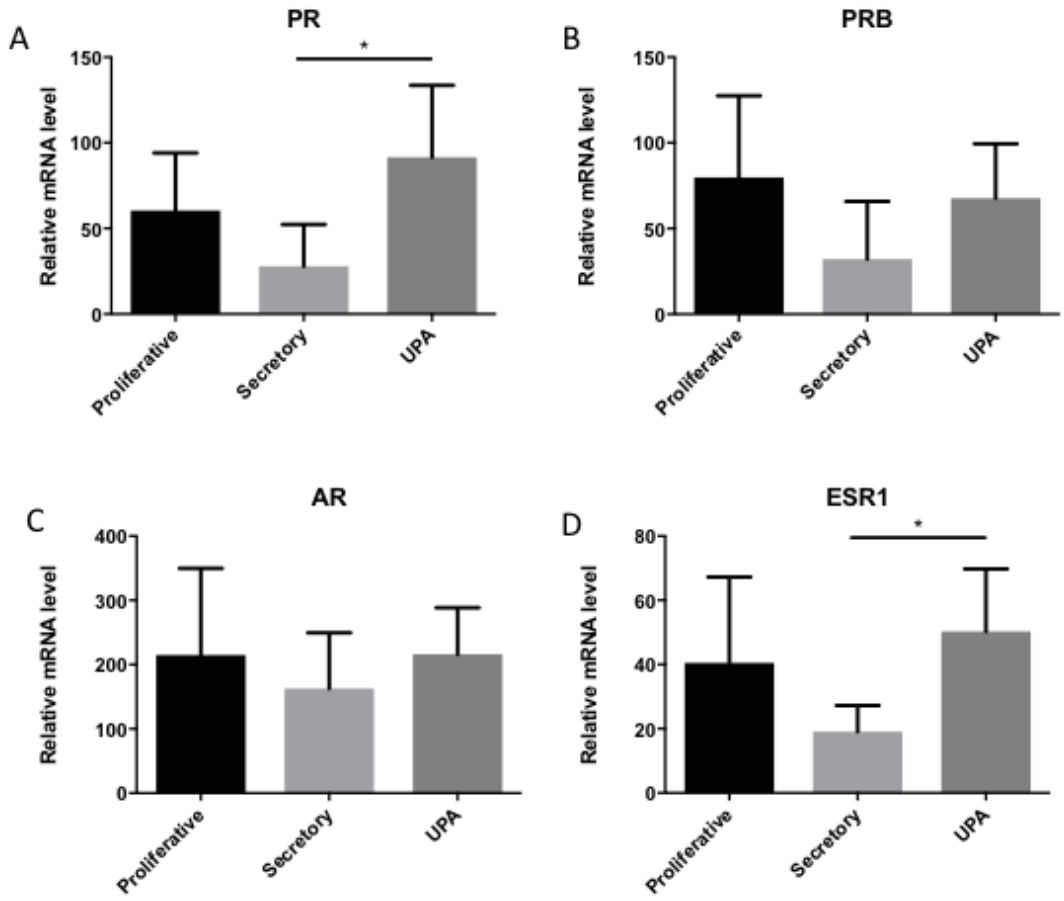

Figure 3.15 Administration of selective progesterone receptor modulator, ulipristal acetate (UPA) modulates relative mRNA levels of progesterone receptor (PR) and Oestrogen receptor alpha (ERα) in the fallopian tube

Relative mRNA levels of PR (A Kruskal-Wallis p = 0.0152), PRB (B Kruskal-Wallis p = 0.1881), androgen receptor (AR; C Kruskal-Wallis p = 0.7402) and oestrogen receptor S1 (ESR1; D Kruskal-Wallis p = 0.0116) from woman with fibroids during proliferative and secretory stages and after UPA administration. Samples from UPA-treated women had increased mRNA levels of PR and ERα compared to women in the secretory phase. PRB and AR mRNA levels were not statistically different: n=6 for each group. * *P*<0.05. Bars +/- SEM.

appeared only moderate in secretory phase (Figure 3.16F). This has not been quantified. Whilst epithelial staining was intense within the epithelium of ampulla from UPA exposed women, a less dense immunopositivity was observed in the epithelium of the fimbrial end (Figure 3.16D & H). There was intermittent light stromal immunostaining irrespective of stage of cycle or UPA treatment.

In keeping with PR immunopositivity, PRB immunoreactivity was most marked in ampullary epithelial nuclei, with occasional moderate stromal staining (Figure 3.17). Stromal staining was unaffected by stage of cycle or UPA treatment (Figure 3.17E-H). Ampullary epithelial immunopositivity was most dense in proliferative phase (Figure 3.17A & E), was slightly less ubiquitous following UPA treatment (Figure 3.17C & G) and appeared less dense in the secretory phase (Figure 3.17B & F). PRB immunopositivity in the fimbrial end phenocopied ampullary staining (Figure 3.17D & H). AR ampullary epithelial immunopositivity mirrored that of PRB with the most dense staining evident in the proliferative phase (Figure 3.18A & E) and somewhat less extensive in the secretory phase (Figure 3.18B and F) and following UPA treatment (Figure 3.18C & G). Only occasional stromal immunoreactivity was observed and the pattern of staining in the fimbriae of UPA exposed women was similar to that observed at the ampulla (Figure 3.18D & H).

Ampullary epithelial ERα immunopositivity was widespread in both proliferative (Figure 3.19A & E) and secretory (Figure 3.19B & F) phase fallopian tubes as well as following UPA treatment (Figure 3.19C & G). Immunopositivity appeared most dense in UPA exposed women and appeared slightly reduced in secretory phase compared to proliferative phase. Intermittent but moderate stromal immunoreactivity was present irrespective of phase of cycle or following treatment with UPA (Figure 3.19E-G). Fimbrial epithelial immunopositivity was present but appeared less than when compared with the ampulla (Figure 3.19D & H).

3.5.2.4 Summary of impact of UPA on sex-steroid receptor expression and localisation in the fallopian tube

The results of the effect of UPA upon sex-steroid receptors in the fallopian tube are summarised in Table 3.6.

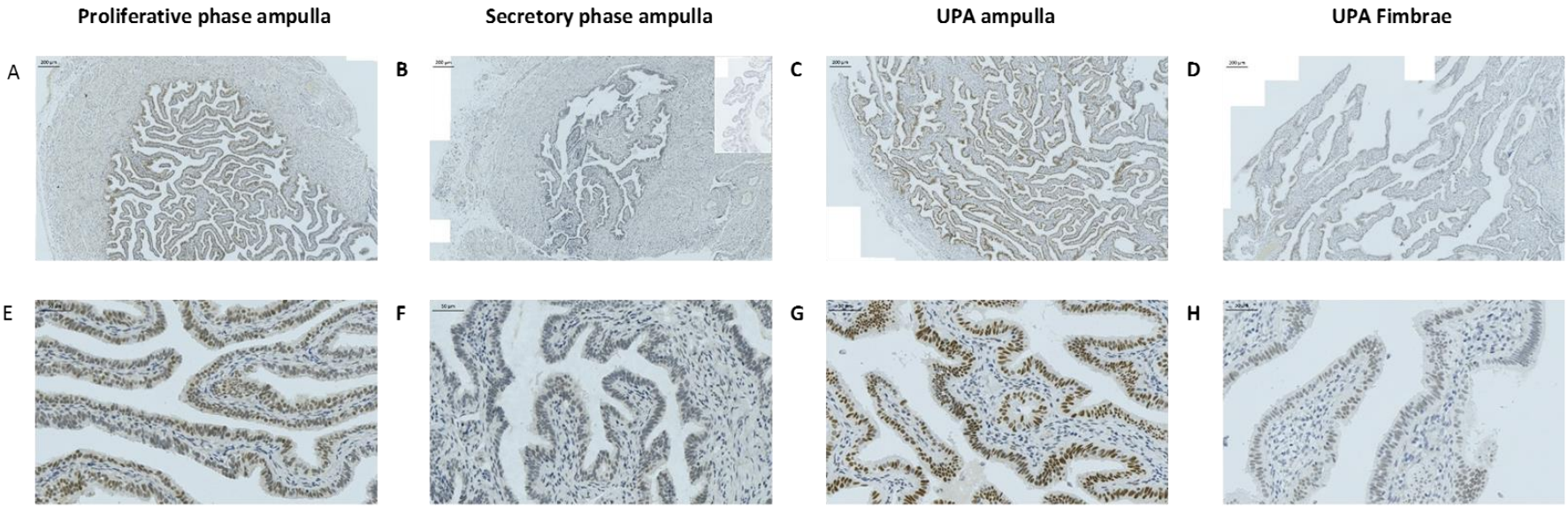

Figure 3.16 Administration of selective progesterone receptor modulator, ulipristal acetate (UPA), increases ampullary epithelial progesterone receptor (PR) expression

Representative images low- (A-D) and high-power (E-H) immuno-localisation of PR in fallopian tube (FT) biopsies from woman during proliferative and secretory stages of the menstrual cycle and after UPA administration. Samples from FT ampulla of UPA-treated women (C&G) displayed intense immunopositive epithelial nuclei with only a few immunopositive cells in the stroma, this immunostaining was less marked at fimbriae ends (D&H). In contrast to UPA, epithelial staining in the FT ampulla was less intense in proliferative phase epithelium (A & E) and further reduced in secretory (B & F) epithelium. There was light intermittent immunopositive nuclear staining of stroma irrespective of phase of cycle or UPA treatment.
Lower power (scale bar = 200µm) and high power magnification (scale bar = 50 µm); Negative controls shown as inserts on secretory fallopian tube low power image.

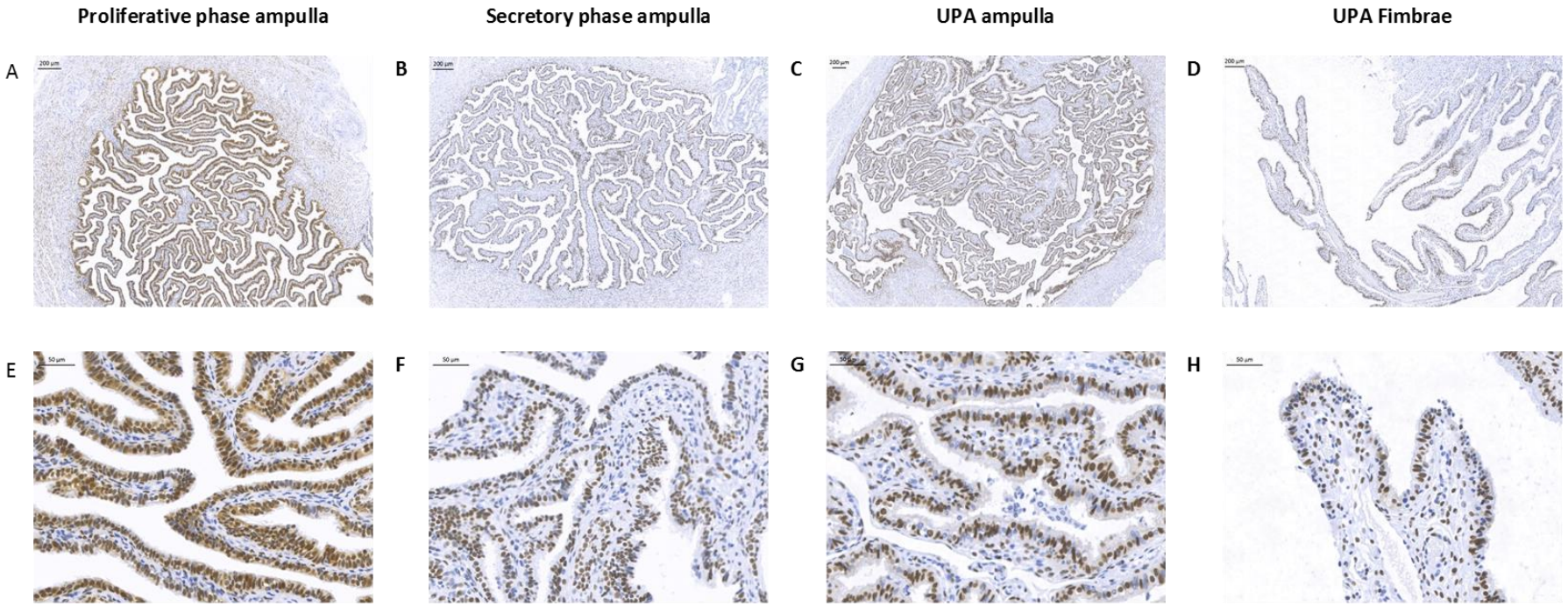

Figure 3.17 Administration of selective progesterone receptor modulator, ulipristal acetate (UPA), does not alter ampullary epithelial progesterone receptor B (PRB) expression

Representative images low- (A-D) and high-power (E-H) immuno-localisation of PRB in fallopian tube (FT) biopsies from woman during proliferative and secretory stages of the menstrual cycle and after UPA administration. Samples from FT ampulla of UPA-treated women (C&G) displayed intense immunoreactive staining in most epithelial nuclei with some immunopositive cells in the stroma, this pattern was replicated at fimbriae ends (D&H). The ampullary pattern of epithelial staining was stronger in the proliferative phase (A&E) and appeared slightly less in secretory phase (B&F). Stromal immunostaining was unchanged irrespective of cycle phase or treatment with UPA (E-H). Lower power (scale bar = 200µm) and high power magnification (scale bar = 50 µm); Negative controls shown as inserts on secretory fallopian tube low power image.

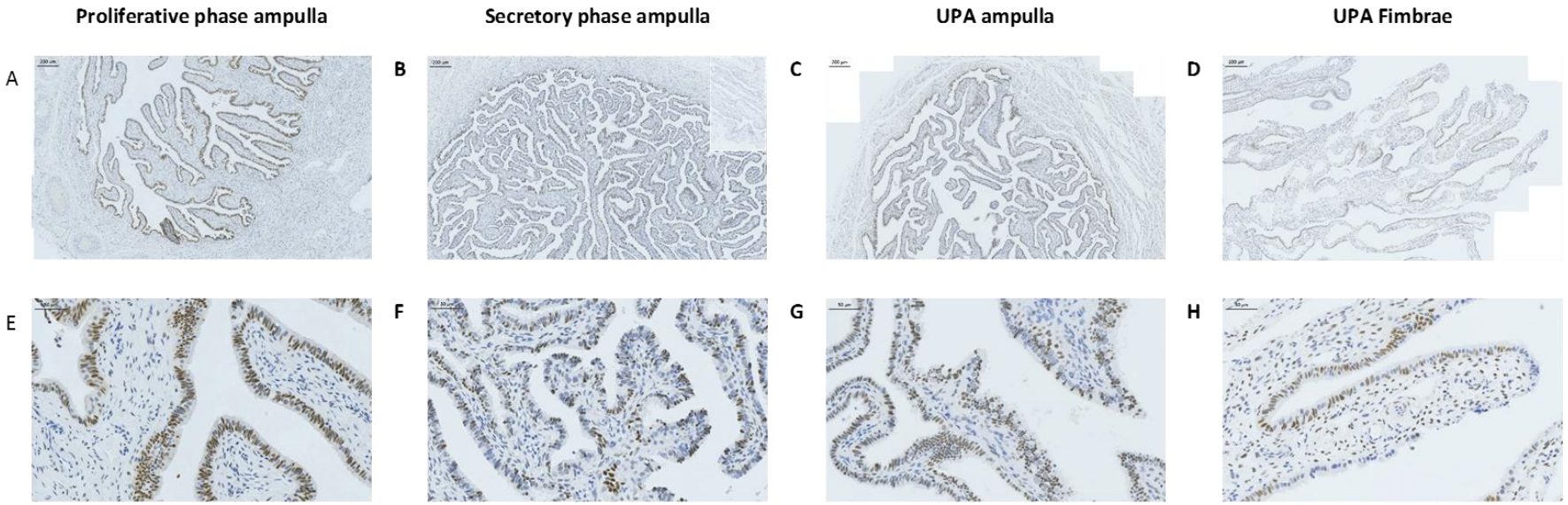

Figure 3.18 Administration of selective progesterone receptor modulator, ulipristal acetate (UPA), does not alter ampullary epithelial androgen receptor (AR) expression

Representative images low- (A-D) and high-power (E-H) immuno-localisation of AR in fallopian tube (FT) biopsies from woman during proliferative and secretory stages of the menstrual cycle and after UPA administration. Epithelial nuclei in ampullary samples from UPA-treated women (C&G) displayed intense immunoreactivity in most epithelial nuclei with some immunopositive cells in the stroma, this pattern was replicated at fimbriae ends (D&H). The ampullary pattern of epithelial staining was stronger in proliferative phase (A&E) and appeared slightly reduced in the secretory phase (B&F). Stromal immunostaining was unchanged irrespective of cycle phase or treatment with UPA.
Lower power (scale bar = 200µm) and high power magnification (scale bar = 50 µm); Negative controls shown as inserts on secretory fallopian tube low power image.

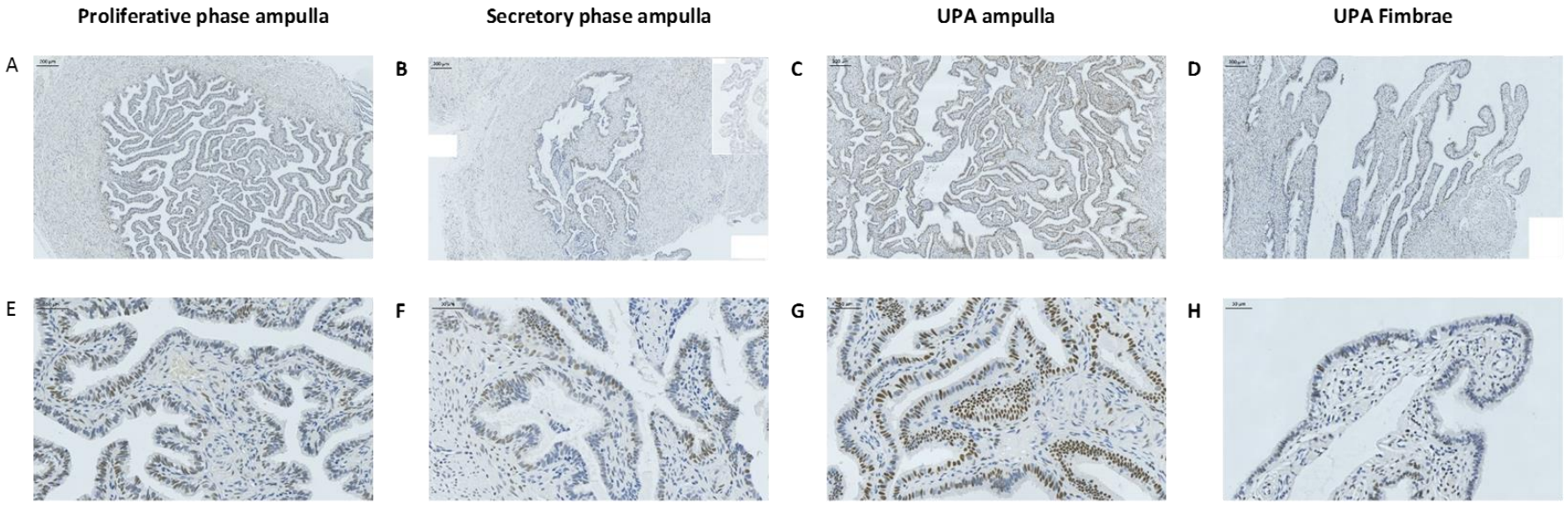

Figure 3.19 Administration of selective progesterone receptor modulator, ulipristal acetate (UPA), increases ampullary epithelial oestrogen receptor alpha (ERα) expression

Representative low- (A-D) and high-power (E-H) immuno-localisation of ERα in fallopian tube (FT) biopsies from woman during proliferative and secretory stages of the menstrual cycle and after UPA administration. Samples from UPA-treated women (C&G) displayed intense immunopositive epithelial nuclei, this immunoreactivity was less marked at fimbriae ends (D&H). In contrast to UPA, epithelial staining was less intense in proliferative phase epithelium (A & E) and secretory (B & F) epithelium. There was light positive staining of most stroma nuclei irrespective of phase of cycle or UPA treatment.
Lower power (scale bar = 200µm) and high power magnification (scale bar = 50 µm); Negative controls shown as inserts on secretory fallopian tube low power image.

Table 3.6 Summary of impact of UPA administration on ampullary fallopian sex-steroid mRNA levels and protein expression and localisation

SSR	Relative mRNA level	Protein expression and localisation					
		Proliferative		Secretory		UPA	
		G	S	G	S	G	S
PR	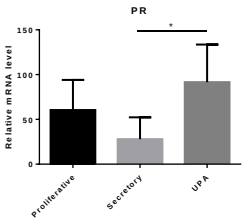	++	+/-	++	+/-	+++	+/-
PRB	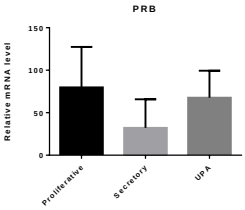	+++	+/-	+	+/-	++	+/-
AR	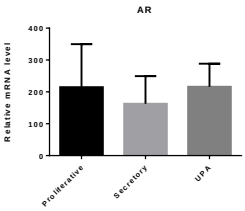	+++	+/-	+	+/-	++	+/-
ERα	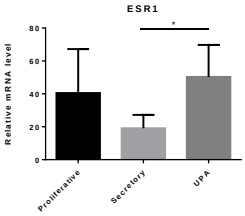	++	+	++	+	+++	+

SSR: sex steroid receptor, G: glandular epithelium; S: stroma PR progesterone receptor; PRB: progesterone receptor B; AR: androgen receptor; ERα: oestrogen receptor alpha.

* p <0.05, ** p <0.01, *** p <0.001

+++ Dense immunopositivity, ++ moderate immunopositivity + light immunopositivity +/- infrequent immunopositivity – absent immunopositivity

3.5.3 Effect of UPA administration upon cervical morphology and sex-steroid receptor expression

3.5.3.1 UPA administration did not alter cervical morphology

Cervical biopsy gross morphology on H&E staining was unchanged between proliferative phase (Figure 3.20A, D & G), secretory phase (Figure 3.20B, E & H) and from women receiving treatment with UPA (3.20C, F & I). There no evidence of cervical intraepithelial neoplasia (CIN) in any samples. Transformation zone epithelium was absent due to sampling artefact in three of the UPA treated women and one from secretory phase. There was evidence of squamous metaplasia in two of the UPA treated women – this was considered to be acceptable physiological variation.

3.5.3.2 Administration of UPA did not alter sex-steroid receptor expression in the cervix

Strong immunopositivity of PR was observed in the stroma, squamous and glandular epithelium of proliferative phase (Figure 3.21A, D & G), secretory phase (Figure 3.21B, E &H) and following UPA treatment (Figure 3.21C, F & I). Similarly there was no difference in staining intensity or frequency between phase of cycle or UPA for PRB immunolocalisation in all cell types (Figure 3.22), although overall positive staining was not present in all stromal nuclei (Figure 3.22G-I). The degree of squamous PRB immunopositivity (with relative sparing of the basement membrane; Figure 3.22A-C) was less compared to PR (Figure 3.21A-C) but unchanged by cycle stage or UPA treatment. AR immunolocalisation was unaltered by stage of cycle or UPA treatment with dense immunopositivity observed in all glandular epithelium (Figure 3.23D-I), stroma (Figure 3.23G-I) and squamous epithelium (including the basement membrane; Figure 3.23A-C). ERα immunoreactivity was also unaltered between proliferative and secretory phase and UPA treatment but appeared less ubiquitous than other sex-steroid receptor immunolocalisation (Figure 3.24). Intermittent immunoreactivity was present in the squamous epithelium with only occasional positive nuclear staining in basement membrane (Figure 3.24A-C). Intermittent but dense staining was present in the stroma and glandular epithelium of proliferative (Figure 3.24D & G), squamous (Figure 3.24E & H) and UPA-treated (Figure 3.24F & I) cervical biopsies.

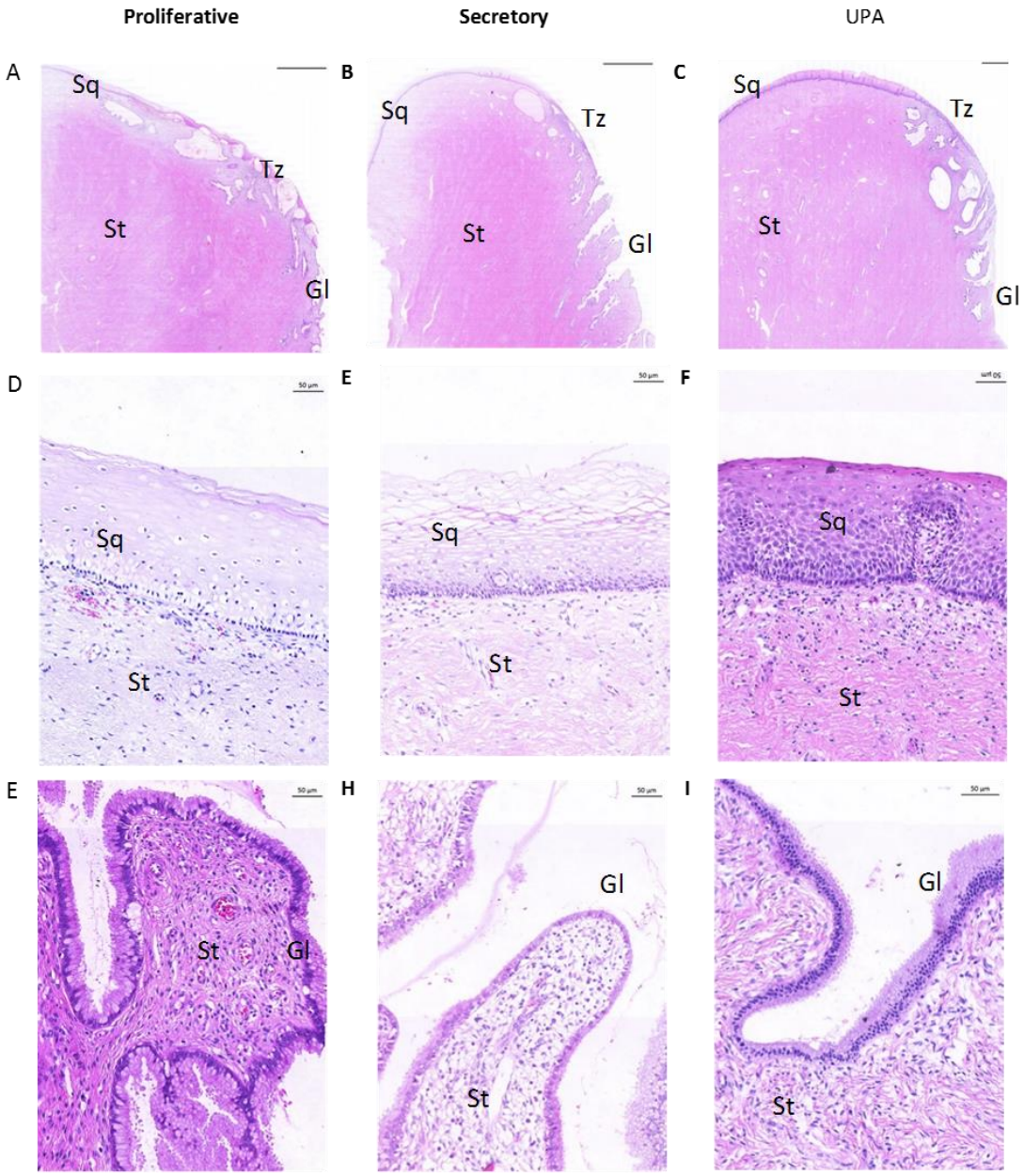

Figure 3.20 Representative H&E images of human uterine cervix

A-C macroscopic images demonstrating ectocervical squamous epithelium (Sq), endocervical glandular epithelium (Gl) and the underlying stroma (St). The transformation zone (Tz) separates the true glandular and squamous epithelium. Samples from women in proliferative phase (A, D & G), secretory phase (B, E & H) and from women receiving treatment with UPA (C, F & I).

Higher power squamous (D-F) and glandular (G-I) demonstrate similar appearance irrespective of stage of the menstrual cycle or UPA treatment.

Scale bars lower power 2000µm high power 50µm

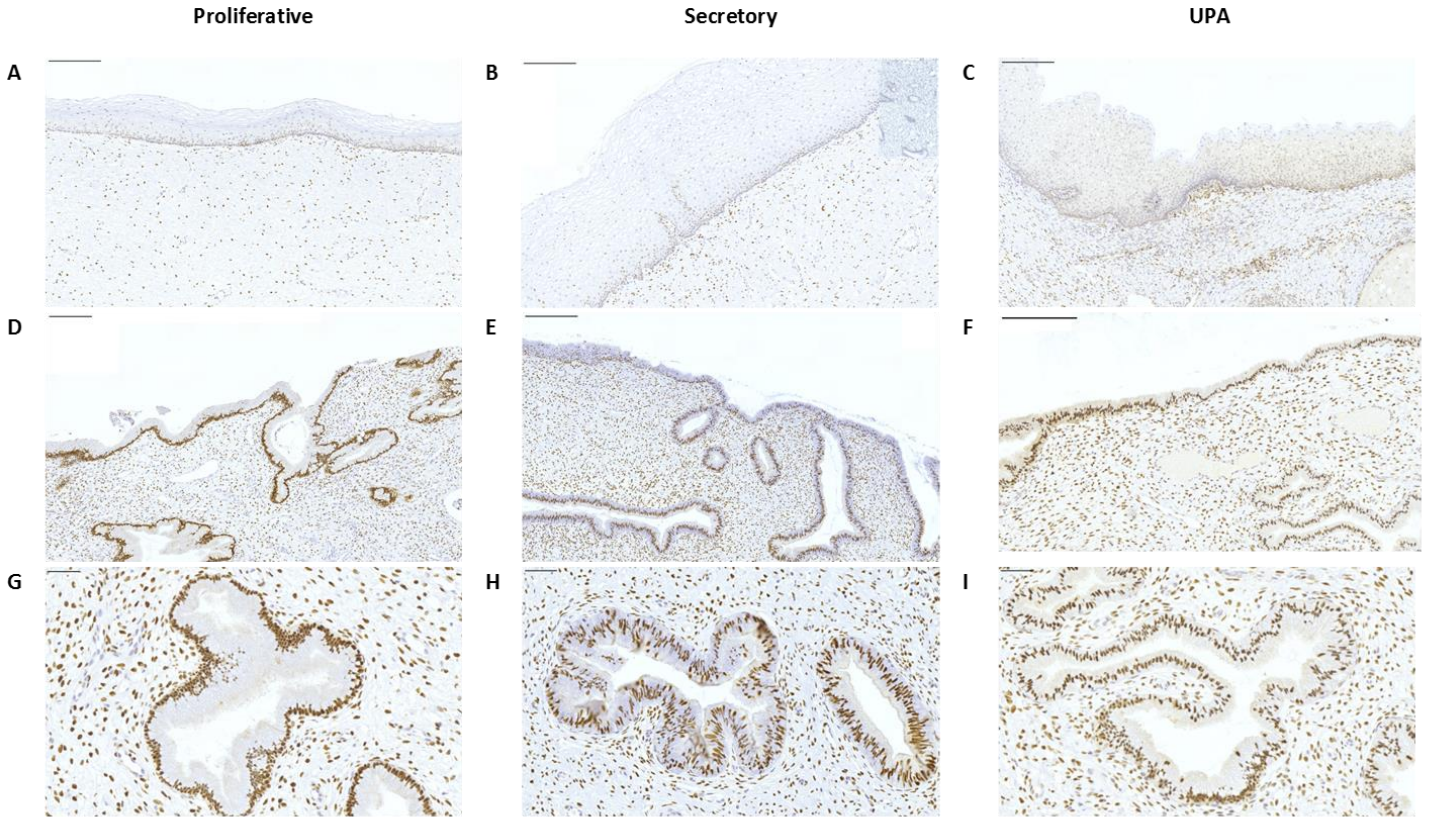

Figure 3.21 Administration of selective progesterone receptor modulator, ulipristal acetate (UPA), does not alter progesterone receptor (PR) localisation or intensity in the endo- or ecto-cervix

Representative low- (A-F) and high-power (G-I) immuno-localisation of PR in cervical biopsies from woman during proliferative (A/D/G) and secretory (B/E/H) stages of the menstrual cycle and after UPA (C/F/I)) administration. Intense immunopositive nuclei were present in the stroma, squamous (D, E F) and glandular (G/H/I) epithelium. Localisation and intensity of immunostaining was unchanged irrespective of stage of cycle or treatment with UPA. Medium power (scale bar = 200µm) and high power magnification (scale bar = 50 µm); Negative controls shown as inserts on secretory cervix.

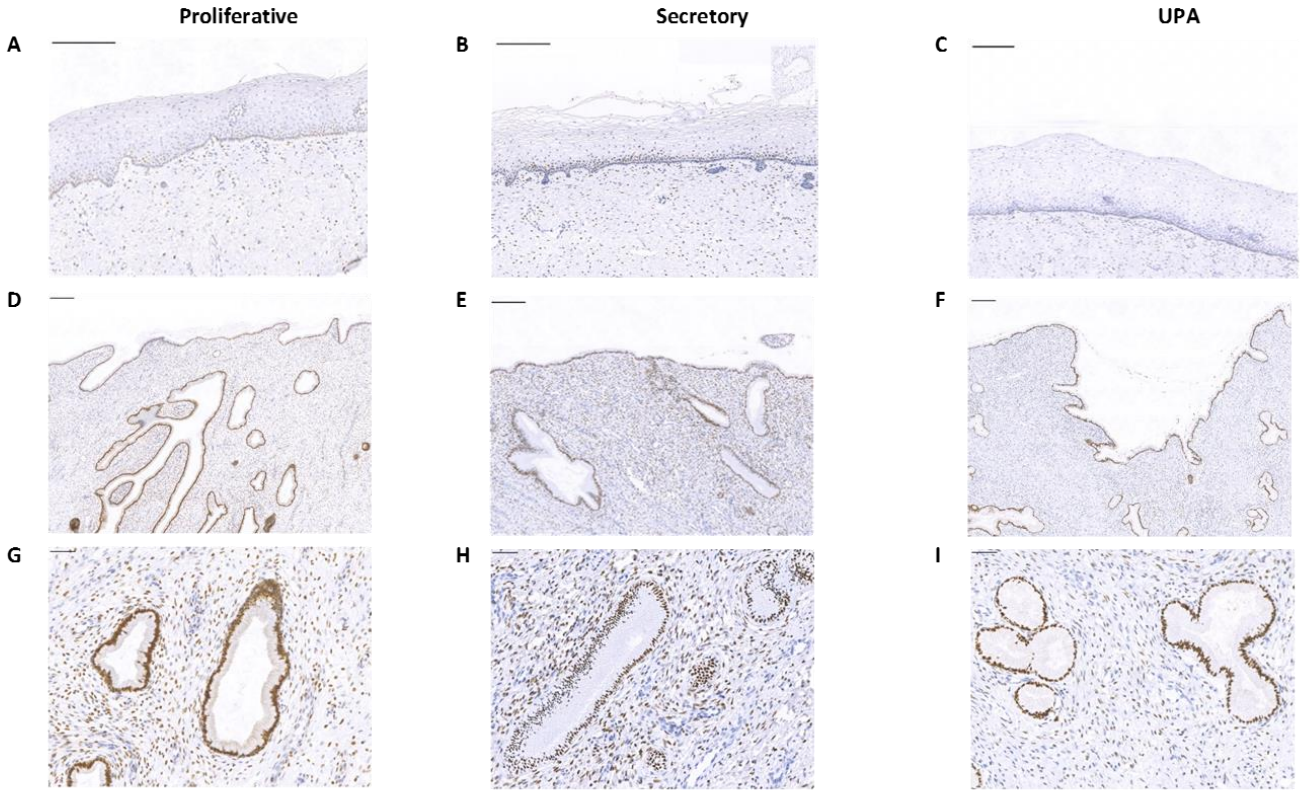

Figure 3.22 Administration of selective progesterone receptor modulator, ulipristal acetate (UPA), does not alter progesterone receptor B (PRB) localisation or intensity in the endo- or ecto-cervix

Representative low- (A-F) and high-power (G-I) immuno-localisation of PR in cervical biopsies from woman during proliferative (A/D/G) and secretory (B/E/H) stages of the menstrual cycle and after UPA (C/F/I)) administration. Intense immunopositive nuclei were present in glandular (G/H/I) epithelium. Less intense immunopositive nuclei were seen in the stroma (G/H/I). Lightly stained immunopositive nuclei were seen in the basement membrane of the squamous epithelium (D, E F) Localisation and intensity of immunostaining was unchanged irrespective of stage of cycle or treatment with UPA. Medium power (scale bar = 200µm) and high power magnification (scale bar = 50 µm); Negative controls shown as inserts on secretory cervix.

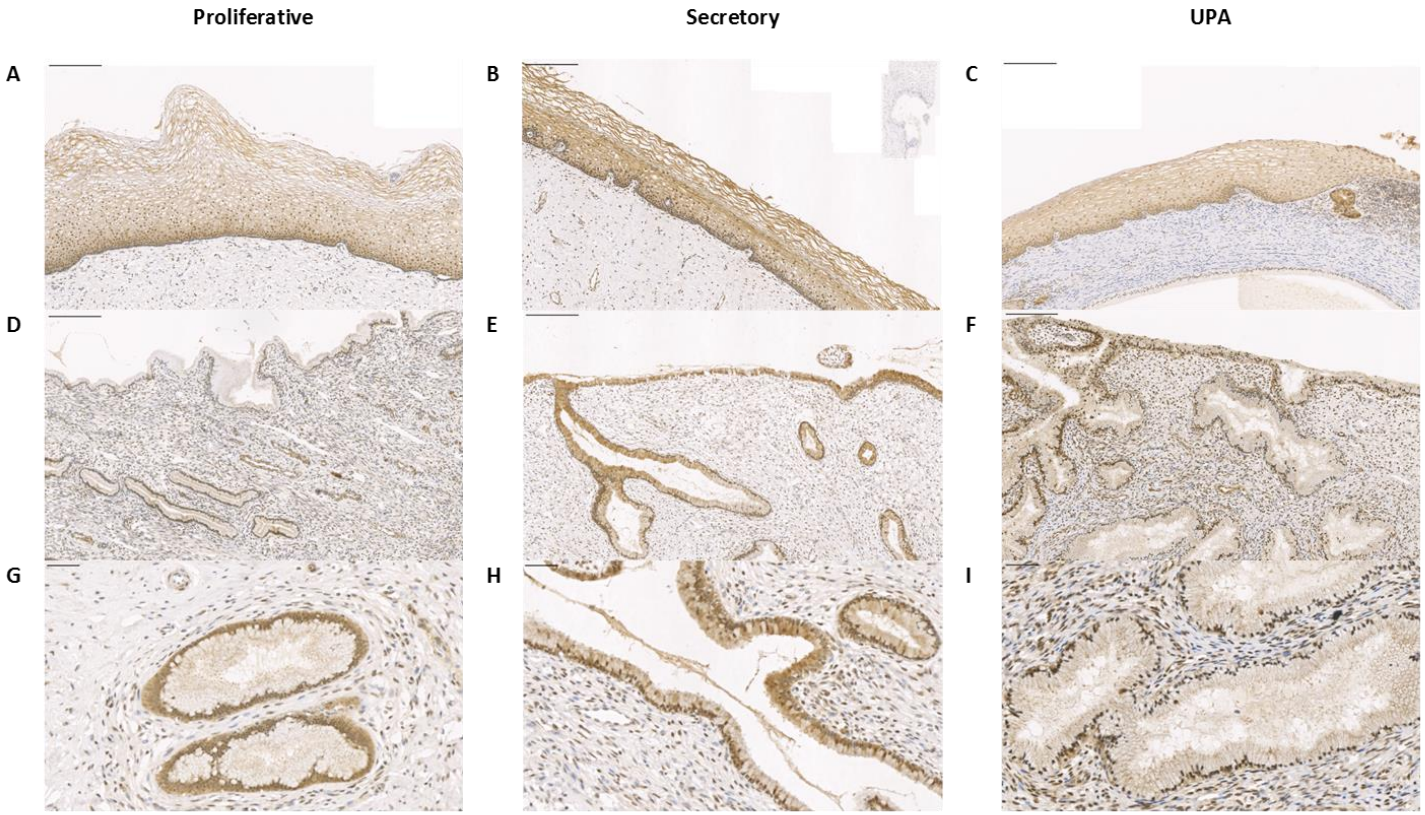

Figure 3.23 Administration of selective progesterone receptor modulator, ulipristal acetate (UPA), does not alter androgen receptor (AR) localisation or intensity in the endo- or ecto-cervix

Representative low- (A-F) and high-power (G-I) immuno-localisation of AR in cervical biopsies from woman during proliferative (A/D/G) and secretory (B/E/H) stages of the menstrual cycle and after UPA (C/F/I)) administration. Intense immunopositive nuclei were present in the stroma, squamous (D, E F) and glandular (G/H/I) epithelium. Localisation and intensity of immunostaining was unchanged irrespective of stage of cycle or treatment with UPA. Medium power (scale bar = 200µm) and high power magnification (scale bar = 50 µm); Negative controls shown as inserts on secretory cervix.

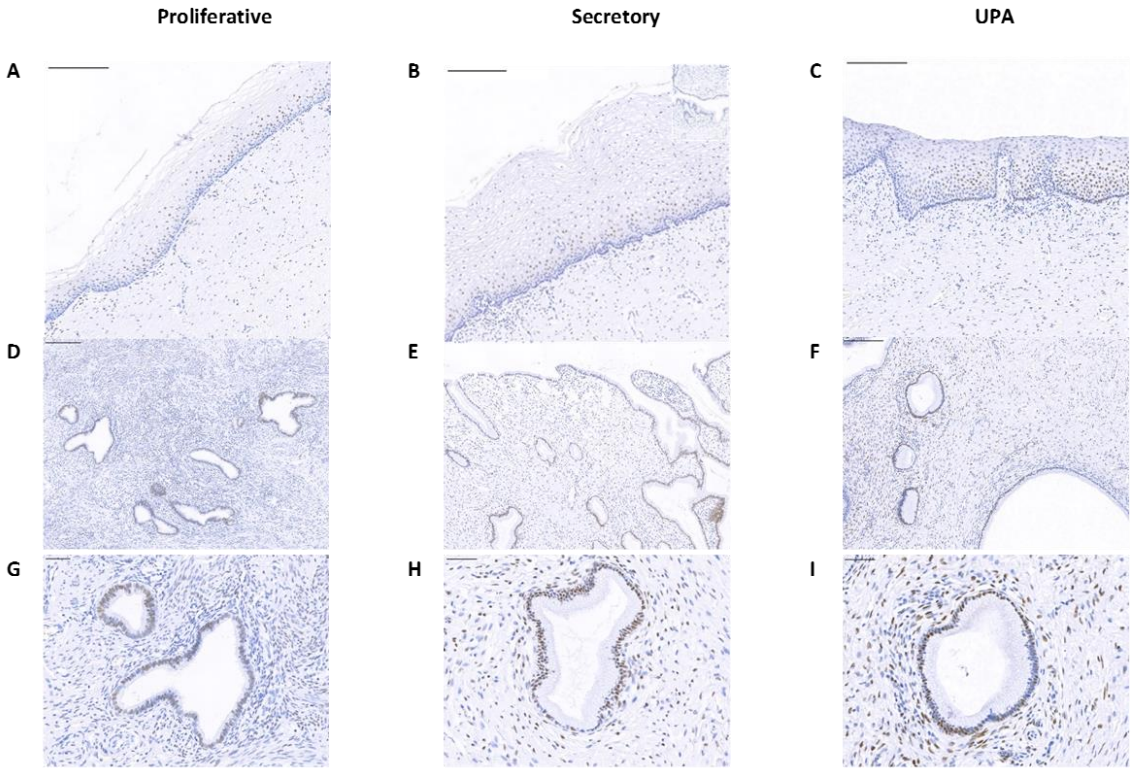

Figure 3.24 Administration of selective progesterone receptor modulator, ulipristal acetate (UPA), replicates secretory phase oestrogen receptor alpha (ERα) localisation and intensity in the endo- and ecto-cervix

Representative low- (A-F) and high-power (G-I) immuno-localisation of AR in cervical biopsies from woman during proliferative (A/D/G) and secretory (B/E/H) stages of the menstrual cycle and after UPA (C/F/I) administration. Immunopositive nuclei were present in the squamous epithelium above the basement membrane of squamous epithelial cells irrespective of stage of cycle or UPA treatment (A/B/C). Light immuno-positive nuclei of glandular epithelium and some stromal cells were visualized in proliferative phase cervical biopsies (A/D/G), in contrast secretory (B/E/H) and UPA-treated (C/F/I) cervix demonstrated more intense immune-positivity of glandular epithelial and stromal nuclei though was not present in all nuclei. Medium power (scale bar = 200µm) and high power magnification (scale bar = 50 µm); Negative controls shown as inserts on secretory cervix

3.5.3.2 Summary of impact of UPA on sex-steroid receptor expression and localisation in the cervix

The results of the effect of UPA upon sex-steroid receptors in the cervix are summarised in Table 3.7.

Table 3.7 Summary of impact of UPA on sex-steroid receptor expression and localisation in the cervix

SSR	Protein expression and localisation								
	Proliferative			Secretory			UPA		
	Squam	G	S	Squam	G	S	Squam	G	S
PR	++	+++	++	++	+++	++	++	+++	++
PRB	+	+++	+	+	+++	+	+	+++	+
AR	+++	+++	++	+++	+++	++	+++	+++	++
ERα	+	++	+	+	++	+	+	++	+

SSR: sex steroid receptor, G: glandular epithelium; S: stroma PR progesterone receptor; PRB: progesterone receptor B; AR: androgen receptor; ERα: oestrogen receptor alpha.

+++ Dense immunopositivity, ++ moderate immunopositivity + light immunopositivity +/- infrequent immunopositivity – absent immunopositivity

3.6 Discussion

Ulipristal acetate (UPA) is a SPRM, which, like other members of this class of compound has mixed agonist and antagonist effects (Chabbert-Buffet, Meduri et al. 2005, Bouchard and Chabbert-Buffet 2016, Wagenfeld, Saunders et al. 2016). The impact of SPRMs is tissue dependent and this may be influenced both by concentrations of different co-repressor and co-activator proteins and bioavailabilty of different PR isoforms in different cell types (Wagenfeld, Saunders et al. 2016). In this study it was demonstrated that UPA administration has profound effects on endometrial morphology and alters the pattern of expression of PR, PRB and AR in the endometrium. This is the first comprehensive description on the impact of in vivo UPA administration on SSR

expression and localisation in human endometrium (Whitaker, Murray et al. 2017). Furthermore, administration of UPA appears to increase expression of PR and ERα in the fallopian tube relative to secretory but not proliferative phase and has no impact on SSR expression in the cervix.

3.6.1 Endometrium

Whilst all endometrial biopsies demonstrated evidence of PAEC, in keeping with established literature (Williams, Bergeron et al. 2012) the degree of histological change within the endometrium varied with some biopsies demonstrating a greater degree of cystic dilatation. The impact of this histological observation upon symptom control is unknown. In our study the degree of cystic dilatation was not correlated with duration of treatment or control of bleeding.

Larger studies have demonstrated PAEC rates of around 74% following a 3-month course of UPA administration (Williams, Bergeron et al. 2012), and this rapidly regressed on cessation of treatment (Donnez, Vazquez et al. 2014, Donnez, Hudecek et al. 2015). It should be noted that suction catheters (e.g. pipelle biopsy catheters) obtained the biopsies assessed in these studies described above. This sampling technique may disrupt the dilated cysts and either render specimens inadequate for assessment or with such disrupted tissue that only those with familiarity of the more subtle manifestations of PAEC may conclude this as the histopathological opinion (Professor ARW Williams, personal communication). In contrast full thickness endometrial biopsies (luminal epithelium to endometrial-myometrial junction), obtained at the time of hysterectomy (as in this thesis), allow comprehensive assessment of a larger biopsy, which has not been unduly distorted by sampling artefact. Familiarity with the features of PAEC remains critical for accurate histopathological assessment.

The true incidence of PAEC whilst on SPRM treatment remains uncertain, and it is unknown as to whether it results in a field change with the endometrium of the entire uterus or results in discrete areas of focal change. Given that two separate biopsies from each individual women, obtained from differing areas of the uterine cavity, both demonstrated PAEC it would imply the former, but detailed descriptions of the extent of histological change within the uterus remains lacking in the literature. The only study to comment on rates of PAEC in discrete separate areas of the uterus (fundus, mid corpus and isthmus) was one of the studies involving the administration of the SPRM, asoprisnil.

That study concluded that rates were similar in each region (Williams, Critchley et al. 2007). Whilst PAEC is considered a 'class effect' (Mutter, Bergeron et al. 2008), variability in reporting classifications (Murji, Whitaker et al. 2017) means that it is impossible at present to draw accurate conclusions as to whether different members of the SPRM class truly have the same likelihood of development of PAEC.

Administration of UPA increases levels of both PR and PRB mRNA. Both the A and B isoforms are expressed in a differential manner within the endometrium in the normally cycling woman (Wang, Critchley et al. 1998, Mote, Balleine et al. 1999). The data herein demonstrate marked upregulation within the glandular epithelium of both PR isoforms and downregulation within the stroma following UPA administration. This pattern of expression neither phenocopied proliferative nor secretory phase endometrium. This is inconsistent with a study of PR expression in the NHP following UPA administration where in that study expression phenocopied proliferative phase (Brenner, Slayden et al. 2010). The striking switch in PR protein localisation observed when compared to secretory phase demonstrated in this thesis is consistent with previous reports studying the effect of another SPRM, asoprisnil, on PR protein localisation in human endometrium (Wilkens, Male et al. 2013). In contrast the SPRM mifepristone does not appear to down regulate stromal expression in both animal models and human studies (Slayden and Brenner 1994, Narvekar, Cameron et al. 2004). The relatively pure P-antagonist ZK 137316 resulted in stromal down regulation of PR protein localisation that was limited to the basal compartment (Slayden, Zelinski-Wooten et al. 1998). In this current study I have demonstrated stromal down regulation of PR and PRB in both the functional and basal layers. It is not clear whether this differing expression pattern is determined by the relative degree of pure PR antagonism associated with mifepristone, ZK 137316 and UPA (Elger, Bartley et al. 2000, Chabbert-Buffet, Meduri et al. 2005) or if other factors contribute to this such as differing interaction of co-regulators such as the nuclear co-receptors (NcoR) (Afhuppe, Sommer et al. 2009).

The data presented in this thesis are the first to describe the effects of UPA on PRB expression (Whitaker, Murray et al. 2017). The apparent slight reduction in immunopositivity of PRB expression compared with PR (A+B isoforms) suggests that both isoforms are differentially expressed following UPA administration, but this has not been formally quantified. This finding of PRB immunolocalistion mirrors that observed with mifepristone in human endometrium (Sun, Christow et al. 2003).

One of the most striking findings in this study was the impact on AR expression. A significant increase in concentrations of *AR* mRNA was demonstrated, which was accompanied by a unique pattern of AR protein expression. This was distinct to that reported in the endometrium of a woman during a normal menstrual cycle or following intra-uterine levonorgestrel exposure (Slayden, Nayak et al. 2001, Burton, Henderson et al. 2003, Marshall, Lowrey et al. 2011). The up-regulation of AR expression in the epithelium with preserved stromal immunopositivity in the human described in this thesis are consistent with reports of assessment of the endometrium from Rhesus macaques following treatment with an intrauterine device containing UPA for three artificial menstrual cycles (Brenner, Slayden et al. 2010). These findings are also noted in both human and animal studies following administration of mifepristone (both following 2mg for 30 days or a single dose of 200mg; (Slayden, Nayak et al. 2001). Studies of the effect of SPRM administration on epithelial AR expression in NHP models have demonstrated that up regulation is limited to the functional layer of the endometrium. The exception to this was ZK 137316 administered to NHP where basal epithelial immunopositivity was observed (Slayden, Nayak et al. 2001). This was consistent with the observations (data presented in this thesis) of up regulation of AR by UPA in both functional and basal layers of the endometrium. This further demonstrates the differing impacts of SPRMs with regard to SSR expression and may be either a product or cause of the variable degree of progesterone antagonism. The effect upon AR expression in women following UPA administration is of particular import as in the NHP AR maybe critical to the anti-proliferative effect following SPRM administration (Slayden and Brenner 2003). This is discussed in further detail in chapter five of this thesis.

The pattern of expression of *ESR1* (ERα) mRNA and protein after treatment with UPA was similar to that of the proliferative phase. This suggests that UPA did not induce PR-dependent down regulation of ERα gene expression. This is consistent with the observation of unaltered ER expression and localisation following the administration of UPA to the NHP (Brenner, Slayden et al. 2010). A similar pattern phenocopying proliferative phase is also observed in NHP (Slayden and Brenner 1994) and women (Narvekar, Cameron et al. 2004) following administration of SPRM, mifepristone.

Whilst the effects on SSR expression have not been quantified in this study, the profound effect upon localisation of PR, PRB and AR protein renders this less critical to conclusion

regarding the impact of UPA on the endometrium. The non-significant rise in mRNA expression of *ESR1* compared to proliferative phase and similar pattern of immunopositivity may suggest quantification to be of importance, particularly given the impact on proliferation and should be considered for future work.

3.6.2 Fallopian tube

The findings with regard to the effect of UPA administration on the fallopian tube complement and extend the existing literature. In keeping with the findings of *in vitro* treatment with UPA on human fallopian tubes, ampullary morphology resembled proliferative phase (Yuan, Zhao et al. 2015). This is also consistent with the effect on morphology with administration of mifepristone in the NHP (Slayden and Brenner 1994). SSR mRNA levels were unchanged relative to proliferative phase but *PR* and *ESR1* were down-regulated relative to secretory phase, consistent with P-antagonism. In contrast to SSR protein expression in the endometrium, ampullary SSR expression demonstrated no alteration in the localisation of SSR expression. Epithelial immunopositivity was increased following UPA administration relative to secretory levels of both PR and ERα. The pattern appeared similar to proliferative with an apparent slight increase in density of staining following UPA but this has not been formally quantified. Given the small number of subjects and lack of quantification in this study limited weight can be given to an inference that UPA up regulates PR and ERα relative to proliferative phase. The up regulation of PR and ERα relative to secretory phase is consistent with the effect of *in vitro* studies of UPA treatment of human fallopian tubes (Yuan, Zhao et al. 2015) and findings in the NHP following *in vivo* mifepristone administration (Slayden and Brenner 1994). In human studies of *in vivo* mifepristone treatment both PR and PRB was markedly up regulated relative to secretory phase (Christow, Sun et al. 2002, Sun, Christow et al. 2003). In contrast, this study of UPA the effect appeared limited to the PRA isoform only at an mRNA level. It is uncertain if this is an effect of a differing SPRM administration, as the NHP study of mifepristone did not assess the impact on the PRB isoform. Equally in this study of UPA, it does appear at a protein level that PRB expression may be slightly reduced in secretory phase relative to UPA but this not been quantified with either stereology or western blot studies. There are no published data regarding impact of SPRMs on AR expression in the Fallopian tube to compare with the findings of studies in this thesis. Lack of significant alteration in mRNA is consistent with no significant alteration in AR in fallopian tube across the cycle

(Horne, King et al. 2009). Thus it is perhaps unsurprising that mRNA and protein expression of AR do not significantly alter following UPA administration.

It has previously been demonstrated that SSR expression of PR and ER is altered in the different regions of the fallopian tube (Amso, Crow et al. 1994). Here in this thesis, it is demonstrated that immunopositivity of PRB and AR is unchanged between the ampulla and the fimbriae, but expression of PR, and ERα is reduced in the fimbriae relative to the ampulla. Limited conclusions can be drawn from this given that untreated fimbriae from women in proliferative and secretory phase were not available to assess relative alteration at this site. This requires further inspection, not least as the fimbrial ends of the fallopian tube are now considered a potential site for the development of future high grade serous ovarian cancer (Crum, Herfs et al. 2013) and any compound that impacts upon SSR expression in this site may have implications for future tumour genesis. Whilst mifepristone has been shown to be ineffective for the treatment of recurrent ovarian cancer (Rocereto, Brady et al. 2010) an RCT is currently underway to assess the impact of mifepristone on women with *BRCA1* & *2* mutations with development of ovarian disease investigated as a secondary measure (https://clinicaltrials.gov/ct2/show/NCT01898312).

3.6.3 Cervix

There was no alteration in morphology and SSR expression in the cervix following administration of UPA. The data presented in this thesis are the first description of the impact of UPA on the non-pregnant human cervix following in vivo treatment with an SPRM, albeit in a small number of samples. mRNA levels were not quantified due to difficulties in consistently sampling the same region and availability of control samples. Laser capture is a technique for future consideration that may facilitate the accurate quantification of transcription in the differing cell compartments.

As previously described, the degree of cyclical change of PR expression in both glandular and stromal epithelium is minimal (Lin 1984, Cano, Serra et al. 1990). *In vitro* studies and data from pregnancy models imply that the effect of mifepristone was predominantly related to the blockade of progesterone-mediated response that resulted in altered functionality. In the former of these high dose P-agonists were administered (Ackerman, Summerfield et al. 2016) and in the latter, pregnancy resulted in altered circulating P4 (Yellon, Dobyns et al. 2013). Given that both these states are consistent

with much higher levels of circulating ligand it is perhaps unsurprising that in the context of normally cycling woman, administration of a SPRM results in minimal alteration of SSR compared to either proliferative or secretory phase. Studies of mifepristone have indicated an alteration in immune-cell (specifically macrophages) populations (Kirby, Heuerman et al. 2016). In the endometrium asoprisnil impacted upon CD56 (a marker of uterine NK cells) expression (Wilkens, Male et al. 2013). Whilst no apparent alteration in SSR expression was observed following UPA administration, the impact on immune-cell populations would merit further inspection.

3.6.4 Future work

The impact of UPA administration on morphology and SSR expression is most dramatic in the endometrium. Described in chapter 3 are some of the existing uncertainties with regard to the effect of UPA in the reproductive tract including true incidence of PAEC, and evidence regarding focality, quantification of SSR expression and localisation in the fallopian tube and cervix. In the fallopian tube, UPA administration relatively phenocopies proliferative phase and in the cervix there is no demonstrable difference following UPA administration. All three structures arise from the paramesonephric duct but differentiate into their separate structures. *Wnt* signalling and *Hox* genes help regulate this process and expression of *HOX* genes continues through adult life. This functional differentiation may explain why, though SSR are expressed in all three anatomical regions, the response to UPA is altered. The impact upon HOXA10 is assessed in chapter 4, but *Hoxa9, -11* and *-13* have not been assessed in this study.

The effect of sex-steroid action is regulated by the availability of the ligand (be it endogenous or synthetic) and the cognate receptor. The amount of free ligand can be modified by steroid metabolising enzymes, in the human these include the 17-βhydroxysteroid dehydrogenase family (17βHSD) (Lathe and Kotelevtsev 2014). The type 2 isoform (17βHSD2) has a major role in regulating the conversion of more potent E2 to the less potent oestrone (Thomas and Potter 2013). It also activates progesterone and converts androgens to less potent forms (Burton, Henderson et al. 2003). 17βHSD2 is expressed in the glandular endometrium and is up regulated by progesterone (Maentausta, Svalander et al. 1993). However whilst the synthetic progestin levonorgestrel initially increases *17βHSD2* mRNA expression, over time this declines (Burton, Henderson et al. 2003). There is evidence that the SPRM mifepristone can block

the expression of 17βHSD2 (Sivik and Jansson 2012). There is no published evidence of the impact of UPA on 17βHSD2 expression and this merits further investigation given the critical role 17βHSD2 plays in the availability of sex-steroid ligands.

This study is limited to the sex-steroids receptors. Only the alpha subunit of ER was investigated. ERβ was outwith the scope of this study but merits further study. It is postulated to attenuate response of ERα to E2 in the endometrium (Hapangama, Kamal et al. 2015) and is differentially expressed in the fallopian tube depending upon stage of menstrual cycle (Horne, King et al. 2009).

Other steroid receptors exist within the endometrium including the glucocorticoid receptor (GR) and the mineralocorticoid (MR) (Henderson, Saunders et al. 2003, McDonald, Henderson et al. 2006). GR is expressed in endometrial stromal cells and MR is present in both stromal and glandular compartments (McDonald, Henderson et al. 2006). Glucocorticoids may play a significant role in endometrial function and repair (Critchley and Maybin 2011, Maybin and Critchley 2015). Inactivation of cortisol is associated with HMB (Rae, Mohamad et al. 2009). UPA exhibits GR binding, albeit with a much-reduced affinity than mifepristone (Attardi, Burgenson et al. 2004) but data regarding impact of SPRMs upon protein expression of GR and MR within the endometrium are lacking.

Availability of active cortisol is regulated by the 11β-HSD family (McDonald, Henderson et al. 2006) with 11β-HSD1 increasing local tissue availability of cortisol and 11β-HSD2 decreasing availability by conversion to inactive cortisone (Rae, Mohamad et al. 2009, Thiruchelvam, Maybin et al. 2016). This further underscores the need to assess the impact of SPRMs on the 11β-HSD family as well as GR and MR.

There is one outstanding epithelial component of the reproductive tract that has not been assessed: the squamous epithelium of the vagina. SSR are expressed in the vagina and respond to menstrual cycle stage hormonal fluctuations; E2 stimulates vaginal epithelial proliferation and P4 promotes epithelial maturation (Ayehunie, Islam et al. 2015). A previous study of mifepristone administration demonstrated no effect on morphology, SSR expression or localisation (Narvekar, Lakha et al. 2007) and thus the effect of UPA on vaginal epithelium was not considered a priority for this current series

of investigations. The effects upon UPA on fibroids and myometrial SSR are also outwith the scope of this thesis.

3.7 Conclusions

The results presented within this chapter demonstrate that UPA administration has profound effects on endometrial morphology, and the data presented herein extend the published literature. This is the first description of the impact of *in vivo* treatment with UPA on the morphology of the human fallopian tubes, which resemble proliferative phase, in keeping with the effects observed with other SPRMs. UPA does not alter human cervical morphology. Sex-steroid receptor mRNA levels of PR, PRB, ERα and AR are altered in the endometrium by treatment with UPA. There is alteration in ampullary sex-steroid receptor mRNA levels in the fallopian tube but this is limited to PR and ERα and this is relative only to the secretory phase. This is thus the first extensive description of the impact of UPA administration on localisation of sex-steroid receptor in the reproductive tract. Within the endometrium PR, PRB and AR all demonstrate profound spatial alteration in the localisation of protein expression which does not replicate either proliferative or secretory patterns of expression. In the ampullary fallopian tube localisation appeared unaltered, and immunopositivity most closely resembled proliferative phase. This suggests the impact of UPA in the fallopian tube is limited to blockade of the usual secretory phase progesterone-driven antagonism of the action of oestradiol only. Sex-steroid receptor expression in the cervix was unchanged by UPA. Thus in conclusion treatment with ulipristal acetate appears to have an "endometrial specific" effect upon the morphology and sex-steroid receptor expression in the epithelium of the human reproductive tract.

Chapter 4.

The impact of selective progesterone receptor modulator (SPRM), ulipristal acetate (UPA), administration on progesterone receptor responsive genes in the endometrium

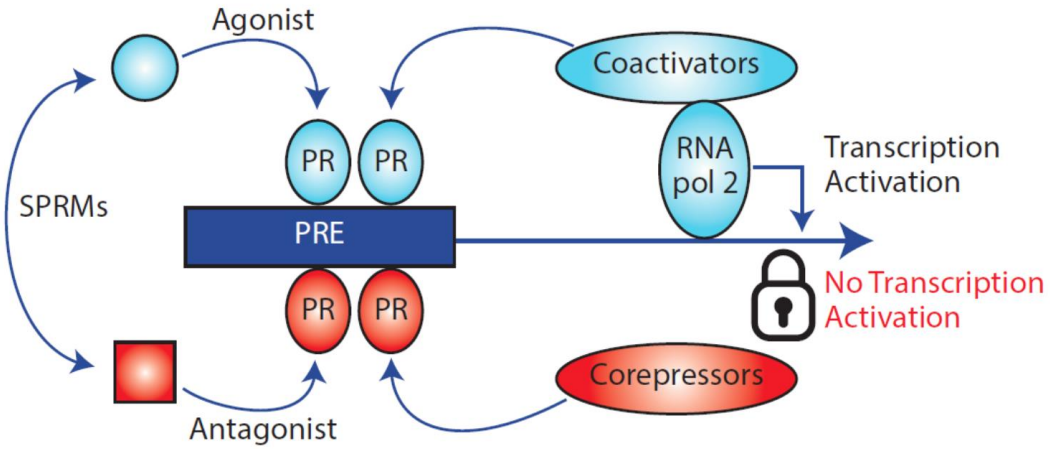

Figure 4.1 Activation of the progesterone receptor (PR) by progesterone receptor ligands.

Binding of progesterone to the inactive progesterone receptor complex induces a conformational change. This results in dissociation of heat shock proteins, dimerization and translocation of PR to the nucleus.

The PR then binds to the progesterone response element (PRE) in promoter regions of target genes and subsequent communication with the RNA polymerase RNA POL2 results in alteration of gene transcription. This process is modified by co-regulatory proteins, that may either increase or decrease gene transcription.

Other ligands (including SPRMs) for the PR results in differing recruitment of co-activators and co-repressors, altering transcriptional activity. The same SPRM may have different relative agonist and antagonist effects, dependent upon target tissue.

4.1 Background

4.1.1 Progesterone regulation of transcription

Progesterone (P4), as described in Chapter 3, is a 21 carbon sex-steroid hormone (**Figure 3.5**). It has key roles in female reproduction related tissues, regulating development, differentiation and normal functioning of target tissues. It may act both by ligand binding to its cognate receptor, the progesterone receptor (PR) (Tsai and O'Malley 1994), a member of the nuclear hormone receptor superfamily (Mangelsdorf, Thummel et al. 1995), and via non-genomic signalling following cytoplasmic binding to membrane bound receptors (Gellersen, Fernandes et al. 2009). As with others of this family, PR has an N-terminal A/B region, a DNA binding domain (DBD, C), a hinge region (D) and a C-terminal (E) which contains the ligand binding domain (LBD) (**Figure 3.6**). PR has two protein isoforms: PRA and PRB, both of which are encoded by the same gene. Both PRA and PRB act as ligand activated transcription factors (Patel, Elguero et al. 2015).

Unbound PR is located in the cytoplasm, complexed with a heat shock protein (HSP). On binding with a ligand, there is a conformational change and the HSP dissociates. This process is partly curated by the co-chaperone imunophilin proteins (FKBP), FKBP51 and FKBP52 (Jaaskelainen, Makkonen et al. 2011). These are implicated in most sex-steroid receptor signalling and with respect to PR, FKBP51 attenuates PR mediated transcription, whereas FKBP52 enhances transcription (Sanchez 2012).

Following HSP dissociation from the ligand-receptor complex, the ligand bound PR translocates to the nucleus, prior to binding with hormone response elements (PREs) at the promoter regions of target genes and subsequent communication with the RNA polymerase RNA POL2 (Figure 4.1). This process is further modified by co-regulatory proteins, that may either increase or decrease transcription (Critchley and Saunders 2009). Over 300 co-regulators are reported to interact with the PR (Scarpin, Graham et al. 2009). Classical co-activators include members of the steroid receptor co-activator family (SRC) and co-repressors include nuclear receptor corepressor (NCoR) and silencing mediator of retinoic acid and thyroid hormone receptor (SMRT) (Chabbert-Buffet, Meduri et al. 2005). The degree of relative recruitment of co-activators and co-repressors are thus key regulators of subsequent transcriptional activity (Figure 4.1). PR can also interact with other transcription factors such as specificity protein 1 (SP1), Forkhead Box O1 (FOXO1), activator protein 1 (AP1) and the p65 subunit of nuclear

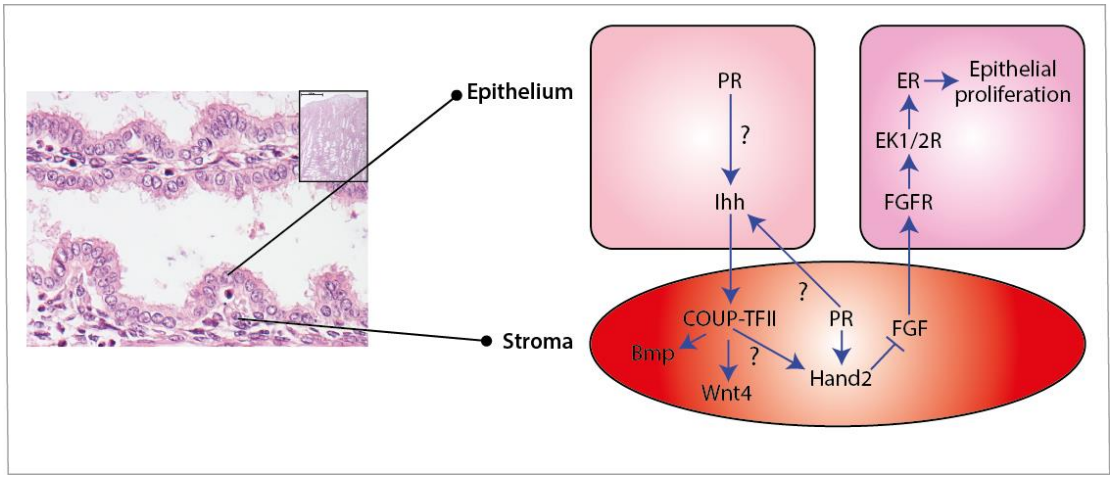

Figure 4.2 Evidence of PR-mediated paracrine signalling in the endometrium and key progesterone regulated pathways derived from murine models

Key signaling pathways at the time of embryo implantation, derived from murine knockout models. Indian Hedgehog (*Ihh*) is a progesterone target activated within the epithelium which signals downstream to COUP-TFII (activating *Bmp2* and *Wnt4*) in the stroma establishing the *Ihh*–COUP-TFII axis across the epithelial and stromal compartment.

Both COUP-TFII and PR directly may also play a role in the activation of *Hand2* in the stroma leading to the inhibition of the FGF pathway, a pathway known to be involved in the promotion of epithelial proliferation by oestrogen signaling.

Adapted and redrawn from Wetendorf and DeMayo 2012

factor-κB (NF-κB) (Gellersen and Brosens 2003, Kim, Kurita et al. 2013) and with proto-oncogene tyrosine-protein kinase Src (Src kinase) to activate mitogen-activated protein kinases (MAPK) signalling (Migliaccio, Piccolo et al. 1998)

As described in **Chapter 1**, SPRMs are ligands for the PR, and they can result in differing degrees of progesterone antagonism depending upon the individual compound. The action of ligand binding, HSP dissociation, dimerization and binding to PRE appears to be unaffected by SPRMs (Chabbert-Buffet, Meduri et al. 2005), rather it is the relative recruitment of co-regulators that results in subsequent progesterone antagonism (Smith and O'Malley 2004). Alteration in both SRC-1 and SMRT has been observed following administration of the SPRMs mifepristone (RU-486) and asoprisnil (J867) (Madauss, Grygielko et al. 2007, Afhuppe, Beekman et al. 2010, Amazit, Roseau et al. 2011). The degree of interaction between the co-repressor NCoR appears to alter between the differing SPRMs mifepristone, onapristone (ZK 89299) and lonaprisan (ZK 230211) (Afhuppe, Sommer et al. 2009).

4.1.2 Progesterone regulated genes

Within the endometrium P4 regulates gene expression to induce an endometrium that is receptive to, and can support a developing pregnancy. During the P4 dominated secretory phase, oestrogen driven endometrial proliferation is supressed and the endometrium undergoes differentiation and maturation, characterised by secretory transformation of glands and influx of inflammatory cells (Strowitzki, Germeyer et al. 2006).

Mouse models have identified key P-regulated genes and P-regulated functions through the use of *PR*-knockout mice (Wang and Dey 2006). Work by DeMayo and colleagues in murine models has identified pivotal P-regulated genes including the indian hedgehog – chicken ovalbumin upstream transcription factor II (IHH – COUP-TFII) pathway (and its downstream effect upon wingless related MMTV integration site/bone morphogenetic protein (Wnt/Bmp) signalling and Heart and neural crest derivatives expressed 2 (Hand2) signalling pathway (Figure 4.2) which are critical to endometrial decidualisation, proliferation and cell survival (Wetendorf and DeMayo 2012).

Key markers of decidualisation are Insulin-like growth factor-binding protein 1 (IGFBP1), prolactin (PRL) and interleukin-15 (IL-15), all of which are P-regulated (Dunn, Critchley et al. 2002, Gellersen and Brosens 2003). Homeobox A10 (HOXA10) regulates expression of these markers and is itself P-regulated (Gellersen and Brosens 2003, Eun Kwon and Taylor 2004).

Other known P-regulated genes include B-Cell CLL/Lymphoma 6 (*BCL6*) (Li, Large et al. 2013), and the kruppel-like factor (KLF) family. Perturbation of the KLFs has been observed in reproductive tract pathologies, in particular KLF-4, -9 and -15 have been implicated in infertility, endometriosis and endometrial cancer (Ray and Pollard 2012, Simmen, Heard et al. 2015).

There is evidence that the gynaecological disorder endometriosis is associated with changes in the eutopic endometrium (the uterine endometrium, in a woman with endometriosis). These include increased proliferation and decreased apoptosis, altered cellular immunity and diminished response to progesterone, termed progesterone resistance (Young and Lessey 2010). P-regulated genes found to be altered in the presence of co-existing endometriosis include (but are not limited to) PRB (Shen, Yan et al. 2015) and the co-chaperone proteins FKBP51 (Yang, Zhou et al. 2012) and FKBP52 (Joshi, Miyadahira et al. 2017). P-regulated genes for example, FOXO1 (Su, Strug et al. 2015), HOXA10 (Kim, Taylor et al. 2007), KLF-9 (Heard, Simmons et al. 2014) and BCL6 (Evans-Hoeker, Lessey et al. 2016) have all been demonstrated to be altered in the setting of co-existing endometriosis.

Finally the tumour suppressor gene Phosphatase and tensin homolog (PTEN) is present in the endometrium and loss of this is considered a pivotal event in the development of endometrial cancer (Mutter, Lin et al. 2000). PTEN null glands may be shed at menstruation and exogenous progestins may also play a role in elimination of null glands (Orbo, Rise et al. 2006). PTEN is also a negative regulator of phosphoinositide 3-kinase (PI3K) signalling, which is a key regulator of cell growth and survival (Carracedo and Pandolfi 2008).

In **Chapter 3**, the significant increase of *PR* and *PRB* mRNA levels and striking alteration in localisation of both isoforms following administration of the SPRM Ulipristal acetate (UPA) was described. Little is known regarding the effect of SPRMs on the P-regulated

genes described above. Asoprisnil administration significantly reduced *IL-15* and reassuringly did not alter levels of PTEN. Microarray and sequencing studies of mifepristone, asoprisnil and UPA have identified differentially expressed transcripts (Catalano, Critchley et al. 2007, Wilkens, Male et al. 2013, Cuevas, Tapia-Pizarro et al. 2016, Lira-Albarran, Durand et al. 2017) but have reported conflicting differential gene transcripts (Tapia, Vilos et al. 2011), the majority of which are unvalidated, and the effects of administration of UPA on the key genes described above is largely unknown.

4.2 Hypothesis

SPRM administration impacts upon progesterone-regulated genes in the human endometrium

4.3 Aim

To study the impact of SPRM administration on progesterone-regulated genes in the human endometrium

Research questions

- What is the impact upon known endometrial P-regulated gene transcription?
- Is there alteration in protein localisation of P-regulated genes under investigation?
- Does the presence of co-existing endometriosis alter response of endometrial P-regulated genes?
- Does administration of SPRM, UPA alter clearance of PTEN null glands in the endometrium?

4.4 Materials and Methods

Women with symptomatic fibroids underwent hysterectomy following treatment with the SPRM, Ulipristal acetate (UPA) 5mg orally once daily for up to 15 weeks prior to surgery (minimum nine weeks of SPRM treatment). They had given informed consent and the study had Research Ethics Committee (REC) approval (12/SS/0238 and 16/ES/0007; section **2.1.1**). At the time of surgery, biopsies were collected from the endometrium. Samples were processed as previously described (section **2.2.1.1**) and

tissue taken for RNA extraction for RT-qPCR and formalin fixation prior to immunohistochemistry. Corresponding control biopsies from women with symptomatic fibroids in proliferative and secretory phase of cycle were obtained from tissue archives (section **2.1.1**). Subjects were well characterised (section **2.4.1, Table 2.4-5**). These samples were utilised for RT-qPCR and immunohistochemistry.

Further paired endometrial biopsies were obtained from women prior to, and whilst on SPRM (daily) treatment following administration of UPA 5mg once daily for at least ten weeks (section **2.2.1.2, Table 2.6-7**). The baseline samples were well characterised and staged as previously described (section **2.3**). These samples were utilised for immunohistochemistry of PTEN.

RNA was extracted, quality checked and cDNA produced prior to performing RT-qPCR (as previously described; section **2.5**) for the co-chaperones *FKBP51, FKBP52*, P-regulated genes *IHH, COUP-TFII, BMP2, HAND2, HOXA10, FOXO1, FOXM1, BCL6, KLF-4, -9* and *15,* and the markers of decidualisation *IGFBP1* and *IL-15* (**Table 2.12)**. For the majority of genes an "n" of nine was used for each group (proliferative, secretory and following SPRM (UPA) administration) with the exception of *KLF-4* and *KLF-15* (n=6). Comparison of gene expression, as assessed by RT-qPCR, of *PR*, *PRB, FKBP51, FKBP52, FOXO1, HOXA10*, *KLF-9* and *BCL6* was also undertaken from women administered SPRM (UPA) either with and without endometriosis (n=7 in each group).

FFPE sections were cut for immunolocalisation of HAND2, FOXO1, BCL6 and PTEN on full thickness endometrial biopsies from the women exposed to SPRM (UPA) prior to hysterectomy and appropriate archival controls from women in the proliferative and secretory phase as described above (n=6-9). PTEN immunolocalisation was also performed on paired endometrial biopsies (n=17). These paired endometrial biopsies were obtained from 17 women with symptomatic fibroids treated with UPA 5mg daily with ethical approval and written informed consent (**Table 2.4&2.5**). Samples were obtained using a pipelle endometrial biopsy sampler (Pipelle de Cornier Mark II, Laboratoire CCD, France) as described in section **2.2.1.2**. A baseline biopsy was obtained prior to commencement of treatment and phase of the menstrual cycle (staged as described in section **2.3.2**; histological appearance based on Noyes criteria, LMP and circulating progesterone and oestradiol). Detailed of IHC protocols and antibodies utilised can be found in section **2.6** and **Table 2.13-14**.

Statistical analysis of RT-qPCR results was performed using Graphpad prism software (Graphpad, USA). Data were subjected to the D'Agostino-Pearson omnibus normality test. Data with a Guassian distribution had an unpaired t-test applied when two comparators, and one-way ANOVA when 3 comparators (proliferative, secretory and following SPRM (UPA) treatment), to determine difference between groups. For non-parametric data Kruskal-Wallis test was used to determine differences between sample groups when three comparators, and Mann-Whitney test when two. Following ANOVA/Kruskal-Wallis test post-hoc testing was performed if appropriate using Tukey's or Dunn's multiple comparison. Results are presented as ±minimum and maximum. $p < 0.05$ was considered to be statistically significant. To assess impact of endometriosis on bleeding control, a 2-by2 table was constructed, Fischer's exact test was then applied and an odds ratio calculated.

4.5 Results

4.5.1 Treatment with SPRM, UPA, alters relative mRNA levels of P-regulated genes in human endometrium

Administration of the SPRM UPA significantly decreases mRNA levels of the co-chaperone *FKBP51* relative to secretory levels (Figure 4.3A) but does not alter *FKBP52*, which also demonstrated no significant alteration between proliferative and secretory phase mRNA levels (Figure 4.3B). *IHH* mRNA levels were significantly increased following UPA administration and in proliferative phase, compared to secretory phase levels (Figure 4.3C). However neither *COUP-TFII* nor *BMP2* demonstrated cyclical alteration in mRNA levels and these were not affected by SPRM (UPA) administration (Figure 4.3D-E). In contrast *HAND2* mRNA levels were markedly increased in secretory phase but significantly reduced both in proliferative phase and following UPA administration (Figure 4.3F).

In proliferative phase and following SPRM (UPA) administration, mRNA levels of the transcription factor *HOXA10* were significantly increased relative to secretory phase (Figure 4.4A). In keeping with histological absence of decidualisation (**Figure 3.7-8**), both markers of decidualisation *IGFBP1* and *IL-15* demonstrated low mRNA levels, which were significantly reduced compared to secretory levels, and similar to proliferative phase levels (Figure 4.4B-C). A similar pattern was demonstrated by mRNA levels of

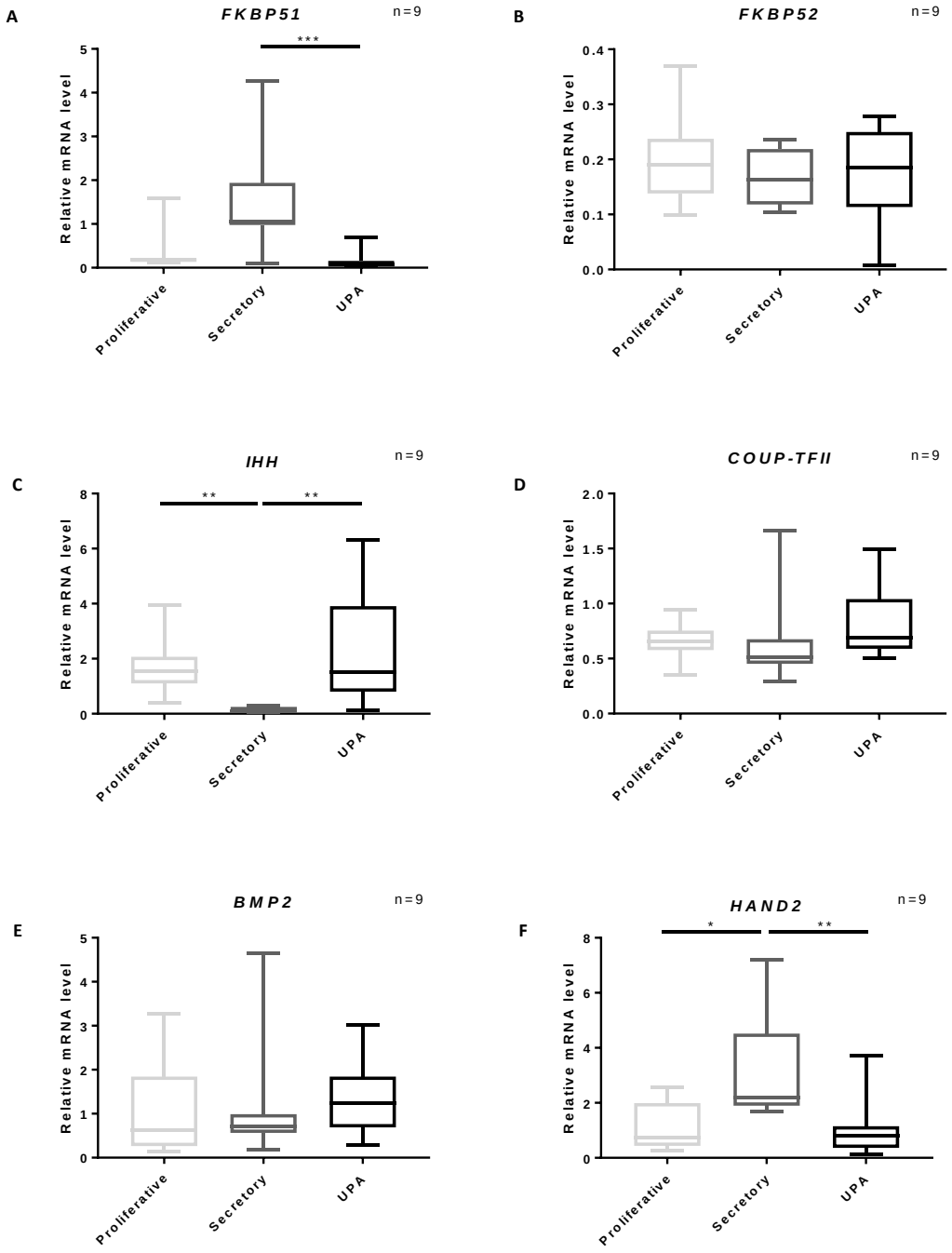

Figure 4.3 Treatment with selective progesterone receptor modulator, ulipristal acetate (UPA), increased the concentration of mRNAs encoding genes involved in progesterone signalling in tissue extracts from human endometrium as determined by RT-qPCR

Relative mRNA levels of *FKBP51* (A Kruskal-Wallis p = 0.0010), *FKBP52* (B ANOVA p = 0.6578), *IHH* (C Kruskal-Wallis p = 0.004), *COUP-TFII* (D Kruskal-Wallis p = 0.01629), *BMP2* (E Kruskal-Wallis p = 0.4373) and *HAND2* (F Kruskal-Wallis p = 0.0049) from woman with fibroids during proliferative and secretory stages of menstrual cycle and following UPA administration. n=9 for each group. * *P*<0.05, ** p<0.01, ***p<0.001. Box and whisker: box indicates first/third quartile and median, whiskers minimum and maximum

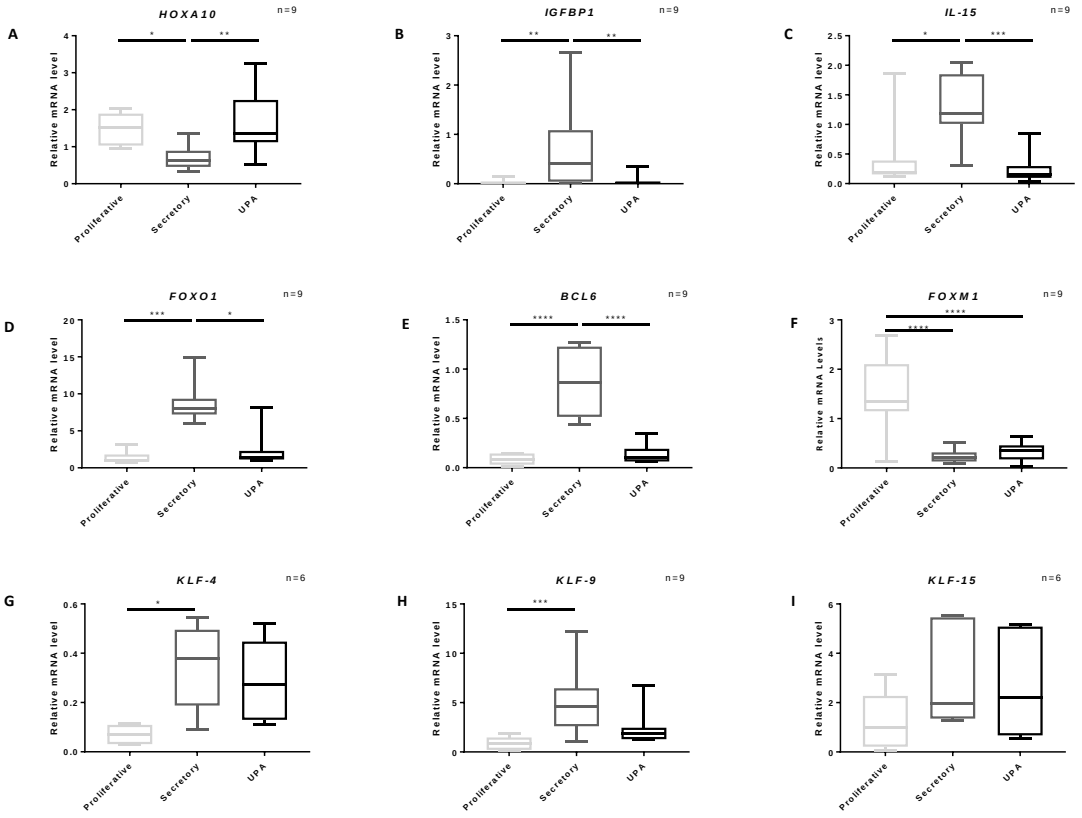

Figure 4.4 Treatment with selective progesterone receptor modulator, ulipristal acetate (UPA), increased the concentration of mRNAs encoding genes involved in progesterone signalling and markers of decidualisation in tissue extracts from human endometrium as determined by RT-qPCR

Relative mRNA levels of *HOXA10* (A ANOVA p = 0.0035), *IGFBP1* (B Kruskal-Wallis p = 0.0007), *IL-15* (C Kruskal-Wallis p = 0.0007), *FOXO1* (D Kruskal-Wallis p = 0.0003), *BCL-6* (E ANOVA p < 0.0001) *FOXM1* (F ANOVA p < 0.0001), *KLF-4* (G ANOVA p = 0.0109), *KLF-9* (H Kruskal-Wallis p = 0.0010) and *KLF-15* (I Kruskal-Wallis p = 0.2274) from woman with fibroids during proliferative and secretory stages of the menstrual cycle and following UPA administration. n=6 or 9 for each group. * *P*<0.05, ** p<0.01, ***p<0.001, **** p<0.0001. Box and whisker: box indicates first/third quartile and median, whiskers minimum and maximum

FOXO1 and *BCL6* (Figure 4.4D-E). In contrast *FOXM1* mRNA levels were significantly decreased in both secretory phase and following UPA administration, compared with proliferative phase (Figure 4.4F). The kruppel-like factors 4, 9 and 15 mRNA levels were all increased in secretory phase compared with proliferative phase although this increase did not achieve statistical significance for KLF-15. In contrast UPA administration did not significantly alter mRNA levels relative to either secretory or proliferative phase levels (Figure 4.4G-I).

4.5.2 SPRM (UPA) administration decreases immunoexpression of HAND2, FOXO1 and BCL6 but does not alter location within the endometrium

HAND2 is expressed predominantly in the endometrial stroma and immunoreactivity is increased in secretory phase (Figure 4.5B) relative to proliferative phase (Figure 4.5A). Following SPRM (UPA) administration, weakly immunopositive stromal nuclei for HAND2, with occasional weak glandular immunoreactivity were observed (Figure 4.5C). The level of stromal immunopositivity following UPA administration was consistent with that observed in proliferative phase, and markedly less than that observed in the secretory phase.

Immunopositivity of FOXO1 was weakly present in both endometrial glands and stroma in samples from women in the proliferative phase of the menstrual cycle (Figure 4.5D). Samples from women in the secretory phase demonstrated strong immunopositivity in glandular cells and moderate immunoreactivity in stromal cells (Figure 4.5E). In contrast samples from UPA-treated women displayed almost negligible immunopositivity of FOXO1 in both endometrial glands and stroma (Figure 4.5F).

BCL6 is predominantly expressed in the endometrial glandular epithelium, with some weak stromal immunopositivity (Figure 4.6). Immunoreactivity was maximal in the secretory phase, with intense glandular immunopositivity, and some weak stromal immunoreactivity (Figure 4.6B). In contrast following SPRM (UPA) administration immunoreactivity was almost complete absent in both glands and stroma (Figure 4.6C), a pattern of immunopositivity that phenocopied the proliferative phase (Figure 4.6A). Only one subject administered UPA exhibited evidence of BCL6 immunopositivity with occasional weak immunoreactivity predominantly in the glands: this subject had active endometriosis at the time of hysterectomy (Figure 4.6D).

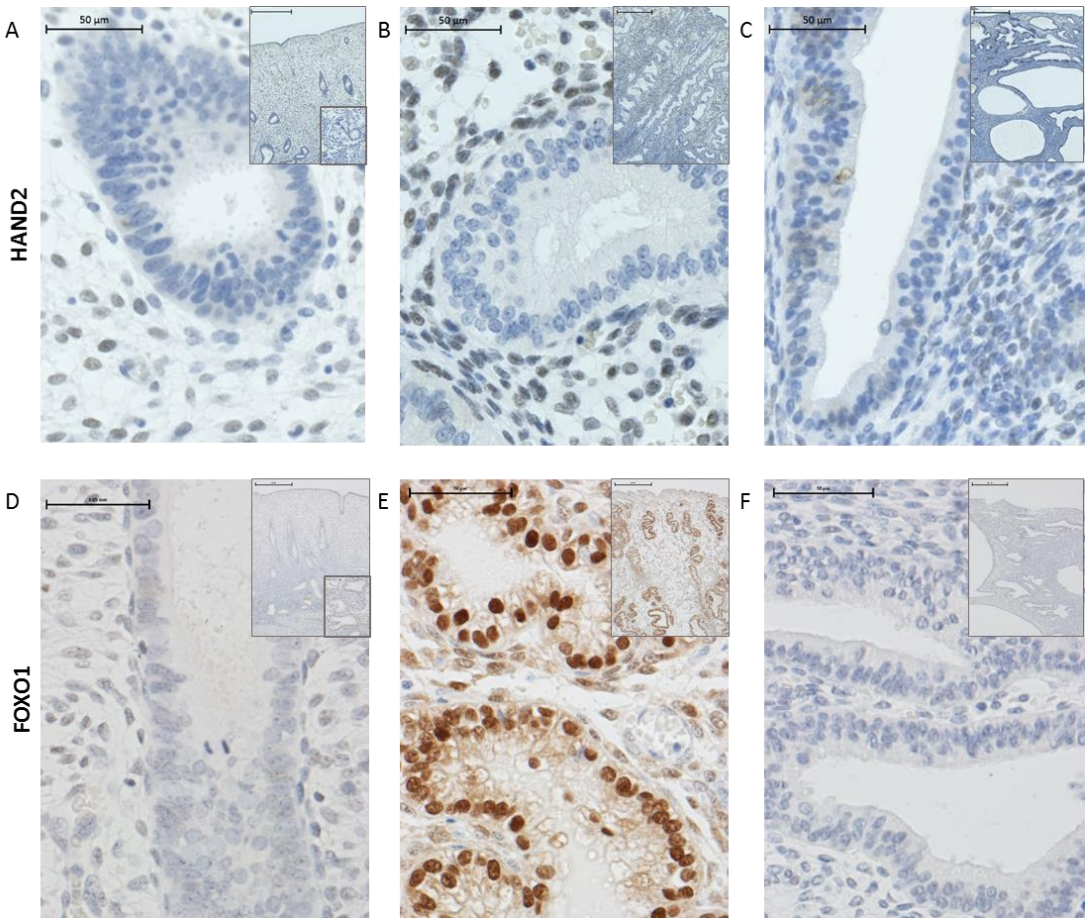

Figure 4.5 Administration of selective progesterone receptor modulator, ulipristal acetate (UPA), modulates HAND2 and FOXO immunoreactivity

Representative low-power (inserts) and high-power immuno-localisation of HAND2 (A-C) and FOXO1 (D-F) in endometrium from woman with fibroids during proliferative (A&D) and secretory stages (B&E) of the menstrual cycle and after UPA administration (C&F).

Samples from UPA-treated women (C) displayed weakly immunopositive stromal cell nuclei for HAND2, with occasional weak glandular cell immunoreactivity. The level of stromal cell immunopositivity following UPA administration was consistent with that observed in the proliferative phase (A). In contrast endometrial samples from women in the secretory phase displayed strong immunopositivity in stromal cells (B).

Samples from UPA-treated women (F) displayed negligible immunopositivity of FOXO1 in both glands and stroma. This was less than immunopositivity observed in proliferative phase (weak staining in both glands and stroma (D). In samples from women in the secretory phase strong immunopositivity was observed in endometrial glandular cells and moderate immunoreactivity in stromal cells (E)

Lower power (scale bar = 500µm) and high power magnification (scale bar = 50 µm); Negative controls shown as inserts on proliferative low power endometrium (A&D).

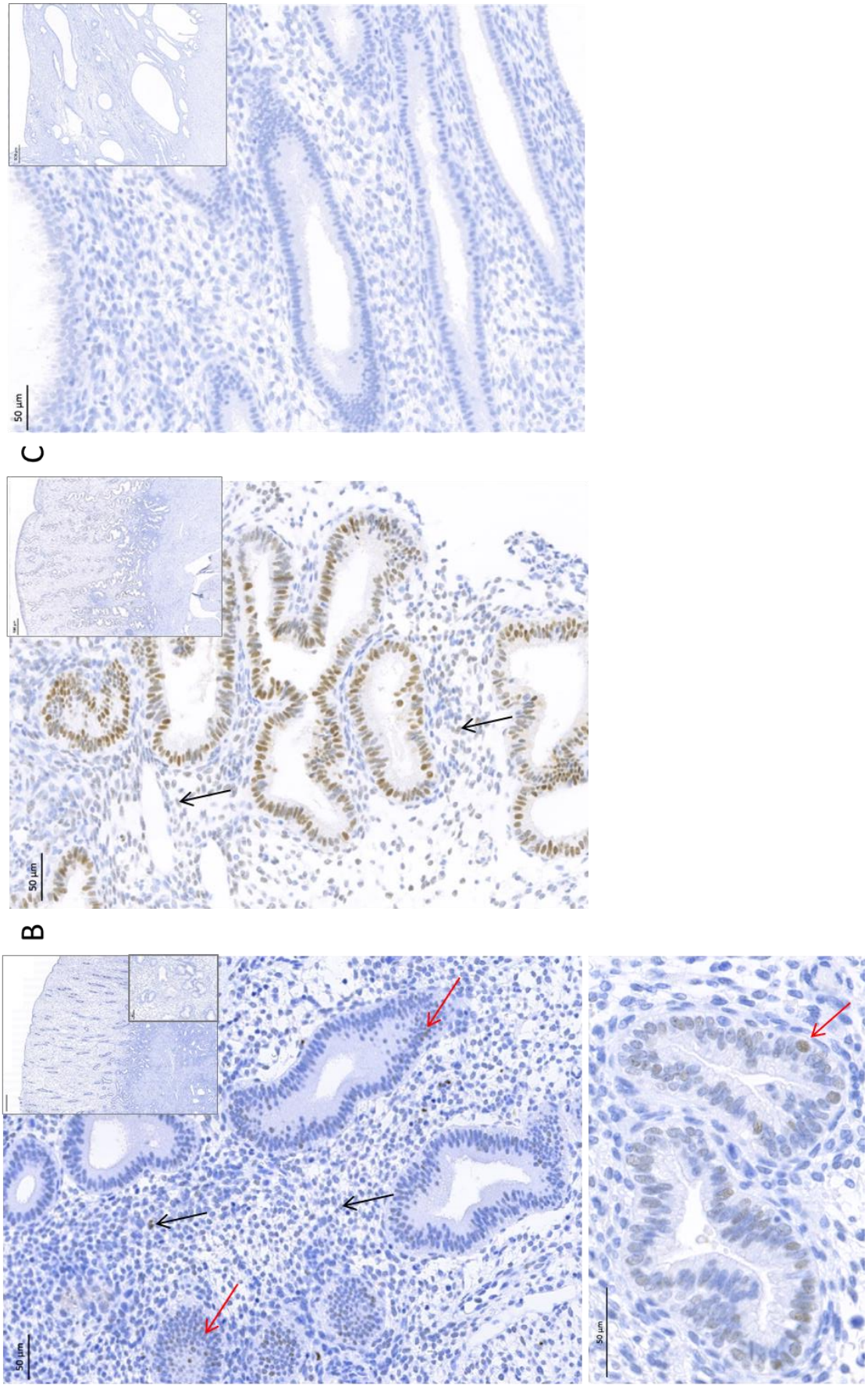
C
50 µm
B
50 µm
A
50 µm
D
50 µm

Figure 4.6 Administration of selective progesterone receptor modulator, ulipristal acetate (UPA), modulates BCL6 immunolocalisation in human endometrium

Representative low-power (inserts) and high-power immuno-localisation of BCL6 in endometrium from woman with fibroids during proliferative (A) and secretory stages (B) and after UPA administration (C&D).

Samples from most UPA-treated women (C) displayed negligible immunopositivity of BCL6 in both glands and stroma. This was less than immunopositivity observed in proliferative phase (A) where occasional weak immunoreactivity was observed in both glands (↑) and stroma (↑). In samples from women in secretory (B) phase strong immunopositivity was observed in glandular cells and occasional moderate immunoreactivity in stromal cells (↑).One exception of UPA-treated subject (with co-exisiting endometriosis) displayed weak glandular immunopositivity (↑, D).

Lower power (scale bar = 500µm) and high power magnification (scale bar = 50 µm); Negative controls shown as inserts on proliferative low-power endometrium (A).

4.5.3 Co-existing endometriosis is associated with a trend towards lower rates of amenorrhoea but does not alter mRNA levels of progesterone receptor and key genes associated with progesterone resistance following SPRM (UPA) administration.

In total samples from 38 women who were administered the SPRM, UPA, have been utilised in the thesis, and of these 10 women had a diagnosis of co-existing endometriosis (**Table 2.4 & 2.6**). Data were not available regarding stage of disease, or whether the diagnosis was historical or of active endometriosis noted at the time of sample collection (if the sample was obtained at the time of hysterectomy). Recorded rates of amenorrhoea following UPA administration were higher in those without endometriosis (72%) compared to those women with a diagnosis of endometriosis, in whom only 50% achieved amenorrhoea (Figure 4.7A). The odds of amenorrhoea were not statistically different but there did appear to be a trend towards poorer control of bleeding for those women with endometriosis, with an odds ratio of achieving amenorrhoea of 0.4 (95% confidence interval 0.08-1.837) compared to women without endometriosis. Of note, of the three women with histologically proven adenomyosis, all were rendered amenorrhoeic by UPA administration. Data regarding impact of UPA administration on any pain symptoms (dysmenorrhoea, chronic pelvic pain, dyspareunia, dyschezia or dysuria) were not available.

There was no significant difference in mRNA levels of *PR* or *PRB* (Figure 4.7B&C), or genes associated with progesterone resistance in the setting of endometriosis. These included *FKBP51* (Figure 4.7D), *FKBP52* (Figure 4.7E), *FOXO1* (Figure 4.7F), *HOXA10* (Figure 4.7G), *KLF-9* (Figure 4.7H) and *BCL6* (Figure 4.7I). There was marked variation in gene mRNA levels within both groups. For subjects with endometriosis, information regarding stage of endometriosis had not been collected.

4.5.4 Impact of SPRM (UPA) administration on presence of PTEN null glands in the endometrium

The majority of subjects undergoing hysterectomy exhibited evidence of strong immuno-staining of all endometrial glands with PTEN irrespective of stage of cycle or following SPRM (UPA) administration (Figure 4.8A-C). However PTEN null glands were observed in two women in the proliferative phase of the menstrual cycle (Figure 4.8D&G), two in the secretory phase (Figure 4.8E&H), and three who had had administration of UPA prior

to surgery (Figure 4.8F&I). In all subjects these PTEN null glands were present in the basal layer (Figure 4.8D-F).

Of the 17 "paired" endometrial samples, described in 4.4, 11 women had no evidence of PTEN null glands in either the baseline pre-treatment sample or following UPA administration (Table 4.1). Three women had PTEN null glands present in their index sample (18%), of these only one had convincing evidence of residual PTEN null glands in the biopsy obtained when on UPA. Of note one of these 'normal' UPA samples was of poor quality due to small quantities of highly fragmented tissue (Sample CT1366E3, Table 4.1). Three women appeared to have developed PTEN null glands whilst administered UPA that were not present in their baseline endometrial biopsy. All of these three women were amenorrheic and displayed histological signs of UPA administration. No subjects displayed evidence of hyperplasia or malignancy.

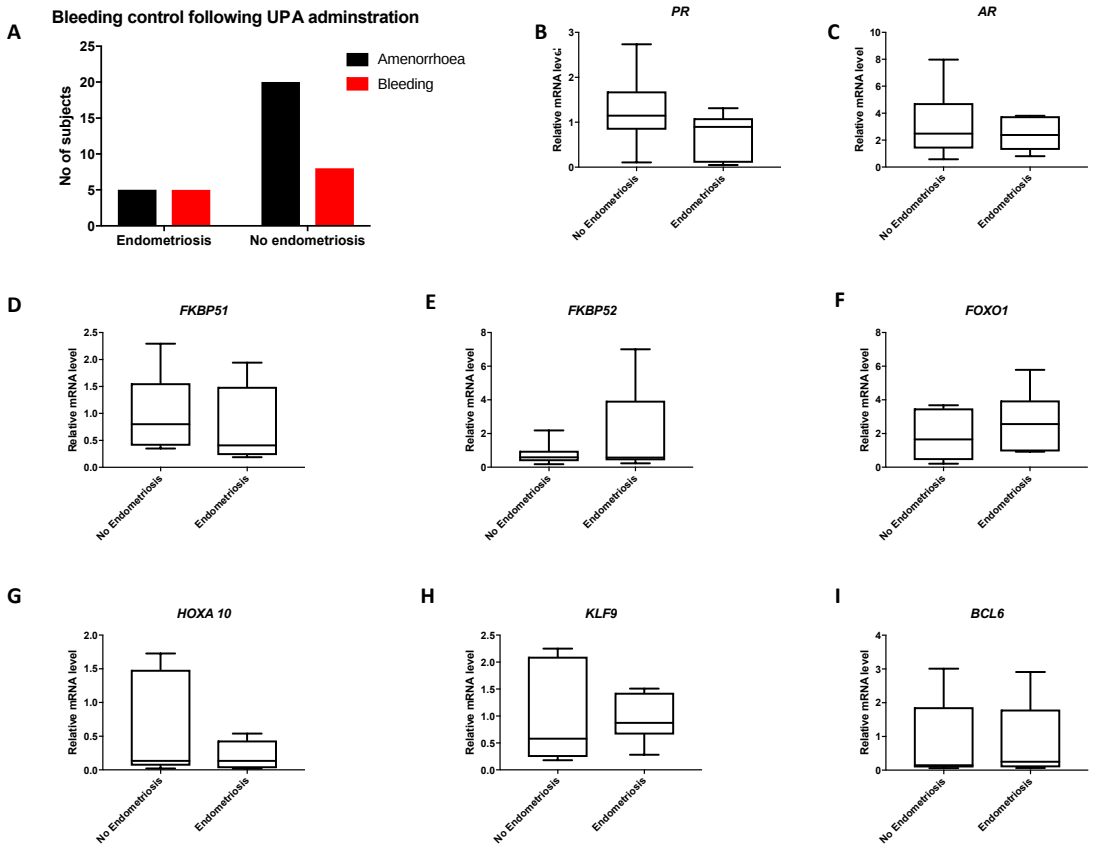

Figure 4.7 Presence of co-existing endometriosis may alter menstrual bleeding control but does not alter mRNA levels of progesterone receptor and key genes associated with progesterone resistance in women treated with selective progesterone receptor modulator, ulipristal acetate (UPA), as determined by RT-qPCR

Menstrual bleeding control following treatment with UPA (A), Relative mRNA levels of *PR* (B), *PRB* (C), *FKBP51* (D), *FKBP52* (E), *FOXO1* (F), *HOXA10* (G), *KLF-4* (H) and *BCL6* (I) from woman with fibroids administered UPA, with and without co-existing endometriosis. n=7 for each group. Box and whisker: box indicates first/third quartile and median, whiskers minimum and maximum

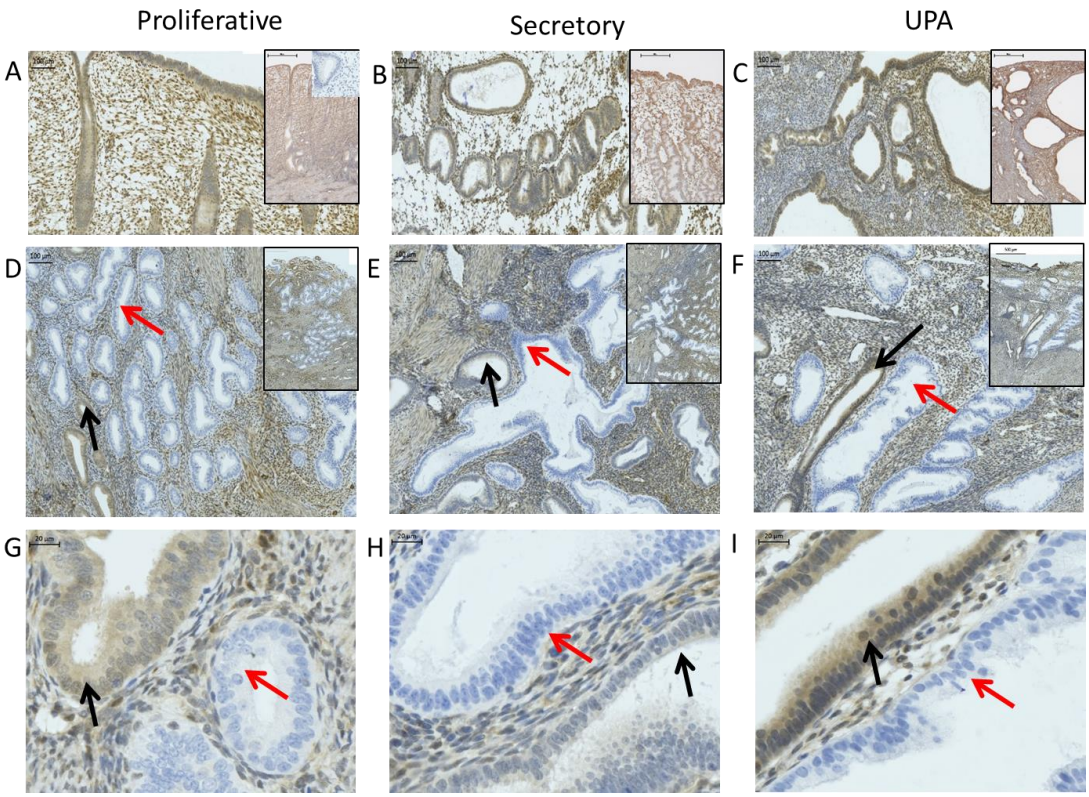

Figure 4.8 PTEN null glands are present irrespective of stage of menstrual cycle or following administration of selective progesterone receptor modulator, ulipristal acetate (UPA)

Representative low-power (inserts, A-F) medium-power (A-F) and high-power (G-I) images of immuno-localisation of PTEN in endometrium from woman with fibroids during proliferative (A&D) and secretory stages (B&E) and after UPA administration (C&F). The majority of subjects had immunopositive staining for PTEN in glands following UPA treatment (C), or in proliferative (A) or secretory phase (B) of the menstrual cycle. However PTEN null glands were observed in two subjects in both proliferative (D&G), in secretory phase (E&H) and also following administration of UPA (F&I). None of these subjects with PTEN null glands had evidence of endometrial hyperplasia or malignancy.

Low power (scale bar = 500µm), medium-power (scale bar = 100µm) and high power magnification (scale bar = 20 µm); Negative controls shown as inserts on proliferative low power endometrium (A).

Table 4.1 Alteration in rates of PTEN null glands following treatment with selective progesterone receptor modulator, Ulipristal acetate (UPA)

Subject	Index sample					Sample whilst administered UPA							
Participant No	Study code No	Sample No	Final pathology	No Null	PTEN null	Study code No	Sample No	Duration of Rx (days)	Days off Rx	Control	Histology	No Null	PTEN null
5777	CT1262E2	1678	Proliferative	x		CT1262E3	1938	81	0	Amenorrhoea	Inactive with no atypia#	x	
8522	CT1929E	1724	Proliferative		**x**	CT1929E2	1941	80	0	Lighter	PAEC		**x**
8002	CT1366E2	1723	Disordered proliferative		**x**	CT1366E3	1942	66	0	Amenorrhoea	Disordered proliferative#	x	
8100	CT1463E	1920	Proliferative	x		CT1463E2	1949	82	0	Amenorrhoea	Consistent with UPA#		**x**
8097	CT1460E	1916	Proliferative	x		CT1460E2	1951	70	0	Amenorrhoea	Inadequate#	x	
5795	CT1280E	1679	Proliferative	x		CT1280E2	1960	77	8[2]	Amenorrhoea	PAEC		**x**
9055	CT1685E	2036	Proliferative		**x**	CT1685E2	2063	79	0	Lighter	PAEC	x	
7886	CT1162E2	1935	Proliferative	x		CT1162E3	2062	60	0	Amenorrhoea	Inactive with no atypia#	x	
5817	CT1691E	2053	Disordered proliferative	x		CT1691E2	1988	80	0	Amenorrhoea	PAEC	x	
8122	CT1485E	1953	Secretory	x		CT1485E2	1981	69	0	Amenorrhoea	PAEC	x	
8124	CT1487E	1955	Secretory	x		CT1487E2	1986	81	0	Amenorrhoea	Consistent with UPA#	x	
8130	CT1493E	1963	Secretory	x		CT1493E2	1987	70	0	Amenorrhoea	PAEC	x	
8045	CT1409E2	2050	Secretory	x		CT1409E3	2062	76	0	Amenorrhoea	PAEC	x	
8123	CT1486E	1954	Menstrual	x		CT1486E2	1980	75	0	Amenorrhoea	PAEC		**x**
5790	CT1275E	1671	Proliferative	x		CU1275E[1]	1684	791	0	Unchanged	Mildly disordered proliferative	x	
5785	CT1270E2	1673	Proliferative	x		CU1270E3[1]	1958	781	0	Amenorrhoea	Secretory (some non-physiological)	x	
8506	CT1903E2	1917	Proliferative	x		CU1903E3[1]	1903	821	0	Lighter	Proliferative	x	

PAEC: progesterone receptor modulator associated endometrial changes

#: Minimal tissue in biopsy or fragmented sample. Sufficient tissue may be available to exclude malignancy but may be insufficient to assess for features of PAEC or to unequivocally state PAEC as diagnosis [1]: sample from UCON subject – pipelles taken in final week of second 12 week cycle of treatment [2]: sample taken 8 days after stopping UPA. Patient remained amenorrhic at the time of biopsy

Samples highlighted: Absence of PTEN null glands prior to treatment, but PTEN null glands present in sample obtained following treatment with UPA
Samples highlighted: PTEN Null glands present prior to treatment but not present in sample obtained following treatment with UPA
Sample highlighted: PTEN Null glands present both prior to treatment and following treatment with UPA

4.6 Discussion

Ulipristal acetate (UPA) is a SPRM which, like other class members, exhibits both agonist and antagonist activities *in vitro* and may be influenced both by bioavailability of different PR isoforms and the concentrations of different co-repressor and co-activator proteins (Wagenfeld, Saunders et al. 2016). The data presented here, demonstrate that administration of the SPRM, UPA, to women with symptomatic fibroids, results in alteration of many key P-regulated genes, indicating that in the endometrium, UPA acts with low P-agonism on many key genes associated with reproductive function.

4.6.1 Co-Chaperones FKBP51 and FKBP52

FKBP51 mRNA levels were significant reduced compared to secretory phase of the menstrual cycle, similar to those seen in proliferative phase, whereas levels of *FKBP52* mRNA were unchanged.

The effect of SPRM (UPA) administration on FKBP51 has not been published but is consistent with the effect observed following administration with the SPRM mifepristone. In healthy women administered a single dose of mifepristone *FKBP51* mRNA was reduced relative to secretory phase (Cuevas, Tapia-Pizarro et al. 2016). FKBP51 has been demonstrated to be increased in decidual cells (Jaaskelainen, Makkonen et al. 2011) and following administration of progestin (Hubler, Denny et al. 2003) and so decrease in *FKBP51* mRNA levels relative to secretory phase following UPA administration is consistent with UPA acting with low PR-agonist activity. SPRMs have previously been described as having unaltered ligand binding, HSP dissociation, dimerization and binding to PRE (Chabbert-Buffet, Meduri et al. 2005), and down-stream effects related to relative recruitment of co-regulators that results in altered activity (Smith and O'Malley 2004). It is unclear what the alteration in *FKBP51* mRNA levels described here may have on HSP dissociation from PR and subsequent mobilisation from the cytoplasm to the nucleus. Co-localisation of PR and FKBP51 by immunofluorescence may provide insights into functional effects of UPA administration.

No cyclical alteration in *FKBP52* mRNA levels was observed. Other groups have observed a rise in secretory phase relative to proliferative (Yang, Zhou et al. 2012). Microarray performed by another group observed a 3 fold increase in *FKBP52* mRNA levels in the

endometrium from women administered a single dose of mifepristone compared to women in the secretory phase of the cycle, although this was not validated either by PCR or immunohistochemistry (Catalano, Critchley et al. 2007). However there are potential explanations for why the data present herein are inconsistent with established literature both with respect to alteration in expression between proliferative and secretory phase of the cycle, and following administration of an SPRM.

FKP52 is partly regulated by HOXA10 (Yang, Zhou et al. 2012), itself normally increased in secretory phase, but HOXA10 expression may be decreased in the presence of fibroids (Yang, Zhou et al. 2012, Kulp, Mamillapalli et al. 2016). This was also demonstrated in the endometrium of the women presented in this thesis (who had co-existing fibroids), in whom *HOXA10* mRNA levels were also reduced in the secretory phase. The blunted alteration in HOXA10 may explain the apparent absence of cyclical variation of *FKBP52* demonstrated here in this thesis, and makes interpretation of *FKBP52* mRNA levels following UPA administration more challenging. It is uncertain if the impact of UPA directly on *FKBP52* mRNA levels occurs by acting with low P-agonism, or if it is alteration in HOXA10 due to underlying fibroids that impacts upon *FKBP52* mRNA levels. However ongoing studies assessing the impact of UPA administration on the endometrium of women both with and without fibroids, such as the current UCON trial (Ulipristal acetate versus conventional management of heavy menstrual bleeding; EudraCT 2014-003408-65) described in **Chapter 2** (**2.2.1.2**) may facilitate the assessment FKBP52 mRNA levels in women with structurally normal uteri following SPRM administration.

4.6.2 Progesterone regulated genes

Murine knockout models have identified key P-regulated signalling pathways in the development of a receptive endometrium, in particular the IHH – COUP-TFII pathway and HAND2 signalling (Wetendorf and DeMayo 2012, Pawar, Hantak et al. 2014).

IHH is signalling protein that acts in a paracrine fashion from epithelial cells to initiate a cascade of gene expression in the stromal cell compartment (Takamoto, Zhao et al. 2002). Loss of *IHH* in murine models resulted in a total loss of typical uterine P4 responses, suggesting that IHH is an obligate mediator of uterine P4 function (Lee, Jeong et al. 2006). There is some conflict in the literature regarding expression of IHH within human endometrium of the normal cycling woman. Some groups have demonstrated

that IHH protein expression was increased in secretory phase when compared to proliferative phase endometrium (Wei, Levens et al. 2010) though others have observed that the secretory rise was abrogated in the presence of co-existing endometriosis (Smith, Alnifaidy et al. 2011). This description however was determined from protein expression in women without fibroids, and a genome wide molecular phenotyping study that was derived from nearly 50% of women with fibroids indicated that IHH was downregulated during the progression of the endometrium from proliferative phase through the secretory phase (Talbi, Hamilton et al. 2006). The data presented in this present thesis are consistent with the latter study, with an observed reduction in *IHH* mRNA levels in the secretory phase relative to the proliferative phase. Of the subjects studied in the secretory phase and contributing to RT-qPCR data presented here, all of the women had fibroids and two women had a history of endometriosis.

IHH has previously been assessed in women exposed to SPRMs. One group of women received a higher dose of UPA (10mg and 20mg), and changes in mRNA level change relative to proliferative phase only, studied. They observed that IHH expression was significantly increased following UPA administration, and it was unclear if protein expression was increased relative to the secretory phase. A study of mifepristone administration compared with secretory phase endometrium (no-treatment group) revealed an increase in *IHH* following SPRM administration (Cuevas, Tapia-Pizarro et al. 2016). Further validation of the findings presented here in this thesis, by protein expression studies, and sub grouped by presence of co-existing endometriosis would further elucidate whether UPA is acting with low or high P-agonism on IHH expression.

One mechanism of action of IHH is to bind to the transmembrane receptor patched-1 (PTCH1), resulting in loss of inhibition of smoothened (SMO) (Wetendorf and DeMayo 2012). This then results in activation of COUP-TFII (Krishnan, Elberg et al. 1997). The expression of COUP-TFII is reported to alter across the menstrual cycle, but in a contrasting fashion depending on location within the endometrium. Expression decreases in the functional layer, but increases in the basal layer following the proliferative to secretory transition (Li, Large et al. 2013). No cyclical alteration in mRNA levels was observed in data presented in this thesis, but the endometrium used to extract RNA was obtained from biopsies obtained at the time of hysterectomy, and so contained both basal and functional layer endometrium, and as such may have obscured relative

cyclical change. This is also true for assessing the effects of UPA, and assessment of effects of UPA administration of protein localisation would be of utility.

Bone morphogenetic proteins (BMPs) are members of the transforming growth factor-beta (TGFβ) superfamily. BMP-2 is P-regulated, a downstream target of COUP-TFII (Wetendorf and DeMayo 2012) and is implicated in control of HOXA10 expression (Sinclair, Mastroyannis et al. 2011). *BMP-2* knockout mice are embryonic lethal but conditional knockout results in inability to decidualise and subsequent infertility (Lee, Jeong et al. 2007). *BMP-2* mRNA levels are increased in decidualised endometrial stromal cells compared to undecidualised stromal cells from the proliferative phase (Li, Kannan et al. 2007). There was no cyclical alteration in *BMP-2* mRNA levels in the data presented here in this thesis. It is unclear if this was a result of unaltered *COUP-TFII*, or due to altered response of *BMP-2* due to co-existing pathology such as fibroids in the women from whom the endometrium utilised in this thesis were obtained. Endometrial deficiency of *BMP-2* has been demonstrated in the stromal cells of women with fibroids (Sinclair, Mastroyannis et al. 2011). UPA administration did not significantly alter *BMP-2* mRNA levels, consistent with an absence of differential expression in previous transcriptional arrays following both UPA (Lira-Albarran, Durand et al. 2017) and mifepristone administration (Catalano, Critchley et al. 2007, Cuevas, Tapia-Pizarro et al. 2016). This still requires confirmation by assessment of impact on protein expression, both in those women with and without fibroids. It would be of utility to assess impact of UPA administration on TGF-β3, which regulates the BMP-2 receptor and has also been demonstrated to be altered in stromal cells from women with fibroids (Sinclair, Mastroyannis et al. 2011).

Whilst the downstream targets of IHH, *COUP-TFII* and *BMP-2* were unchanged by UPA administration, the transcription factor HAND2 was significantly reduced relative to secretory phase and similar levels of expression relative to proliferative phase were observed, consistent with UPA acting with low P-agonism. This was demonstrated both by mRNA levels and protein expression. This is consistent with the effect demonstrated by other groups following UPA administration (Lira-Albarran, Durand et al. 2017) and following mifepristone administration (Li, Kannan et al. 2011). HAND2 may be regulated by COUP-TFII but also directly by PR (Wetendorf and DeMayo 2012). The striking reduction in HAND2 following UPA administration in the presence of unaltered COUP-TFII may mean that the latter mechanism of control is more relevant with regard to

HAND2 expression following UPA administration. The abrogation of PR within the stroma following UPA administration, described in **Chapter 3**, may also be implicated in the alteration of HAND2 expression following UPA administration. In addition to the role of HAND2 in regulating endometrial receptivity, it is also implicated in inhibition of fibroblast growth factors (FGF), thereby preventing activation of extracellular-signal-related kinases (ERK) and epithelial cell proliferation (Li, Kannan et al. 2011). Loss of HAND2 by methylation is a common occurrence in endometrial cancer (Jones, Teschendorff et al. 2013). However despite reduction in HAND2, UPA administration is not associated with increased proliferation endometrial cell (Whitaker, Murray et al. 2017), and discussed further in **Chapter 5**.

As described in **Chapter 3** a series of *Hox* genes are critical for the differentiation of the developing reproductive tract. HOXA10 is expressed in the developing uterus and is important in determining tissue boundaries (Mullen and Behringer 2014). Expression continues into reproductive life and it remains an important transcription factor, both for endometrial development and decidualisation. HOXA10 is expressed in both glandular and stromal compartments of the endometrium and expression is regulated by both oestradiol and progesterone (Eun Kwon and Taylor 2004). Whilst HOXA10 does not regulate PR directly, it is hypothesised to regulate PR co-factors (Daftary and Taylor 2004), and these have subsequently been demonstrated to include IGFBP1, FOXM1 and KLF-9 (Kim, Taylor et al. 2003, Du, Sarno et al. 2010, Gao, Bian et al. 2015). In healthy women expression peaks during the mid-secretory phase and its expression is considered an important factor in endometrial receptivity (Kulp, Mamillapalli et al. 2016). In women with uterine fibroids secretory phase upregulation may be impaired (Makker, Goel et al. 2017) and as all the subjects studied in this element of this thesis had fibroids this may explain why a reduced mRNA levels of *HOXA10* from the secretory endometrium compared with proliferative phase was observed. In those subjects exposed to the SPRM UPA, *HOXA10* mRNA levels were similar to the proliferative phase. Impact of UPA administration on HOXA10 has not previously been assessed but mifepristone administration in mice are reported to reduce expression. However as described above, the presence of fibroids in a human model may explain the contrasting data presented herein. Repetition of the experiment with endometrium from women without fibroids either in the various phases of the menstrual cycle or following UPA administration may yield useful further insights into the impact of SPRM administration on HOXA10 expression.

As described above, HOXA10 regulates IGBPB1, and as such it is unsurprising that mRNA levels of *IGFBP1* were reduced relative to secretory phase following UPA administration. This was consistent with an observed absence of decidualisation (previously described in **Chapter 3**). Equally HAND2 regulates IGFBP1 (Huyen and Bany 2011) and so the absence of decidualisation maybe a product of alteration of multiple aspects of PR signaling. Use of genetically manipulated "knockout mice" may further elucidate the mechanism, particularly if administration of either HAND2 or HOXA10 might rescue decidualisation. Another marker of decidualisation is IL-15 (Gellersen and Brosens 2014), which, as with *IGFBP1*, was significantly reduced following UPA administration. This was in keeping with the effect observed following administration a single dose of UPA (Lira-Albarran, Durand et al. 2017) and following administration of the SPRM asoprisnil (Wilkens, Male et al. 2013). The effect of reduction by UPA administration on *IL-15* mRNA levels on one of the downstream targets, CD56 positive uterine natural killer cells (uNK), has not been investigated. The morphological effects of asoprisnil administration on the architecture of the endometrium are slightly different and striking thick-walled vessels are widespread, an observation that is far less frequently observed following UPA administration. uNK cells may remodel endometrial vessels (Fraser, Whitley et al. 2015) and so the effect on uNK cell population may not be consistent between SPRMs. Indeed, *in vitro* treatment with mifepristone of human endometrial explants resulted in an increase of CD56 positive cells (Zhu, Zhang et al. 2009). However the effect associated with mifepristone potentially may be mediated by glucorticoids (Chen, Wang et al. 2012); as mifepristone binds GR with much greater affinity than other SPRMs (Attardi, Burgenson et al. 2004).

Consistent with previous reports, mRNA encoded by *FOXO1* was significantly increased in secretory phase control samples compared with those in proliferative phase (Fan, Li et al. 2012). Treatment with UPA resulted in mRNA concentrations similar to the proliferative phase and significantly lower than the secretory phase, corroborated by the impact upon protein expression, again suggesting UPA results in limited PR-dependent agonism in endometrium. This reduction in FOXO1 expression has not previously been demonstrated with other SPRMs, nor has been identified as a candidate gene in previous arrays or sequencing experiments. *FOXO1* is progesterone regulated, with expression of *FOXO1* in endometrial stromal cells up-regulated by cAMP and progesterone (Labied, Kajihara et al. 2006) and previous work using human endometrial stromal cells treated

with a decidualisation stimulus has suggested that HAND2 may regulate FOXO1 expression (Huyen and Bany 2011). Thus the reduction in FOXO1 may be in part due to reduction in HAND2 expression. Furthermore, a genomic screen of human endometrial stromal cells treated with a decidualisation protocol showed 15% of the genes induced were aberrantly expressed if FOXO1 was "knocked down" (Vasquez, Mazur et al. 2015). As FOXO1 binding sites are present in the majority of DNA regions associated with PR binding (Vasquez, Mazur et al. 2015) the finding of reduced expression of FOXO1 in UPA-treated women may explain some of the changes in PR-dependent genes.

BCL6 is a nuclear gene repressor associated with cell proliferation (Shaffer, Yu et al. 2000) and also may decrease the Indian Hedgehog (IHH) pathway involving COUP-TFII (Evans-Hoeker, Lessey et al. 2016). Consistent with other groups (Evans-Hoeker, Lessey et al. 2016), *BCL6* mRNA levels were significantly increased in the secretory phase of the menstrual cycle relative to the proliferative phase, and immunopositivity observed both in the glandular epithelium and stromal fibroblasts in secretory phase endometrium. UPA administration significantly decreased mRNA levels of *BCL6* relative to the secretory phase, and this was reflected in reduced protein expression, most evident in the glandular epithelium. This is consistent with a reduction in *BCL6* transcript levels noted in a microarray of endometrium from normal healthy women in mid secretory phase following a single dose of 30mg UPA (Lira-Albarran, Durand et al. 2017) but was not demonstrated to be altered in the two published microarrays of mifepristone (Catalano, Critchley et al. 2007, Cuevas, Tapia-Pizarro et al. 2016). It is unclear if this discrepancy between the differing SPRMS is due to the compound, dosing schedules or associated pathology.

Interestingly one of the subjects administered UPA had some persistent weak glandular immunopositivity of BCL6. This subject had active endometriosis at the time of surgery. Co-existing endometriosis is associated with significant increased transcription and protein expression of BCL6 in the eutopic endometrium (Evans-Hoeker, Lessey et al. 2016), and it may be that this was implicated in the persistent immunopositivity despite UPA administration. However this was not a consistent effect as three other women in the current study, who had a history of endometriosis, had no immunopositivity following UPA administration and mRNA levels were not significantly altered between women with and without endometriosis. Equally these three subjects all achieved amenorrhoea or markedly reduced bleeding, whereas the subject with persistent BCL6

immunopositivity also had no improvement in bleeding symptoms following UPA administration.

FOXM1 is a transcription factor, critical for cell cycle progression at the G_1-S and G_2-M transitions (Kalin, Ustiyan et al. 2011). Consistent with previously reports, *FOXM1* was highest in the proliferative phase (Jiang, Liao et al. 2015), but in contrast with many of the P-regulated genes described above, mRNA levels following UPA administration were consistent with the secretory phase rather than proliferative phase levels. The effect of SPRM administration on FOXM1 has not previously been examined, and previous microarrays of human endometrium have not identified it as differentially expressed gene. This is perhaps unsurprising as the published literature with regard to SPRM microarray and RNA-Seq have been relative to secretory phase, suggesting that transcription of *FOXM1* in the secretory phase is similar to that following SPRM administration. Of note the microarray of differentially expressed transcripts in human endometrium relative to proliferative phase performed for this thesis and described in **Chapter 5**, independently identified *FOXM1* as being decreased by UPA administration. The mechanism for this is unclear, and is likely separate to that of UPA acting with low P-agonism described above. Regulation of *FOXM1* by HOXA10 has previously been demonstrated (Gao, Bian et al. 2015). In this cohort *HOXA10* was reduced in the secretory phase compared with the proliferative phase or following UPA administration and so does not adequately explain the pattern of transcription of *FOXM1* observed and bears further investigation. This is particularly pertinent given that FOXM1 inhibition has been demonstrated to reduce cyclin B1 expression (Jiang, Liao et al. 2015) and so may be critical in the observed anti-proliferative effect of SPRM UPA and impact upon cell cycle described in **Chapter 5**.

Consistent with previous data, in the data presented herein there was increase in the secretory phase mRNA levels relative to proliferative phase of *KLF-4* (Shimizu, Takeuchi et al. 2010) and *KLF-9* (Pabona, Simmen et al. 2012). No statistical difference relative to either secretory phase or proliferative was noted in mRNA levels of *KLF-4, -9* or *-15* following administration of UPA. For both *KLF-4* and *KLF-15* this may have been due to a smaller sample size but the medians were very similar to secretory phase and so increasing the number of samples may not result in a statistical difference being observed. For *KLF-9*, a trend towards treatment effect relative to secretory phase was observed but the heterogeneity in response prevented this from being statistically

significant. The secretory group where not sub-divided into early, mid and late secretory and the differing expression of *KLF-9* across the luteal phase may have impacted upon outcomes (Pabona, Simmen et al. 2012). Some women in the UPA group had adenomyosis or endometriosis and this may have impacted on mRNA levels. However no kruppel like factors (KLFs) were differentially expressed in other previously reported studies of UPA and mifepristone (Catalano, Critchley et al. 2007, Cuevas, Tapia-Pizarro et al. 2016, Lira-Albarran, Durand et al. 2017) so the findings in the current thesis may represent true effect. However given that *KLF-4* and *KLF-15* both are known to regulate the proliferative response to oestradiol (Ray and Pollard 2012) and *KLF-9* has key roles in both progesterone and oestrogen function in the endometrium (Simmen, Heard et al. 2015) a reassessment of the genes in women in all phases of the menstrual cycle (including subdivision of the secretory phase) and following UPA administration would be of value. The impact on KLF protein expression would also be of import as UPA may alter localisation, as HOXA10 impacts upon epithelial but not stromal expression of KLF-9 (Du, Sarno et al. 2010) and location specific alteration following UPA administration may be assessed.

4.6.3 Endometriosis

The data presented herein suggest that there is a trend towards women who have endometriosis being less likely to achieve amenorrhoea when administered UPA, although this is not statistically significant. The numbers are small and this is a retrospective observation only, and may be affected by selection bias. Whilst this finding is consistent with observation data by our clinical team, in that women who reported poor control of bleeding whilst undergoing treatment with UPA, were often where found to have active endometriosis at the time of surgery, an appropriately powered study with potential bias corrected would be necessary to further explore this most interesting observation.

The data presented herein suggest that co-existing endometriosis does not result in differing mRNA levels of key genes implicated in progesterone resistance following treatment with UPA, when compared to women administered UPA who do not have endometriosis. However limited conclusions can be drawn from these data. The observations have not been confirmed with studies concerning protein expression and localisation, the sample size is small and corresponding controls of women in

proliferative phase and secretory phase with endometriosis were not available. The subjects were poorly characterised with regard to their endometriosis. The anonymised database in which clinical information is recorded of subjects recruited to the "in-house" Female Reproductive Tract Tissue Resource (REC approval 16/ES/0007) does not differentiate between a previous diagnosis of endometriosis (and ensuing treatment) and that of active endometriosis prior to commencing UPA or observed at the time of sample collection. The stage of endometriosis is not recorded and the eutopic endometrium gene profiles has been previously shown, by others, to be altered depending upon stage of endometriosis (Wu, Strawn et al. 2006).

It is thus uncertain if an absence of difference in mRNA levels between the two groups is due to small sample size and potential heterogeneous samples with regard to disease stage and activity, if UPA overcomes relative progesterone resistance associated with endometriosis, or low P-agonism reflects merely pre-existing P-resistance. Only three of the paired biopsies (biopsy prior to and whilst on UPA treatment) had a diagnosis of endometriosis, and all had different histological staging of the baseline sample (proliferative, menstrual and disordered proliferative), as such it is not possible with study on the samples collected to date to assess the impact of UPA administration on genes associated with progesterone resistance in the context of endometriosis. As tissue collection in the embedded mechanistic arm of the UCON study continues (Ulipristal acetate versus conventional management of heavy menstrual bleeding; EudraCT 2014-003408-65) described in **Chapter 2** (**2.2.1.2**), information may be obtained regarding the impact of endometriosis on alteration in gene expression following UPA administration. An alternative would be to explore the effect of *in vitro* administration of UPA on cultured endometrial cells obtained from women with and without endometriosis. Given the paracrine effects of P-signalling between the epithelial and stromal compartments there would be utility in performing this experiment both in isolated stromal cells, isolated epithelial cells and co-culture systems containing both epithelial and stromal cells.

Further exploration of the effect of UPA administration in the context of endometriosis would be of utility as if one could phenotype patients prior to treatment it might be possible to better predict those who would have improved bleeding outcomes, thereby facilitating more 'personalised' medicine. Furthermore SPRMs are increasingly being considered as a treatment for women suffering from the symptoms of endometriosis

without co-existing HMB or fibroids. Promising results from animal studies have shown positive results with regard to regression of lesions following administration of the SPRMs mifepristone (Grow, Williams et al. 1996), onapristone and ZK 136799 (Stoeckemann, Hegele-Hartung et al. 1995). In clinical trials reduction in endometriosis-associated pain was observed following administration of both mifepristone (Kettel, Murphy et al. 1998), and asoprisnil (Chwalisz, Perez et al. 2005). Preliminary reports of a phase II trial of the effects of UPA on endometriosis also reported amelioration of symptoms and reduction in lesion size (Simpson, Lonsdale et al. 2017, Simpson, Lonsdale et al. 2017).

4.6.4 PTEN

Whilst women with heavy menstrual bleeding (and thus likely to be offered SPRMs if co-existing fibroids) overall have a low risk of endometrial cancer (Pennant, Mehta et al. 2017), there have been historical concerns regarding the safety of the SPRMs given the potential risk of normal circulating oestrogen, absence of ovulation, and administration of a compound with low P-agonism. Despite this, there is accumulating high volume evidence suggesting that SPRM administration is not associated with the development of premalignant or malignant disease (Williams, Bergeron et al. 2012).

PTEN is present in the endometrium and acts as a tumour suppressor (Sanderson, Critchley et al. 2017). There is cyclical variation in expression (Mutter, Lin et al. 2000) but inactivation of PTEN is a common feature of endometrial cancer, particularly endometrioid subtypes, and often predates morphological evidence of malignancy and pre-malignant precursors (Mutter, Baak et al. 2000). PTEN deletion has been demonstrated in benign endometrium of nearly a fifth of healthy women (Yang, Meeker et al. 2015). Whilst there was little cyclical variation or impact of UPA on PTEN expression, consistent with effect noted after asoprinil (Wilkens, Williams et al. 2009), null glands were observed in some cases at both the proliferative and secretory phase of the menstrual cycle, and following UPA administration. In no cases was this associated with evidence of malignancy or hyperplasia. Reassuringly in paired samples from the same women obtained prior to treatment and whilst administered UPA, treatment did not appear to affect clearance of PTEN null glands, and was not associated with significant rates of new acquisition. This is particularly relevant given that exogenous

progestins may play an important role in elimination of PTEN-null glands (Orbo, Rise et al. 2006).

It should be noted that interpretation of samples was occasionally compromised by the quality of the tissue obtained, which was occasionally highly fragmented following UPA administration. There would be utility assessing PTEN deletion in paired samples from women prior to commencing UPA, with the subsequent section from the same women obtained from a full thickness biopsy (lumen to endometrial-myometrial interface) at the time of hysterectomy (thereby obtaining greater architectural preservation to better assess the presence of PTEN null glands) in order to add weight to these conclusions.

4.6.5 Future work

The data presented herein would benefit from additional work. For many of the genes discussed, protein validation has yet to be undertaken. Given the alteration in PR and PR localisation described in **Chapter 3,** immunolocalisation in sequential sections and compared against PR/PRB expression, or co-localization with PR/PRB may provide additional insights.

Furthermore, given the impact of fibroids upon expression of key genes such as *IHH*, *BMP-2* and *HOXA10,* exploration of effect of UPA administration on the endometrium in women without fibroids would be of interest. The impact of UPA administration on other key genes implicated in P-signalling including *WNT4, FGF, FGFR, ERK1/2, HIC-5, SRC-2* and *STAT* has yet to be undertaken. In addition the impact upon the co-repressors NcoR and SMRT has yet to be ascertained and the former of these has previously been demonstrated to have differing alteration depending on SPRM utilised (Afhuppe, Sommer et al. 2009).

Further examination of the mechanism of the SPRM UPA action is somewhat hampered by the lack of bioidentical model. Well-validated murine models are available of menstruation itself, (Cousins, Murray et al. 2014) but are time consuming and expensive and there are occasional differences in P-signalling between the mouse and humans. Use of culture systems may provide insights, but given the complex interaction and paracrine effects between the epithelial and stromal compartments, co-culture systems, which have inherent challenges, are likely to be required to more accurately assess mechanism.

The limitations of the experimental design to assess the impact of endometriosis on the effects of UPA administration have already been comprehensively discussed in section **4.6.2.** The impact of co-existing adenomyosis has not been examined, and as recruitment to the "in-house" Female Reproductive Tract Tissue Resource (REC approval 16/ES/0007) is ongoing, may potentially be assessed alongside the impact of endometriosis in the future. The impact of endometriosis and adenomyosis should also not be considered on gene expression and localisation in isolation, but also the impact upon bleeding control and symptomatology.

4.7 Conclusions

In conclusion the data presented herein demonstrate that for many key progesterone regulated genes, UPA administration alters mRNA levels, consistent with UPA acting with low P-agonism. Alteration in *HAND2, FOXO1* and *BCL2* mRNA levels was reflected in altered protein expression but not localisation. In contrast to the majority of genes, mRNA levels of *FOXM1* reflected UPA acting as a P-agonist and may be implicated in the anti-proliferative effect discussed further in **Chapter 5**. For many of these genes this was the first assessment of UPA endometrial effect following *in vivo* administration, and also validates other candidates highlighted by RNA-sequencing and microarray of UPA and mifepristone effect described by other groups. Reassuringly, also presented here, despite overall low P-agonism, there does not appear to be increased levels of PTEN null gland acquisition, adding further mechanistic data to the histological observation of unaltered rates of pre-malignancy and malignancy following UPA administration.

Furthermore it is demonstrated that the effect of UPA administration on genes implicated in P-resistance appear to be unaltered in the presence of endometriosis but further characterisation of this is required. This is of particular importance as in this small sample size there appears to be a trend towards co-existing endometriosis resulting in poorer bleeding control following UPA administration.

Further work is required to better describe this effect of low P-agonism, including protein characterisation, exploration on size of effect relative to the different stages of the secretory phase of the menstrual cycle and the relative impact of co-existing fibroids, as well further exploration of function in appropriate models, and crucially correlation

with bleeding control. However the data presented herein provide novel early insights into the effects of UPA administration on key P-regulated genes within the human endometrium.

Chapter 5.

The impact of selective progesterone receptor modulator (SPRM), Ulipristal acetate (UPA), administration on cell proliferation in the human female reproductive tract

5.1 Background

The endometrium in the human female undergoes repeated cycles of proliferation followed by secretory differentiation and subsequent shedding at the time of menstruation. As described in chapter one (section **1.2.3**, **Figure 1.3**), under the influence of oestradiol (E2), proliferating epithelial and stromal cells arise from the basal layer to form the functional layer of the endometrium.

5.1.1 The cell cycle

Cell proliferation (replication) results from a tightly controlled sequence of events called the cell cycle.

The majority of cells exist in a quiescent state (G_0) where they are not dividing. Under an appropriate stimulus, such as signals from growth factors or from the extracellular matrix (ECM) via integrins, they enter the cell cycle to eventually undergo cell division (mitosis; M). There are three distinct points in the cell cycle prior to mitosis, Gap 1, (pre-synthesis; G_1), synthesis (DNA synthesis; S) and Gap 2 (pre-mitotic; G_2) collectively known as interphase (Figure 5.1).

The cell cycle is highly regulated, and as well as tightly controlled entry by growth factor and integrin signalling, there are multiple checkpoints and internal controls. Each phase of the cycle is dependent on the proper activation and completion of the previous step, and the cycle is further limited by appropriate expression of cell cycle proteins.

Entry into G_1 is either directly from mitosis (for continually replicating cells) or from G_0. The transition from quiescent cell to G_1 is regulated by transcriptional activation of a large number of genes, including proto-oncogenes, and genes required for ribosome synthesis and protein translation. The G_1/S transition is a restriction point, which is a rate-limiting step, and progression beyond this point means that the cell is irreversibly committed to DNA replication. Progression through this point is tightly regulated by the cyclin group of proteins and their associated enzymes, the cyclin-dependant kinases (CDKs). These form complexes with the cyclins, and thus acquire catalytic activity, allowing phosphorylation of proteins critical for transitions through the cell cycle.

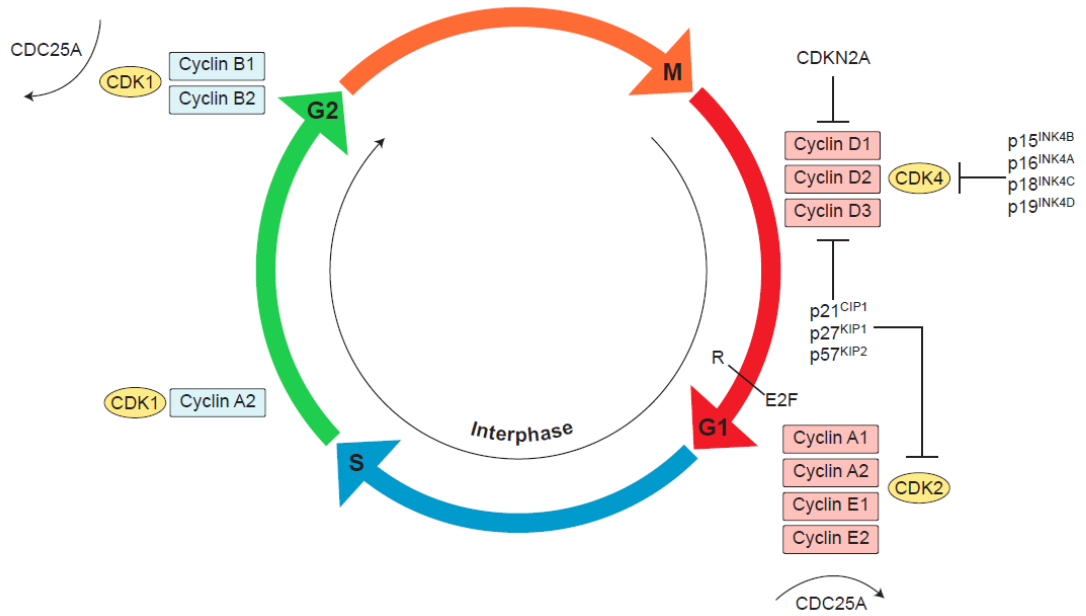

Figure 5.1 The mitotic cell cycle

Representative images of the eukaryotic cell cycle. Cells transition though the cell cycle to eventually undergo cell division (mitosis; M). There are three distinct points in the cell cycle prior to M: Gap 1, (pre-synthesis; G_1), synthesis (DNA synthesis; S) and Gap 2 (pre-mitotic; G_2) collectively known as interphase.

Progression is tightly regulated by cyclins which are regulated by cyclin-dependant kinases (CDK) and there are other regulatory proteins. In G_1 there is restriction point (R), beyond which cells are irrevocable committed to DNA replication

Further CDK-cyclin complexes have activity in subsequent cell cycle phases. Activity of the CDKs is regulated by CDK inhibitors (Figure 5.1). Furthermore there are DNA integrity check points at G_1/S and G_2/M. If damaged DNA is sensed the repair mechanisms are activated, or if too severe, the cell either undergoes apoptosis or enters senescence, a non-replicative state (primarily through p53 regulated mechanisms).

Within the endometrium, the predominant growth factor driving cells into G_1 is E2 (Groothuis, Dassen et al. 2007).

5.1.2 The proliferative paradox of SPRMs

In chapter three the profound effects of Ulipristal acetate (UPA) administration on the human endometrium have been described. In keeping with other SPRMs extensive cystic glandular dilatation is often observed. Prior to the recognition of progesterone receptor modulator associated endometrial changes (PAEC) as a distinct histological variant (Mutter, Bergeron et al. 2008), this characteristic appearance following treatment with an SPRM was often interpreted as simple hyperplasia (Murphy, Kettel et al. 1995, Eisinger, Meldrum et al. 2003, Levens, Potlog-Nahari et al. 2008, Bagaria, Suneja et al. 2009). The reclassification of the endometrial effects following SPRM administration has led to reassurance regarding the histological appearance but the paradox of why women administered SPRMs do not develop endometrial cancer at an increased rate remains.

As previously described in section **1.4**, using the McPhail test both mifepristone and UPA are relatively pure P-antagonists (Elger, Bartley et al. 2000). The majority of women receiving mifepristone are anovulatory due to impaired follicular development and blockade of the LH surge (Croxatto, Salvatierra et al. 1993, Croxatto, Salvatierra et al. 1995, Cameron, Critchley et al. 1996) and circulating E2 levels are consistent with mid follicular phase levels (Baird, Brown et al. 2003). Similar circulating levels of E2 are observed following UPA administration (Donnez, Tatarchuk et al. 2012, Donnez, Tomaszewski et al. 2012). Unopposed E2 is one of the main risk factors for developing endometrial pre-malignancy and endometrioid endometrial cancer (Trimble, Method et al. 2012, Chlebowski, Anderson et al. 2016). Despite this, administration of SPRMs has not been associated with cases of endometrial cancer. The largest studies follow UPA administration in the PEARL studies: 1049 women were allocated to UPA and increase in rates of endometrial malignancy or hyperplasia were not observed (Donnez,

Tatarchuk et al. 2012, Donnez, Tomaszewski et al. 2012, Donnez, Vazquez et al. 2014, Donnez, Hudecek et al. 2015).

Early insights into why UPA administration does not result in unrestrained endometrial proliferation can be derived from the action of SPRMs on other tissue types and previous observed findings in the endometrium of other SPRM class members.

5.1.3 SPRM effects upon cell proliferation

Uterine fibroids

SPRMs have an anti-proliferative effect upon uterine fibroids. These benign tumours of the myometrium express both PR and ER, and with greater abundance than the adjacent myometrium (Englund, Blanck et al. 1998). Macroscopically administration of the SPRMs mifepristone (Engman, Granberg et al. 2009), asoprisnil (Chwalisz, Larsen et al. 2007) and UPA (Donnez, Tatarchuk et al. 2012, Donnez, Tomaszewski et al. 2012) all result in in fibroid shrinkage. *In vitro* work has shown anti-proliferative and pro-apoptotic effects on fibroid cells associated with administration of mifepristone (Yin, Lin et al. 2010), asoprisnil (Yoshida, Ohara et al. 2010) and UPA (Luo, Yin et al. 2010). Mifepristone administration was associated with reduced PCNA and KLF-11 protein expression (Yin, Lin et al. 2010). UPA down regulated PCNA and BCL-2 and upregulated cleaved caspase 3 (Xu, Takekida et al. 2005).

Breast

Anti-proliferative effects of mifepristone has been described in normal human breast tissue with reduction in Ki67 index (Engman, Skoog et al. 2008), an effect replicated in non-human primate (NHP) studies both by mifepristone and asoprisnil (Chwalisz, Garg et al. 2006, Engman, Skoog et al. 2008). In addition, administration of mifepristone prevented development of tumours in *Brca1*-deficient mice (Poole, Li et al. 2006).

Fallopian tube

The fallopian tube also expresses sex-steroid receptors (SSR), as described in chapter 3. Within the fallopian tube, as demonstrated in in this thesis, UPA alters SSR expression relative to secretory phase only, consistent with blockade of P-antagonism. With regard to proliferation there is evidence that SPRMs may reduce proliferation slightly. Mifepristone administration to a NHP resulted in preservation of ciliation and oviductal

wet weight consistent with proliferative phase morphology and unaltered apoptosis. However a modest reduction in epithelial Ki67 was observed (Slayden, Hirst et al. 1993, Slayden and Brenner 1994). The SPRM ZK 137316 also maintained oviductal wet weight but Ki67 was not assessed (Slayden, Zelinski-Wooten et al. 1998). The effect of UPA on cell proliferation within the human fallopian tube and cervix has not previously been assessed.

5.1.4 Known SPRM effects on endometrial cell proliferation

Mifepristone, Asoprisnil, ZK 137316 and ZK230211

In keeping with the impact upon SSR expression described in chapter 3, much of the early understanding of the impact of SPRMs upon endometrial proliferation was gained from studies utilising mifepristone in both NHP and human studies. In the NHP mifepristone administration resulted in endometrial atrophy with both reduction in thickness and wet weight, however in this study, despite morphological atrophy, there was no reduction in cell proliferation as assessed by Ki67 although increased apoptosis was noted (Slayden, Hirst et al. 1993). However subsequent studies did demonstrate a reduction in mitotic indices (no of mitoses per 1000 epithelial cells; (Slayden and Brenner 1994)). This inconsistent finding in the first study may be due to treatment schedules. Anti-proliferative effects have been consistently noted with other SPRMS in NHP models. The SPRM asoprisnil reduced endometrial thickness and decreased epithelial Ki67 and PH3 immunopositivity (Chwalisz, Garg et al. 2006). Similarly ZK 137316 inhibited mitosis (as assessed by Ki67 immunopositivity) in both epithelial and stromal cells and this was observed in both basal and functional layers, in addition to the reduction in thickness and wet weight (Slayden, Zelinski-Wooten et al. 1998). A reduction in wet weight and thickness, as well as reduction in mitotic indices was also observed after administration of the SPRM ZK 230211 (Slayden and Brenner 2003, Slayden and Brenner 2004).

Human studies have been predominantly limited to mifepristone and asoprisnil. Mifepristone, whilst increasing endometrial thickness (Baird, Brown et al. 2003) has been consistently shown to reduce proliferation, as assessed by number of mitotic figures, as well as Ki67 immunopositivity (Cameron, Critchley et al. 1996, Baird, Brown et al. 2003, Engman, Granberg et al. 2009). This reduction in Ki67 expression was observed in both glands and stroma. Asoprisnil did not increase endometrial thickness in the largest published study (Chwalisz, Larsen et al. 2007). Mitotic figures were

reduced (Williams, Critchley et al. 2007) and Ki67 immunoexpression decreased, though this was limited to the stroma and compared only to secretory phase endometrium (Wilkens, Williams et al. 2009).

In both NHP and human studies this observed anti-proliferative effect has been considered a potential factor involved in the reduction of menstrual bleeding resulting from administration of an SPRM (Spitz 2003).

Ulipristal acetate

As with other SPRMS, initial information can be gained from NHP models. Intrauterine administration of UPA resulted in endometrial atrophy and histological proliferation appeared reduced. This was further confirmed utilising the proliferation marker Ki67 and PH3 both of which were reduced by UPA administration (Brenner, Slayden et al. 2010). In human studies, whilst an increase in endometrial thickness is often observed (Donnez, Donnez et al. 2016), mitotic activity appears low on histological examination (H&E of fixed tissue sections;(Williams, Bergeron et al. 2012)). To date we are the only group to quantitatively demonstrate that proliferation is reduced following UPA administration compared to the proliferative phase (Whitaker, Murray et al. 2017). We demonstrated that there is a reduction in Ki67 immunopositivity both overall in the endometrium and specifically in the stromal compartment (Figure 5.2). The reduction in the glandular compartment did not quite achieve statistical significance ($p = 0.069$).

The mechanism by which this reduction in proliferation is brought about is poorly understood. Some studies of in vitro models of other disease systems have suggested that mifepristone and onapristone results in cell cycle arrest by up regulation of cyclin dependant kinase inhibitors p21 in a murine breast cancer model (Peters, Vanzulli et al. 2001). Mifepristone also increases the CDK inhibitor p27 in a similar mouse model (Vanzulli, Soldati et al. 2005) and in metastatic murine cell lines (Vanzulli, Efeyan et al. 2002). In ovarian cancer cells mifepristone administration is associated with low E2F and reduced CDK2 (Goyeneche, Caron et al. 2007) and this and other SPRMs (including UPA) upregulate p21 and p27 and reduce cyclin E levels (Goyeneche, Seidel et al. 2012). Somewhat surprisingly, little is published with regard to effects of SPRMs on cell cycle

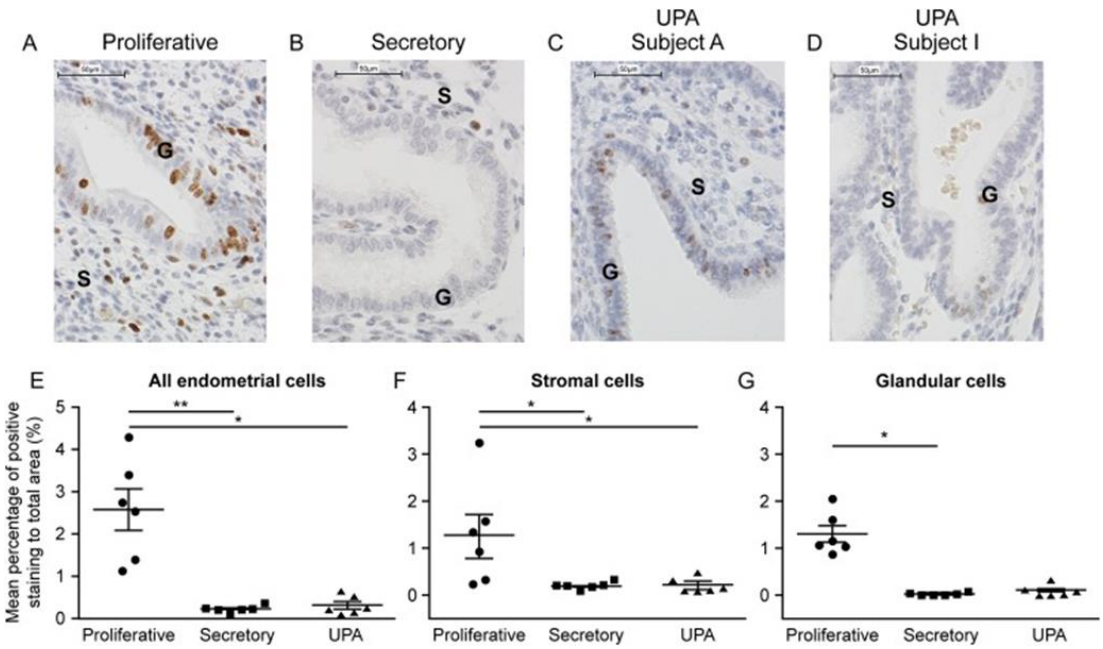

Figure 5.2 Selective progesterone receptor modulator, ulipristal acetate (UPA), administration does not increase endometrial cell proliferation

Proliferation assessed by Ki67 immunohistochemistry and stereological quantification. Subject A shows endometrium in which PAEC is characterised by extensive cystic glandular dilatation; Subject I has PAEC with minimal cystic change. x40 magnification (scale bar = 50µm); LE: Luminal epithelium, G: Glands, S: Stroma. Negative controls shown as inserts on secretory endometrium. Kruskal-Wallis statistical test *p <0.05, **p <0.01

Reproduced with permission (open access) from:

Whitaker LH, Murray AA *et al* (2017)
Selective progesterone receptor modulator (SPRM) ulipristal acetate (UPA) and its effects on the human endometrium
Human Reproduction 32(3):531-543

factors in the endometrium. Ishikawa cancer cells demonstrate reduction in cycle progression but the point of arrest appears conflicting (Goyeneche and Telleria 2015). In a different endometrial cancer cell line (Hex-1A) p21 was also increased (Schneider, Gibb et al. 1998). In a NHP model mifepristone cyclin B was increased but not p21 (Heikinheimo, Hsiu et al. 1996).

In summary, as a class, SPRMs appear to reduce cell proliferation in some tissues, including the endometrium. The effect of UPA administration upon fallopian tube and cervix cell proliferation is unknown. Other SPRMs have a limited effect upon fallopian tube proliferation, suggesting a relatively endometrial specific effect. The mechanism by which endometrial proliferation is reduced by UPA is unknown, and there does not appear to be published evidence of the impact of *in vivo* UPA administration upon cell cycle function in the endometrium of women.

5.2 Hypothesis

SPRM administration has an anti-proliferative effect within the epithelium of the human reproductive tract

5.3 Aim

To study the mechanisms whereby SPRM administration reduces cell proliferation in the epithelium of the human female reproductive tract.

Research Questions

- Is there reduction in cell proliferation in the fallopian tube and cervix following UPA administration?
- What candidate genes are implicated in the anti-proliferative effect within the endometrium?
- Is there alteration in mRNA levels and protein expression in the endometrial cell cycle?

5.4 Materials and Methods

5.4.1 Ki67 Immunohistochemistry of human fallopian tube and cervix biopsies

Nine women with symptomatic fibroids underwent hysterectomy following treatment with Ulipristal acetate (UPA) 5mg orally once daily for up to 15 weeks prior to surgery (minimum nine weeks of treatment). They had given informed consent and the study had REC approval (12/SS/0238; section **2.1.1**). At the time of surgery, biopsies were collected from the fallopian tube and cervix if removed concurrently. Samples were processed as previously described (section **2.2**) and tissue taken for formalin fixation prior to immunohistochemistry. Corresponding control biopsies from women with symptomatic fibroids in proliferative and secretory phases of cycle were obtained from tissue archives (section **2.1.1**). Subjects were well characterised (section **2.4.1 Table 2.8-11**). FFPE sections were cut for histology (H&E staining) and immunolocalisation of Ki67 was performed (section **2.6, Table 2.13-14**). This was performed on the fallopian tube (n=6 in each group of UPA, proliferative or secretory phase of the menstrual cycle) and cervix (n = 8 UPA, 4 proliferative and 5 secretory).

5.4.2 Gene expression Microarray in human endometrium exposed to SPRM

5.4.2.1 Sample characteristics

For gene microarray, paired endometrial biopsies were obtained from six women with symptomatic fibroids treated with UPA 5mg daily with ethical approval and written informed consent (see below for power calculation). Samples were obtained using a pipelle endometrial biopsy sampler (Pipelle de Cornier Mark II, Laboratoire CCD, France) as described in section **2.2.1.2**. A baseline biopsy was obtained prior to commencement of treatment when women were in the proliferative phase of the menstrual cycle (staged as described in section **2.3.2**; histological appearance based on Noyes criteria, LMP and circulating progesterone and oestradiol Table 5.1).

A follow-up sample was taken whilst on treatment after at least eight weeks of UPA administration (Table 5.2). One sample (CT1280E2) was form a patient who had unexpectedly stopped treatment a week prior to her scheduled biopsy but had no bleeding. Consensus was that this sample was acceptable for use in the array as exposure had been for 77 days and progesterone and oestradiol levels suggested that ovulation had not occurred (Table 5.2).

Table 5.1 Sample characteristics of endometrial biopsies from proliferative phase of the menstrual cycle for gene microarray

Participant No	REC	Date of collection	Sample No	Study code No	Age	BMI	Parity	HMB	Fib	Endo	LMP	Cycle	E2	P4	Histology	RIN	cRNA concentration
5777	B	23/11/2015	1678	CT1262E2	52	29.6	1+2	Yes	Yes	No	05/11/2015	7/24-29	145	0.4	P	8.6	624 µg/µl
5795	B	07/01/2016	1679	CT1280E	46	22.9	2+1	Yes	Yes	No	14/12/2015	8/21-25	522	4.7	P	8.1	222 µg/µl
7886	B	25/02/2016	1935	CT1162E2	46	21.3	0+0	Yes	Yes	No	18/02/2016	6-14/28-46	104	5.1	P	8.2	555 µg/µl
8097	B	29/10/2015	1916	CT1460E	40	28.9	0+1	Yes	Yes	No	20/10/2015	3-8/21-28	224	2.5	P	7.7	317 µg/µl
8522	B	14/12/2015	1724	CT1929E	46	38.6	0+3	Yes	Yes	No	25/11/2015	4-8/35-43	312	8.5	P	8.3	583 µg/µl
9055	B	03/12/2015	2036	CT1685E	47	25.9	1+1	Yes	Yes	Yes	18/11/2015	7-10/21	207	4.5	P	10.0	244 µg/µl

REC: Research ethics committee (approval) BMI: Body mass index HMB: Heavy menstrual bleeding Fib: Fibroids Endo: Endometriosis LMP: Last menstrual period E2: oestradiol P4: progesterone
P: Proliferative phase of menstrual cycle

Table 5.2 Sample characteristics of endometrial biopsies following administration of ulipristal acetate (UPA) for gene microarray

Participant No	REC	Date of collection	Sample No	Study code No	Duration of UPA Rx	Days off Rx	Control	E2	P4	Histology	RIN	cRNA concentration
5777	A	08/03/2016	1938	CT1262E3	81	0	Amenorrhoea	55	5.2	Inactive with no atypia[#]	7.6	125 µg/µl
5795	A	03/05/2016	1960	CT1280E2	77	8[2]	Amenorrhoea	359	0.2	PAEC	8.4	193 µg/µl
7886	A	19/05/2016	1964	CT1162E3	60	0	Amenorrhoea	319	0.5	Inactive with no atypia[#]	9.4	230 µg/µl
8097	A	29/03/2016	1951	CT1460E2	70	0	Amenorrhoea	149	2.7	Inadequate[#]	7.5	112 µg/µl
8522	A	14/03/2016	1941	CT1929E2	80	0	Lighter	302	3.6	PAEC	8	565 µg/µl
9055	A	02/06/2016	2063	CT1685E2	79	0	Lighter	135	0.2	PAEC	7.5	436 µg/µl

REC: Research ethics committee (approval) E2: oestradiol P4: progesterone PAEC: progesterone receptor modulator associated endometrial changes
[#]: Minimal tissue in biopsy or fragmented sample. Sufficient tissue available to exclude malignancy but may be insufficient to assess for features of PAEC or to unequivocally state PAEC as diagnosis
[2]: sample taken 8 days after stopping UPA. Patient remained amenorrhoeic at the time of biopsy

Table 5.3 Sample characteristics of endometrial biopsies from proliferative phase of the menstrual cycle for gene microarray validation

Participant No	REC	Date of collection	Sample No	Study code No	Age	BMI	Parity	HMB	Fib	Endo	LMP	Cycle	E2	P4	Histology	RIN
5790	B	12/05/2015	1671	CT1275E+	39	26.8	3+0	Yes	Yes	No	29/04/2015	5-16/28-31	477	21.7[1]	P	9.1
8100	B	26/11/2015	1920	CT1463E+	48	46.4	2+0	Yes	Yes	No	NS	10/14-21	229	3.1	P	8.3
8131	A	23/06/2016	1976	CT1494E	47	25.6	2+0	Yes	Yes	No	15/06/2016	7/14	1376	0.8	P	9.5
8085	A	23/07/2015	1904	CT1448E	46	32.7	1+0	Yes	No	No	13/07/2015	5-7/26-30	199	1.8	P	9.2
5785	B	28/07/2015	1673	CT1270E2+	44	34.6	3+0	Yes	No	No	06/07/2015	5-6/26-27	331	3.6	P	9.6
8506	B	24/11/2015	1917	CT1903E2+	41	23.8	3+1	Yes	No	No	13/11/2015	5/28-29	430	1.3	P	10.0

REC: Research ethics committee (approval) BMI: Body mass index HMB: Heavy menstrual bleeding Fib: Fibroids Endo: Endometriosis LMP: Last menstrual period E2: oestradiol P4: progesterone NS: Not stated P: Proliferative phase

+: sample has a paired UPA treated sample [1]: sample had elevated P4 but day of cycle sampling and histology review suggested proliferative phase. Subsequent first day of menstruation also was in keeping with the sample having been taken in proliferative phase

Table 5.4 Sample characteristics of endometrial biopsies from women administered ulipristal acetate (UPA)

Pt No	REC	Date of collection	Sample No	Study code No	Age	BMI	Parity	HMB	Fib	Endo	Duration of UPA Rx	Days off Rx	Control	E2	P4	Histology	RIN
Samples after 3 months of treatment																	
8002	A	16/03/2016	1942	CT1366E3	51	20.9	1+1	Yes	Yes	Yes	66	0	Amenorrhoea	819	21.8	Disordered proliferative#	7.5
8100	A	24/03/2016	1949	CT1463E2+	49	46.4	2+0	Yes	Yes	No	82	0	Amenorrhoea	60	3.4	Consistent with UPA#	7.9
8123	A	05/07/2016	1980	CT1486E2	41	39.9	3+1	Yes	Yes	Yes	75	0	Amenorrhoea	162	0.2	PAEC	9.2
8124	A	18/07/2016	1986	CT1487E2	49	30.5	1+1	Yes	Yes	No	81	0	Amenorrhoea	97	0.2	Consistent with UPA#	NA
8117	A	18/07/2016	1985	CT1480E2	40	32.3	2+0	Yes	Yes	No	77	0	Lighter	317	50.3	PAEC	9.2
5817	A	21/07/2016	1988	CT1691E2	48	22.7	2+0	Yes	Yes	No	80	0	Amenorrhoea	1491	1.7	PAEC	9.1
Samples after 6 months of treatment																	
5790	E	22/01/2016	1684	CU1275E+	40	NS	3+0	Yes	Yes	No	79[1] (163)	0	Unchanged	NS	NS	Mildly disordered proliferative	9.6
5805	E	18/10/2016	1812	CU1289E2	48	22.0	2+1	Yes	Yes	No	81[1] (165)	0	Amenorrhoea	1665	0.5	Inactive with no atypia#	8.8
8126	E	09/11/2016	1867	CU1489E2	45	30.4	0+1	Yes	Yes	No	81[1] (165)	0	Amenorrhoea	114	<0.2	PAEC	9.2
5785	E	27/04/2016	1958	CU1270E3+	44	34.6	3+0	Yes	No	No	78[1] (162)	0	Amenorrhoea	303	15.7	Secretory (some non-physiological)	9.0
8506	E	12/08/2016	1807	CU1903E3+	41	23.5	3+0	Yes	No	No	82[1] (166)	0	Lighter	237	1.6	Proliferative	9.1
9046	E	24/08/2016	1993	CU1676E2	44	30.1	5+0	Yes	No	No	80[1] (164)	0	Amenorrhoea	432	<0.2	Inadequate#	NA

REC: Research ethics committee (approval) BMI: Body mass index HMB: Heavy menstrual bleeding Fib: Fibroids Endo: Endometriosis Rx: treatment LMP: Last menstrual period E2: oestradiol P4: progesterone NS: Not stated PAEC: progesterone receptor modulator associated endometrial changes NS: Not stated +: sample has a paired control sample #: Minimal tissue in biopsy or fragmented sample. Sufficient tissue available to exclude malignancy but may be insufficient to assess for features of PAEC or to unequivocally state PAEC as diagnosis [1]: sample from UCON subject (Ulipristal acetate versus conventional management of heavy menstrual bleeding clinical trial): pipelles taken in final week of second 12 week cycle of treatment (total treatment days)

Additional endometrial samples were utilised for validation of the array outputs. For RT-qPCR endometrial biopsies from six women with HMB in proliferative phase were obtained from archival resources (REC approval 16/ES/0007, 14/LO/1602). Three women had fibroids and three women did not (Table 5.3). A further six samples were obtained from women (all with symptomatic fibroids) after administration of UPA (5mg once daily) for at least nine weeks (Table 5.4). A further treatment set was obtained from women participating in the mechanistic arm of the UCON trial (described in section **2.2.1.2**) in the final week of the second cycle of treatment (Table 5.4). Three had fibroids and three women did not. Three of the UCON UPA samples had had paired biopsies in the proliferative phase of the menstrual cycle. All biopsies for RT-qPCR validation of the array were obtained by pipelle biopsy sampler (Pipelle de Cornier Mark II, Laboratoire CCD, France) as described in section **2.2.1.2**. RNA was extracted and quality checked as described previously (section **2.5.1**).

Full thickness endometrial biopsies (luminal epithelium to endometrial-myometrial junction) were obtained from nine women with symptomatic fibroids at the time of hysterectomy following treatment with Ulipristal acetate (UPA) 5mg orally once daily for up to 15 weeks (section **2.2.1.1 Table 2.4**). Control biopsies from nine women in the proliferative phase were obtained at the time of hysterectomy and utilised for comparison (**Table 2.5**). FFPE sections were cut for immunolocalisation of cell division cycle 25A (CDC25A, Figure 5.1) as previously described (section **2.6, Table 2.13-14**).

5.4.2.2 Power calculation

A power calculation for the number of samples required for micro array was generated using data from a prior unrelated study (Talbi, Hamilton et al. 2006). All microarray raw data files were downloaded and subject to RMA probe set summation and normalisation. After box and whiskers plots used to analyse consistency of data distribution, no samples were removed due to an obvious gross differences in data. The raw files were again normalised without array outlier and data used as input for Power calculation analysis in R statistical software.

A statistical power calculation for a two-sided statistical test determines that n=6 independent samples per group should provide the ability to detect a 2-fold change in

expression with 80% power at p=0.05 (adjusted) for 95% of the gene probes on the array.

5.4.2.3 Array RNA processing and biotinylation

Total RNA was isolated from endometrial samples and quality checked as previously described (tissue homogenisation, Qiagen RNAeasy mini kit, nano dropped and Agilent RNA 600nano kit; section **2.5.1**). Three samples required concentration to yield acceptable RNA concentrations (CT1460E2, CT1262E3 and CT1685E2). This was performed according the manufacturer's protocol utilising a Zymo RNA Clean and Concentrator™-5 kit (Zymo Research, USA). Despite fragmentation of some samples on H&E acceptable RIN were obtained (7.5-10.0; Table 5.1&5.2). Samples were then diluted to 150ng/µl.

RNA samples were amplified and labelled with biotin to produce biotinylated anti-sense RNA (cRNA). This was performed according to manufacturer's protocol using an Illumina® TotalPrep™ RNA Amplification kit (Life Technologies, USA). In summary 500ng of total RNA underwent reverse transcription to create first strand cDNA, second strand cDNA was then synthesised from this. The cDNA was then purified and incubated overnight in a thermal cycler with an in vitro transcription enzyme and biotin-UTP to synthesise biotinylated cRNA. The biotinylated cRNA was then purified and eluted into 100µl of nuclease free water. Concentration was assessed using Agilent RNA 600nano kit in conjunction with Agilent 2100 Bioanalyser system as previously described (section **2.5.1**) and stored at -80°C.

5.4.2.4 Illumina platform Gene expression Microarray

Illumina Whole Genome Gene Expression Profiling was performed by the Genetics Core, based in the Wellcome Trust Clinical Research Facility at the Western General Hospital, Edinburgh.

Following assessment of adequacy utilising the Agilent results performed above the 12 samples were placed on an Illumina HumanHT-12 BeadChip and underwent direct hybridization assay with readout utilising iScan. The beadchip contains probes from the National Center for Biotechnology Information Reference Sequence (NCBI RefSeq Release 38, 2009) with additional probe design based upon UniGene release 188. Overall

48,804 transcripts (both coding and non-coding) were analysed in each sample. Internal quality control was performed and raw data exported for transfer to FIOS Genomics (Fios Genomics, UK) for external quality control, statistical analysis and some limited bioinformatics interogation.

5.4.2.5 Data Processing

Quality control (QC)

Raw data were analysed by Fios genomics using the arrayQualityMetrics package in Bioconductor (Kauffmann and Huber 2010). Arrays were scored (outliers identified) on the basis of 3 metrics (maplot, boxplot, heatmap).

MA plots: M and A are defined as

- $M = \log_2(I_1) - \log_2(I_2)$
- $A = 1/2\ (\log_2(I_1) + \log_2(I_2))$

where I_1 is the intensity of the array studied and I_2 is the intensity of a "pseudo"-array, which has the median values of all the arrays. Typically, it is expected that the mass of the distribution in an MA plot is concentrated along the M = 0 axis, and there should be no trend in the mean of M as a function of A. A trend in the lower range of A usually indicates that the arrays have different background intensities, this may be addressed by background correction. A trend in the upper range of A usually indicates saturation of the measurements, in mild cases, this may be addressed by non-linear normalisation (e.g. quantile normalisation).

Box plots: Each box corresponds to one array. It gives a simple summary of the distribution of feature intensities across all arrays. Typically, one expects the boxes to have similar size (IQR) and y position (median). If the distribution of an individual array is very different from the others, this may indicate an experimental problem.

Heat map: The heatmap shows the correlation (Pearson) of the raw data ($\log_2$ intensities), prior to QC. Individual arrays are shown along both the X and Y axes, with the degree of correlation indicated by the colour (red: higher correlation, blue: lower correlation), as shown in the colour key/histogram in the top left of image. Clustering (Euclidean distance) is shown by the dendrograms above and to the left of the image

Boxplots of the raw, transformed and normalised data were also assessed manually, as were outlier and sample relation plots generated for all stages of the processing. Exploratory analysis using principle component analysis (orthogonal transformation to convert a set of observations of possibly correlated variables into a set of values of linearly uncorrelated variables) and hierarchical clustering to determine if there was separation of the samples based on the on treatment group.

Non-specific filtering

Following QC, the data set was filtered to remove features that were not detected at last once across all the arrays. Raw data were log2 transformed prior to normalisation across all arrays using the robust spline normalisation (RSN) method.

Statistical hypothesis testing

Normalised data provide the input for statistical hypothesis testing, in order to identify features that are statistically significantly different between sample groups. Fold change (FC, the degree of difference) was also assessed. In the output, the fold-changes (logFC) are given as $\log_2$ values, with a positive logFC representing up-regulation, and a negative logFC indicating down-regulation.

A single comparison (Post- vs pre- treatment) was undertaken using linear modelling to identify differentially expressed genes (DEG). The null hypothesis was that there was no difference between the groups being compared. As pre- and post-treatment samples were available from each individual in the study, a paired statistical comparison approach was used in order to account for baseline differences between the treated individuals. The Bioconductor package limma was used (Smyth 2005). Significance was tested using a moderated t-test. The statistical significance of the DEGs was assessed by Fios Genomics with a raw (unadjusted) p-value < 0.01 and a fold change >= 1.3. A subsequent comparison was performed utilising (FC>2, adjusted p<0.05). The latter has a power of 80%.

Pathway analysis

An overview of the underlying biological changes occurring within each comparison was obtained by functional enrichment analysis. This was performed from two perspectives,

namely Kyoto Encyclopedia of genes and Genome (KEGG) pathway membership (http://www.kegg.jp) and Gene Ontology (GO) terms (http://www.geneontology.org)

Significant genes with raw p <0.01 and fold change ≥1.3 from each comparison were analysed for enrichment of KEGG pathway membership and of enrichment of GO terms across all three GO ontologies using a hypergeometric test. Enrichment (p <0.05) was assessed for up- and down-regulated genes separately.

5.4.2.6 Validation of gene targets

5.4.2.6a Quantitative reverse transcription polymerase chain reaction (RT-qPCR) of gene targets

Candidates for validation were selected both from the differentially expressed gene list and altered genes within the most significantly down regulated KEGG pathway.
RT-qPCR was performed on RNA submitted for array for internal validation, and then on independent sets of women in proliferative phase (n = 6) and whilst receiving treatment with UPA. The latter group was further subdivided by women in their first cycle of treatment (n = 6) and those at the end of a second cycle of treatment (n = 6) (5.4.2.2).

RT-qPCR performed in triplicate for candidate genes identified by the array as previously described (section **2.5.3**). Primers and probes can be found in **Table 2.12**. ATBP5 and SHDA were used as housekeeper genes. Data were analysed using the $\Delta\Delta C_q$ method as described in section **2.5.3**.

Statistical analysis of RT-qPCR results was performed using Graphpad prism software (Graphpad, USA). Data were subjected to the D'Agostino-Pearson omnibus normality test. Data with a Guassian distribution had an unpaired t-test applied when two comparators, and one-way ANOVA when 3 comparators (proliferative, secretory and following SPRM (UPA) treatment), to determine difference between groups. For non-parametric data Kruskal-Wallis test was used to determine differences between sample groups when three comparators, and Mann-Whitney test when two. $p < 0.05$ was considered to be statistically significant.

5.4.2.6b Immunohistochemistry of gene targets

FFPE sections were cut for histology (H&E staining) and immunolocalisation of Ki67 was performed (**2.6**). This was performed on the baseline and post treatment biopsies submitted for the array (n=6 in each group, Table 5.1&5.2). Immunolocalisation was semi-quantitated by histoscoring as previously described (section **2.6.5.1**). Immunolocalisation of CSC25A was performed on full thickness endometrial biopsies from women receiving UPA or in proliferative phase (n=9 in each group) (section **2.6**). Immunolocalisation was semi-quantitated by histoscoring as above.

5.5 Results

5.5.1 Effect of UPA administration upon cell proliferation in the fallopian tube and cervix.

5.5.1.1 UPA administration reduces cell proliferation in the fallopian tube relative to proliferative phase of the menstrual cycle

In all samples cell proliferation, as assessed in the ampulla using an antibody to Ki67, was relatively infrequent but appeared lower in women in secretory phase (5.3B & F) and following UPA administration (5.3C & G) compared to women in proliferative phase of the menstrual cycle (5.3A & E). Women in proliferative phase had between 0 and 58 positive nuclei per sample (mean 21) compared to secretory (2-30 positive nuclei per sample, mean 11.6) and UPA (0-4, mean 12.3). A formal index of cell proliferation was not performed. Immunopositivity for Ki67 in the fimbrial ends of the fallopian tubes from women treated with UPA (5.3D & H) was consistent with ampullary immunoreactivity for Ki67 (5.3C & G).

5.5.1.2 UPA administration does not appear to alter cell proliferation in the cervix

Cell proliferation, as assessed using an antibody to Ki67, appeared low in all groups of women and administration of UPA did not appear to alter cell proliferation in the cervix. Immunopositive nuclei were infrequently present in the para basal layer of the squamous epithelium (5.4A-C). Localisation and intensity of immunostaining in the squamous epithelium was unchanged irrespective of stage of cycle or treatment with UPA. There was a complete absence of immunopositive nuclei present in the stroma,

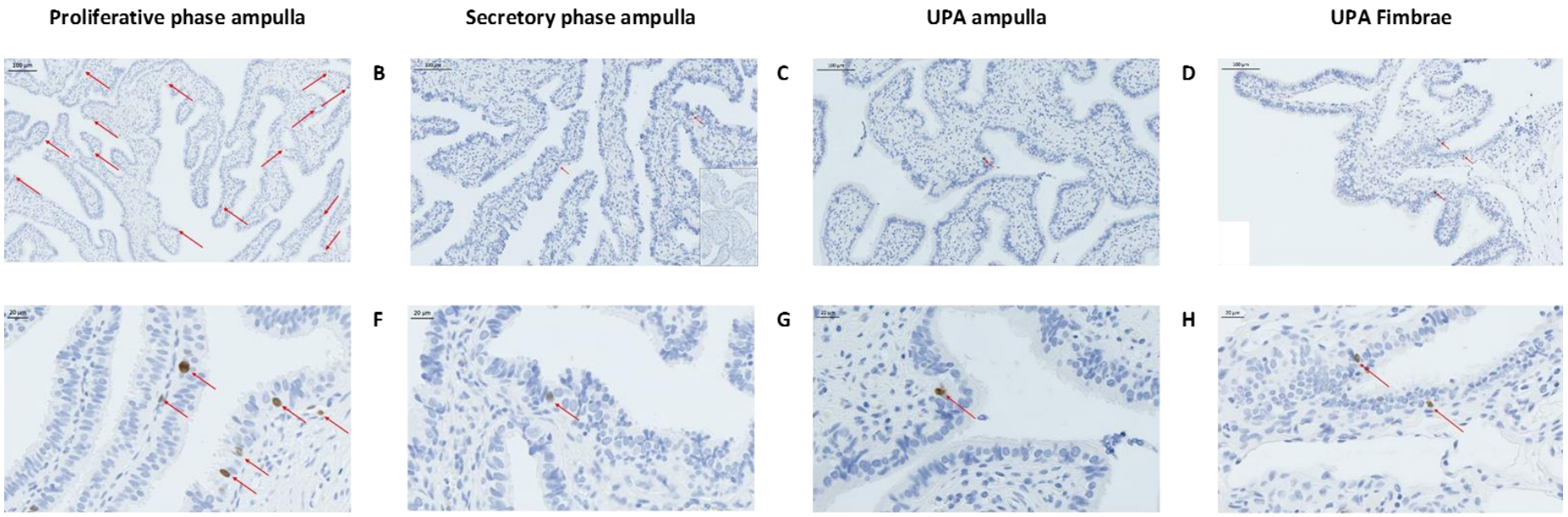

Figure 5.3 Administration of selective progesterone receptor modulator, ulipristal acetate (UPA), appears to decrease cell proliferation marker Ki67 expression in the ampulla of the fallopian tube relative to proliferative phase.

Representative images low- (A-D) and high-power (E-H) immuno-localisation of Ki67 in fallopian tube (FT) biopsies from woman during proliferative and secretory stages of the menstrual cycle and after UPA administration. Samples from FT ampulla of UPA-treated women (C&G) displayed very rare immunopositive nuclei (indicated by red arrows), this immunostaining was consistently observed at the fimbriae ends (D&H). Infrequent Ki67 immunopositivity was also observed in the ampulla from women in secretory (B & F) phase of the menstrual cycle.

In contrast samples from women in proliferative (A & E) phase of the menstrual cycle appeared to have more frequent immunopositive cells

Red arrows indicate towards immunopositive nuclei. Lower power (scale bar = 100µm) and high power magnification (scale bar = 20 µm); Negative controls shown as inserts on secretory phase fallopian tube low power image (B)

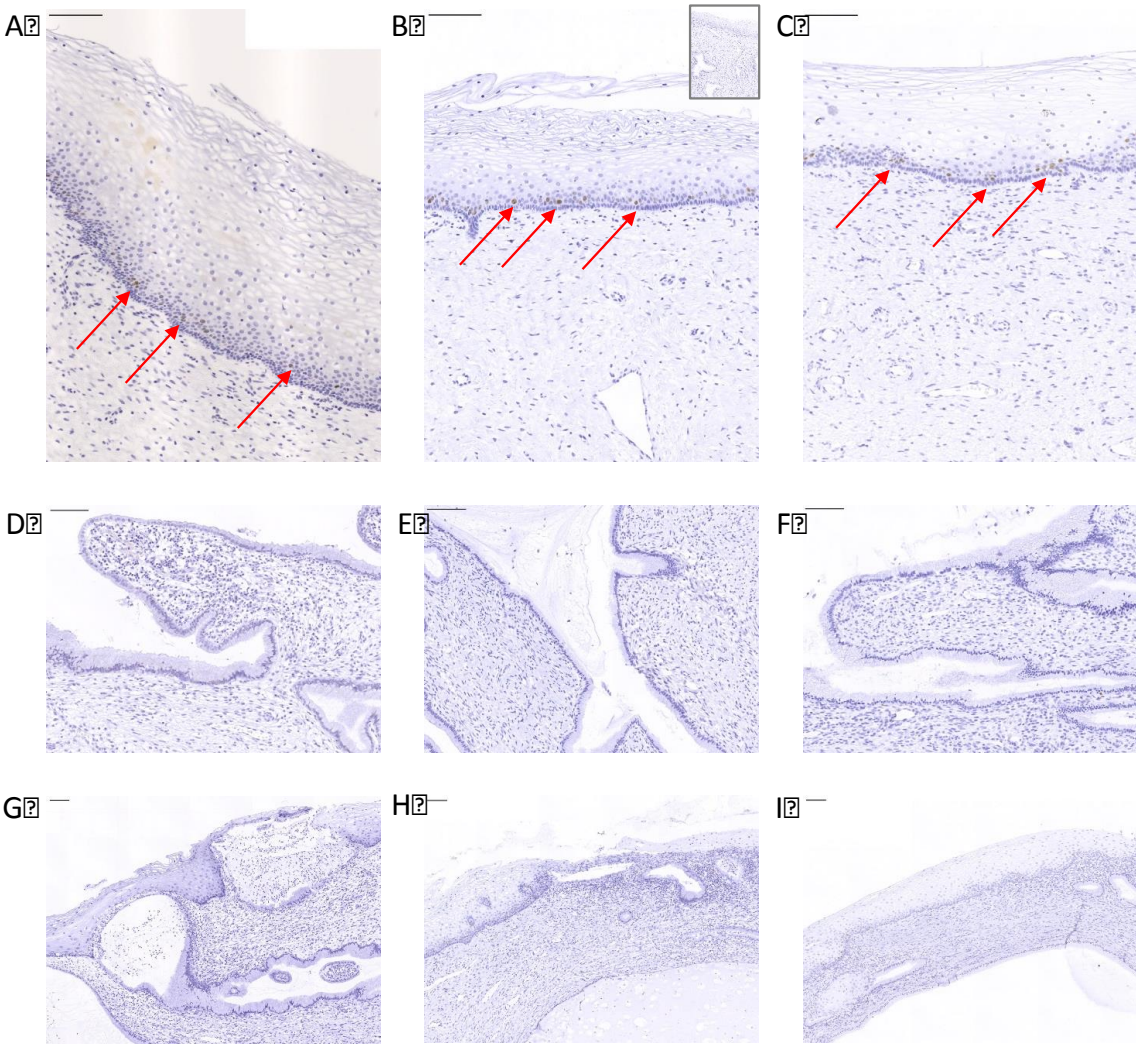

Figure 5.4 Administration of selective progesterone receptor modulator, ulipristal acetate (UPA), does not alter cell proliferation marker Ki67 localisation or intensity in the endo- or ecto-cervix

Representative immuno-localisation of Ki67 in cervical biopsies from woman during proliferative (A/D/G) and secretory (B/E/H) stages of the menstrual cycle and after UPA (C/F/I)) administration. Immunopositive nuclei (indicated by red arrows) were infrequently present in the para basal layer of the squamous epithelium (A-C). There were no immunopositive nuclei present in the stroma, glandular (D, E F) and transitional zone (G/H/I) epithelium. Localisation and intensity of immunostaining in the squamous epithelium was unchanged irrespective of stage of cycle or treatment with UPA.
Red arrows indicate towards immunopositive nuclei. Scale bar = 100 µm; Negative controls shown as inserts on secretory phase cervix (B).

glandular (5.4D-F) and transitional zone (5.4G-I) epithelium in women in proliferative and secretory phase and following administration of UPA. Immunopositivity has not been quantitated either with histoscoring or utilising stereology but given the very low frequency of immunopositivity this was not considered to be of use.

These findings in the fallopian tube and cervix suggest that the impact upon cell proliferation previously observed within the endometrium is not specific to the endometrial region of epithelium of the female human reproductive tract.

5.5.2 Gene Microarray results

5.5.2.1 Quality control (QC)

QC of the Illumina microarray raw data was performed as described above by Fios Genomics:

MA plots: The mass of distribution is concentrated around the M=0 axis and symmetrical which is reassuring (Figure 5.5A). The trend in the lower range of A suggest that the arrays have different background intensities. This was corrected for by subsequent normalisation.
Box plots: The box plots have a relatively similar sizes and y positions (Figure 5.5B). Overall the pre-treatment samples appeared to have slightly wider IQR, the widest was CT1262E2 (5777_Pre).
Heat map: The data were normalised and the top 25% most variable features within the processed dataset were subsetted prior to sample relatedness being assessed by Euclidean distance using a complete linkage algorithm (Figure 5.5C). The heatmap shows the correlation (Pearson) of the raw data (log_2 intensities), prior to QC (Figure 5.5D) and following normalisation (Figure 5.5E)

Boxplots of the raw, transformed and normalised data were also assessed manually by Fios, as were outlier and sample relation plots generated for all stages of the processing.

Based on the three metrics (MAplot, Boxplot and Heatmap), one sample (CT1262E2) was flagged as a moderate outlier based on automated QC checks. After manual inspection however it was decided to include this sample as it did not show any major differences relative to the remaining samples.

A

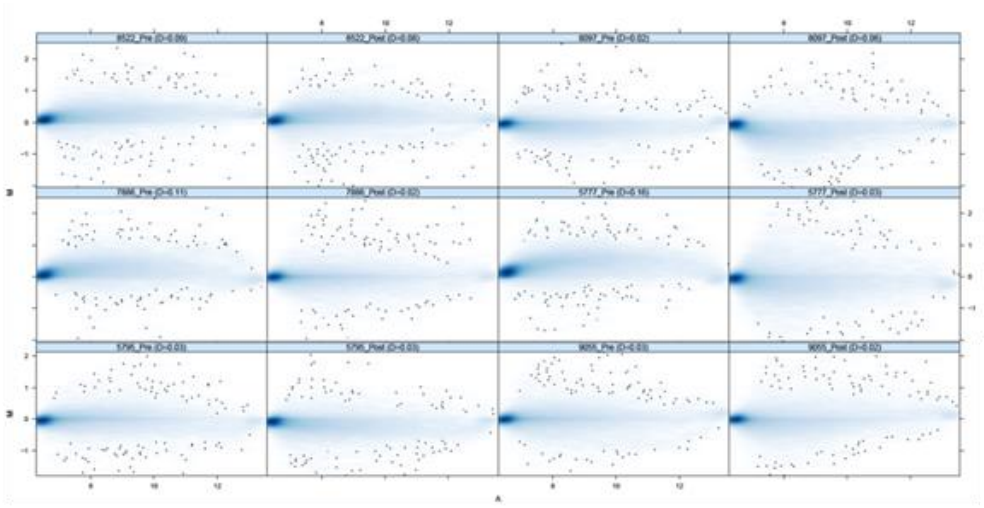

B

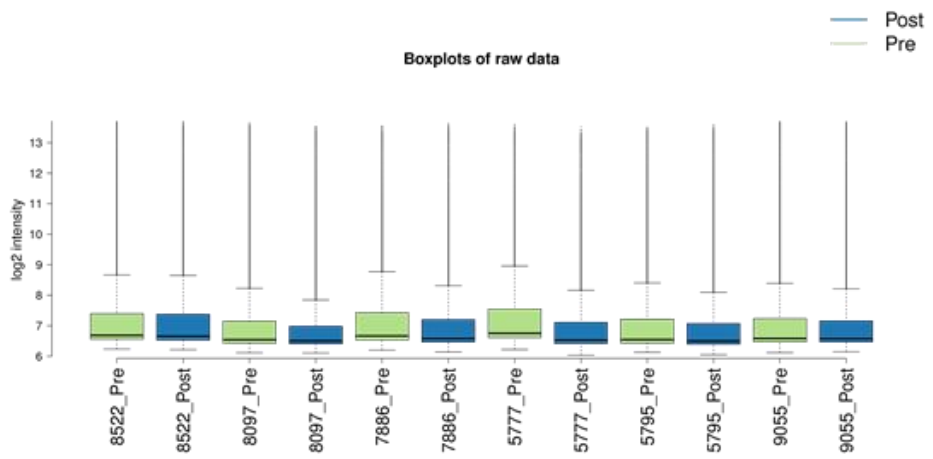
Post
Pre
Boxplots of raw data
log2 intensity
13
12
11
10
9
8
7
6
8522_Pre
8522_Post
8097_Pre
8097_Post
7886_Pre
7886_Post
5777_Pre
5777_Post
5795_Pre
5795_Post
9055_Pre
9055_Post

C

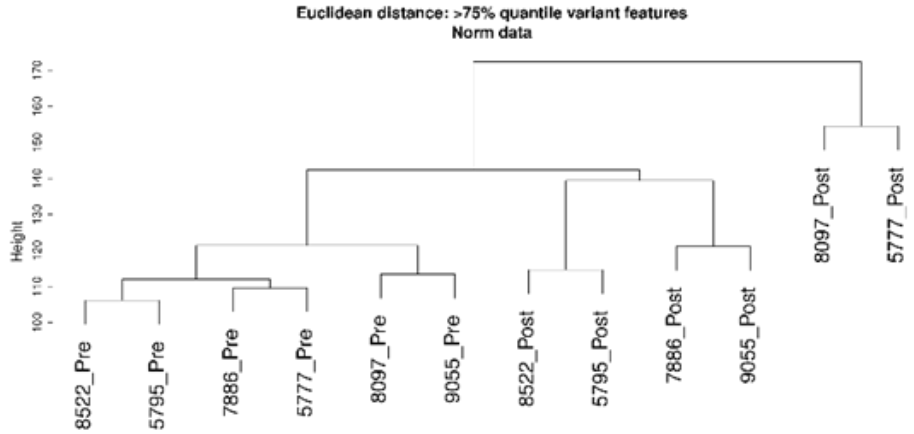
Euclidean distance: >75% quantile variant features
Norm data
Height
170
160
150
140
130
120
110
100
8522_Pre
5795_Pre
7886_Pre
5777_Pre
8097_Pre
9055_Pre
8522_Post
5795_Post
7886_Post
9055_Post
8097_Post
5777_Post

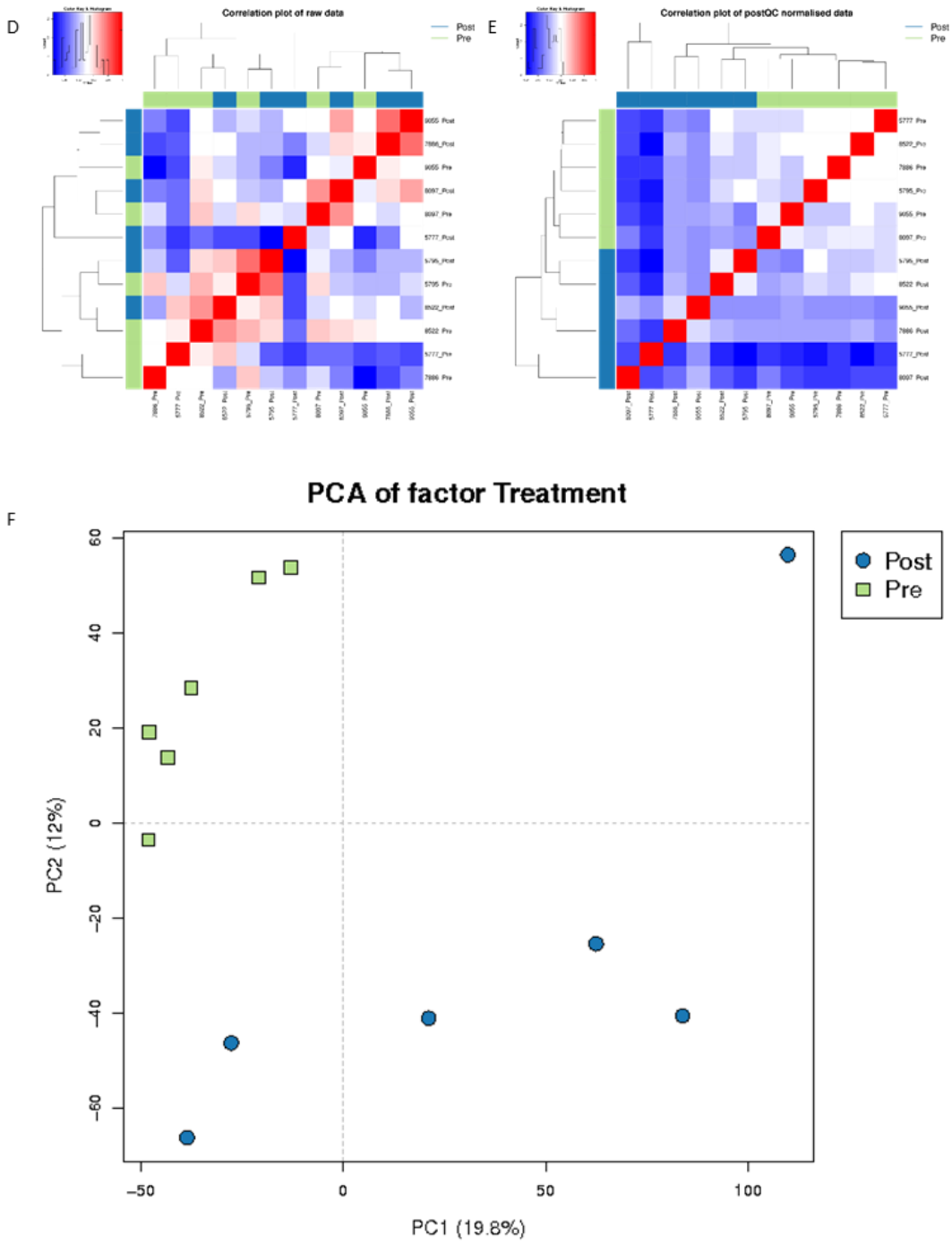

Figure 5.5 Quality control (QC) of the Illumina gene microarray

QC metric MA plots (A), Box plots (B) were reassuring with clear separation between pre-treatment and on treatment samples as assessed by Euclidean distance (C). Heatmap shows the correlation (Pearson) of the raw data (log_2 intensities), prior to QC (D) and following normalization (E). Exploratory analysis using Principal Component Analysis (PCA) and hierarchial clustering showed a clear separation of the samples based on the treatment status of the sample (F)

Exploratory analysis using Principle Component Analysis and hierarchial clustering showed a clear separation of the samples based on the treatment status of the sample (Figure 5.5F). The 3rd principle component was related to patient variation.

5.5.2.2 Non-specific filtering

After QC, the dataset was filtered to remove features that were not detected at least once across all arrays. This reduced the number of features from 47,323 to 24,097.

5.5.2.3 Statistical hypothesis testing

Fios Genomics initially performed statistical hypothesis testing using a raw (unadjusted) p-value < 0.01 and a fold change >= 1.3. With these thresholds 1331 genes were differentially expressed between the pre and on treatment groups (664 genes up-regulated and 667 genes down-regulated; Figure 5.6A). These separated into clear pre and on treatment groups (Figure 5.6B). A full list of differentially expressed genes at this statistical level is to be found in the Appendix (supplementary Tables 1&2). Of note the apoptosis marker caspase 3 was both up and down regulated (FC -1.3 p = 0.03, FC 1.3, p = 0.28) and three transcript variants of *BCL-2* were upregulated (FC 1.5 p = 0.08, FC 1.6, p = 0.10, FC 1.3 p = 0.30).

Utilising a FC>2, adjusted p <0.05 (80% power) 48 genes were differentially expressed between the pre-treatment and treatment group. 16 were up-regulated by UPA administration (Table 5.5) and 32 were down regulated (Table 5.6). Of those genes down-regulated 4 genes were not associated with a named gene and 2 were non-coding mRNAs. At this level of statistical robustness, no core cell cycle genes were differentially expressed.

5.5.2.4 Pathway analysis

KEGG

Functional enrichment of the up- and down-regulated DEG lists obtained from the contrast of on-treatment vs. pre-treatment resulted in 19 KEGG pathways enriched for up-regulated genes (Figure 5.7A, Table 5.7), and two KEGG pathways enriched for down-regulated genes (Figure 5.7B Table 5.8) at an adjusted enrichment p-value < 0.05.

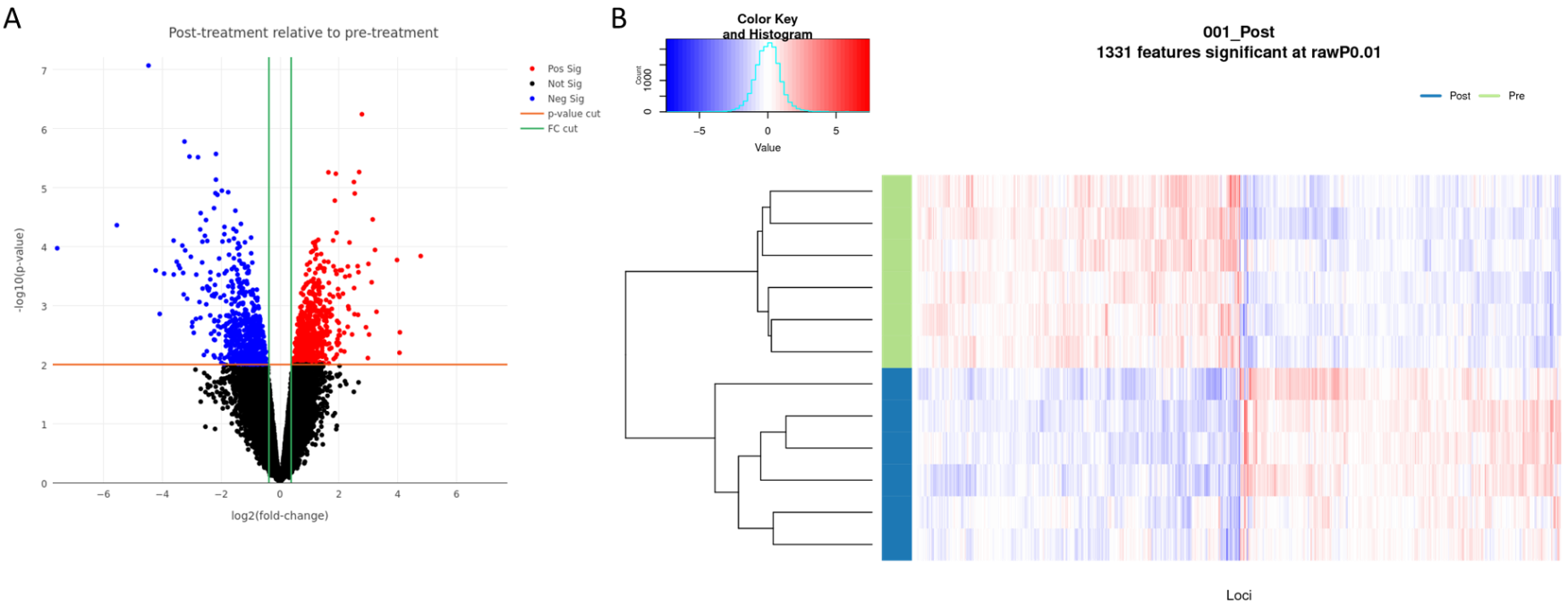

Figure 5.6 Selective progesterone receptor modulator, ulipristal acetate (UPA) administration results in differentially expressed genes within the endometrium compared to proliferative phase

1331 genes (p <0.01, fold change >2; FC>2) were altered following UPA administration in paired endometrial biospies from six women (index sample in proliferative phase of the menstrual cycle). A similar number were up-regulated (red) and down-regulated (blue; A). When samples were arranged by individual subjects there was clear differentiation between the proliferative phase and subsequent UPA treatment but some differing patterns of gene alteration (B).

Table 5.5 Differentially expressed gene candidates in human endometrium up-regulated by administration of ulipristal acetate (UPA)

Symbol	Name	Function	FC	Pvalue	adj P value
SLC13A5	solute carrier family 13 member 5	Sodium-dependant citrate co-transporter	6.874	5.69E-07	6.86E-03
RNF39	ring finger protein 39	On MHC1 ?early synaptic plasticity	6.441	5.44E-06	1.56E-02
MUC1	mucin 1, cell surface associated	These proteins play a role in intracellular signalling. Overexpression, aberrant intracellular localization, and changes in glycosylation of this protein have been associated with carcinomas.	3.122	5.50E-06	1.56E-02
MUC1	mucin 1, cell surface associated		3.72	5.81E-06	1.56E-02
EGLN3	egl-9 family hypoxia-inducible factor 3		5.695	8.03E-06	1.76E-02
MUC1	mucin 1, cell surface associated		5.807	1.26E-05	1.99E-02
ABCC3	ATP binding cassette subfamily C member 3		3.632	1.66E-05	2.35E-02
SOX9	SRY-box 9	Acts with SRY-1 to regulate AMH transcription	8.862	3.46E-05	3.88E-02
HAMP	hepcidin antimicrobial peptide	Iron homeostasis	3.789	5.81E-05	4.63E-02
TNFSF10	tumor necrosis factor superfamily member 10	This protein preferentially induces apoptosis in transformed and tumour cells, but does not appear to kill normal cells	2.459	7.66E-05	4.63E-02
LRRN2	leucine rich repeat neuronal 2	Cell-adhesion molecules or as signal transduction receptors	3.492	7.86E-05	4.63E-02
WDR72	WD repeat domain 72		2.31	8.23E-05	4.63E-02
SORL1	sortilin-related receptor, L(DLR class) A repeats containing	Epidermal growth factor repeat	5.13	8.51E-05	4.63E-02
ABTB1	ankyrin repeat and BTB domain containing 1	This gene encodes a protein with an ankyrin repeat region and two BTB/POZ domains, which are thought to be involved in protein-protein interactions. Expression of this gene is activated by PTEN	2.183	8.57E-05	4.63E-02
SPINT1	serine peptidase inhibitor, Kunitz type 1	Regulation of the proteolytic activation of HGF in injured tissue	2.264	8.84E-05	4.63E-02
GIMAP5	GTPase, IMAP family member 5	This gene encodes an anti-apoptotic protein that functions in T-cell survival	2.285	9.77E-05	4.90E-02

Genes with Fold change (FC) >2 and adjusted $p < 0.05$ (80% power)
Descriptions of gene function NCBI gene resource, obtained at https://www.ncbi.nlm.nih.gov/gene

Table 5.6 Differentially expressed gene candidates in human endometrium down-regulated by administration of ulipristal acetate (UPA)

Gene	Name	Description	logFC	FC	adj P value
GREM2	gremlin 2, DAN family BMP antagonist	Activation of Wnt/β-catenin signalling	-4.468	-22.133	2.05E-03
GJB2	gap junction protein beta 2	Cell-to-cell channels that facilitate the transfer of ions and small molecules between cells	-3.246	-9.485	1.23E-02
GJA4	gap junction protein alpha 4	Intercellular channels that provide a route for the diffusion of low molecular weight materials from cell to cell	-2.178	-4.524	1.23E-02
GPER1	G protein-coupled estrogen receptor 1	The protein binds oestrogen, play a role in the rapid nongenomic signaling events widely observed following stimulation of cells and tissues with oestrogen	-2.787	-6.903	1.23E-02
OPN3	opsin 3	Guanine nucleotide-binding protein (G protein)-coupled receptor superfamily	-1.976	-3.934	1.99E-02
LINC00461	long intergenic non-protein coding RNA 461	Non-protein coding	-1.762	-3.392	1.99E-02
DIO3OS	DIO3 opposite strand/antisense RNA (head to head)	Non-protein coding	-2.126	-4.366	1.99E-02
GLA	galactosidase alpha	Homodimeric glycoprotein ta hydrolyses the terminal alpha-galactosyl moieties from glycolipids and glycoproteins	-2.243	-4.732	2.98E-02
PAPSS1	3'-phosphoadenosine 5'-phosphosulfate synthase 1	3'-phosphoadenosine-5'-phosphosulfate (PAPS) is the sulfate donor cosubstrate for all sulfotransferase (SULT) enzymes	-1.517	-2.862	3.12E-02
SGCD	sarcoglycan delta	One of the four known components of the sarcoglycan complex	-2.697	-6.484	3.25E-02
FXYD4	FXYD domain containing ion transport regulator 4	Modulates the properties of the Na, K-ATPase	-2.515	-5.716	3.88E-02
PAPSS1	3'-phosphoadenosine 5'-phosphosulfate synthase 1	Sulfate donor cosubstrate for all sulfotransferase (SULT) enzymes	-1.329	-2.512	4.31E-02
PAGE4	PAGE family member 4	Strongly expressed in prostate and prostate cancer. It is also expressed in female reproductive tissues including fallopian tube, uterus, and placenta, as well as in testicular cancer and uterine cancer	-5.544	-46.651	4.35E-02
ZCCHC12	zinc finger CCHC-type containing 12	This gene encodes a downstream effector of bone morphogenetic protein (BMP) signalling	-1.888	-3.702	4.46E-02
KAZALD1	Kazal type serine peptidase inhibitor domain 1	Secreted member of the insulin growth factor-binding protein (IGFBP) superfamily	-1.584	-2.998	4.56E-02
GPER1	G protein-coupled estrogen receptor 1	Binds oestrogen, resulting in intracellular calcium mobilisation and synthesis of phosphatidylinositol 3,4,5-trisphosphate in the nucleus	-2.713	-6.555	4.56E-02
TCF19	transcription factor 19	Encoded protein plays a role proliferation	-1.488	-2.805	4.63E-02
CEACAM21	carcinoembryonic antigen related cell adhesion molecule 21		-1.892	-3.711	4.63E-02
SGK1	serum/glucocorticoid regulated kinase 1	Involvement in the regulation of processes such as cell survival	-2.552	-5.866	4.63E-02
RAB15	RAB15, member RAS oncogene family	G-protein	-1.565	-2.959	4.63E-02
TUBA3D	tubulin alpha 3d	Microtubules maintain cellular structure, function in intracellular transport, and play a role in spindle formation during mitosis	-3.617	-12.265	4.63E-02
FAM13C	family with sequence similarity 13 member C		-1.735	-3.329	4.63E-02
HIST1H2BH	histone cluster 1, H2bh	Replication-dependent histone that is a member pf the histone H2B family	-1.956	-3.879	4.63E-02
SGK1	serum/glucocorticoid regulated kinase 1	Activates certain K, Na and Cl channels suggesting an involvement in the regulation of processes such as cell survival	-2.638	-6.226	4.63E-02
ARSG	arylsulfatase G	involved in hormone biosynthesis	-1.193	-2.286	4.63E-02
COL17A1	collagen type XVII alpha 1	Endcodes the alpha chain of type XVII collagen	-1.421	-2.678	4.63E-02
LRRC26	leucine rich repeat containing 26	Expressed in normal salivary and prostate tissue. Increased expression associated with reduced tumourgenesis	-3.318	-9.976	4.90E-02
EDN3	endothelin 3	Altered expression of this gene is implicated in tumorigenesis	-1.371	-2.586	4.92E-02

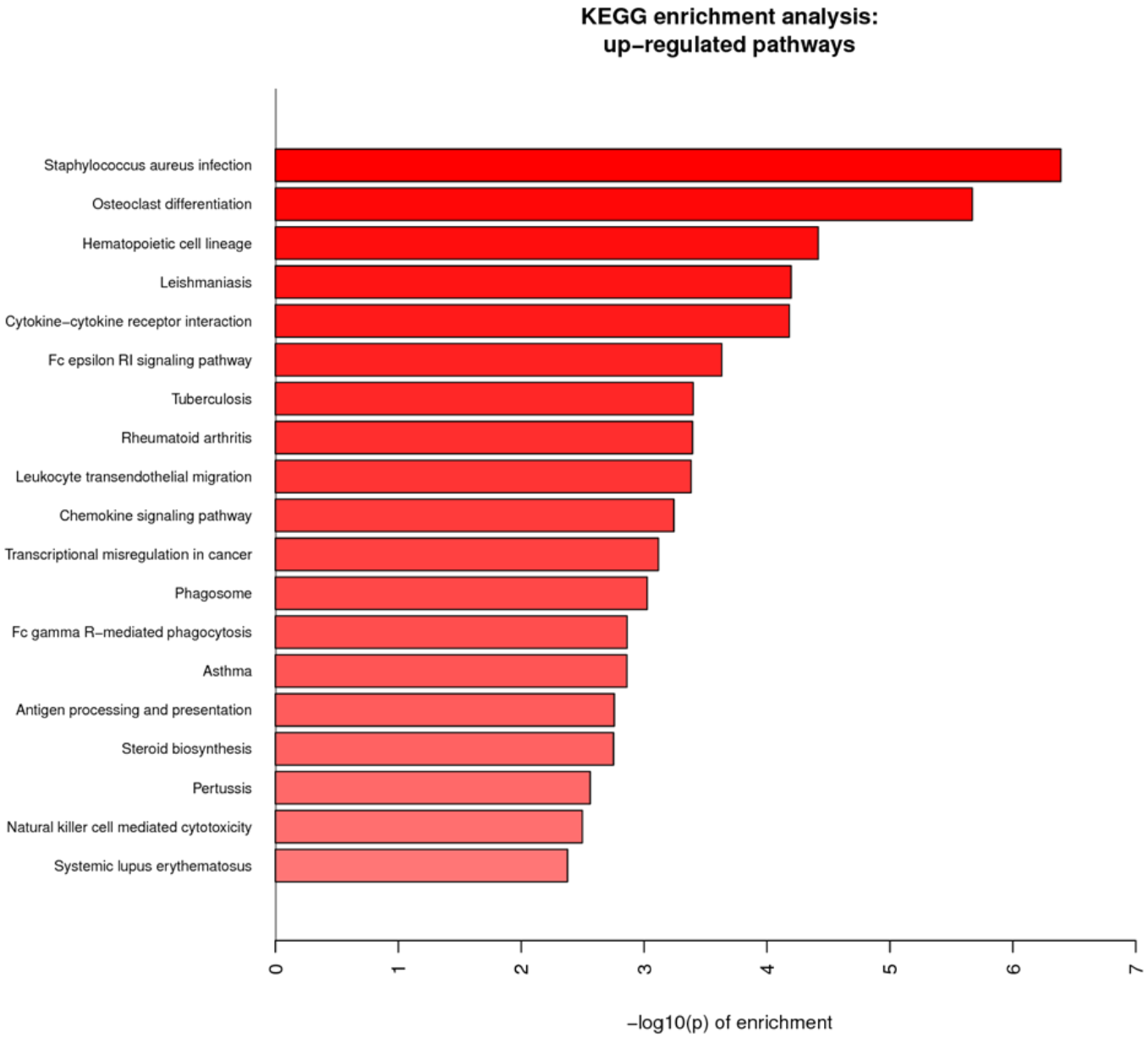
KEGG enrichment analysis:
up−regulated pathways
Staphylococcus aureus infection
Osteoclast differentiation
Hematopoietic cell lineage
Leishmaniasis
Cytokine−cytokine receptor interaction
Fc epsilon RI signaling pathway
Tuberculosis
Rheumatoid arthritis
Leukocyte transendothelial migration
Chemokine signaling pathway
Transcriptional misregulation in cancer
Phagosome
Fc gamma R−mediated phagocytosis
Asthma
Antigen processing and presentation
Steroid biosynthesis
Pertussis
Natural killer cell mediated cytotoxicity
Systemic lupus erythematosus
0
1
2
3
4
5
6
7
−log10(p) of enrichment

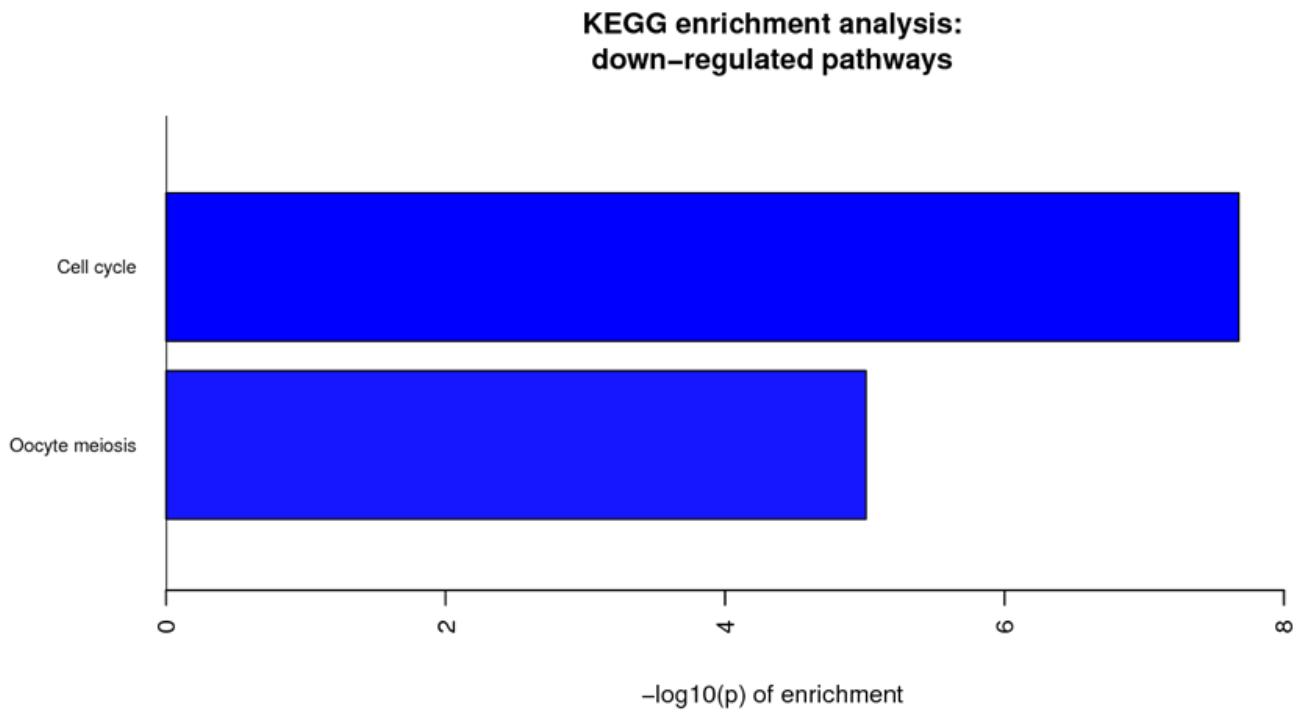

Figure 5.7 Treatment with selective progesterone receptor modulator, ulipristal acetate (UPA) results in KEGG pathway enrichment for both up and down regulation of genes

Functional enrichment of the up- and down-regulated differentially expressed gene lists obtained from the contrast of on-treatment with UPA vs. pre-treatment proliferative phase resulted in 19 KEGG pathways enriched for up-regulated genes (A), and two KEGG pathways enriched for down-regulated genes (B). Adjusted enrichment p-value < 0.05.

Table 5.7 KEGG pathways enriched for up-regulated genes

KEGG Pathway	Significant genes (p < 0.01, FC> 1.3)	S	N	N/S (%)	OR	Adjusted p
Staphylococcus aureus infection	C1QB, C1QC, C3AR1, CFH, FCGR2A, FCGR2B, FPR3, HLA-DPA1, HLA-DPB1, HLA-DRB4, ITGAM, ITGB2	12	44	27.27	8.11	8.65E-05
Osteoclast differentiation	BTK, CYBB, FCGR2A, FCGR2B, FOS, FOSL2, GAB2, LILRB4, NCF2, NCF4, PLCG2, PPP3CA, RELB, SPI1, TNF, TNFRSF11B, TREM2, TYROBP	18	110	16.36	4.29	2.28E-04
Hematopoietic cell lineage	CD14, CD1C, CD1E, CD33, CD37, CD3D, CD4, CD9, HLA-DRB4, ITGAM, KIT, TNF	12	66	18.18	4.78	2.72E-03
Leishmaniasis	FCGR2A, FOS, HLA-DPA1, HLA-DPB1, HLA-DRB4, ITGAM, ITGB2, NCF2, NCF4, PRKCB, TNF	11	59	18.64	4.91	2.80E-03
Cytokine-cytokine receptor interaction	ACVR2A, CCL14, CCL15, CCL2, CCL3L3, CTF1, CX3CL1, CX3CR1, CXCL10, CXCL9, CXCR3, IL25, KIT, PDGFB, TNF, TNFRSF10C, TNFRSF11B, TNFRSF6B, TNFSF10, TNFSF13B	20	166	12.05	3	2.80E-03
Fc epsilon RI signaling pathway	BTK, FCER1G, GAB2, INPP5D, MAP2K3, PLA2G4C, PLCG2, PRKCB, TNF, VAV3	10	57	17.54	4.54	8.28E-03
Tuberculosis	CD14, CD74, CORO1A, CTSD, FCER1G, FCGR2A, FCGR2B, HLA-DPA1, HLA-DPB1, HLA-DRB4, ITGAM, ITGB2, LAMP2, PPP3CA, SPHK1, TNF	16	134	11.94	2.93	9.81E-03
Rheumatoid arthritis	ATP6V1B1, CCL2, CCL3L3, CD86, FOS, HLA-DPA1, HLA-DPB1, HLA-DRB4, ITGB2, TNF, TNFSF13B	11	72	15.28	3.86	9.81E-03
Leukocyte transendothelial migration	CYBB, GNAI1, ITGAM, ITGB2, MMP9, NCF2, NCF4, PLCG2, PRKCB, PXN, RASSF5, VASP, VAV3	13	96	13.54	3.36	9.81E-03
Chemokine signaling pathway	CCL14, CCL15, CCL2, CCL3L3, CX3CL1, CX3CR1, CXCL10, CXCL9, CXCR3, DOCK2, ELMO1, GNAI1, HCK, PRKCB, PXN, STAT3, VAV3	17	152	11.18	2.73	1.22E-02
Transcriptional misregulation in cancer	ARNT2, CD14, CD86, CDKN2C, CEBPA, HPGD, ITGAM, MAX, MMP9, MYCN, PROM1, SLC45A3, SPI1, SPINT1, SUPT3H, TSPAN7	16	142	11.27	2.74	1.48E-02
Phagosome	ATP6V1B1, CD14, CORO1A, CYBB, FCGR2A, FCGR2B, HLA-DPA1, HLA-DPB1, HLA-DRB4, ITGAM, ITGB2, LAMP2, MARCO, NCF2, NCF4	15	131	11.45	2.78	1.67E-02
Fc gamma R-mediated phagocytosis	DOCK2, FCGR2A, FCGR2B, GAB2, HCK, INPP5D, PLCG2, PRKCB, SPHK1, VASP, VAV3	11	83	13.25	3.26	2.10E-02
Asthma	FCER1G, HLA-DPA1, HLA-DPB1, HLA-DRB4, TNF	5	19	26.32	7.51	2.10E-02
Antigen processing and presentation	CD4, CD74, HLA-DPA1, HLA-DPB1, HLA-DRB4, IFI30, LGMN, TAPBP, TNF	9	61	14.75	3.67	2.36E-02
Steroid biosynthesis	CYP51A1, DHCR7, FAXDC2, SC5D, TM7SF2	5	20	25	7.01	2.36E-02
Pertussis	C1QB, C1QC, CASP7, CD14, FOS, GNAI1, ITGAM, ITGB2, TNF	9	65	13.85	3.41	3.44E-02
Natural killer cell mediated cytotoxicity	CD48, FCER1G, ITGB2, PLCG2, PPP3CA, PRKCB, TNF, TNFRSF10C, TNFSF10, TYROBP, VAV3	11	92	11.96	2.89	3.76E-02
Systemic lupus erythematosus	C1QB, C1QC, CD86, FCGR2A, H2AFJ, HIST2H2BE, HLA-DPA1, HLA-DPB1, HLA-DRB4, TNF	10	82	12.2	2.95	4.71E-02

S: No of significant genes N: No of genes in pathway OR: Odds ratio

Table 5.8 KEGG pathways enriched for down-regulated genes

KEGG Pathway	Significant genes (p < 0.01, FC> 1.3)	S	N	N/S (%)	OR	Adjusted p
Cell cycle	ANAPC4, CCNA1, CCNA2, CCNB1, CCNB2, CCNE2, CDC20, CDC25A, CDC7, CDK1, CDKN2A, CHEK2, E2F2, ESPL1, MAD2L1, MYC, PCNA, PTTG1	18	114	15.79	6.07	4.21E-06
Oocyte meiosis	ADCY7, ANAPC4, AURKA, CCNB1, CCNB2, CCNE2, CDC20, CDK1, ESPL1, ITPR2, MAD2L1, PTTG1, SGOL1	13	94	13.83	5.04	9.81E-04

S: No of significant genes N: No of genes in pathway OR: Odds ratio

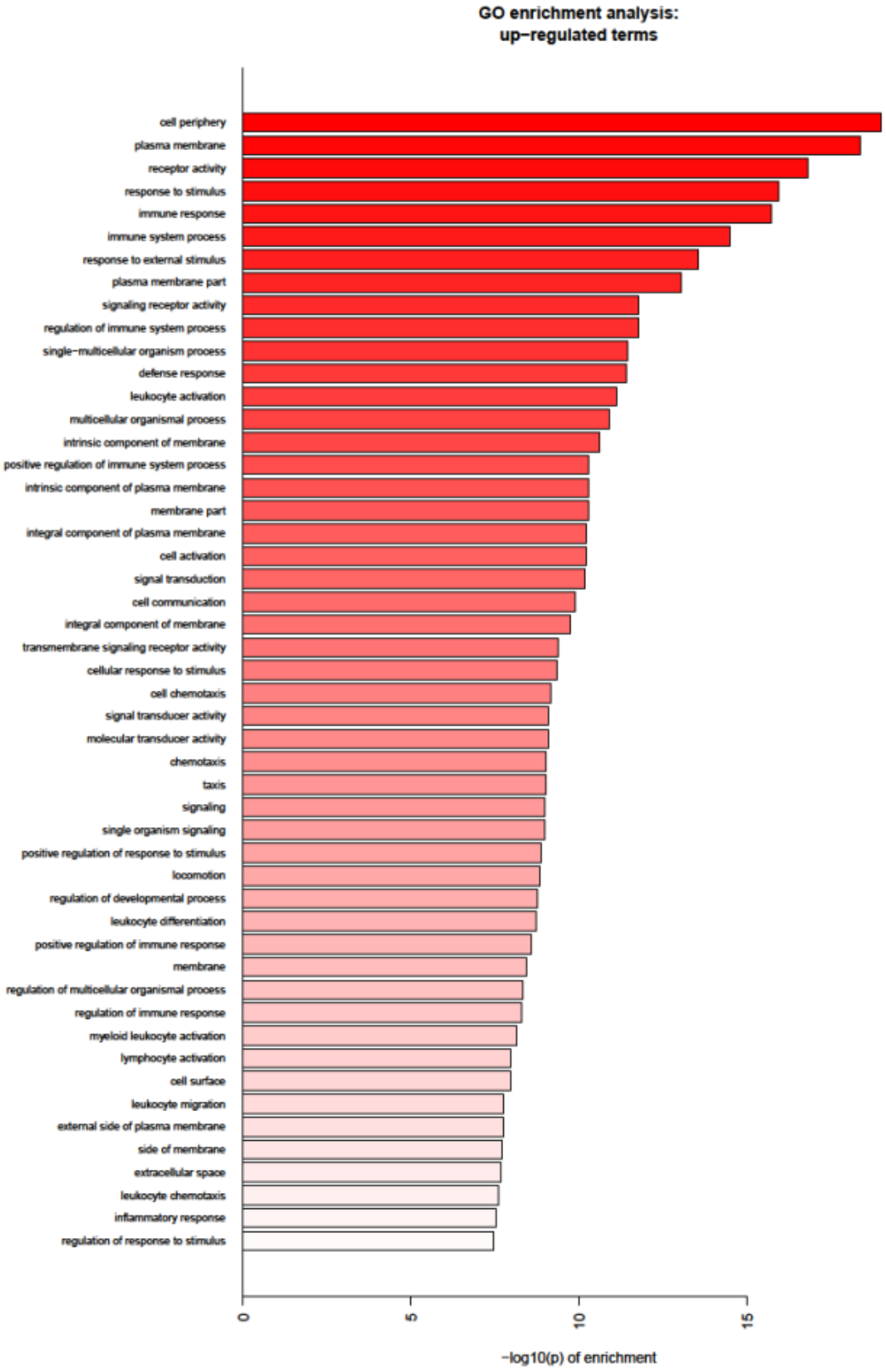
GO enrichment analysis:
up−regulated terms
cell periphery
plasma membrane
receptor activity
response to stimulus
immune response
immune system process
response to external stimulus
plasma membrane part
signaling receptor activity
regulation of immune system process
single−multicellular organism process
defense response
leukocyte activation
multicellular organismal process
intrinsic component of membrane
positive regulation of immune system process
intrinsic component of plasma membrane
membrane part
integral component of plasma membrane
cell activation
signal transduction
cell communication
integral component of membrane
transmembrane signaling receptor activity
cellular response to stimulus
cell chemotaxis
signal transducer activity
molecular transducer activity
chemotaxis
taxis
signaling
single organism signaling
positive regulation of response to stimulus
locomotion
regulation of developmental process
leukocyte differentiation
positive regulation of immune response
membrane
regulation of multicellular organismal process
regulation of immune response
myeloid leukocyte activation
lymphocyte activation
cell surface
leukocyte migration
external side of plasma membrane
side of membrane
extracellular space
leukocyte chemotaxis
inflammatory response
regulation of response to stimulus
0
5
10
15
−log10(p) of enrichment

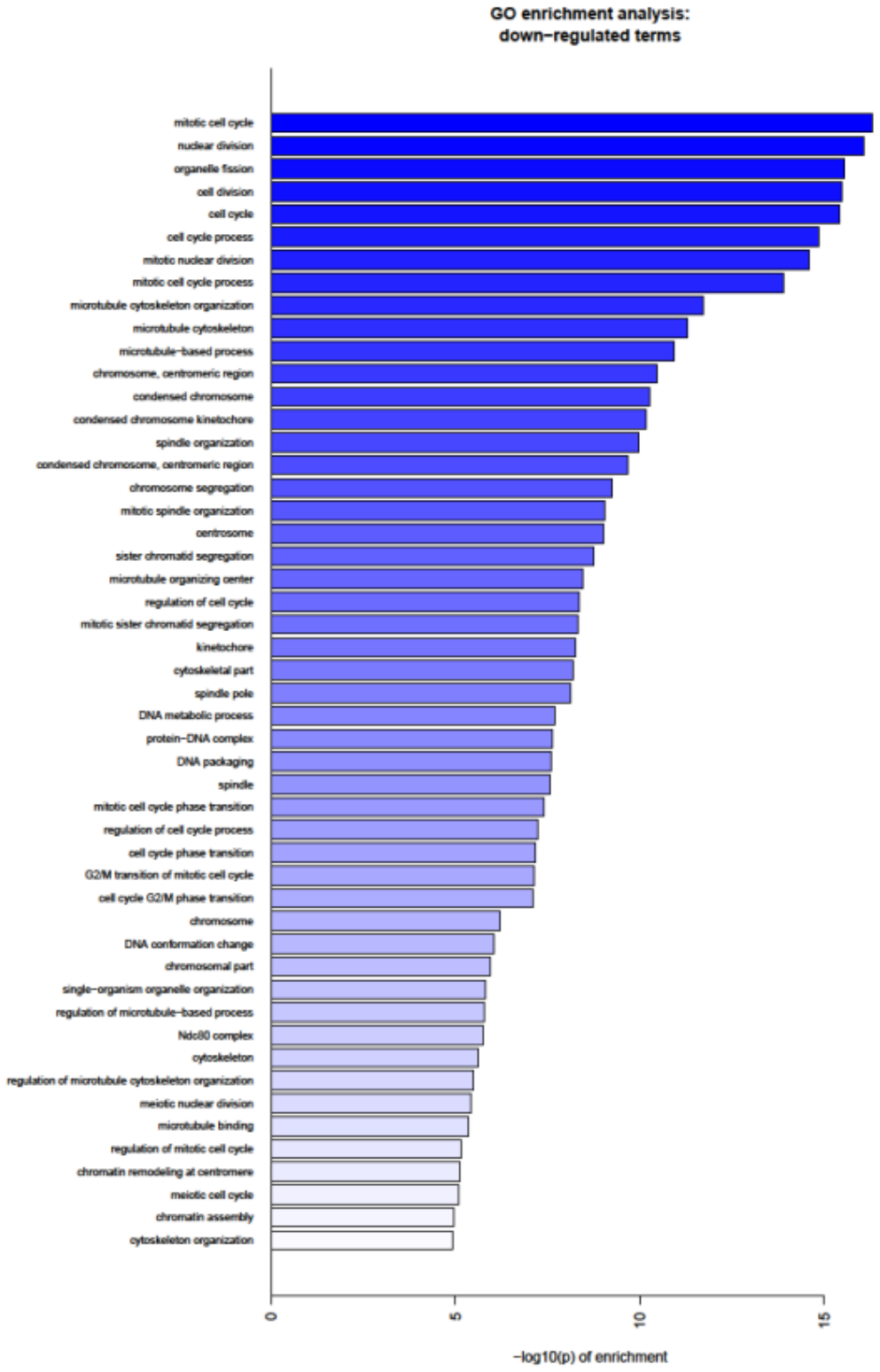

Figure 5.8 Altered gene ontology (GO) terms
Top 25 up and down-regulated GO terms following enrichment analysis. Statistical significance at an adjusted p <0.05

The top three KEGG pathways enriched for up-regulated genes were:

- Staphylococcus aureus infection
- Osteoclast differentiation
- Hematopoietic cell lineage

There was additionally enrichment in a relatively large set of pathways involved in infection and inflammatory responses in the upregulated genes.

The two KEGG pathways enriched for down regulated genes were:

- Cell cycle
- Oocyte meiosis

GO

The enrichment analysis in GO terms resulted in a large number of terms reaching statistical significance at an adjusted p-value <0.05 (416 up- and 103 down-regulated terms). The top 50 for up regulation and down regulation are displayed in Figure 5.8.

Up-regulated GO terms largely relate to membrane processes and immune response. Down-regulated GO terms largely relate to cell-cycle processes and DNA replication.

5.5.3 Validation of array outputs

5.5.3.1 Differentially expressed genes: GREM2 and MUC1

The most significantly down regulated gene following treatment with UPA was *GREM2* (adjusted p = 0.002). The most significantly up-regulated gene was the sodium dependant citrate co-transporter *SLC13A5* (adjusted p = 0.0086). However *MUC1* transcripts accounted for half of the six most up regulated genes and MUC1 is known to be P-regulated and as result this gene was selected for validation along with *GREM2* (adjusted p = 0.0156 – 0.0199).

Both genes validated on the original gene microarray samples (p <0.0001 and p <0.01; Figure 5.9A & D), despite considerable patient variation in *MUC1* following UPA administration (Figure 5.9G). This variability in response was also observed in the three and six month treatment independent sample sets (Figure 5.9E&F H&I). After 3 months of treatment with UPA two patients had no alteration in *MUC1* mRNA levels compared to samples from women in proliferative phase; the same was observed in the group of women who received six months of treatment with UPA (Figure 5.9H&I). This attenuated response was observed in subjects both with and without fibroids and no subject had endometriosis. In both these independent sets the maximal level of *MUC1* increase following UPA administration was less that that observed in the array samples

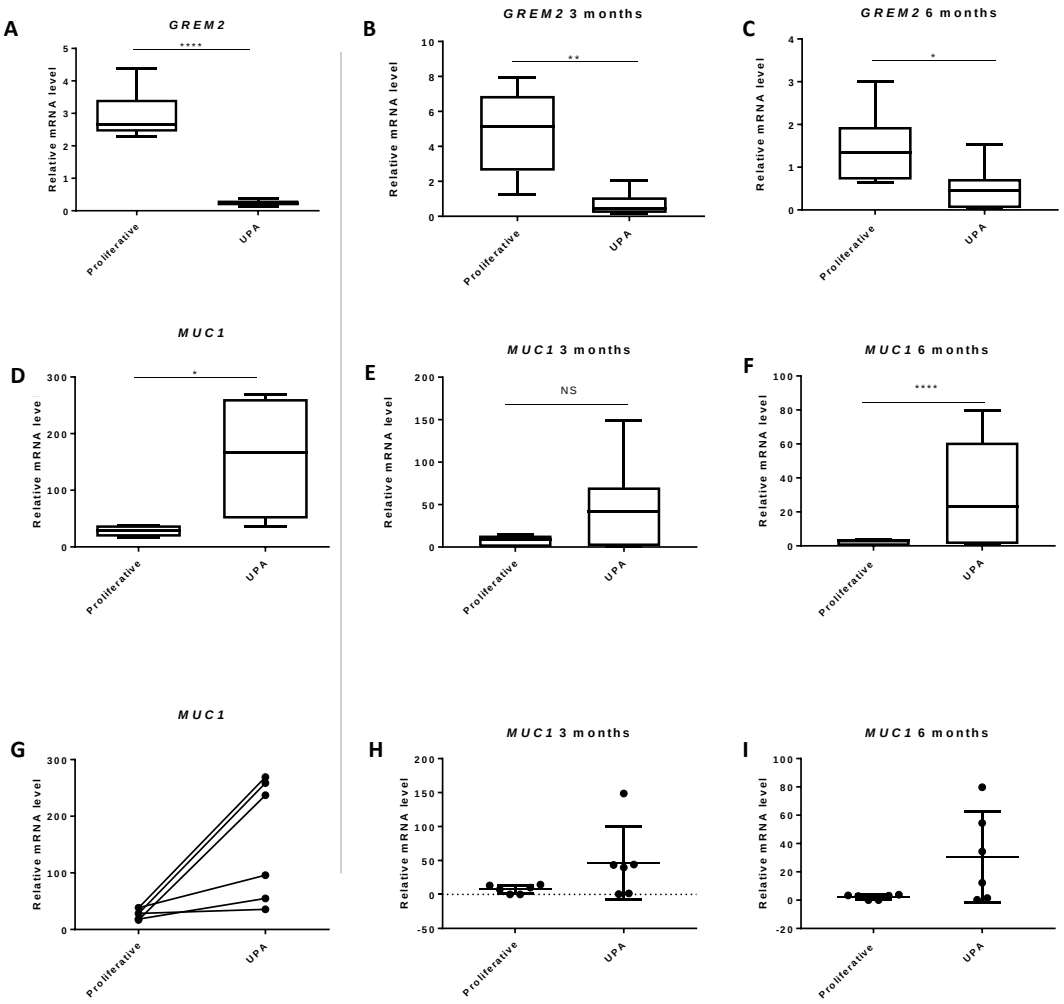

Figure 5.9 Validation by RT-qPCR of differentially expressed genes in the endometrium following treatment with selective progesterone receptor modulator, ulipristal acetate (UPA)

Relative mRNA levels of *GREM2* and *MUC1* in the endometrium of women in proliferative phase and after UPA administration. Endometrial biopsy after UPA administration was either paired to a proliferative phase endometrial sample (A D & G) or were independent samples of endometrium, not submitted to the microarray after 3 months of UPA treatment (B, E & H); or after six months of treatment with a 4 week mid-point break (C, F & I). G-I indicate heterogeneity of alteration of *MUC1* alteration following UPA administration
n=6 for each group. * p <0.05, ** p <0.01, **** p <0.0001. NS not significant.
A-F Box and whisker, whiskers: median, minimum and maximum
G Scatter plot
H-I Scatter plot, mean and standard deviation

and there was no statistical difference between proliferative phase and following UPA treatment in the 3 month group, though an alteration was observed in the 6 month group (Figure 5.9E&F).

GREM2 validated in both the three and six month independent sample sets ($p < 0.01$ and $p < 0.05$; (Figure 5.9B & C).

5.5.3.2 Genes within the cell-cycle KEGG pathway are altered following administration of UPA

The most significantly down-regulated enriched pathway was the cell cycle (Figure 5.7B). This was supported by the GO analysis where the majority of down-regulated GO terms largely relate to cell-cycle processes and DNA replication.

Reduction of cell proliferation was confirmed using Ki67 immunolocalisation of the paired endometrial samples from women prior to and whilst receiving treatment with UPA (Figure 5.10). Whilst some samples had less reduction in immunopositivity following UPA administration (Figure 5.10E-F, reduction in Ki67 immunopositivity limited to the stroma only) than others (Figure 5.10A-D), overall there was significant reduction in immunopositivity ($p < 0.001$; Figure 5.10G) which was more marked in the glands ($p < 0.001$ Figure 5.10H) than the stroma ($p < 0.05$ Figure 5.10I). Circulating E2 levels were not statistically different between the pre-treatment proliferative phase samples and following UPA administration (Figure 5.10J & K).

The KEGG cell cycle pathway contains 18 significantly down regulated genes (Table 5.8&5.9, Figure 5.11). In addition to those genes down regulated in cell cycle, three were up-regulated: cyclin-dependant kinase inhibitor 2C (*CDKN2C*, also known as p18 and INK4C; FC 1.86 p = 4.42e-4), cyclin-dependant kinase inhibitor 2B (*CDKN2B*, also known as p15 INK4B; FC 1.99 p = 8.26e-3) and growth arrest and DNA damage inducible alpha (*GADD45A*; FC 1.72 p = 6.62e-3).

For onward validation it was decided to limit to down-regulated genes involved in G1, S and G2 phase of the cell cycle (Figure 5.1 & 5.11). *CDKN2A* and *CHEK2* were subsequently excluded as functioning primers could not be obtained.

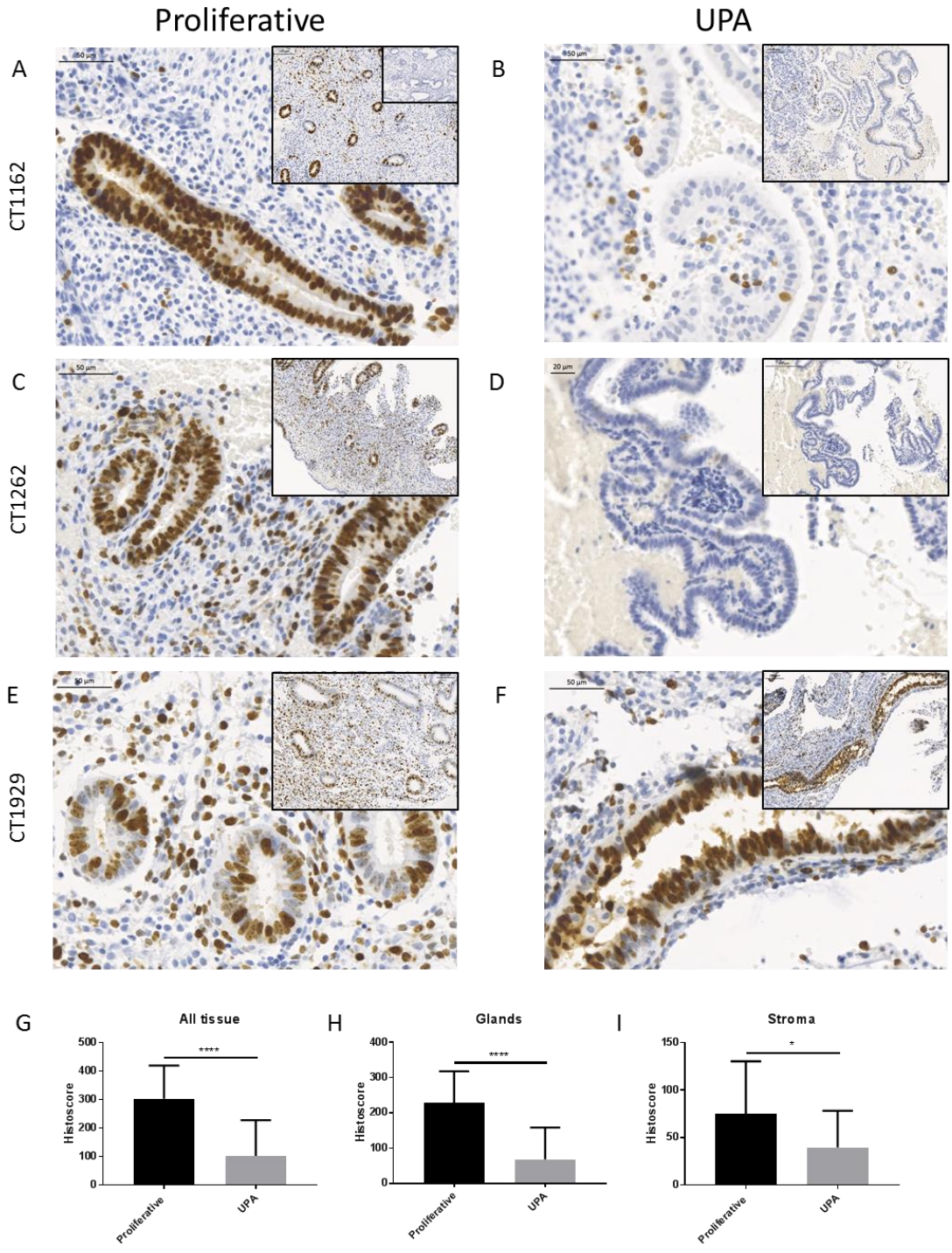
Proliferative
UPA
A
B
CT1162
C
D
CT1262
E
F
CT1929
G
All tissue
Histoscore
****
Proliferative
UPA
H
Glands
****
I
Stroma
*

Serum Oestradiol levels (pmol/L) at the time of endometrial biopsy

J

Subject	Proliferative	UPA	Control
CT1162	104	319	Amenorrhoea
CT1262	145	55	Amenorrhoea
CT1929	312	302	Lighter
CT1280	522	359	Amenorrhoea
CT1460	224	149	Amenorrhoea
CT1685	207	135	Lighter

K

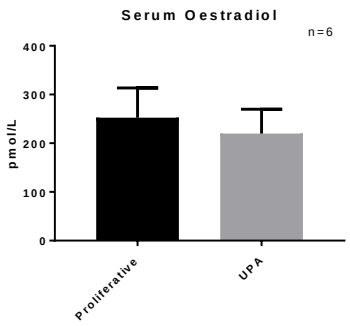

Figure 5.10 Selective progesterone receptor modulator, ulipristal acetate (UPA) administration reduces endometrial cell proliferation

Representative immunolocalisation of Ki67 in endometrium from 3 women in the proliferative phase of the menstrual cycle (A, C & E) and following UPA administration (B, D & F). There is down regulation of Ki67 in both glands and stromal cells in the majority of subjects (B&D) though the reduction was not consistent in all (F). Immunopositivity overall was significantly reduced following UPA treatment (G), though this was more marked in glandular than stromal cell nuclei (H-I).

Circulating oestradiol levels were not significantly altered by UPA treatment J and K (data presented as mean +/- SEM) and did not impact upon control of menstrual bleeding (J).

Scale bars 100µm low power, 50µm high power, negative control shown as insert on proliferative phase low power endometrium image (A). N= 6 in each group * $p < 0.05$ **** $p < 0.0001$ Bars +/- SEM

Table 5.9 Down-regulated genes differentially expressed in enriched KEGG Cell cycle

Gene	Code in diagram	Description	logFC	FC	P.value	adj.P.value
CDC25A	Cdc25A	cell division cycle 25A	-1.569	-2.967	0.0001577	0.05897
ANAPC4	APC/C	anaphase promoting complex subunit 4 also known as APC4	-1.603	-3.037	0.0004937	0.07621
CCNA1	CycA	cyclin A1	-2.423	-5.364	0.0005527	0.07834
ESPL1	Esp1	extra spindle pole bodies like 1, separase	-1.549	-2.926	0.001385	0.113
MYC	c-Myc	v-myc avian myelocytomatosis viral oncogene homolog	-0.905	-1.872	0.001556	0.1136
CHEK2	Chk 2	checkpoint kinase 2	-0.716	-1.642	0.001744	0.1174
CDKN2A	ARF	cyclin-dependent kinase inhibitor 2A (also known as p16, INK4A)	-0.834	-1.783	0.003143	0.1298
E2F2	E2F 2	E2F transcription factor 2	-1.085	-2.121	0.003276	0.1315
CCNE2	CycE	cyclin E2	-1.803	-3.489	0.00471	0.1478
CCNA2	CycA	cyclin A2	-1.222	-2.333	0.006487	0.1654
PCNA	PCNA	proliferating cell nuclear antigen	-0.645	-1.564	0.006523	0.1655
CDC20	Cdc20	cell division cycle 20	-1.493	-2.814	0.006807	0.1673
CCNB2	CycB	cyclin B2	-1.349	-2.547	0.006999	0.1683
CDK1	CDCK1	cyclin-dependent kinase 1	-1.474	-2.777	0.00762	0.1707
PTTG1	PTTG	pituitary tumor-transforming 1	-1.258	-2.391	0.007952	0.1727
MAD2L1	Mad2	MAD2 mitotic arrest deficient-like 1 (yeast)	-1.188	-2.278	0.008578	0.1759
CDC7	Cdc7	cell division cycle 7	-1.036	-2.051	0.009082	0.1782
CCNB1	CycB	cyclin B1	-1.211	-2.314	0.009377	0.1784

Highlighted genes Involved in G1, S and G2 phase of cell cycle, selected for onward validation

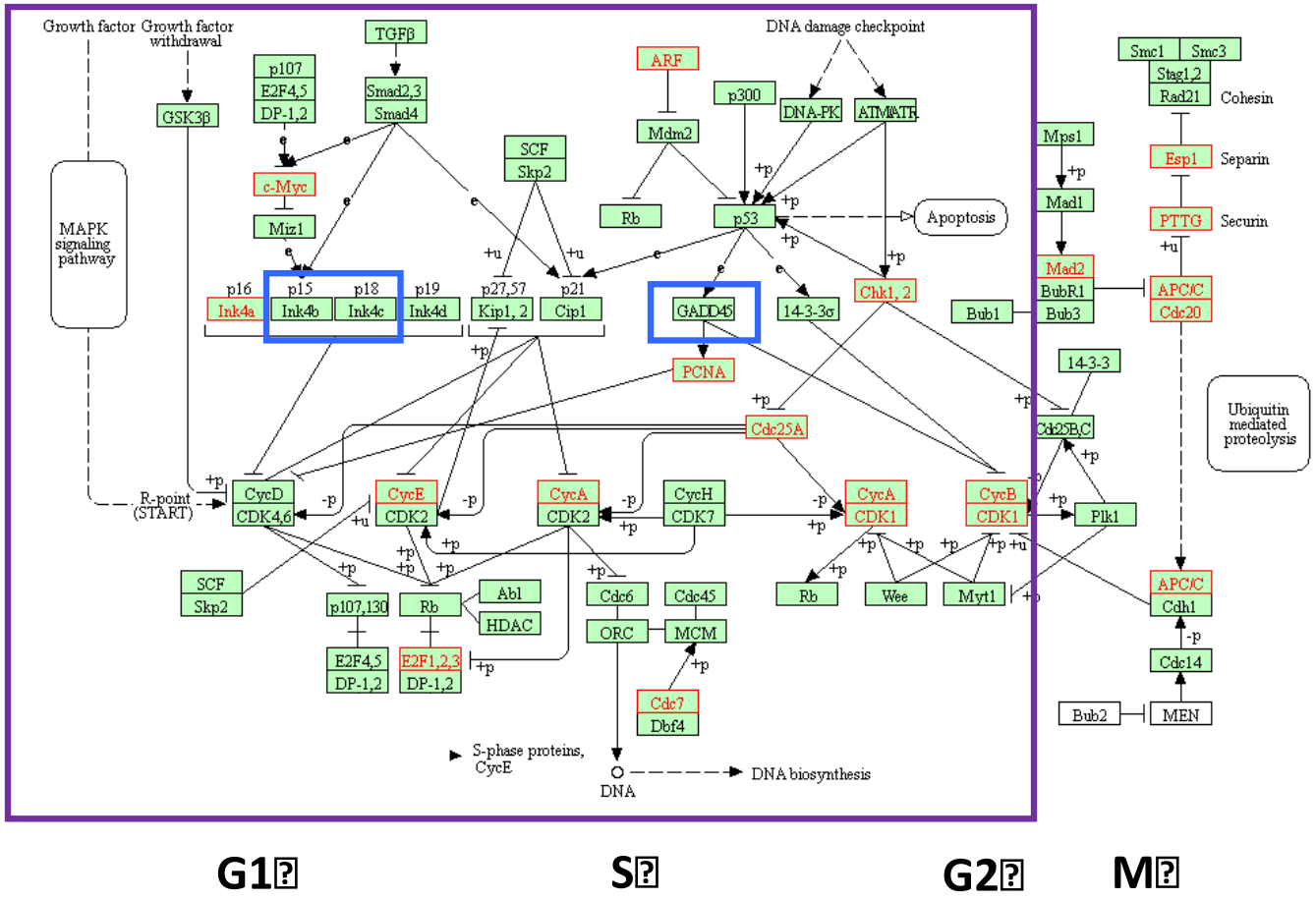

Figure 5.11 KEGG Cell cycle

Genes implicated in the cell cycle as identified by KEGG (http://www.genome.jp/kegg-bin/show_pathway?map=hsa04110&show_description=show) Diffentially expressed genes following UPA (downregulated) in red. Upregulated genes idenitfied by blue boxes. Downregulated genes within G1, S and G2 (enclosed within purple box) were selected for onward validation

Some but not all genes validated from the original array samples (Figure 5.12). A statistical outlier was identified (Grubbs alpha = 0.5) for *CDC25A*, with an unusual pattern of response for many other genes (Figure 5.13). This was sample CT1280E2, the subject who had inadvertently stopped treatment eight days prior to sampling. Given the potential for biological difference due to clearance of the drug this sample was excluded from all validation analysis.

Further validation of candidate genes identified by the microarray was undertaken utilising independent sets of endometrial biopsies from women in proliferative phase or from women who had received 3 or 6 months of treatment with UPA.

In addition to the eight genes that validated on the original array samples (*CDC25A, CCNA1*, *MYC, CCNA2*, *CCNB2*, *CDK1*, *E2F2* and *CCNB1*) *CCNE2*, *PCNA* and *CDC7* all validated in the independent 3 months of UPA administration samples (Figure 5.14). After 6 months of treatment only *MYC* failed to validate (Figure 5.15). Three of the six subjects in the proliferative phase of cycle and three of the subjects biopsied after 6 months of UPA treatment did not have fibroids. However presence or absence of fibroids did not correlate with degree of alteration of mRNA levels and did not contribute to the non-significance of *MYC* levels.

A summary of statistically altered genes in the three different subject groups (array UPA, 3 months of UPA administration and 6 month (x2 3-months) administration of UPA) is presented in Table 5.10.

5.5.3.3 CDC25A immunolocalisation in the endometrium is altered by UPA administration

CDC25A was the most significantly altered cell-cycle gene identified by the gene microarray and validated both internally and in the independent biopsies collected from women administered UPA for 3 and 6 month (Table 5.10). CDC25A regulates elements of G_1, S and G_2 phase of the cell cycle and for these reasons was selected for assessment of impact of UPA on protein expression (Figure 5.16).

Samples from women in the proliferative phase displayed intense immunopositive staining in the luminal epithelium, glands and stroma (Figure 5.16A, F & K). Intensity of

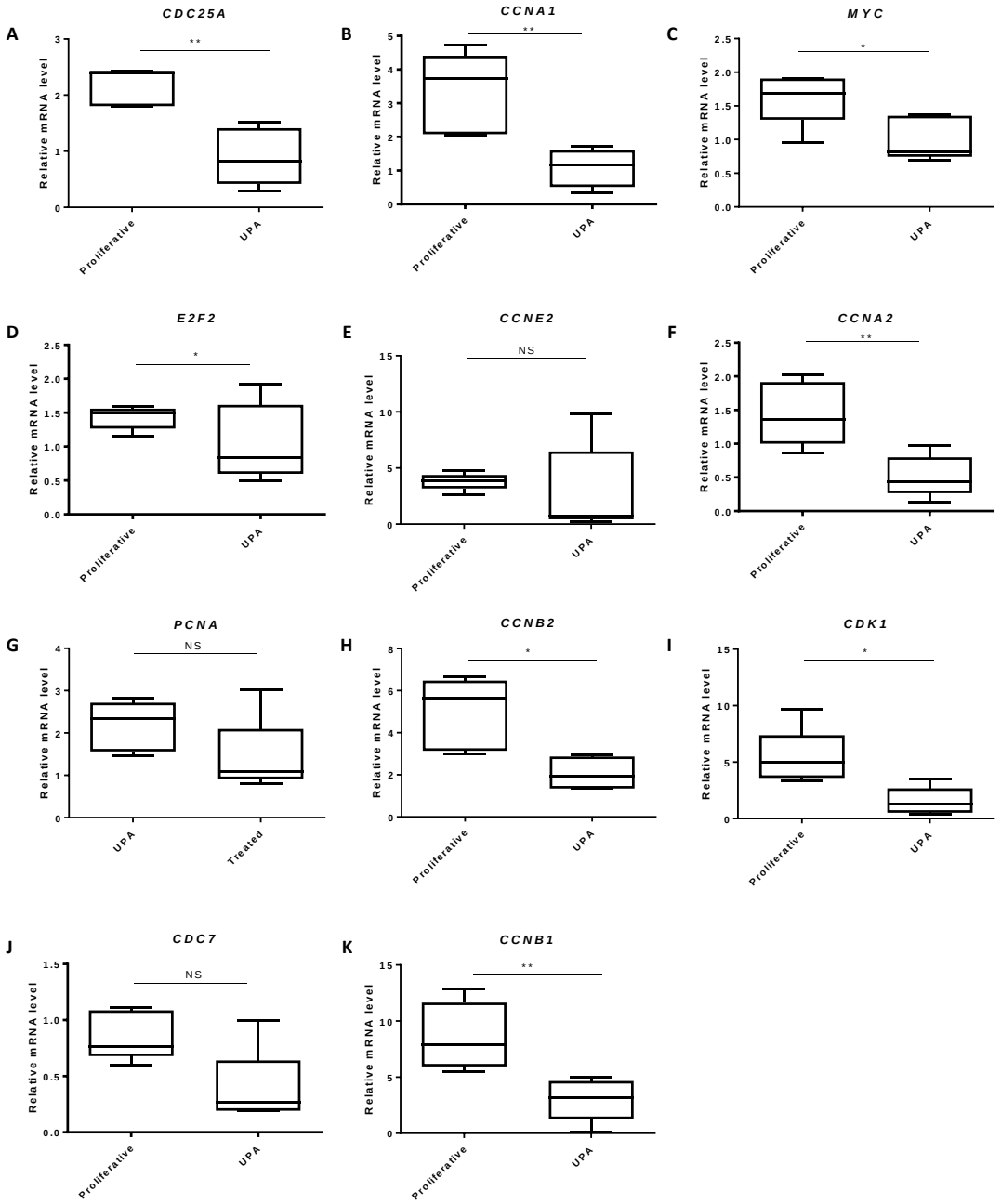

Figure 5.12 Internal validation by RT-qPCR of differentially expressed down regulated cell cycle genes in the endometrium following treatment for 3 months with selective progesterone receptor modulator, ulipristal acetate (UPA)

Relative mRNA levels of selected cell cycle genes in paired samples from the endometrium of women in proliferative phase and then following subsequent UPA administration for up to twelve weeks.

n=6 for each group. * p <0.05, ** p <0.01. NS not significant. Box and whisker, whiskers: median, minimum and maximum

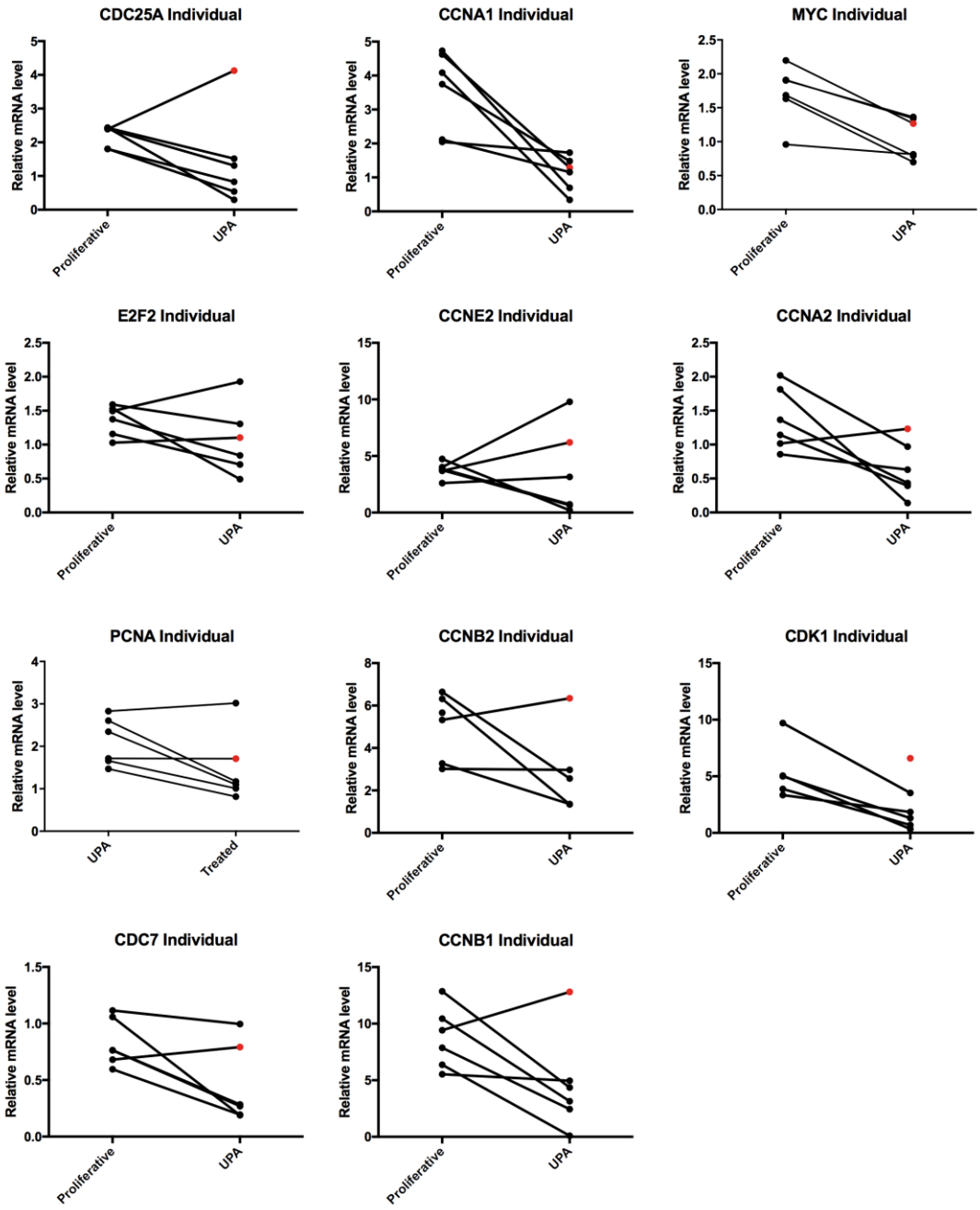

Figure 5.13 Premature cessation of selective progesterone receptor modulator, ulipristal acetate (UPA) appears to affect mRNA levels of differentially expressed cell cycle genes as assessed by RT-qPCR

Individual relative mRNA levels of cell cycles genes in the endometrium from six women in the proliferative phase of the menstrual cycle and then following subsequent UPA administration for up to 12 weeks. One sample (CT1280E2, red dot) was from a subject who had stopped UPA eight days prior to sampling.

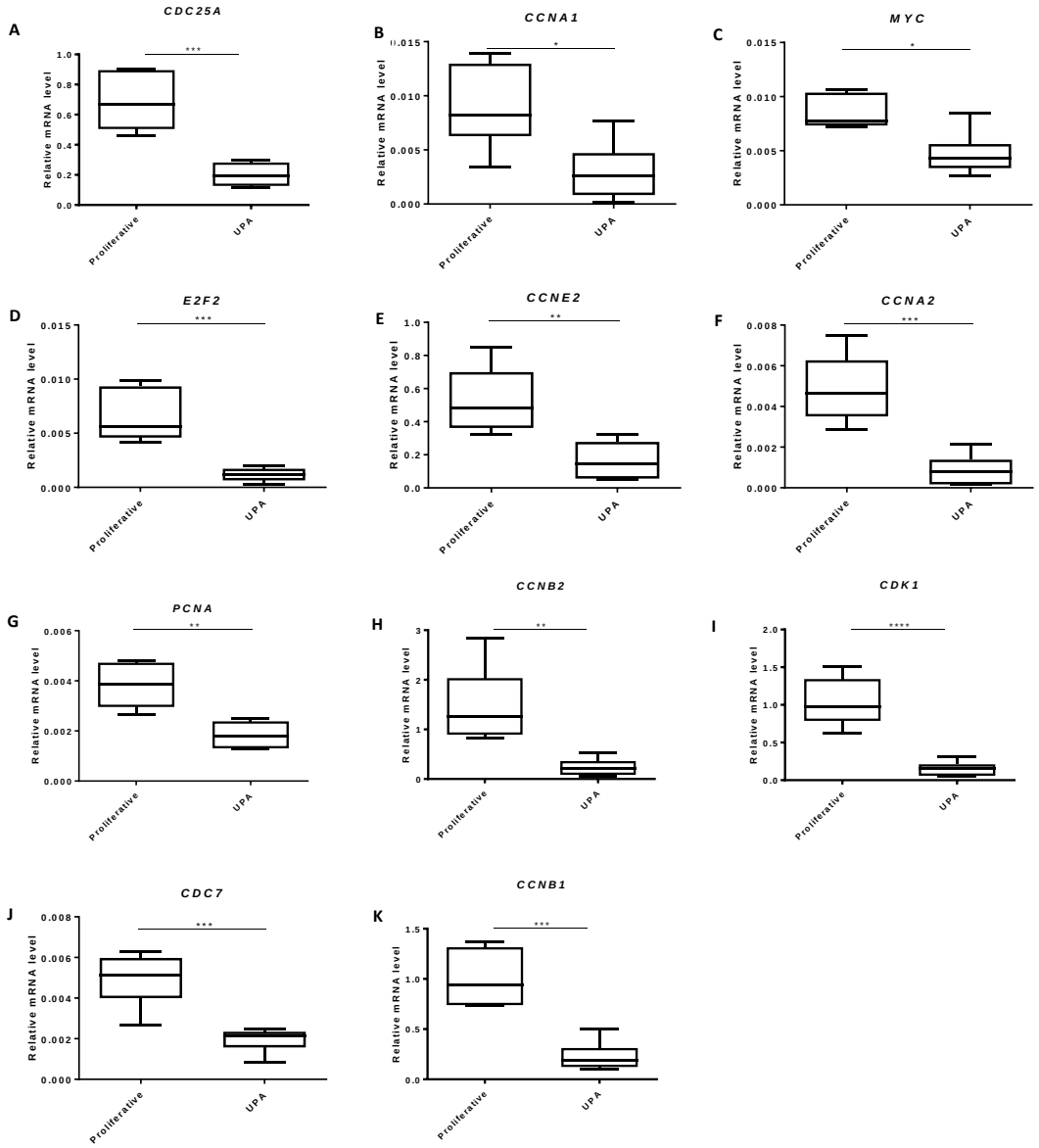

Figure 5.14 Validation by RT-qPCR of differentially expressed down regulated cell cycle genes in the endometrium following treatment for three months with selective progesterone receptor modulator, ulipristal acetate (UPA)

Relative mRNA levels of selected cell cycle genes in samples from the endometrium of women either in proliferative phase or following UPA administration for up to twelve weeks. n=6 for each group. * p <0.05, ** p <0.01, *** p <0.001, **** p <0.0001. NS not significant. Box and whisker, whiskers: median, minimum and maximum

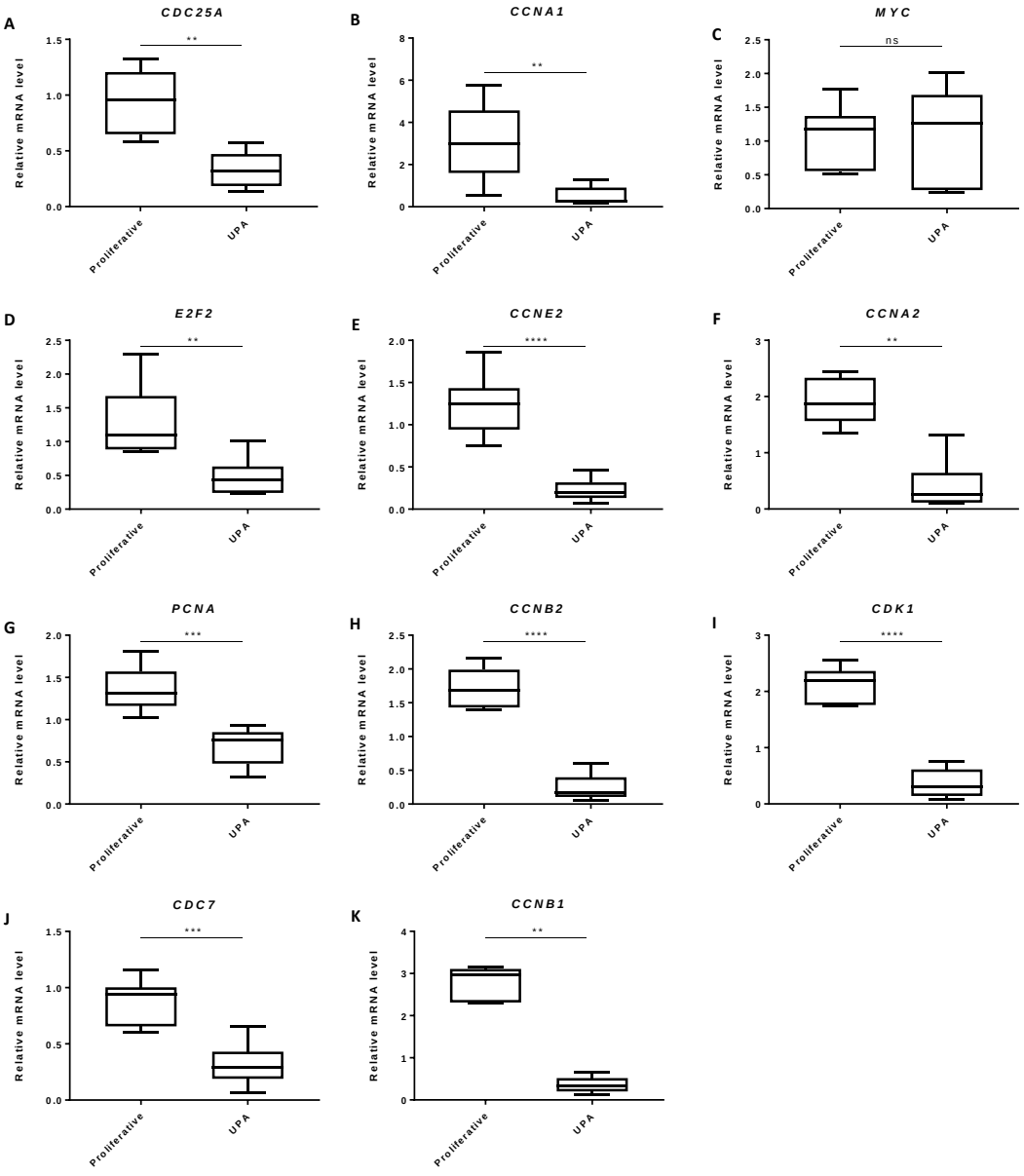

Figure 5.15 Validation by RT-qPCR of differentially expressed down regulated cell cycle genes in the endometrium following treatment for six months with selective progesterone receptor modulator, ulipristal acetate (UPA)

Relative mRNA levels of selected cell cycle genes in samples from the endometrium of women either in proliferative phase or following UPA administration for up to six months with a 4-week midpoint treatment break.
n=6 for each group. * p <0.05, ** p <0.01, *** p <0.001, **** p <0.0001. NS not significant.
Box and whisker, whiskers: median, minimum and maximum

Table 5.10 Summary of PCR validation of genes of interest identified by gene microarray

Gene	FC	P.value	Effect of UPA	Array samples	3 month samples	6 month samples
GREM2	-22.133	0.0000001	↓	****	**	*
MUC1	3.122	0.0000055	↑	**	NS	****
CDC25A	-2.967	0.0001577	↓	**	***	**
CCNA1	-5.364	0.0005527	↓	**	*	**
MYC	-1.872	0.0015560	↓	*	*	NS
E2F2	-2.121	0.0032760	↓	*	**	**
CCNE2	-3.489	0.0047100	↓	NS	**	****
CCNA2	-2.333	0.0064870	↓	**	***	**
PCNA	-1.564	0.0065230	↓	NS	**	***
CCNB2	-2.547	0.0069990	↓	*	**	****
CDK1	-2.777	0.0076200	↓	*	****	****
CDC7	-2.051	0.0090820	↓	NS	***	***
CCNB1	-2.314	0.0093770	↓	**	**	**

* p <0.05, ** p <0.01, *** p <0.001, **** p <0.0001 NS not significant

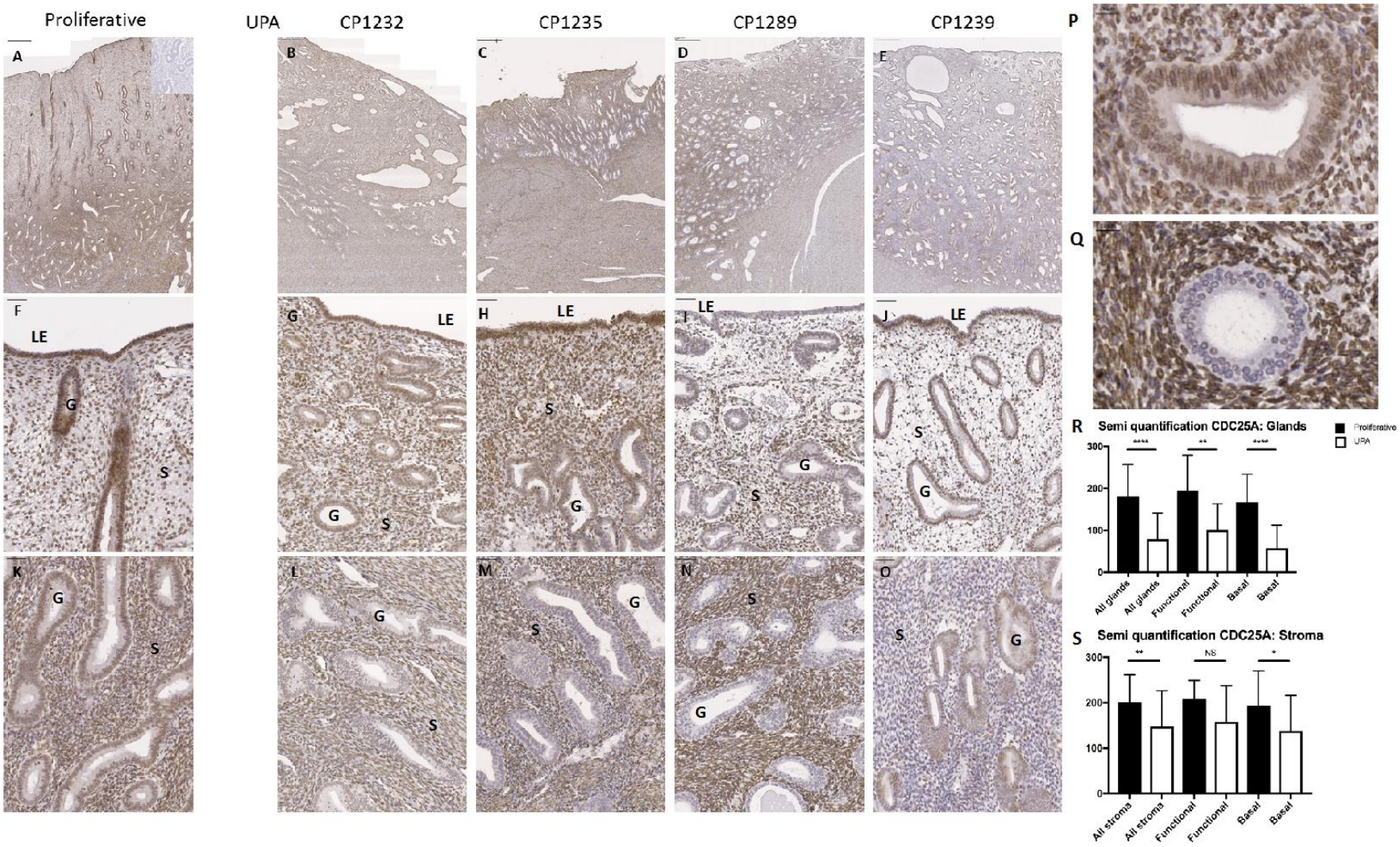
Proliferative
UPA
CP1232
CP1235
CP1289
CP1239
A
B
C
D
E
F
G
H
I
J
K
L
M
N
O
P
Q
R
S
LE
G
S
Semi quantification CDC25A: Glands
Proliferative
UPA
****
**
****
300
200
100
0
All glands
All glands
Functional
Functional
Basal
Basal
Semi quantification CDC25A: Stroma
**
NS
*
All stroma
All stroma
Functional
Functional
Basal
Basal

Figure 5.16 Administration of selective progesterone receptor modulator, ulipristal acetate (UPA) appears to reduce endometrial CDC25A expression

Representative low- (A-E) and high-power (F-O) immuno-localisation of CDC25A in endometrium from woman with fibroids during proliferative (A, F, K, P) and after UPA administration (B-E, G-J, L-O, Q).

Samples from women in proliferative phase displayed intense immunopositivity in the luminal epithelium (LE) glands (G) and stroma (S) (LE+G+S+). Intensity of epithelial immunopositivity appeared less in the basal layer (K) compared with the functional layer (F). UPA-treated women displayed variable alteration in immunopositivity. The majority had positive luminal epithelium (G, H, J) though in some subject the immunoreactivity was less dense (I). Epithelial immunopositivity reduced (R), most evident in the basal layer in most subjects (L-N, Q) when compared to proliferative phase (K, P). In one woman there was also reduced epithelial immunopositivity in the functional layer (I). There was one exception where the patient has similar epithelial expression as proliferative phase (J&O).

All women administered UPA had persistent stromal immunopositivity (G-J & L-O) but the intensity was reduced (S). In one subject stromal staining was markedly reduced in the basal layer (O).

Lower power (scale bar = 500μm), high power magnification (scale bar = 50 μm), glands (scale bar = 20 μm); Negative controls shown as inserts on proliferative endometrium (A). * $p < 0.05$ ** $p < 0.01$ **** $p < 0.0001$

epithelial immunopositivity appeared less in the basal layer (Figure 5.16K) compared with the functional layer (Figure 5.16F).

The localisation of CDC25A within the endometrium of women treated with UPA was variable. The majority had positive luminal epithelium (Figure 5.16G, H & J) though in some this was less dense (Figure 5.16I). Epithelial immunopositivity was reduced (Figure 5.16P-R) and this was most marked in the basal layer in most subjects (Figure 5.16L-N) when compared to proliferative phase (Figure 5.16K). In one sample there was clear reduction in epithelial immunopositivity in the functional layer (Figure 5.16I) and overall this was significantly reduced (Figure 5.16R). All women administered UPA appeared to have persistent stromal immunopositivity (Figure 5.16G-J & L-O), though this was reduced in intensity (Figure 5.15S). In one subject (Figure 5.16O) stromal immunopositivity was almost entirely absent.

There was one of the nine women administered UPA, CP1239, who had an entirely different pattern of immunolocalisation with similar epithelial expression observed as proliferative phase and reduction in stromal immunopositivity as described above (Figure 5.16J&O).

5.6 Discussion

This is the first description of the effect of *in vivo* administration of UPA upon cell proliferation in the human fallopian tube (FT) and uterine cervix. Cell proliferation appeared reduced in the fallopian tube from women administered UPA relative to those from women in the proliferative phase, and in the cervix was low irrespective of cycle stage or following UPA administration.

This is also the first unbiased description of the impact of UPA administration upon gene expression in the endometrium compared with proliferative phase endometrium. Furthermore, in keeping with the anti-proliferative effect observed in the endometrium, administration of UPA alters gene expression of multiple elements of the cell cycle, many of which are novel compared to those identified following administration of other SPRMs by previous groups.

5.6.1 Fallopian Tube

When ampullary cell proliferation was assessed it appeared that whilst proliferation (as assessed by Ki67 immunopositivity) overall was low, proliferation was further reduced by UPA administration relative to the proliferative phase. Other studies have demonstrated that whilst numbers of Ki67 positive cells are low, there is alteration in immunopositivity between fallopian tubes from women in proliferative and secretory phase of the menstrual cycle (George, Milea et al. 2012) with progesterone (exogenous or endogenous) reducing cell proliferation (Donnez, Casanas-Roux et al. 1985). This reduction in cell proliferation between proliferative and secretory phase of the menstrual cycle was consistent with that observed in this small sample of fallopian tube biopsies.

In chapter 3 it was demonstrated that UPA alters cell morphology and steroid receptor expression in the fallopian tube relative to secretory phase only, suggesting that UPA administration was resulting in blockage of the antagonistic effect of progesterone on E2 action. As such one would expect proliferation to also be consistent between fallopian tubes from women in proliferative phase and following UPA administration. Whilst these findings have not been formally quantified it does appear that in contrast to this expectation, UPA reduces cell proliferation in the ampulla of the fallopian tube. This observation is consistent with the effect of other SPRMs (mifepristone) on Ki67 expression in NHP oviducts (Slayden, Hirst et al. 1993, Slayden and Brenner 1994). The mechanism by which cell morphology and SSR expression is preserved relative to proliferative phase, but cell proliferation is reduced is unclear, and suggests that whilst UPA results in loss of P-antagonism within the fallopian tube, there are also other indirect effects on the fallopian tube. This impact upon cell proliferation requires further interrogation, particularly given the fimbrial ends of the fallopian tube are now considered a potential site for the development of future high grade serous ovarian cancer (Crum, Herfs et al. 2013). As cell proliferation is reduced this may indicate that despite preservation of PR and ERα in the fallopian tube, SPRMs may hold the potential to have a protective role against the future development of epithelial ovarian cancer. As previously discussed in Chapter 3, the rate of ovarian malignancy is currently under investigation as a secondary outcome in high risk women with *BRCA* mutations administered an SPRM (Danielsson).

5.6.2 Cervix

In the cervix Ki67 immunopositivity was limited to the squamous epithelium and was unaltered by UPA administration. The uterine cervix is ordinarily relative quiescent but Ki67 immunopositivity reflecting proliferating cells may be observed in the squamous cells and glandular cells of the normal cervix (Calil, Edelweiss et al. 2014, Stewart and Crook 2015). As with SSRs, there is a relative dearth of evidence regarding both cyclical variation of protein expression of Ki67 in the squamous and endoglandular compartments of the normal cervix and the effects of SPRM administration upon this. The data presented in this thesis suggest that cell turnover in the cervix is very low and is not increased by administration of an SPRM. This is perhaps unsurprising given the lack of impact upon SPRM administration upon SSR expression in the cervix as demonstrated in Chapter 3 of this thesis. Further, in other cell types SPRM administration appears to reduce rather than increase cell proliferation.

The age of the control specimens may have contributed slightly to the degree of cell proliferation observed. Ki67 expression is altered by the age of the specimen with 10% loss of protein expression by 5 years from collection (Combs, Han et al. 2016). The control cervical samples from women in the proliferative and secretory phases had been collected between eight and twelve years prior to the timing of collection of the UPA specimens (which themselves were three years old at the time of sectioning and staining). This may have impacted upon immunopositivity slightly but whilst the sample size is small, antigen degeneration is unlikely to cause complete abrogation of immunopositivity seen in the glandular cells of all samples and is thus unlikely to have impacted significantly on current conclusions.

5.6.3 Endometrium

In Chapter 4 it was demonstrated that UPA administration typically either alters P-regulated genes relative to secretory phase only (e.g. FOXO1, HOXA10 and HAND2), or has no effect (e.g. *COUP-T11*). *FOXM1* was the only exception where altered levels of gene expression relative to proliferative phase rather than secretory was identified by this candidate approach. Techniques such as sequencing and gene microarray interrogation allow an unbiased approach and may identify novel transcript targets. However an unbiased approach needs to be cognisant of the difference between a statistically significant and biologically significant effect.

Alteration of the transcriptome by SPRMs has been assessed previously. However many of these either assess alteration in cell lines (Tamm-Rosenstein, Simm et al. 2013), other tissues such as fibroids (Engman, Varghese et al. 2013) or in murine and NHP models (Bagchi, Li et al. 2005, Ghosh, Sharkey et al. 2009). In studies assessing the effect of *in vivo* administration of a SPRM on human endometrium, the majority of the literature concerns administration of mifepristone (Catalano, Critchley et al. 2007, Cuevas, Tapia-Pizarro et al. 2016) and to date only one study has investigated UPA (Lira-Albarran, Durand et al. 2017). However, in contrast to the data presented in this thesis, all these studies assess the alteration in mRNA levels between secretory phase and SPRM administration. It is thus unsurprising that very different transcripts are identified when compared to the data presented in this thesis as the comparator groups reflect a very different functional and hormonal status.

5.6.3.1 Differentially expressed genes: GREM2 and MUC1

Neither *GREM2* nor *MUC1* have previously been identified as differentially expressed in gene microarray studies of the endometrium of women exposed to SPRMs.

GREM2

GREM2 was the most significantly altered gene following administration of UPA and was markedly down-regulated compared to the proliferative phase (FC -22.1, $p = 8.5 \times 10^{-8}$). GREM2 is a cytokine and acts as an antagonist of bone morphogenetic proteins (BMP), particularly BMP-2 and BMP-4 (Zuniga, Rippen et al. 2011). In addition Grem2 also promotes nuclear translocation of β-catenin (Wu, Tang et al. 2015). It is expressed in multiple tissues in the human including all tissues of the female reproductive tract with the exception of the vagina (http://www.proteinatlas.org/ENSG00000180875-GREM2/tissue Accessed 27/3/17).

The function of *GREM2* in normal endometrium has not been assessed. However one of its targets, BMP-2 has a role in the endometrium. It increases the progesterone co-chaperone *FKBP52* and *Wnt4* (Lee, Jeong et al. 2007), and knockout murine models are unable to decidualise (Lee, Jeong et al. 2007). In humans it is critical for decidualisation (Wetendorf and DeMayo 2012) and an endometrial deficiency has been demonstrated in the stromal cells of women with fibroids (Sinclair, Mastroyannis et al. 2011). Furthermore in this study treatment with UPA slightly increased *BMP-2* levels but not

significantly (FC 1.3, p = 0.18), despite the significant down-regulation of its antagonist. This finding of a non-significant rise of *BMP-2* levels following UPA administration is in keeping with PCR data presented in **Chapter 4** (**Figure 4.3E**). Furthermore BMP-2 is also regulated by TGF-β3, also known to be increased in the presence of fibroids and may down-regulate the expression of the receptor for BMP-2 (Sinclair, Mastroyannis et al. 2011). However the impact of *GREM2* mRNA down-regulation upon GREM2, BMP-2 and TGF-β3 protein expression and function is unknown.

GREM2 is also expressed in the ovary and has roles in late follicular development (Sudo, Avsian-Kretchmer et al. 2004). There is also some evidence it may regulate the transition of primordial follicles to primary follicles within the ovary and can directly bind to AMH and inhibit its effects (Nilsson, Larsen et al. 2014). Women receiving treatment with SPRMs are typically anovulatory, with E2 levels in the mid-follicular range and normal circulating levels of LH and FSH (Baird, Thong et al. 1995, Chabbert-Buffet, Pintiaux-Kairis et al. 2007). If the reduction of *GREM2* RNA levels is reflected in reduced protein expression, loss of AMH inhibition may contribute to the anovulatory effect.

As previously described *GREM2* promotes β-catenin translocation. β-catenin is an integral Wnt signaling component and implicated in cell proliferation and survival (Moradi, Ghasemi et al. 2017). Mutation is associated with endometrial cancer and a poorer disease free survival (Kurnit, Kim et al. 2017). Furthermore a single study assessing differentially expressed genes in endometrial cancers observed a reduction in GREM2, and that *in vitro* treatment with GREM2 inhibited tumour cell growth (Tsubamoto, Sakata et al. 2016). The array performed in this thesis demonstrated that despite significant down-regulation of *GREM2*, *β-catenin* was not differentially altered by UPA treatment. The finding by Tsubamoto is of note, but has not been substantiated by other sequencing studies of endometrial cancers (Chang, Huang et al. 2017, Garcia-Sanz, Trivino et al. 2017, Jones, Xiu et al. 2017) and the significance of down-regulation of *GREM2* in healthy endometrium is unknown.

MUC1

The most significantly up regulated gene was *SLC13A5* but, as previously described, three of the six most up regulated genes were *MUC1* transcripts and as such it was thus decided that this should be the candidate gene taken forward for validation. *MUC1* is a

glycoprotein which belongs to a family of very large and heavily glycosylated proteins that are present upon the apical surfaces of almost all simple epithelial tissues and function to maintain cell surface lubrication as well as environmental control and protection from pathogens (Hattrup and Gendler 2008). They protect from apoptosis, and dysregulation is associated with cancer (Hollingsworth and Swanson 2004, Ren, Agata et al. 2004). Within the endometrium expression is progesterone regulated (Meseguer, Aplin et al. 2001). Mucins play a key role in embryo implantation (Dharmaraj, Gendler et al. 2009) and altered expression within the uterus is associated with infertility (Horne, Lalani et al. 2005). Whilst MUC1 expression is progesterone mediated, it is the PRB isoform that is predominantly responsible for up-regulation whereas PRA antagonizes PRB-mediated stimulation (Brayman, Julian et al. 2006).

The data presented in the thesis demonstrated that *MUC1* levels were differentially expressed in paired samples from the same women prior to and following administration of UPA with significant up-regulation observed. This is somewhat surprising given that MUC1 expression is typically increased by progesterone (Meseguer, Aplin et al. 2001) but may reflect alteration of relative PR isoform expression. The finding of up-regulation of *MUC1* following UPA treatment is also in contrast to that observed by one group following administration of the SPRM mifepristone, where MUC1 was reported to be down regulated (Meng, Andersson et al. 2009). However this was following *in vitro* administration of mifepristone to an endometrial co-culture of primary endometrial stromal and epithelial cells. As a result it is difficult to ascertain if their contrasting observations are a result of a differing SPRM effect on PR isoform or a reflection of *in vitro* treatment of a co-culture model.

The finding of increased expression of *MUC1* demonstrated in this thesis requires further investigation to determine the relevance of this observation. Firstly increased mRNA levels have not yet been subsequently validated by alteration in protein expression. Furthermore, a differential expression was not confirmed in independent cohorts. In all groups there was a very heterogeneous response of *MUC1* to administration of UPA. The samples utilized in the array validated by PCR, but three samples had a very marked increase in mRNA levels whereas in the other three this increase was very much attenuated. In the independent groups again some subjects had an attenuated or absent change in *MUC1* and this was not explained by presence or absence of fibroids. Quantification of protein expression may provide valuable insights into this variability

and confirm the up-regulation observed in paired samples. MUC1 is an epithelial expressed protein and a significant variation in the degree of cystic dilatation (and thus relative glandular to stromal ratios) may impact upon relative expression levels of mRNA. Previous studies in endometriosis have demonstrated that normalizing expression against epithelial cell markers has a significant impact upon perceived cyclical alteration of mRNA levels (Dharmaraj, Chapela et al. 2014). It is impossible to correlate *MUC1* levels in this study against the degree of cystic dilatation: endometrial biopsies obtained by suction catheter often have significant distortion and fragmentation of the sample by this sampling method, as was the case in the samples utilized here. Correlation between mRNA levels and protein expression in endometrium obtained at the time of hysterectomy, where the fixation of a full thickness biopsy may allow for more accurate assessment of the degree of dilatation will allow further interrogation of possible explanations for the variability in *MUC1* alteration.

Other biological relevance of this alteration in *MUC1* is unclear. Given the association of increased MUC1 expression with infertility, up-regulation may be increased with an alteration in receptivity of the endometrium, contributing to its potential for prevention of unplanned pregnancy. If a correlation between MUC1 and the degree of cystic dilatation is demonstrated it raises the intriguing possibility of the role that MUC1 might play in the development of the striking cystic dilatation often observed in many, but not all, subjects following administration of an SPRM. Increased glycosylation of the apical surface may alter the osmotic potential of the lumen of an endometrial gland. However there would be significant challenges in demonstrating causality given the lack to date of an effective co-culture system that can demonstrate the histological features of PAEC.

5.6.3.2 Cell Cycle

Consistent with data previously presented by our group (Whitaker, Murray et al. 2017), down-regulation of proliferation in human endometrium following administration of UPA is described herein. This is in keeping with an anti-proliferative effect observed following *in vivo* administration of mifepristone and asoprisnil (Engman, Granberg et al. 2009, Wilkens, Williams et al. 2009). One of the most striking observations presented in this thesis is the alteration in endometrial mRNA levels of multiple elements of the cell cycle following administration of UPA. Down-regulation was identified both by KEGG pathway enrichment and by GO interrogation and selected candidates were confirmed

by RT-qPCR and IHC. This effect also persisted in subjects who had had repeated courses of UPA and in those with and without fibroids.

The data presented in this thesis provide fresh insights into the potential mechanisms by which the anti-proliferative effect might be caused, and identify different candidates implicated within the cell cycle compared to other SPRMs. Whilst the degree of fold change of these candidates may have been less dramatic than many of the differentially expressed genes observed with greater statistical stringency, the biological relevance is of great import, particular given the confirmation of reduced cell proliferation as assessed by Ki67 immunopositivity.

Cell cyclins

Critical to progression through the cell cycle are the cyclins. The novel data presented in this thesis suggest that whilst A, B and E cyclins mRNA are all down regulated in the endometrium by i*n vivo* treatment with UPA, D cyclins were unaltered. *CDK1* but not *CDK2* was also downregulated. B Cyclins are regulated by CDK1, E by CDK2 and D by CDK4. A cyclins are regulated by both CDK1 and CDK2. The down-regulation of CDK1 may in part explain the subsequent down-regulation of A and B cyclins, but the down-regulation of E cyclins suggests a mechanism independent of CDK2. To date there have been no published studies of the effect of UPA of endometrial expression of cyclins. In ovarian cancer cell lines UPA reduced cyclin E, but this was less marked that other SPRMs and was associated with a reduction in CDK2 (Goyeneche, Seidel et al. 2012).

CDK2

In the data presented in this thesis there was no significant alteration in *CDK2* observed following UPA treatment. Studies on the effect of mifepristone on cell cycle have demonstrated that cell cycle arrest occurs predominantly in the G_1 phase and involves up-regulation of the CDK inhibitors $p21^{cip1}$ and $p27^{kip1}$ and these result in inhibition of CDK2 (Goyeneche and Telleria 2015).

This effect was observed in murine breast cancer models (Vanzulli, Soldati et al. 2005). This finding has also been replicated following *in vitro* treatment of breast cancer cell lines (Vanzulli, Efeyan et al. 2002) and endometrial cancer cell lines (Schneider, Gibb et al. 1998). Multiple SPRMs, including UPA increase $p21^{cip1}$ and $p27^{kip1}$ (Goyeneche and

Telleria 2015) expression with consequent reduction in CDK2 in ovarian cancer cell lines, however UPA was the least potent with regard to this effect (Goyeneche, Seidel et al. 2012).

In contrast to these studies in other cell types, the data presented in this thesis revealed that in the endometrium of women with fibroids, $p21^{cip1}$ and $p27^{kip1}$ are not increased, and that CDK2 was not reduced. It is uncertain whether this is result of differing cell types, or due to pharmacological differences between mifepristone and UPA. Interestingly FOXM1 affects G_1/S by diminishing $p21^{cip1}$ and $p27^{kip1}$ (Costa 2005) however in Chapter 4 data are presented that demonstrate a reduction in *FOXM1* relative to proliferative phase followed administration of UPA. As such the mechanism by which $p21^{cip1}$ and $p27^{kip1}$ are maintained remains unclear.

CDC25A

CDK-cyclin complexes are the only known substrates for CDC25 phosphatases. The CDC25 proteins dephosphorylate and thereby activate the CDK-complex. There are 3 isoforms: A, B & C. All three act as key regulators of the G_1-S and G_2-M transitions. CDC25A mainly activates CDK2 complexes with cyclin E and A in the G_1-S transition and CDK1-cyclin B at the G_2-M (Boutros, Lobjois et al. 2007). CDC25B and C are primarily required for entry into mitosis (Millar, Blevitt et al. 1991, Lammer, Wagerer et al. 1998) but also contribute to S-phase progression (Boutros, Dozier et al. 2006).

Only *CDC25A* of the CDC25 phosphatases was significantly altered in the data presented from this array, and this down-regulation was confirmed by protein expression. This is the first evidence of alteration by UPA of CDC25A expression. Down-regulation was most evident in epithelial cells, but a reduction of intensity of staining in individual nuclei was also noted in stroma cells when semi-quantified. This has not been further quantified either by stereology or immunofluorescence.

This has also not previously been observed with administration of other SPRMs. This may contribute to the down-regulation of CDK1-cyclin B activity and may also contribute to the down-regulation of cyclin A/E despite preserved CDK2.

Other cell cycle targets

Other cell cycle candidates validated by this array include *MYC*, *E2F2* and *CDC7*. *MYC* is a proto-oncogene that encodes a transcription factor that is essential for cell proliferation (Dominguez-Sola, Ying et al. 2007). E2F2 is one of the E2F family of transcription factors that bind to retinoblastoma (Rb) tumour suppressor protein (Liban, Thwaites et al. 2016). E2F2 is a transcription activator and so down-regulation may thus contribute to reduction in cell cycle progression at the G_1/S transition. CDC7 regulates DNA replication (Yamada, Masai et al. 2014) and this down-regulation may alter S-phase transition.

5.6.4 Limitations of the gene microarray

One of the significant strengths of this array was that the endometrial biopsies compared were "paired" samples: both the comparator and the on treatment groups were derived from the same women. There is often significant heterogeneity between individual women regarding underlying pathology (such as fibroid size and location), co-morbidities and clinical response. This is evident in the principal component analysis, which identified individual variation as the third highest principal component discriminator. Subjects had variable circulating progesterone and oestradiol levels following UPA administration, and it is uncertain what impact this has on cell proliferation irrespective of UPA treatment. Equally it should be noted that the subjects with the least and greatest reduction in proliferation (as assessed by Ki67 immunopositivity), had almost identical circulating E2 levels (302 and 319pmol/L respectively). All biopsies were obtained by the same technique and by the same operator and this may reduce variation between relative proportions of functional versus basal sampling. All samples were immediately fixed and so alteration in phosphorylation due to prolonged ischaemia was avoided. This has previously been noted in samples obtained at the time of hysterectomy, when ligation of the blood supply to the uterus may precede by some time the final removal of the specimen and subsequent fixation (Sivalingam, Kitson et al. 2016).

One sample in the array (CT1280E2) was from a subject who had stopped her UPA administration eight days prior to endometrial sampling. She had not had a withdrawal bleed, her circulating progesterone and oestradiol levels suggested she had not ovulated and her endometrial histology demonstrated that she had PAEC. As such it was jointly agreed that she was suitable for inclusion in the UPA treatment group for the gene

microarray study. This was a pragmatic approach given the difficulty of obtaining paired samples from women who had had their index sample in the proliferative phase and were willing to have a repeated sample for the purposes of research. Whilst in the array QC this sample did not appear to be an outlier, at the stage of validation this sample was a statistical outlier for several genes, most notably *CDC25A*. The half-life of UPA is around 38 hours (Esmya Summary of product characteristics http://esmya.co.uk/wp-content/uploads/2016/06/Apr-2016-SPC-UK-clean.pdf Accessed 27th May 2017). As such by 8 days, assuming standard pharmacokinetics less than 4% of UPA would have been circulating. Whilst morphology would be unlikely to change until ovulation then subsequent shedding of the functional layer, the impact of the significant reduction in circulating UPA concentration on cell cycle activity is unknown. Given a robust biological reason for outlier status it was decided to exclude this sample from the RT-qPCR validation. Whilst this may have introduced bias, the cell cycle genes still validated in the independent sets (with the exception of *MYC* in the group who had received treatment for 2 cycles of UPA). As such the interpretation of these genes being significantly down regulated by UPA appears valid.

The level of statistical significance for functional analysis (KEGG pathway enrichment and GO interrogation) would normally be chosen to be the most stringent level at which 1% of the features were, on average, significant (which would have been adjusted p-value <0.01). In this instance, as the number of significant features across the comparisons was quite skewed, the significance threshold was manually chosen to be raw p-value < 0.01. Given that targets identified by this method validated by RT-qPCR, this decision appears justified for the cell cycle targets but may not necessarily hold true for other pathways identified as altered, and as ever, candidates identified from a microarray require external validation prior to robust conclusions being drawn.

The use of gene microarrays for assessing the transcriptome has been well established (Zhao, Fung-Leung et al. 2014) but this technology is increasing being superseded by newer techniques such as RNA-sequencing (RNA-seq). RNA-Seq has the benefits of not being limited by a fixed number of known probes, (and is thus less biased), and in contrast to microarrays may more readily identify alteration in splice junctions, allele-specific expression and detection of novel transcripts (Mutz, Heilkenbrinker et al. 2013). However at present, data analysis of RNA-Seq is a more costly option and and data

analysis is complex, particularly when combined with proteomics (Kumar, Bansal et al. 2016).

In the validation set not all biopsies were from women with fibroids. Whilst there was no evidence of clustering between fibroid/non fibroid groups and this does not appear to have affected the validation of candidates, it is a potential source of error, particularly given the small numbers in the validation sets. As previously discussed in both chapter 4 and in this chapter presence of fibroids may alter endometrial mRNA levels and protein expression (Sinclair, Mastroyannis et al. 2011, Makker, Goel et al. 2017). It is uncertain if SPRMs have a differing effect on the transcriptome of the endometrium in the presence or absence of fibroids. Tissue collection of samples following repeated cycles of UPA is ongoing and this will allow an increase in n numbers in validation sets of subject both with and without fibroids to facilitate further enquiry.

5.6.5 Future work

A pragmatic approach was taken with regard to selection of candidates for onward validation. Clearly the outstanding targets from the cell cycle (both up and down-regulated) need to be completed initially. These include *CDKN2A, Chek2, ANAPC4, ESPL1, CDC20, PTTG1* and *MAD2L1* (down-regulated) and *CDKN2C*, *CDKN2B* and *GADD45A*. All differentially expressed genes then need to undergo assessment of alteration in protein expression. Given the apparent contrast between effect of mifepristone and UPA upon cell cycle genes, further assessment of the effect of UPA administration on alteration of mRNA levels and protein expression of CDK2, p21 and p27 would also be of utility.

Functional studies then need to be undertaken. One strategy would be *in vitro* treatment of cultured endometrial cells with UPA. An assessment of cell proliferation could then be assessed by a functional assay such as a 3-(4,5-dimethylthiazol-2-yl)-2,5-diphenyltetrazolium bromide (MMT) assay or a DNA synthesis assay. Alteration in protein expression (if sufficient quantity) may be assessed by western blot. One limitation of endometrial cell culture systems is that *in vivo* there is a complex interplay between endometrial epithelial and stromal cells (Wetendorf and DeMayo 2012). Co-culture models have historically been challenging but methods have now been established (Eritja, Llobet et al. 2010) and may allow a more precise interrogation of the *in vitro* effects of UPA administration.

Consideration of assessment of micro-RNA (miRNA) involved in cell cycle would be of potential utility, particularly if there is discordance between mRNA levels and protein expression. P-regulated miRNA have previously been implicated in the control of endometrial proliferation (Pan, Yuan et al. 2017) and so some alteration of miRNA levels may be evident. It is also unclear that whilst cell cycle genes appear affected at many points of the cell cycle, whether the majority of cells actually arrest in G_1/S.

Cell proliferation can be assessed in a number of ways and commonly used antigens include Ki67, PCNA and Phospho Histone 3 (PH3). Ki-67 is a nuclear protein expressed during all stages of the cell cycle except G_0 and is a standard index of overall cellular proliferation (Yerushalmi, Woods et al. 2010), and is frequently used specifically in endometrial studies (Kitson, Sivalingam et al. 2017). Because histone 3 is phosphorylated only during mitosis and is expressed only in mitotic chromosomes, PH3 staining provides a direct indication of mitotic activity (Brenner, Slayden et al. 2003). As such specific assessment of alteration of PH3 may give further insight into anti-proliferative effect.

The data presented in this thesis offers insights into targets potentially implicated in the endometrial anti-proliferative effect but does not explain the mechanism by which this is brought about. One possible factor that should be further explored is the role of the androgen receptor (AR). In Chapter three it was demonstrated that UPA administration has a striking effect on AR expression with an increase in mRNA levels and protein expression which was evident in both the endometrial stroma and the glands. This is similar to the effect observed in NHP models following administration of the SPRM ZK 230211 (Slayden, Nayak et al. 2001). In the NHP SPRM administration was also associated with a reduction in endometrial wet weight, thickness and mitotic indices. However this anti-proliferative effect was abrogated by administration of the anti-androgen flutamide (Slayden and Brenner 2003). Androgens are known to suppress E2 action in the endometrium and thus the authors postulated that local up-regulation of AR may suppress stromally derived, E2-dependent growth factors (Brenner, Slayden et al. 2003). Given the class effect of reduced proliferation by the SPRMs this may well be implicated in the anti-proliferative effect observed in the endometrium following UPA administration. Without access to NHP models one option would be to treat primary endometrial cells in vitro with UPA and then assess the effect of co-administration of

flutamide on functional proliferation assays, cell cycle mRNA levels and protein expression. Ideally this would be done in a co-culture system but some information may be derived from culture of endometrial stromal cells only. Further exploration of this effect may be undertaken by *in silico* studies – particularly analysis of common genes to both androgen pathways and those differentially expressed following UPA treatment. This includes both those identified by the array and from the candidate-based approach with known roles in proliferation such as HAND2, FOXM1 and KLF-4, -9 & -15.

Finally this chapter has predominantly focused upon the impact of UPA on the cell cycle. This may in part explain why increased levels of malignancy and pre-malignancy are not observed following administration of a progesterone antagonist. However the complement to proliferation is apoptosis. This process was not identified by this array as a significantly altered KEGG pathway but both apoptosis markers *Caspase-3* and *BCL-2* were altered, albeit not at the most stringent statistical level. These merit further investigation and validation, not least as both *in vivo* and *in vitro* treatment of fibroids with UPA up regulates caspase-3 with an associated increase in apoptosis and *in vitro Bcl-2* was down regulated (Xu, Takekida et al. 2005, Yun, Seong et al. 2015). In addition, gene microarray studies assessing the impact on the endometrium following exposure to mifepristone have demonstrated down-regulation of anti-apoptosis transcripts (Cuevas, Tapia-Pizarro et al. 2016) although these analyses were in comparison to secretory phase endometrium.

5.7 Conclusions

This chapter demonstrates that administration of UPA reduces proliferation in the endometrium and fallopian tube but not the cervix. This is the first demonstration of effect of UPA on Ki67 expression in the human fallopian tube and cervix. Administration of UPA has a highly significant impact upon *GREM2* mRNA levels, but up-regulation of *MUC1* is highly variable between subjects. Furthermore that the data presented herein demonstrate for the first time that administration of UPA impacts upon mRNA levels of critical cell cycle genes in the endometrium. This was reflected in reduced expression of the cyclin-dependant kinase regulator CDC25A what was particularly striking in the

glandular epithelium. The effect on protein expression of other cell cycle candidates has not yet been assessed.

Chapter 6.
Final Summary

6.1 Summary of findings

Progesterone receptors (PR) are present throughout the human female reproductive tract. The synthetic ligand for the PR, ulipristal acetate (UPA), a member of the family of selective progesterone receptor modulators (SPRMs), hold promise for the amelioration of numerous gynaecological conditions. Whilst the effect upon endometrial morphology is well recognised, to date data have been lacking of the effect of administration upon key aspects of the epithelial layers of the reproductive tract. The data presented herein provide novel descriptions of the effect of UPA administration upon sex steroid receptor (SSR) expression, and proliferation within the endometrium, fallopian tubes and cervix of women with symptomatic fibroids. Furthermore the effect of UPA administration upon key progesterone regulated genes is described. Candidates implicated in the anti-proliferative effect within the endometrium are also identified.

In keeping with established literature, profound effects upon endometrial morphology were observed, but with greater prevalence than previously described. This is the first description of the impact of *in vivo* treatment with UPA on the morphology of the fallopian tubes, which resemble proliferative phase, in keeping with the effects observed with other SPRMs. However UPA administration does not alter cervical morphology. The morphological effects of UPA in the fallopian tube are consistent with UPA acting with low P-agonism within this region however the morphological changes within the endometrium do not phenocopy either proliferative or secretory phase, suggesting UPA has an "endometrial specific" effect within the human uterus.

Within the endometrium UPA administration increases both PR and PRB mRNA levels and localisation with a particular pattern of protein expression that is not observed either in proliferative or secretory phase endometrium. UPA binds the PR but has minimal affinity for other SSR such as the oestrogen receptor (ER) and androgen receptor (AR). Despite this, UPA administration results in alteration of ER and AR mRNA levels. Protein expression is also increased both in the stromal fibroblasts and glandular epithelium, for AR this reflects a spatial alteration in the localisation of protein expression which does not replicate either proliferative or secretory patterns of expression. There is alteration in ampullary sex-steroid receptor mRNA levels in the fallopian tube but this is limited to PR and ERα and this is relative only to the secretory phase. SSR protein localisation appeared unaltered, and immunopositivity most closely resembled the proliferative phase. This suggests the impact of UPA in the fallopian tube

is limited to blockade of P-antagonism only. Sex-steroid receptor expression in the cervix was unchanged by UPA. Thus it appears, despite PR being present in all three locations, consistent with the effect upon morphology, UPA appears to have an "endometrial specific" effect upon the SSR expression in the epithelium of the human reproductive tract.

To assess the endometrial impact of altered SSR expression, the effect of UPA administration on key P-regulated genes was examined. An alteration relative to secretory levels was frequently observed, consistent with UPA acting with low P-agonism. However despite alteration in SSR localisation between glands and stroma, localisation of protein expression of selected P-regulated genes was similar to the proliferative phase. Furthermore other P-regulated genes were unaltered. Further characterisation is required to assess the impact of UPA on the complex paracrine signalling environment within the endometrium.

Genes implicated in P-resistance associated with endometriosis were demonstrated to have similar mRNA levels as women without endometriosis but it remains unclear whether UPA is acting to overcome the putative P-resistance associated with endometriosis, or merely reflects pre-existing altered levels. Further investigation would be of value as there appears to be a trend towards poorer bleeding control following UPA administration in those women with co-existing endometriosis. Alteration in the eutopic endometrium of these women may render them less able to achieve the bleeding control obtained by those women without endometriosis.

Reassuringly, also presented here, despite overall low P-agonism, and normal circulating oestradiol levels there was no increased rates of hyperplasia or malignancy. Furthermore, despite absence of endometrial shedding and the altered hormonal milieu described above, UPA administration was not associated with accumulation of PTEN null glands.

Despite P-regulated genes reflecting low P-agonism UPA has previously been demonstrated to have an anti-proliferative effect within the endometrium. It was determined here that UPA administration may also reduce proliferation within the fallopian tube.

Unbiased microarray studies of the endometrium identified the cell cycle as the most down regulated pathway following UPA administration relative to proliferative phase. Multiple aspects from all phases of the cell cycle were identified as being down-regulated and were confirmed by PCR in independent samples from women both and without fibroids. Many of these candidates were novel compared to those identified by interrogation of other SPRMs. The mechanism for this anti-proliferative effect is unclear. Demonstrated here was alteration of the transcription factor *FOXM1* relative to proliferative phase within the endometrium, both this and the up-regulation of AR may potentially be implicated in the endometrial anti-proliferative effect but require further investigation in functional studies.

6.2 Further work and future directions

In each chapter suggestion for further work to address deficiencies in current knowledge are suggested and their rationale explained. A summary of key future work is given below:

Endometrium:

- Steroid receptors: Impact of UPA administration upon expression and localisation of ERβ, MR and GR
- Availability of ligands: modulation of steroid metabolising enzymes, 11β- and 17β-hydroxysteroid dehydrogenases
- Assessment on UPA administration on co-repressors NCoR and SMRT
- P-regulated genes:
    - Protein expression of (+/-co-localisation with PR) of co-chaperones, IHH pathway, TGFβ3 signalling and HOXA10
    - Impact of UPA on Wnt4, FGF, FGFR, CRK, His-5, SRC
    - uNK cell population (given impact on IL-15)
- Endometriosis:
    - well phenotyped patients ideally with paired biopsies (pre and on treatment) to assess impact of UPA on P-regulated genes previously demonstrated to be aberrantly expressed in the context of endometriosis
    - In vitro treatment with UPA of stromal cells/co-culture models from women with and without endometriosis

    - Exploration of differences between those with and without control of bleeding
- Array outputs:
    - GREM2 protein localisation, impact upon β-catenin
    - MUC1 immunolocalisation
- Reduction in proliferation:
    - Assessment of mRNA levels of remaining candidates identified in cell cycle, along with p21 and p27 and CDK2, with subsequent immunolocalisation
    - *In vitro* treatment with UPA and other SPRMs of cell culture models: functional proliferation assay, impact upon cell cycle, and impact of co-administration of flutamide (anti-androgen) to determine role of AR in the anti-proliferative effect
    - Further exploration of role of FOXM1 in the anti-proliferative effect

Fallopian tube:

- Assessment of impact upon sex steroid receptors and proliferation in the fimbriae
- Quantification of Ki67 immunopositivity in the fallopian tube and impact upon cell-cycle genes

Cervix:

- Impact of UPA administration upon the immune cell populations

6.3 Overall conclusions

UPA has previously been demonstrated to be an effective and acceptable medical agent for establishing bleeding control in those women with symptomatic fibroids. UPA also has potential for utility in those with HMB in the context of structurally normal uteri, and in the management of endometriosis. These conditions are often incapacitating and have significant socioeconomic costs. The novel data presented in this thesis considerably extend the data available to date concerning the actions of the SPRM, UPA, on the female reproductive tract, and increases knowledge regarding a compound with promising utility for the management of debilitating gynaecological conditions.

Bibliography

Aasmundstad, T. A., O. A. Haugen, E. Johannesen, A. L. Hoe and S. Kvinnsland (1992). "Oestrogen receptor analysis: correlation between enzyme immunoassay and immunohistochemical methods." J Clin Pathol **45**(2): 125-129.

Ackerman, W. E. t., T. L. Summerfield, S. Mesiano, F. Schatz, C. J. Lockwood and D. A. Kniss (2016). "Agonist-Dependent Downregulation of Progesterone Receptors in Human Cervical Stromal Fibroblasts." Reprod Sci **23**(1): 112-123.

Adesanya-Famuyiwa, O. O., J. Zhou, G. Wu and C. Bondy (1999). "Localization and sex steroid regulation of androgen receptor gene expression in rhesus monkey uterus." Obstet Gynecol **93**(2): 265-270.

Afhuppe, W., J. M. Beekman, C. Otto, D. Korr, J. Hoffmann, U. Fuhrmann and C. Moller (2010). "In vitro characterization of ZK 230211--A type III progesterone receptor antagonist with enhanced antiproliferative properties." J Steroid Biochem Mol Biol **119**(1-2): 45-55.

Afhuppe, W., A. Sommer, J. Muller, W. Schwede, U. Fuhrmann and C. Moller (2009). "Global gene expression profiling of progesterone receptor modulators in T47D cells provides a new classification system." J Steroid Biochem Mol Biol **113**(1-2): 105-115.

Allen, W. M. and O. Wintersteiner (1934). "Crystalline progestin." Science **80**(2069): 190-191.

Amazit, L., A. Roseau, J. A. Khan, A. Chauchereau, R. K. Tyagi, H. Loosfelt, P. Leclerc, M. Lombes and A. Guiochon-Mantel (2011). "Ligand-dependent degradation of SRC-1 is pivotal for progesterone receptor transcriptional activity." Mol Endocrinol **25**(3): 394-408.

Amso, N. N., J. Crow, J. Lewin and R. W. Shaw (1994). "A comparative morphological and ultrastructural study of endometrial gland and fallopian tube epithelia at different stages of the menstrual cycle and the menopause." Hum Reprod **9**(12): 2234-2241.

Attardi, B. J., J. Burgenson, S. A. Hild and J. R. Reel (2004). "In vitro antiprogestational/antiglucocorticoid activity and progestin and glucocorticoid receptor binding of the putative metabolites and synthetic derivatives of CDB-2914, CDB-4124, and mifepristone." J Steroid Biochem Mol Biol **88**(3): 277-288.

Ayehunie, S., A. Islam, C. Cannon, T. Landry, J. Pudney, M. Klausner and D. J. Anderson (2015). "Characterization of a Hormone-Responsive Organotypic Human Vaginal Tissue Model: Morphologic and Immunologic Effects." Reprod Sci **22**(8): 980-990.

Bagaria, M., A. Suneja, N. B. Vaid, K. Guleria and K. Mishra (2009). "Low-dose mifepristone in treatment of uterine leiomyoma: a randomised double-blind placebo-controlled clinical trial." The Australian & New Zealand journal of obstetrics & gynaecology **49**(1): 77-83.

Bagchi, I. C., Q. Li, Y. P. Cheon, S. R. Mantena, A. Kannan and M. K. Bagchi (2005). "Use of the progesterone receptor antagonist RU 486 to identify novel progesterone receptor-regulated pathways in implantation." Semin Reprod Med **23**(1): 38-45.

Baird, D. D., D. B. Dunson, M. C. Hill, D. Cousins and J. M. Schectman (2003). "High cumulative incidence of uterine leiomyoma in black and white women: ultrasound evidence." Am J Obstet Gynecol **188**(1): 100-107.

Baird, D. T., A. Brown, H. O. Critchley, A. R. Williams, S. Lin and L. Cheng (2003). "Effect of long-term treatment with low-dose mifepristone on the endometrium." Hum Reprod **18**(1): 61-68.

Baird, D. T., K. J. Thong, C. Hall and S. T. Cameron (1995). "Failure of oestrogen induced luteinizing hormone surge in women treated with mifepristone (RU 486) every day for 30 days." Hum Reprod **10**(9): 2270-2276.

Binelli, M. and B. D. Murphy (2010). "Coordinated regulation of follicle development by germ and somatic cells." Reprod Fertil Dev **22**(1): 1-12.

Bitzer, J., O. Heikinheimo, A. L. Nelson, J. Calaf-Alsina and I. S. Fraser (2015). "Medical management of heavy menstrual bleeding: a comprehensive review of the literature." Obstet Gynecol Surv **70**(2): 115-130.

Bokström, H. and A. Norström (1995). "Effects of mifepristone and progesterone on collagen synthesis in the human uterine cervix." Contraception **51**(4): 249-254.

Borah, B. J., S. K. Laughlin-Tommaso, E. R. Myers, X. Yao and E. A. Stewart (2016). "Association Between Patient Characteristics and Treatment Procedure Among Patients With Uterine Leiomyomas." Obstet Gynecol **127**(1): 67-77.

Bouchard, P. and N. Chabbert-Buffet (2016). "The history and use of the progesterone receptor modulator ulipristal acetate for heavy menstrual bleeding with uterine fibroids." Best Pract Res Clin Obstet Gynaecol.

Bouchard, P., N. Chabbert-Buffet and B. C. J. M. Fauser (2011). "Selective progesterone receptor modulators in reproductive medicine: Pharmacology, clinical efficacy and safety." Fertility and Sterility **96**(5): 1175-1189.

Boutros, R., C. Dozier and B. Ducommun (2006). "The when and wheres of CDC25 phosphatases." Curr Opin Cell Biol **18**(2): 185-191.

Boutros, R., V. Lobjois and B. Ducommun (2007). "CDC25 phosphatases in cancer cells: key players? Good targets?" Nat Rev Cancer **7**(7): 495-507.

Brache, V., L. Cochon, M. Deniaud and H. B. Croxatto (2013). "Ulipristal acetate prevents ovulation more effectively than levonorgestrel: analysis of pooled data from three randomized trials of emergency contraception regimens." Contraception **88**(5): 611-618.

Brache, V., R. Sitruk-Ware, A. Williams, D. Blithe, H. Croxatto, N. Kumar, S. Kumar, Y. Y. Tsong, I. Sivin, A. Nath, H. Sussman, L. Cochon, M. J. Miranda, V. Reyes, A. Faundes and D. Mishell, Jr. (2012). "Effects of a novel estrogen-free, progesterone receptor modulator contraceptive vaginal ring on inhibition of ovulation, bleeding patterns and endometrium in normal women." Contraception **85**(5): 480-488.

Brayman, M. J., J. Julian, B. Mulac-Jericevic, O. M. Conneely, D. P. Edwards and D. D. Carson (2006). "Progesterone receptor isoforms A and B differentially regulate MUC1 expression in uterine epithelial cells." Mol Endocrinol **20**(10): 2278-2291.

Brenner, R. M., M. C. McClellan, N. B. West, M. J. Novy, G. J. Haluska and M. D. Sternfeld (1991). "Estrogen and progestin receptors in the macaque endometrium." Ann N Y Acad Sci **622**: 149-166.

Brenner, R. M. and O. D. Slayden (1994). Cyclic changes in the primate oviduct and endometrium. The physiology of reproduction. E. Knobil and J. D. Neill. New York, Raven Press. **1:** 541-565.

Brenner, R. M. and O. D. Slayden (2012). "Molecular and functional aspects of menstruation in the macaque." Rev Endocr Metab Disord **13**(4): 309-318.

Brenner, R. M., O. D. Slayden, A. Nath, Y. Y. Tsong and R. Sitruk-Ware (2010). "Intrauterine administration of CDB-2914 (Ulipristal) suppresses the endometrium of rhesus macaques." Contraception **81**(4): 336-342.

Brenner, R. M., O. D. Slayden, N. R. Nayak, D. T. Baird and H. O. D. Critchley (2003). "A role for the androgen receptor in the endometrial antiproliferative effects of progesterone antagonists." Steroids **68**(10-13): 1033-1039.

Brenner, R. M., O. D. Slayden, W. H. Rodgers, H. O. Critchley, R. Carroll, X. J. Nie and K. Mah (2003). "Immunocytochemical assessment of mitotic activity with an antibody to phosphorylated histone H3 in the macaque and human endometrium." Hum Reprod **18**(6): 1185-1193.

Brenner, R. M., N. B. West and M. C. McClellan (1990). "Estrogen and progestin receptors in the reproductive tract of male and female primates." Biol Reprod **42**(1): 11-19.

Briton-Jones, C., I. H. Lok, C. K. Cheung, A. L. Po, T. T. Chiu and C. Haines (2005). "Ratio of mRNA expression of progesterone receptor isoforms AB is to B in human oviduct mucosal cells during the ovulatory cycle." J Assist Reprod Genet **22**(11-12): 429-435.

Brosens, J. J., N. Hayashi and J. O. White (1999). "Progesterone Receptor Regulates Decidual Prolactin Expression in Differentiating Human Endometrial Stromal Cells1." Endocrinology **140**(10): 4809-4820.

Brosens, J. J., J. Tullet, R. Varshochi and E. W. Lam (2004). "Steroid receptor action." Best Pract Res Clin Obstet Gynaecol **18**(2): 265-283.

Bulun, S. E. (2013). "Uterine fibroids." N Engl J Med **369**(14): 1344-1355.

Burton, K. A., T. A. Henderson, S. G. Hillier, J. I. Mason, F. Habib, R. M. Brenner and H. O. Critchley (2003). "Local levonorgestrel regulation of androgen receptor and 17beta-hydroxysteroid dehydrogenase type 2 expression in human endometrium." Hum Reprod **18**(12): 2610-2617.

Calil, L. N., M. I. Edelweiss, L. Meurer, C. N. Igansi and M. C. Bozzetti (2014). "p16 INK4a and Ki67 expression in normal, dysplastic and neoplastic uterine cervical epithelium and human papillomavirus (HPV) infection." Pathol Res Pract **210**(8): 482-487.

Cameron, S. T., H. O. Critchley, K. J. Thong, C. H. Buckley, A. R. Williams and D. T. Baird (1996). "Effects of daily low dose mifepristone on endometrial maturation and proliferation." Hum Reprod **11**(11): 2518-2526.

Cano, A., V. Serra, J. Rivera, R. Monmeneu and C. Marzo (1990). "Expression of estrogen receptors, progesterone receptors, and an estrogen receptor-associated protein in the human cervix during the menstrual cycle and menopause." Fertil Steril **54**(6): 1058-1064.

Carbonell, J. L., R. Acosta, Y. Perez, R. Garces, C. Sanchez and G. Tomasi (2013). "Treatment of uterine myoma with 2.5 or 5 mg mifepristone daily during 3 months with 9 months posttreatment followup: Randomized clinical trial." ISRN Obstetrics and Gynecology **2013**(649030).

Cardozo, E. O., A. D. Clark, N. K. Banks, M. B. Henne, B. J. Stegmann and J. H. Segars (2012). "The estimated annual cost of uterine leiomyomata in the United States " American Journal of Obstetrics & Gynecology **206**(3): 211.e211-211.e219.

Carlson, B. M. (2008). Human Embryology and Developmental Biology. Philadelphia, Mosby.

Carracedo, A. and P. P. Pandolfi (2008). "The PTEN-PI3K pathway: of feedbacks and cross-talks." Oncogene **27**(41): 5527-5541.

Catalano, R. D., H. O. Critchley, O. Heikinheimo, D. T. Baird, D. Hapangama, J. R. Sherwin, D. S. Charnock-Jones, S. K. Smith and A. M. Sharkey (2007). "Mifepristone induced progesterone withdrawal reveals novel regulatory pathways in human endometrium." Mol Hum Reprod **13**(9): 641-654.

Chabbert-Buffet, N., G. Meduri, P. Bouchard and I. M. Spitz (2005). "Selective progesterone receptor modulators and progesterone antagonists: mechanisms of action and clinical applications." Human Reproduction Update **11**(3): 293-307.

Chabbert-Buffet, N., A. Pintiaux-Kairis and P. Bouchard (2007). "Effects of the progesterone receptor modulator VA2914 in a continuous low dose on the hypothalamic-pituitary-ovarian axis and endometrium in normal women: a prospective, randomized, placebo-controlled trial." J Clin Endocrinol Metab **92**(9): 3582-3589.

Chang, Y. S., H. D. Huang, K. T. Yeh and J. G. Chang (2017). "Identification of novel mutations in endometrial cancer patients by whole-exome sequencing." Int J Oncol.

Chauchereau, A., J. F. Savouret and E. Milgrom (1992). "Control of biosynthesis and post-transcriptional modification of the progesterone receptor." Biol Reprod **46**(2): 174-177.

Chen, Y., Y. Wang, Y. Zhuang, F. Zhou and L. Huang (2012). "Mifepristone increases the cytotoxicity of uterine natural killer cells by acting as a glucocorticoid antagonist via ERK activation." PLoS One **7**(5): e36413.

Chlebowski, R. T., G. L. Anderson, G. E. Sarto, R. Haque, C. D. Runowicz, A. K. Aragaki, C. A. Thomson, B. V. Howard, J. Wactawski-Wende, C. Chen, T. E. Rohan, M. S. Simon, S. D. Reed and J. E. Manson (2016). "Continuous Combined Estrogen Plus Progestin and

Endometrial Cancer: The Women's Health Initiative Randomized Trial." J Natl Cancer Inst **108**(3).

Christow, A., X. Sun and K. Gemzell-Danielsson (2002). "Effect of mifepristone and levonorgestrel on expression of steroid receptors in the human Fallopian tube." Mol Hum Reprod **8**(4): 333-340.

Chwalisz, K., R. M. Brenner, U. U. Fuhrmann, H. Hess-Stumpp and W. Elger (2000). "Antiproliferative effects of progesterone antagonists and progesterone receptor modulators on the endometrium." Steroids **65**(10-11): 741-751.

Chwalisz, K., R. Garg, R. Brenner, O. Slayden, C. Winkel and W. Elger (2006). "Role of nonhuman primate models in the discovery and clinical development of selective progesterone receptor modulators (SPRMs)." Reproductive Biology and Endocrinology **4**(SUPPL. 1).

Chwalisz, K., L. Larsen, C. Mattia-Goldberg, A. Edmonds, W. Elger and C. A. Winkel (2007). "A randomized, controlled trial of asoprisnil, a novel selective progesterone receptor modulator, in women with uterine leiomyomata." Fertility & Sterility **87**(6): 1399-1412.

Chwalisz, K., M. C. Perez, D. Demanno, C. Winkel, G. Schubert and W. Elger (2005). "Selective progesterone receptor modulator development and use in the treatment of leiomyomata and endometriosis." Endocrine Reviews **26**(3): 423-438.

Combs, S. E., G. Han, N. Mani, S. Beruti, M. Nerenberg and D. L. Rimm (2016). "Loss of antigenicity with tissue age in breast cancer." Lab Invest **96**(3): 264-269.

Costa, R. H. (2005). "FoxM1 dances with mitosis." Nat Cell Biol **7**(2): 108-110.

Cousins, F. L., A. Murray, A. Esnal, D. A. Gibson, H. O. D. Critchley and P. T. K. Saunders (2014). "Evidence from a Mouse Model That Epithelial Cell Migration and Mesenchymal-Epithelial Transition Contribute to Rapid Restoration of Uterine Tissue Integrity during Menstruation." PLoS ONE **9**(1): e86378.

Critchley, H. O., R. M. Brenner, T. A. Henderson, K. Williams, N. R. Nayak, O. D. Slayden, M. R. Millar and P. T. Saunders (2001). "Estrogen receptor beta, but not estrogen receptor alpha, is present in the vascular endothelium of the human and nonhuman primate endometrium." J Clin Endocrinol Metab **86**(3): 1370-1378.

Critchley, H. O., R. W. Kelly, R. M. Brenner and D. T. Baird (2001). "The endocrinology of menstruation--a role for the immune system." Clin Endocrinol (Oxf) **55**(6): 701-710.

Critchley, H. O. and J. A. Maybin (2011). "Molecular and cellular causes of abnormal uterine bleeding of endometrial origin." Semin Reprod Med **29**(5): 400-409.

Critchley, H. O., J. Osei, T. A. Henderson, L. Boswell, K. J. Sales, H. N. Jabbour and N. Hirani (2006). "Hypoxia-inducible factor-1alpha expression in human endometrium and its regulation by prostaglandin E-series prostanoid receptor 2 (EP2)." Endocrinology **147**(2): 744-753.

Critchley, H. O. and P. T. Saunders (2009). "Hormone receptor dynamics in a receptive human endometrium." Reprod Sci **16**(2): 191-199.

Croxatto, H. B., A. M. Salvatierra, H. D. Croxatto and B. Fuentealba (1993). "Effects of continuous treatment with low dose mifepristone throughout one menstrual cycle." Hum Reprod **8**(2): 201-207.

Croxatto, H. B., A. M. Salvatierra, B. Fuentealba and L. Leiva (1995). "Follicle stimulating hormone-granulosa cell axis involvement in the antifolliculotrophic effect of low dose mifepristone (RU486)." Hum Reprod **10**(8): 1987-1991.

Crum, C. P., R. Drapkin, A. Miron, T. A. Ince, M. Muto, D. W. Kindelberger and Y. Lee (2007). "The distal fallopian tube: a new model for pelvic serous carcinogenesis." Curr Opin Obstet Gynecol **19**(1): 3-9.

Crum, C. P., M. Herfs, G. Ning, J. G. Bijron, B. E. Howitt, C. A. Jimenez, S. Hanamornroongruang, F. D. McKeon and W. Xian (2013). "Through the glass darkly: intraepithelial neoplasia, top-down differentiation, and the road to ovarian cancer." J Pathol **231**(4): 402-412.

Cuevas, C. A., A. Tapia-Pizarro, A. M. Salvatierra, D. J. Munroe, L. Velasquez and H. B. Croxatto (2016). "Effect of single post-ovulatory administration of mifepristone (RU486) on transcript profile during the receptive period in human endometrium." Reproduction **151**(4): 331-349.

Cullingford, T. E. and J. W. Pollard (1988). "RU 486 completely inhibits the action of progesterone on cell proliferation in the mouse uterus." J Reprod Fertil **83**(2): 909-914.

Daftary, G. S. and H. S. Taylor (2004). "Pleiotropic effects of Hoxa10 on the functional development of peri-implantation endometrium." Mol Reprod Dev **67**(1): 8-14.

Danielsson, K. G. The Effect of a Progesterone Receptor Modulator on Breast Tissue in Women With BRCA-1 and -2 Mutations - a Placebo Controlled RCT., Karolinska Institutet.

de la Fuente, E., M. D. Borras, M. Rubio and N. Abril (2016). "Ulipristal Acetate in Myomectomy Optimization in an Infertile Patient with Giant Myomas." Case Rep Med **2016**: 5135780.

Demers, L. M., G. J. Macdonald, A. T. Hertig, N. W. King and J. J. Mackey (1972). "The cervix uteri in Macaca mulatta, Macaca arctoides, and Macaca fascicularis--a comparative anatomic study with special reference to Macaca arctoides as a unique model for endometrial study." Fertil Steril **23**(8): 529-534.

Dharmaraj, N., P. J. Chapela, M. Morgado, S. M. Hawkins, B. A. Lessey, S. L. Young and D. D. Carson (2014). "Expression of the transmembrane mucins, MUC1, MUC4 and MUC16, in normal endometrium and in endometriosis." Hum Reprod **29**(8): 1730-1738.

Dharmaraj, N., S. J. Gendler and D. D. Carson (2009). "Expression of human MUC1 during early pregnancy in the human MUC1 transgenic mouse model." Biol Reprod **81**(6): 1182-1188.

Dominguez-Sola, D., C. Y. Ying, C. Grandori, L. Ruggiero, B. Chen, M. Li, D. A. Galloway, W. Gu, J. Gautier and R. Dalla-Favera (2007). "Non-transcriptional control of DNA replication by c-Myc." Nature **448**(7152): 445-451.

Donnez, J., F. Casanas-Roux, J. Caprasse, J. Ferin and K. Thomas (1985). "Cyclic changes in ciliation, cell height, and mitotic activity in human tubal epithelium during reproductive life." Fertil Steril **43**(4): 554-559.

Donnez, J., O. Donnez and M. M. Dolmans (2016). "Safety of treatment of uterine fibroids with the selective progesterone receptor modulator, ulipristal acetate." Expert Opin Drug Saf **15**(12): 1679-1686.

Donnez, J., R. Hudecek, O. Donnez, D. Matule, H. J. Arhendt, J. Zatik, Z. Kasilovskiene, M. C. Dumitrascu, H. Fernandez, D. H. Barlow, P. Bouchard, B. C. Fauser, E. Bestel, P. Terrill, I. Osterloh and E. Loumaye (2015). "Efficacy and safety of repeated use of ulipristal acetate in uterine fibroids." Fertil Steril **103**(2): 519-527 e513.

Donnez, J., T. F. Tatarchuk, P. Bouchard, L. Puscasiu, N. F. Zakharenko, T. Ivanova, G. Ugocsai, M. Mara, M. P. Jilla, E. Bestel, P. Terrill, I. Osterloh, E. Loumaye and P. I. S. Group (2012). "Ulipristal acetate versus placebo for fibroid treatment before surgery." New England Journal of Medicine **366**(5): 409-420.

Donnez, J., J. Tomaszewski, F. Vazquez, P. Bouchard, B. Lemieszczuk, F. Baro, K. Nouri, L. Selvaggi, K. Sodowski, E. Bestel, P. Terrill, I. Osterloh, E. Loumaye and P. I. S. Group (2012). "Ulipristal acetate versus leuprolide acetate for uterine fibroids." New England Journal of Medicine **366**(5): 421-432.

Donnez, J., F. Vazquez, J. Tomaszewski, K. Nouri, P. Bouchard, B. C. Fauser, D. H. Barlow, S. Palacios, O. Donnez, E. Bestel, I. Osterloh, E. Loumaye, Pearl, III and P. I. E. S. Group (2014). "Long-term treatment of uterine fibroids with ulipristal acetate." Fertil Steril **101**(6): 1565-1573 e1561-1518.

Dorozynski, A. (1997). "Boycott threat forces French company to abandon RU486." BMJ : British Medical Journal **314**(7088): 1150-1150.

Du, H., J. Sarno and H. S. Taylor (2010). "HOXA10 Inhibits Kruppel-Like Factor 9 Expression in the Human Endometrial Epithelium." Biology of Reproduction **83**(2): 205-211.

Du, H. and H. S. Taylor (2004). "Molecular regulation of mullerian development by Hox genes." Ann N Y Acad Sci **1034**: 152-165.

Dunn, C. L., H. O. Critchley and R. W. Kelly (2002). "IL-15 regulation in human endometrial stromal cells." J Clin Endocrinol Metab **87**(4): 1898-1901.

Eisinger, S. H., S. Meldrum, K. Fiscella, H. D. le Roux and D. S. Guzick (2003). "Low-dose mifepristone for uterine leiomyomata." Obstetrics & Gynecology **101**(2): 243-250.

Elger, W., J. Bartley, B. Schneider, G. Kaufmann, G. Schubert and K. Chwalisz (2000). "Endocrine pharmacological characterization of progesterone antagonists and progesterone receptor modulators with respect to PR-agonistic and antagonistic activity." Steroids **65**(10-11): 713-723.

Englund, K., A. Blanck, I. Gustavsson, U. Lundkvist, P. Sjoblom, A. Norgren and B. Lindblom (1998). "Sex steroid receptors in human myometrium and fibroids: changes

during the menstrual cycle and gonadotropin-releasing hormone treatment." J Clin Endocrinol Metab **83**(11): 4092-4096.

Engman, M., S. Granberg, A. R. Williams, C. X. Meng, P. G. Lalitkumar and K. Gemzell-Danielsson (2009). "Mifepristone for treatment of uterine leiomyoma. A prospective randomized placebo controlled trial." Hum Reprod **24**(8): 1870-1879.

Engman, M., L. Skoog, G. Soderqvist and K. Gemzell-Danielsson (2008). "The effect of mifepristone on breast cell proliferation in premenopausal women evaluated through fine needle aspiration cytology." Human Reproduction **23**(9): 2072-2079.

Engman, M., S. Varghese, K. Lagerstedt Robinson, H. Malmgren, A. Hammarsjo, B. Bystrom, P. G. Lalitkumar and K. Gemzell-Danielsson (2013). "GSTM1 gene expression correlates to leiomyoma volume regression in response to mifepristone treatment." PLoS One **8**(12): e80114.

Eppig, J. J. (2001). "Oocyte control of ovarian follicular development and function in mammals." Reproduction **122**(6): 829-838.

Eritja, N., D. Llobet, M. Domingo, M. Santacana, A. Yeramian, X. Matias-Guiu and X. Dolcet (2010). "A novel three-dimensional culture system of polarized epithelial cells to study endometrial carcinogenesis." Am J Pathol **176**(6): 2722-2731.

Eun Kwon, H. and H. S. Taylor (2004). "The role of HOX genes in human implantation." Ann N Y Acad Sci **1034**: 1-18.

Evans-Hoeker, E., B. A. Lessey, J. W. Jeong, R. F. Savaris, W. A. Palomino, L. Yuan, D. P. Schammel and S. L. Young (2016). "Endometrial BCL6 Overexpression in Eutopic Endometrium of Women With Endometriosis." Reprod Sci **23**(9): 1234-1241.

Fan, W., S. W. Li, W. H. Li, Y. Wang, Y. Gong, Q. H. Ma and S. Luo (2012). "FOXO1 expression and regulation in endometrial tissue during the menstrual cycle and in early pregnancy decidua." Gynecol Obstet Invest **74**(1): 56-63.

Fauser, B. C., J. Donnez, P. Bouchard, D. H. Barlow, F. Vazquez, P. Arriagada, S. O. Skouby, S. Palacios, J. Tomaszewski, B. Lemieszczuk and A. R. William (2017). "Safety after extended repeated use of ulipristal acetate for uterine fibroids." PLoS One **12**(3): e0173523.

Fernandez, H., T. Schmidt, M. Powell, A. P. Costa, P. Arriagada and C. Thaler (2017). "Real world data of 1473 patients treated with ulipristal acetate for uterine fibroids: Premya study results." Eur J Obstet Gynecol Reprod Biol **208**: 91-96.

Finn, C. A. (1996). "Why do women menstruate? Historical and evolutionary review." Eur J Obstet Gynecol Reprod Biol **70**(1): 3-8.

Finn, C. A. (1998). "Menstruation: a nonadaptive consequence of uterine evolution." Q Rev Biol **73**(2): 163-173.

Fraser, I. S., H. O. Critchley, M. Broder and M. G. Munro (2011). "The FIGO recommendations on terminologies and definitions for normal and abnormal uterine bleeding." Semin Reprod Med **29**(5): 383-390.

Fraser, I. S., S. Langham and K. Uhl-Hochgraeber (2009). "Health-related quality of life and economic burden of abnormal uterine bleeding." Expert Rev. Obstet. Gynecol. **4**(2): 179-189.

Fraser, R., G. S. Whitley, B. Thilaganathan and J. E. Cartwright (2015). "Decidual natural killer cells regulate vessel stability: implications for impaired spiral artery remodelling." J Reprod Immunol **110**: 54-60.

Frick, K. D., M. A. Clark, D. M. Steinwachs, P. Langenberg, D. Stovall, M. G. Munro and K. Dickersin (2009). "Financial and quality-of-life burden of dysfunctional uterine bleeding among women agreeing to obtain surgical treatment." Womens Health Issues **19**(1): 70-78.

Gagne, D., M. Pons and D. Philibert (1985). "RU 38486: a potent antiglucocorticoid in vitro and in vivo." J Steroid Biochem **23**(3): 247-251.

Gao, F., F. Bian, X. Ma, V. V. Kalinichenko and S. K. Das (2015). "Control of regional decidualization in implantation: Role of FoxM1 downstream of Hoxa10 and cyclin D3." Sci Rep **5**: 13863.

Garcia-Sanz, P., J. C. Trivino, A. Mota, M. Perez Lopez, E. Colas, A. Rojo-Sebastian, A. Garcia, S. Gatius, M. Ruiz, J. Prat, R. Lopez-Lopez, M. Abal, A. Gil-Moreno, J. Reventos, X. Matias-Guiu and G. Moreno-Bueno (2017). "Chromatin remodelling and DNA repair genes are frequently mutated in endometrioid endometrial carcinoma." Int J Cancer **140**(7): 1551-1563.

Gellersen, B. and J. Brosens (2003). "Cyclic AMP and progesterone receptor cross-talk in human endometrium: a decidualizing affair." J Endocrinol **178**(3): 357-372.

Gellersen, B. and J. J. Brosens (2014). "Cyclic decidualization of the human endometrium in reproductive health and failure." Endocr Rev **35**(6): 851-905.

Gellersen, B., M. S. Fernandes and J. J. Brosens (2009). "Non-genomic progesterone actions in female reproduction." Hum Reprod Update **15**(1): 119-138.

George, S. H., A. Milea and P. A. Shaw (2012). "Proliferation in the normal FTE is a hallmark of the follicular phase, not BRCA mutation status." Clin Cancer Res **18**(22): 6199-6207.

Ghosh, D., A. M. Sharkey, D. S. Charnock-Jones, S. K. Smith and J. Sengupta (2009). "Effect of low-dose mifepristone administration on day 2 after ovulation on transcript profiles in implantation-stage endometrium of rhesus monkeys." Reproduction **138**(2): 357-370.

Girling, J. E. and P. A. Rogers (2009). "Regulation of endometrial vascular remodelling: role of the vascular endothelial growth factor family and the angiopoietin-TIE signalling system." Reproduction **138**(6): 883-893.

Girling, J. E. and P. A. W. Rogers (2012). "The endometrial lymphatic vasculature: Function and dysfunction." Reviews in Endocrine and Metabolic Disorders **13**(4): 265-275.

Glasier, A. (2014). "The rationale for use of Ulipristal Acetate as first line in emergency contraception: biological and clinical evidence." Gynecol Endocrinol **30**(10): 688-690.

Gleeson, N., M. Devitt, B. L. Sheppard and J. Bonnar (1993). "Endometrial fibrinolytic enzymes in women with normal menstruation and dysfunctional uterine bleeding." Br. J. Obstet. Gynaecol. **100**(8): 768-771.

Gliklich, R. E., M. B. Leavy, P. Velentgas, D. M. Campion, P. Mohr, R. Sabharwal, D. Whicher, E. R. Myers and W. K. Nicholson (2011). Identification of Future Research Needs in the Comparative Management of Uterine Fibroid Disease
A Report on the Priority-Setting Process, Preliminary Data Analysis, and Research Plan. A. f. H. R. a. Quality.

Gottlieb, S. (2000). "Abortion pill is approved for sale in United States." BMJ : British Medical Journal **321**(7265): 851-851.

Goyeneche, A. A., R. W. Caron and C. M. Telleria (2007). "Mifepristone inhibits ovarian cancer cell growth in vitro and in vivo." Clin Cancer Res **13**(11): 3370-3379.

Goyeneche, A. A., E. E. Seidel and C. M. Telleria (2012). "Growth inhibition induced by antiprogestins RU-38486, ORG-31710, and CDB-2914 in ovarian cancer cells involves inhibition of cyclin dependent kinase 2." Invest New Drugs **30**(3): 967-980.

Goyeneche, A. A. and C. M. Telleria (2015). "Antiprogestins in gynecological diseases." Reproduction **149**(1): R15-33.

Groothuis, P. G., H. H. Dassen, A. Romano and C. Punyadeera (2007). "Estrogen and the endometrium: lessons learned from gene expression profiling in rodents and human." Hum Reprod Update **13**(4): 405-417.

Grow, D. R., R. F. Williams, J. G. Hsiu and G. D. Hodgen (1996). "Antiprogestin and/or gonadotropin-releasing hormone agonist for endometriosis treatment and bone maintenance: a 1-year primate study." J Clin Endocrinol Metab **81**(5): 1933-1939.

Gupta, J. K., J. P. Daniels, L. J. Middleton, H. M. Pattison, G. Prileszky, T. E. Roberts, S. Sanghera, P. Barton, R. Gray and J. Kai (2015). "A randomised controlled trial of the clinical effectiveness and cost-effectiveness of the levonorgestrel-releasing intrauterine system in primary care against standard treatment for menorrhagia: the ECLIPSE trial." Health Technol Assess **19**(88): i-xxv, 1-118.

Gupta, J. K. and N. Johnson (1990). "Effect of mifepristone on dilatation of the pregnant and non-pregnant cervix." Lancet **335**(8700): 1238-1240.

Haines, N. (2016). Births by parents' characteristics in England and Wales: 2015. O. f. N. Statistics.

Hapangama, D. K., A. M. Kamal and J. N. Bulmer (2015). "Estrogen receptor beta: the guardian of the endometrium." Hum Reprod Update **21**(2): 174-193.

Hattrup, C. L. and S. J. Gendler (2008). "Structure and function of the cell surface (tethered) mucins." Annu Rev Physiol **70**: 431-457.

Heard, M. E., C. D. Simmons, F. A. Simmen and R. C. Simmen (2014). "Kruppel-like factor 9 deficiency in uterine endometrial cells promotes ectopic lesion establishment associated with activated notch and hedgehog signaling in a mouse model of endometriosis." Endocrinology **155**(4): 1532-1546.

Heikinheimo, O., J. G. Hsiu, K. Gordon, S. Kim, R. F. Williams, W. E. Gibbons and G. D. Hodgen (1996). "Endometrial effects of RU486 in primates--antiproliferative action despite signs of estrogen action and increased cyclin-B expression." J Steroid Biochem Mol Biol **59**(2): 179-190.

Heikinheimo, O., S. Vani, O. Carpen, A. Tapper, P. Harkki, E. M. Rutanen and H. Critchley (2007). "Intrauterine release of progesterone antagonist ZK230211 is feasible and results in novel endometrial effects: a pilot study." Hum Reprod **22**(9): 2515-2522.

Henderson, T. A., P. T. Saunders, A. Moffett-King, N. P. Groome and H. O. Critchley (2003). "Steroid receptor expression in uterine natural killer cells." J Clin Endocrinol Metab **88**(1): 440-449.

Hodgen, G. D. (1991). "Antiprogestins: the political chemistry of RU486." Fertil Steril **56**(3): 394-395.

Hollingsworth, M. A. and B. J. Swanson (2004). "Mucins in cancer: protection and control of the cell surface." Nat Rev Cancer **4**(1): 45-60.

Horak, P., M. Mara, P. Dundr, K. Kubinova, D. Kuzel, R. Hudecek and R. Chmel (2012). "Effect of a selective progesterone receptor modulator on induction of apoptosis in uterine fibroids in vivo." Int J Endocrinol **2012**: 436174.

Horne, A. W., A. E. King, E. Shaw, S. E. McDonald, A. R. Williams, P. T. Saunders and H. O. Critchley (2009). "Attenuated sex steroid receptor expression in fallopian tube of women with ectopic pregnancy." J Clin Endocrinol Metab **94**(12): 5146-5154.

Horne, A. W., E. N. Lalani, R. A. Margara, T. A. Ryder, M. A. Mobberley and J. O. White (2005). "The expression pattern of MUC1 glycoforms and other biomarkers of endometrial receptivity in fertile and infertile women." Mol Reprod Dev **72**(2): 216-229.

Hubler, T. R., W. B. Denny, D. L. Valentine, J. Cheung-Flynn, D. F. Smith and J. G. Scammell (2003). "The FK506-binding immunophilin FKBP51 is transcriptionally regulated by progestin and attenuates progestin responsiveness." Endocrinology **144**(6): 2380-2387.

Huyen, D. V. and B. M. Bany (2011). "Evidence for a conserved function of heart and neural crest derivatives expressed transcript 2 in mouse and human decidualization." Reproduction **142**(2): 353-368.

Jaaskelainen, T., H. Makkonen and J. J. Palvimo (2011). "Steroid up-regulation of FKBP51 and its role in hormone signaling." Curr Opin Pharmacol **11**(4): 326-331.

Jabbour, H. N., R. W. Kelly, H. M. Fraser and H. O. Critchley (2006). "Endocrine regulation of menstruation." Endocr Rev **27**(1): 17-46.

Jiang, Y., Y. Liao, H. He, Q. Xin, Z. Tu, S. Kong, T. Cui, B. Wang, S. Quan, B. Li, S. Zhang and H. Wang (2015). "FoxM1 Directs STAT3 Expression Essential for Human Endometrial Stromal Decidualization." Scientific Reports **5**: 13735.

Jones, A., A. E. Teschendorff, Q. Li, J. D. Hayward, A. Kannan, T. Mould, J. West, M. Zikan, D. Cibula, H. Fiegl, S. H. Lee, E. Wik, R. Hadwin, R. Arora, C. Lemech, H. Turunen, P. Pakarinen, I. J. Jacobs, H. B. Salvesen, M. K. Bagchi, I. C. Bagchi and M. Widschwendter (2013). "Role of DNA methylation and epigenetic silencing of HAND2 in endometrial cancer development." PLoS Med **10**(11): e1001551.

Jones, N. L., J. Xiu, S. Chatterjee-Paer, A. Buckley de Meritens, W. M. Burke, A. I. Tergas, J. D. Wright and J. Y. Hou (2017). "Distinct molecular landscapes between endometrioid and nonendometrioid uterine carcinomas." Int J Cancer **140**(6): 1396-1404.

Joshi, N. R., E. H. Miyadahira, Y. Afshar, J. W. Jeong, S. L. Young, B. A. Lessey, P. C. Serafini and A. T. Fazleabas (2017). "Progesterone Resistance in Endometriosis Is Modulated by the Altered Expression of MicroRNA-29c and FKBP4." J Clin Endocrinol Metab **102**(1): 141-149.

Kalin, T. V., V. Ustiyan and V. V. Kalinichenko (2011). "Multiple faces of FoxM1 transcription factor: lessons from transgenic mouse models." Cell Cycle **10**(3): 396-405.

Kauffmann, A. and W. Huber (2010). "Microarray data quality control improves the detection of differentially expressed genes." Genomics **95**(3): 138-142.

Kettel, L. M., A. A. Murphy, A. J. Morales and S. S. Yen (1998). "Preliminary report on the treatment of endometriosis with low-dose mifepristone (RU 486)." Am J Obstet Gynecol **178**(6): 1151-1156.

Kim, J. J., T. Kurita and S. E. Bulun (2013). "Progesterone action in endometrial cancer, endometriosis, uterine fibroids, and breast cancer." Endocr Rev **34**(1): 130-162.

Kim, J. J., H. S. Taylor, G. E. Akbas, I. Foucher, A. Trembleau, R. C. Jaffe, A. T. Fazleabas and T. G. Unterman (2003). "Regulation of insulin-like growth factor binding protein-1 promoter activity by FKHR and HOXA10 in primate endometrial cells." Biol Reprod **68**(1): 24-30.

Kim, J. J., H. S. Taylor, Z. Lu, O. Ladhani, J. M. Hastings, K. S. Jackson, Y. Wu, S. W. Guo and A. T. Fazleabas (2007). "Altered expression of HOXA10 in endometriosis: potential role in decidualization." Mol Hum Reprod **13**(5): 323-332.

Kirby, M. A., A. C. Heuerman, M. Custer, A. E. Dobyns, R. Strilaeff, K. N. Stutz, J. Cooperrider, J. G. Elsissy and S. M. Yellon (2016). "Progesterone Receptor-Mediated Actions Regulate Remodeling of the Cervix in Preparation for Preterm Parturition." Reprod Sci **23**(11): 1473-1483.

Kitson, S., V. N. Sivalingam, J. Bolton, R. McVey, M. Nickkho-Amiry, M. E. Powell, A. Leary, H. W. Nijman, R. A. Nout, T. Bosse, A. G. Renehan, H. C. Kitchener, R. J. Edmondson and E. J. Crosbie (2017). "Ki-67 in endometrial cancer: scoring optimization and prognostic relevance for window studies." Mod Pathol **30**(3): 459-468.

Kobayashi, A., W. Shawlot, A. Kania and R. R. Behringer (2004). "Requirement of Lim1 for female reproductive tract development." Development **131**(3): 539-549.

Koji, T., M. Chedid, J. S. Rubin, O. D. Slayden, K. G. Csaky, S. A. Aaronson and R. M. Brenner (1994). "Progesterone-dependent expression of keratinocyte growth factor mRNA in stromal cells of the primate endometrium: keratinocyte growth factor as a progestomedin." J Cell Biol **125**(2): 393-401.

Krishnan, V., G. Elberg, M. J. Tsai and S. Y. Tsai (1997). "Identification of a novel sonic hedgehog response element in the chicken ovalbumin upstream promoter-transcription factor II promoter." Mol Endocrinol **11**(10): 1458-1466.

Kuiper, G. G., E. Enmark, M. Pelto-Huikko, S. Nilsson and J. A. Gustafsson (1996). "Cloning of a novel receptor expressed in rat prostate and ovary." Proc Natl Acad Sci U S A **93**(12): 5925-5930.

Kulp, J. L., R. Mamillapalli and H. S. Taylor (2016). "Aberrant HOXA10 Methylation in Patients With Common Gynecologic Disorders: Implications for Reproductive Outcomes." Reprod Sci **23**(4): 455-463.

Kumar, D., G. Bansal, A. Narang, T. Basak, T. Abbas and D. Dash (2016). "Integrating transcriptome and proteome profiling: Strategies and applications." Proteomics **16**(19): 2533-2544.

Kurnit, K. C., G. N. Kim, B. M. Fellman, D. L. Urbauer, G. B. Mills, W. Zhang and R. R. Broaddus (2017). "CTNNB1 (beta-catenin) mutation identifies low grade, early stage endometrial cancer patients at increased risk of recurrence." Mod Pathol.

Labied, S., T. Kajihara, P. A. Madureira, L. Fusi, M. C. Jones, J. M. Higham, R. Varshochi, J. M. Francis, G. Zoumpoulidou, A. Essafi, S. Fernandez de Mattos, E. W. Lam and J. J. Brosens (2006). "Progestins regulate the expression and activity of the forkhead transcription factor FOXO1 in differentiating human endometrium." Mol Endocrinol **20**(1): 35-44.

Lakha, F., P. C. Ho, Z. M. Van der Spuy, K. Dada, R. Elton, A. F. Glasier, H. O. Critchley, A. R. Williams and D. T. Baird (2007). "A novel estrogen-free oral contraceptive pill for women: multicentre, double-blind, randomized controlled trial of mifepristone and progestogen-only pill (levonorgestrel)." Hum Reprod **22**(9): 2428-2436.

Lammer, C., S. Wagerer, R. Saffrich, D. Mertens, W. Ansorge and I. Hoffmann (1998). "The cdc25B phosphatase is essential for the G2/M phase transition in human cells." J Cell Sci **111 (Pt 16)**: 2445-2453.

Lathe, R. and Y. Kotelevtsev (2014). "Steroid signaling: ligand-binding promiscuity, molecular symmetry, and the need for gating." Steroids **82**: 14-22.

Lee, K., J. Jeong, I. Kwak, C. T. Yu, B. Lanske, D. W. Soegiarto, R. Toftgard, M. J. Tsai, S. Tsai, J. P. Lydon and F. J. DeMayo (2006). "Indian hedgehog is a major mediator of progesterone signaling in the mouse uterus." Nat Genet **38**(10): 1204-1209.

Lee, K. Y., J. W. Jeong, J. Wang, L. Ma, J. F. Martin, S. Y. Tsai, J. P. Lydon and F. J. DeMayo (2007). "Bmp2 is critical for the murine uterine decidual response." Mol Cell Biol **27**(15): 5468-5478.

Lessey, B. A., A. P. Killam, D. A. Metzger, A. F. Haney, G. L. Greene and K. S. McCarty, Jr. (1988). "Immunohistochemical analysis of human uterine estrogen and progesterone receptors throughout the menstrual cycle." J Clin Endocrinol Metab **67**(2): 334-340.

Levens, E. D., C. Potlog-Nahari, A. Y. Armstrong, R. Wesley, A. Premkumar, D. L. Blithe, W. Blocker and L. K. Nieman (2008). "CDB-2914 for uterine leiomyomata treatment: a randomized controlled trial." Obstetrics & Gynecology **111**(5): 1129-1136.

Li, H. W., S. B. Liao, W. S. Yeung, E. H. Ng, W. S. O and P. C. Ho (2014). "Ulipristal acetate resembles mifepristone in modulating human fallopian tube function." Hum Reprod **29**(10): 2156-2162.

Li, Q., A. Kannan, F. J. DeMayo, J. P. Lydon, P. S. Cooke, H. Yamagishi, D. Srivastava, M. K. Bagchi and I. C. Bagchi (2011). "The antiproliferative action of progesterone in uterine epithelium is mediated by Hand2." Science **331**(6019): 912-916.

Li, Q., A. Kannan, W. Wang, F. J. Demayo, R. N. Taylor, M. K. Bagchi and I. C. Bagchi (2007). "Bone morphogenetic protein 2 functions via a conserved signaling pathway involving Wnt4 to regulate uterine decidualization in the mouse and the human." J Biol Chem **282**(43): 31725-31732.

Li, X., M. J. Large, C. J. Creighton, R. B. Lanz, J. W. Jeong, S. L. Young, B. A. Lessey, W. A. Palomino, S. Y. Tsai and F. J. Demayo (2013). "COUP-TFII regulates human endometrial stromal genes involved in inflammation." Mol Endocrinol **27**(12): 2041-2054.

Liban, T. J., M. J. Thwaites, F. A. Dick and S. M. Rubin (2016). "Structural Conservation and E2F Binding Specificity within the Retinoblastoma Pocket Protein Family." J Mol Biol **428**(20): 3960-3971.

Lin, T. T. (1984). "Progesterone receptor in the human uterine cervix." Acta Med Okayama **38**(1): 41-48.

Lira-Albarran, S., M. Durand, M. F. Larrea-Schiavon, L. Gonzalez, D. Barrera, C. Vega, A. Gamboa-Dominguez, C. Rangel and F. Larrea (2017). "Ulipristal acetate administration at mid-cycle changes gene expression profiling of endometrial biopsies taken during the receptive period of the human menstrual cycle." Mol Cell Endocrinol.

Liu, J. P., H. Yang, Y. Xia and F. Cardini (2013). "Herbal preparations for uterine fibroids." Cochrane Database Syst Rev **4**: CD005292.

Luo, X., P. Yin, J. S. Coon, Y. H. Cheng and S. E. Bulun (2010). "The Selective Progesterone Receptor Modulator CDB4124 Inhibits Proliferation and Induces Apoptosis in Uterine Leiomyoma Cells." Reproductive Sciences **17**(3): 271A-271A.

Luyckx, M., J. L. Squifflet, P. Jadoul, R. Votino, M. M. Dolmans and J. Donnez (2014). "First series of 18 pregnancies after ulipristal acetate treatment for uterine fibroids." Fertil Steril **102**(5): 1404-1409.

Madauss, K. P., E. T. Grygielko, S. J. Deng, A. C. Sulpizio, T. B. Stanley, C. Wu, S. A. Short, S. K. Thompson, E. L. Stewart, N. J. Laping, S. P. Williams and J. D. Bray (2007). "A structural and in vitro characterization of asoprisnil: a selective progesterone receptor modulator." Mol Endocrinol **21**(5): 1066-1081.

Maentausta, O., P. Svalander, K. G. Danielsson, M. Bygdeman and R. Vihko (1993). "The effects of an antiprogestin, mifepristone, and an antiestrogen, tamoxifen, on endometrial 17 beta-hydroxysteroid dehydrogenase and progestin and estrogen receptors during the luteal phase of the menstrual cycle: an immunohistochemical study." J Clin Endocrinol Metab **77**(4): 913-918.

Makker, A., M. M. Goel, D. Nigam, V. Bhatia, A. A. Mahdi, V. Das and A. Pandey (2017). "Endometrial Expression of Homeobox Genes and Cell Adhesion Molecules in Infertile Women With Intramural Fibroids During Window of Implantation." Reprod Sci **24**(3): 435-444.

Mangelsdorf, D. J., C. Thummel, M. Beato, P. Herrlich, G. Schutz, K. Umesono, B. Blumberg, P. Kastner, M. Mark, P. Chambon and R. M. Evans (1995). "The nuclear receptor superfamily: the second decade." Cell **83**(6): 835-839.

Marbaix, E., I. Kokorine, P. Moulin, J. Donnez, Y. Eeckhout and P. J. Courtoy (1996). "Menstrual breakdown of human endometrium can be mimicked in vitro and is selectively and reversibly blocked by inhibitors of matrix metalloproteinases." Proc Natl Acad Sci U S A **93**(17): 9120-9125.

Marjoribanks, J., A. Lethaby and C. Farquhar (2016). "Surgery versus medical therapy for heavy menstrual bleeding." Cochrane Database Syst Rev **1**: CD003855.

Markee, J. E. (1940). "Menstruation in intraocular transplants in the rhesus monkey." Contributions to Embryology **28**: 219-308.

Marshall, E., J. Lowrey, S. MacPherson, J. A. Maybin, F. Collins, H. O. Critchley and P. T. Saunders (2011). "In silico analysis identifies a novel role for androgens in the regulation of human endometrial apoptosis." J Clin Endocrinol Metab **96**(11): E1746-1755.

Martin, R. D. (2007). "The evolution of human reproduction: a primatological perspective." Am J Phys Anthropol **Suppl 45**: 59-84.

Maruo, T., N. Ohara, H. Matsuo, Q. Xu, W. Chen, R. Sitruk-Ware and E. D. B. Johansson (2007). "Effects of levonorgestrel-releasing IUS and progesterone receptor modulator PRM CDB-2914 on uterine leiomyomas." Contraception **75**(6): S99-S103.

Maybin, J. A., S. Battersby, N. Hirani, L. L. Nikitenko, H. O. Critchley and H. N. Jabbour (2011). "The expression and regulation of adrenomedullin in the human endometrium: a candidate for endometrial repair." Endocrinology **152**(7): 2845-2856.

Maybin, J. A., H. O. Critchley and H. N. Jabbour (2011). "Inflammatory pathways in endometrial disorders." Mol Cell Endocrinol **335**(1): 42-51.

Maybin, J. A. and H. O. D. Critchley (2015). "Menstrual physiology: implications for endometrial pathology and beyond." Human Reproduction Update.

Maybin, J. A., N. Hirani, P. Brown, H. N. Jabbour and H. O. Critchley (2011). "The Regulation of Vascular Endothelial Growth Factor by Hypoxia and Prostaglandin F2{alpha} during Human Endometrial Repair." J Clin Endocrinol Metab **96**(8): 2475-2483.

McDonald, S. E., T. A. Henderson, C. E. Gomez-Sanchez, H. O. Critchley and J. I. Mason (2006). "11Beta-hydroxysteroid dehydrogenases in human endometrium." Mol Cell Endocrinol **248**(1-2): 72-78.

McPhail, M. K. (1934). "The assay of progestin." J Physiol **83**(2): 145-156.

McPherson, K., I. Manyonda, M. A. Lumsden, A. M. Belli, J. Moss, O. Wu, L. Middleton and J. Daniels (2014). "A randomised trial of treating fibroids with either embolisation or myomectomy to measure the effect on quality of life among women wishing to avoid hysterectomy (the FEMME study): study protocol for a randomised controlled trial." Trials **15**: 468.

Meng, C. X., K. L. Andersson, U. Bentin-Ley, K. Gemzell-Danielsson and P. G. Lalitkumar (2009). "Effect of levonorgestrel and mifepristone on endometrial receptivity markers in a three-dimensional human endometrial cell culture model." Fertil Steril **91**(1): 256-264.

Merrill, R. M. (2008). "Hysterectomy survillance in the United States, 1997 through 2005." Med Sci Monit **14**(1): CR24-31.

Meseguer, M., J. D. Aplin, P. Caballero-Campo, J. E. O'Connor, J. C. Martin, J. Remohi, A. Pellicer and C. Simon (2001). "Human endometrial mucin MUC1 is up-regulated by progesterone and down-regulated in vitro by the human blastocyst." Biol Reprod **64**(2): 590-601.

Messinis, I. E., C. I. Messini and K. Dafopoulos (2014). "Novel aspects of the endocrinology of the menstrual cycle." Reprod Biomed Online **28**(6): 714-722.

Migliaccio, A., D. Piccolo, G. Castoria, M. Di Domenico, A. Bilancio, M. Lombardi, W. Gong, M. Beato and F. Auricchio (1998). "Activation of the Src/p21ras/Erk pathway by progesterone receptor via cross-talk with estrogen receptor." Embo j **17**(7): 2008-2018.

Millar, J. B., J. Blevitt, L. Gerace, K. Sadhu, C. Featherstone and P. Russell (1991). "p55CDC25 is a nuclear protein required for the initiation of mitosis in human cells." Proc Natl Acad Sci U S A **88**(23): 10500-10504.

Moradi, A., F. Ghasemi, K. Anvari, S. M. Hassanian, S. A. Simab, S. Ebrahimi, A. Hesari, M. M. Forghanifard, M. T. Boroushaki, S. ShahidSales and A. Avan (2017). "The Cross-Regulation Between SOX15 and Wnt Signaling Pathway." J Cell Physiol.

Moroni, R. M., W. P. Martins, R. A. Ferriani, C. S. Vieira, C. O. Nastri, F. J. Candido Dos Reis and L. G. Brito (2015). "Add-back therapy with GnRH analogues for uterine fibroids." Cochrane Database Syst Rev **3**: CD010854.

Moss, J. and A. Christie (2016). "Uterine artery embolization for heavy menstrual bleeding." Womens Health (Lond) **12**(1): 71-77.

Mote, P. A., R. L. Balleine, E. M. McGowan and C. L. Clarke (1999). "Colocalization of progesterone receptors A and B by dual immunofluorescent histochemistry in human endometrium during the menstrual cycle." J Clin Endocrinol Metab **84**(8): 2963-2971.

Mullen, R. D. and R. R. Behringer (2014). "Molecular genetics of Mullerian duct formation, regression and differentiation." Sex Dev **8**(5): 281-296.

Munro, M. G. (2012). "Classification of menstrual bleeding disorders." Rev Endocr Metab Disord **13**(4): 225-234.

Munro, M. G., H. O. Critchley and I. S. Fraser (2011). "The FIGO classification of causes of abnormal uterine bleeding: Malcolm G. Munro, Hilary O.D. Crithcley, Ian S. Fraser, for the FIGO Working Group on Menstrual Disorders." Int J Gynaecol Obstet **113**(1): 1-2.

Murad, K. (2016). "Spontaneous Pregnancy Following Ulipristal Acetate Treatment in a Woman with a Symptomatic Uterine Fibroid." J Obstet Gynaecol Can **38**(1): 75-79.

Murji, A., L. Whitaker, T. L. Chow and M. L. Sobel (2017). "Selective progesterone receptor modulators (SPRMs) for uterine fibroids." Cochrane Database Syst Rev **4**: Cd010770.

Murphy, A. A., L. M. Kettel, A. J. Morales, V. Roberts, T. Parmley and S. S. Yen (1995). "Endometrial effects of long-term low-dose administration of RU486." Fertil Steril **63**(4): 761-766.

Murray, A. A., A. R. Williams, M. Nicol, J. A. Maybin, P. T. K. Saunders and H. Critchley (2014). "Impact of Ulipristal Acetate (UPA) on Endometrial Steroid Receptors in Women with Uterine Fibroids." Reproductive Sciences **21**(3): 312A-313A.

Mutter, G. L., J. P. Baak, C. P. Crum, R. M. Richart, A. Ferenczy and W. C. Faquin (2000). "Endometrial precancer diagnosis by histopathology, clonal analysis, and computerized morphometry." J Pathol **190**(4): 462-469.

Mutter, G. L., C. Bergeron, L. Deligdisch, A. Ferenczy, M. Glant, M. Merino, A. R. Williams and D. L. Blithe (2008). "The spectrum of endometrial pathology induced by progesterone receptor modulators." Mod Pathol **21**(5): 591-598.

Mutter, G. L. and A. Ferenczy (2001). Anatomy and histology of the uterine -corpus. Blaustein's pathology of the female genital tract. R. J. Kurman. New York, Springer**:** 383-418.

Mutter, G. L., M. C. Lin, J. T. Fitzgerald, J. B. Kum, J. P. Baak, J. A. Lees, L. P. Weng and C. Eng (2000). "Altered PTEN expression as a diagnostic marker for the earliest endometrial precancers." J Natl Cancer Inst **92**(11): 924-930.

Mutter, G. L., M. C. Lin, J. T. Fitzgerald, J. B. Kum and C. Eng (2000). "Changes in endometrial PTEN expression throughout the human menstrual cycle." J Clin Endocrinol Metab **85**(6): 2334-2338.

Mutz, K. O., A. Heilkenbrinker, M. Lonne, J. G. Walter and F. Stahl (2013). "Transcriptome analysis using next-generation sequencing." Curr Opin Biotechnol **24**(1): 22-30.

Narvekar, N., S. Cameron, H. O. Critchley, S. Lin, L. Cheng and D. T. Baird (2004). "Low-dose mifepristone inhibits endometrial proliferation and up-regulates androgen receptor." J Clin Endocrinol Metab **89**(5): 2491-2497.

Narvekar, N., F. Lakha, H. O. Critchley, A. F. Glasier, A. R. Williams, R. Leminen, O. Heikinheimo, R. W. Kelly and D. T. Baird (2007). "Changes in vaginal morphology, steroid

receptor and natural antimicrobial content following treatment with low-dose mifepristone." Contraception **75**(4): 271-280.

NICE. (2007). "Clinical Guideline 44; Heavy menstrual bleeding ", from http://www.nice.org.uk/nicemedia/pdf/CG44FullGuideline.pdf.

NICE (2016). Addendum to Clinical Guideline 44, Heavy menstrual bleeding: assessment and management
Clinical Guideline Addendum 44.1, National Institute for Health and Care Excellence.

Nieman, L. K., W. Blocker, T. Nansel, S. Mahoney, J. Reynolds, D. Blithe, R. Wesley and A. Armstrong (2011). "Efficacy and tolerability of CDB-2914 treatment for symptomatic uterine fibroids: a randomized, double-blind, placebo-controlled, phase IIb study." Fertility & Sterility **95**(2): 767-772.e761-762.

Nikolaou, M., D. Koumoundourou, P. Ravazoula, M. Papadopoulou, G. Michail and G. Decavalas (2014). "An immunohistochemical analysis of sex-steroid receptors, tumor suppressor gene p53 and Ki-67 in the normal and neoplastic uterine cervix squamous epithelium." Med Pregl **67**(7-8): 202-207.

Nilsson, E. E., G. Larsen and M. K. Skinner (2014). "Roles of Gremlin 1 and Gremlin 2 in regulating ovarian primordial to primary follicle transition." Reproduction **147**(6): 865-874.

Noel, J. C., D. Bucella, I. Fayt, T. Simonart, F. Buxant, V. Anaf and P. Simon (2008). "Androgen receptor expression in cervical intraepithelial neoplasia and invasive squamous cell carcinoma of the cervix." Int J Gynecol Pathol **27**(3): 437-441.

Nordengren, J., R. Pilka, V. Noskova, A. Ehinger, H. Domanski, C. Andersson, G. Hoyer-Hansen, S. R. Hansson and B. Casslen (2004). "Differential localization and expression of urokinase plasminogen activator (uPA), its receptor (uPAR), and its inhibitor (PAI-1) mRNA and protein in endometrial tissue during the menstrual cycle." Mol Hum Reprod **10**(9): 655-663.

Novak, E. and H. S. Everett (1928). "Cyclical and other variations in the tubal epithelium." American Journal of Obstetrics & Gynecology **16**(4): 499-530.

Noyes, R. W., A. T. Hertig and J. Rock (1950). "Dating the endometrial biopsy." Fertil Steril **1**(1): 3-25.

Orbo, A., C. E. Rise and G. L. Mutter (2006). "Regression of latent endometrial precancers by progestin infiltrated intrauterine device." Cancer Res **66**(11): 5613-5617.

Pabona, J. M. P., F. A. Simmen, M. A. Nikiforov, D. Zhuang, K. Shankar, M. C. Velarde, Z. Zelenko, L. C. Giudice and R. C. M. Simmen (2012). "Krüppel-Like Factor 9 and Progesterone Receptor Coregulation of Decidualizing Endometrial Stromal Cells: Implications for the Pathogenesis of Endometriosis." The Journal of Clinical Endocrinology and Metabolism **97**(3): E376-E392.

Pan, J. L., D. Z. Yuan, Y. B. Zhao, L. Nie, Y. Lei, M. Liu, Y. Long, J. H. Zhang, L. J. Blok, C. W. Burger and L. M. Yue (2017). "Progesterone-induced miR-133a inhibits the proliferation of endometrial epithelial cells." Acta Physiol (Oxf) **219**(3): 683-692.

Patel, B., S. Elguero, S. Thakore, W. Dahoud, M. Bedaiwy and S. Mesiano (2015). "Role of nuclear progesterone receptor isoforms in uterine pathophysiology." Hum Reprod Update **21**(2): 155-173.

Pauerstein, C. J. and C. A. Eddy (1979). Morphology of the fallopian tube. The Biology of the Fluids of the Female Genital Tract. F. K. Beller and G. F. B. Chumacher. Amsterdam, Elsevier**:** 299–317.

Pawar, S., A. M. Hantak, I. C. Bagchi and M. K. Bagchi (2014). "Minireview: Steroid-regulated paracrine mechanisms controlling implantation." Mol Endocrinol **28**(9): 1408-1422.

Pennant, M. E., R. Mehta, P. Moody, G. Hackett, A. Prentice, S. J. Sharp and R. Lakshman (2017). "Premenopausal abnormal uterine bleeding and risk of endometrial cancer." BJOG: An International Journal of Obstetrics & Gynaecology **124**(3): 404-411.

Peters, M. G., S. Vanzulli, P. V. Elizalde, E. H. Charreau and M. M. Goin (2001). "Effects of antiprogestins RU486 and ZK98299 on the expression of cell cycle proteins of a medroxyprogesterone acetate (MPA)-induced murine mammary tumor." Oncol Rep **8**(2): 445-449.

Petit-Topin, I., M. Fay, M. Resche-Rigon, A. Ulmann, E. Gainer, M. E. Rafestin-Oblin and J. Fagart (2014). "Molecular determinants of the recognition of ulipristal acetate by oxo-steroid receptors." J Steroid Biochem Mol Biol **144 Pt B**: 427-435.

Pollow, K., J. Inthraphuvasak, B. Manz, H. J. Grill and B. Pollow (1981). "A comparison of cytoplasmic and nuclear estradiol and progesterone receptors in human fallopian tube and endometrial tissue." Fertil Steril **36**(5): 615-622.

Poole, A. J., Y. Li, Y. Kim, S. C. Lin, W. H. Lee and E. Y. Lee (2006). "Prevention of Brca1-mediated mammary tumorigenesis in mice by a progesterone antagonist." Science **314**(5804): 1467-1470.

Prasad, S., N. Varun, A. Kumar and S. Prasad (2013). Effect of low dose mifepristone on uterine leiomyoma in reproductive age group. ASRM, Fertility and Sterility.

Quinn, S. D., J. Vedelago, W. Gedroyc and L. Regan (2014). "Safety and five-year re-intervention following magnetic resonance-guided focused ultrasound (MRgFUS) for uterine fibroids." Eur J Obstet Gynecol Reprod Biol **182**: 247-251.

Rae, M., A. Mohamad, D. Price, P. W. Hadoke, B. R. Walker, J. I. Mason, S. G. Hillier and H. O. Critchley (2009). "Cortisol inactivation by 11beta-hydroxysteroid dehydrogenase-2 may enhance endometrial angiogenesis via reduced thrombospondin-1 in heavy menstruation." J Clin Endocrinol Metab **94**(4): 1443-1450.

Ray, S. and J. W. Pollard (2012). "KLF15 negatively regulates estrogen-induced epithelial cell proliferation by inhibition of DNA replication licensing." Proc Natl Acad Sci U S A **109**(21): E1334-1343.

RCOG (2012). National Heavy Menstrual Bleeding Audit Second Annual Report. London, RCOG.

RCOG (2014). National Heavy Menstrual Bleeding Audit Final Report. London, RCOG.

Reich, O. and H. Fritsch (2014). "The developmental origin of cervical and vaginal epithelium and their clinical consequences: a systematic review." J Low Genit Tract Dis **18**(4): 358-360.

Ren, J., N. Agata, D. Chen, Y. Li, W. H. Yu, L. Huang, D. Raina, W. Chen, S. Kharbanda and D. Kufe (2004). "Human MUC1 carcinoma-associated protein confers resistance to genotoxic anticancer agents." Cancer Cell **5**(2): 163-175.

Rimon-Dahari, N., L. Yerushalmi-Heinemann, L. Alyagor and N. Dekel (2016). "Ovarian Folliculogenesis." Results Probl Cell Differ **58**: 167-190.

Roberts, T. E., A. Tsourapas, L. J. Middleton, R. Champaneria, J. P. Daniels, K. G. Cooper, S. Bhattacharya and P. M. Barton (2011). "Hysterectomy, endometrial ablation, and levonorgestrel releasing intrauterine system (Mirena) for treatment of heavy menstrual bleeding: cost effectiveness analysis." BMJ **342**: d2202.

Rocereto, T. F., W. E. Brady, M. S. Shahin, J. S. Hoffman, L. Small, J. Rotmensch and R. S. Mannel (2010). "A phase II evaluation of mifepristone in the treatment of recurrent or persistent epithelial ovarian, fallopian or primary peritoneal cancer: a gynecologic oncology group study." Gynecol Oncol **116**(3): 332-334.

Sanchez, E. R. (2012). "Chaperoning Steroidal Physiology: Lessons from Mouse Genetic Models of Hsp90 and its Cochaperones." Biochimica et Biophysica Acta **1823**(3): 722-729.

Sanderson, P. A., H. O. Critchley, A. R. Williams, M. J. Arends and P. T. Saunders (2017). "New concepts for an old problem: the diagnosis of endometrial hyperplasia." Hum Reprod Update **23**(2): 232-254.

Sangkomkamhang, U. S., P. Lumbiganon, M. Laopaiboon and B. W. Mol (2013). "Progestogens or progestogen-releasing intrauterine systems for uterine fibroids." Cochrane Database Syst Rev **2**: CD008994.

Scarpin, K. M., J. D. Graham, P. A. Mote and C. L. Clarke (2009). "Progesterone action in human tissues: regulation by progesterone receptor (PR) isoform expression, nuclear positioning and coregulator expression." Nucl Recept Signal **7**: e009.

Schneider, C. C., R. K. Gibb, D. D. Taylor, T. Wan and C. Gercel-Taylor (1998). "Inhibition of endometrial cancer cell lines by mifepristone (RU 486)." J Soc Gynecol Investig **5**(6): 334-338.

Schubert, G., W. Elger, G. Kaufmann, B. Schneider, G. Reddersen and K. Chwalisz (2005). "Discovery, chemistry, and reproductive pharmacology of asoprisnil and related 11beta-benzaldoxime substituted selective progesterone receptor modulators (SPRMs)." Semin Reprod Med **23**(1): 58-73.

Schutt, B., A. Kaiser, M. H. Schultze-Mosgau, C. Seitz, D. Bell, M. Koch and B. Rohde (2016). "Pharmacodynamics and safety of the novel selective progesterone receptor modulator vilaprisan: a double-blind, randomized, placebo-controlled phase 1 trial in healthy women." Hum Reprod **31**(8): 1703-1712.

Segal, T. R., S. M. Zarek, S. L. Mumford, T. C. Plowden, L. K. Nieman, J. H. Segars and A. Y. Armstrong (2014). Radiographic and histopathologic endometrial characteristics of women undergoing treatment with Ulipristal acetate (UPA). ASRM, Fertility and Sterility. **102:** e286.

Shaffer, A. L., X. Yu, Y. He, J. Boldrick, E. P. Chan and L. M. Staudt (2000). "BCL-6 represses genes that function in lymphocyte differentiation, inflammation, and cell cycle control." Immunity **13**(2): 199-212.

Shapley, M., K. Jordan and P. R. Croft (2004). "An epidemiological survey of symptoms of menstrual loss in the community." Br J Gen Pract **54**(502): 359-363.

Shen, F., C. Yan, M. Liu, Y. Feng and Y. Chen (2015). "Decreased expression of mucin-1 in endometriosis endometrium correlated with progesterone receptor B involved in infertility." Arch Gynecol Obstet **291**(2): 439-445.

Shen, Q., Y. Hua, W. Jiang, W. Zhang, M. Chen and X. Zhu (2013). "Effects of mifepristone on uterine leiomyoma in premenopausal women: a meta-analysis." Fertil Steril **100**(6): 1722-1726.e1721-1710.

Sherman, M. R., P. L. Corvol and B. W. O'Malley (1970). "Progesterone-binding components of chick oviduct. I. Preliminary characterization of cytoplasmic components." J Biol Chem **245**(22): 6085-6096.

Shimizu, Y., T. Takeuchi, S. Mita, T. Notsu, K. Mizuguchi and S. Kyo (2010). "Kruppel-like factor 4 mediates anti-proliferative effects of progesterone with G(0)/G(1) arrest in human endometrial epithelial cells." J Endocrinol Invest **33**(10): 745-750.

Simmen, R. C., M. E. Heard, A. M. Simmen, M. T. Montales, M. Marji, S. Scanlon and J. M. Pabona (2015). "The Kruppel-like factors in female reproductive system pathologies." J Mol Endocrinol **54**(2): R89-R101.

Simpson, P., R. Lonsdale, A. R. W. Williams and E. P. Morris (2017). A Study of the Clinical Impact of a Three Month Pre-Operative Course of Ulipristal Acetate in Subjects with Known Pelvic Endometriosis. Society for Endometriosis and Uterine Disorders. Singapore.

Simpson, P., R. Lonsdale, A. R. W. Williams and E. P. Morris (2017). A Study of the Histopathological Changes within Ectopic Endometrial Tissue, in Subjects with Known Pelvic Endometriosis Following Treatment with Ulipristal Acetate. Society for Endometriosis and Uterine Disorders. Singapore.

Sinclair, D. C., A. Mastroyannis and H. S. Taylor (2011). "Leiomyoma simultaneously impair endometrial BMP-2-mediated decidualization and anticoagulant expression through secretion of TGF-beta3." J Clin Endocrinol Metab **96**(2): 412-421.

Singh, S., X. Ren, E. Groettrup-Wolfers, K. Petersdorf and C. Seitz (2017). Efficacy and safety of the new Progesterone Receptor Modulator vilaprisan – data from the phase 2 program. Society for Endometriosis and Uterine Disorders. Singapore.

Sivalingam, V. N., S. Kitson, R. McVey, C. Roberts, P. Pemberton, K. Gilmour, S. Ali, A. G. Renehan, H. C. Kitchener and E. J. Crosbie (2016). "Measuring the biological effect of presurgical metformin treatment in endometrial cancer." Br J Cancer **114**(3): 281-289.

Sivik, T. and A. Jansson (2012). "Progesterone and levonorgestrel regulate expression of 17betaHSD-enzymes in progesterone receptor positive breast cancer cell line T47D." Biochem Biophys Res Commun **422**(1): 109-113.

Skorupskaite, K., J. T. George and R. A. Anderson (2014). "The kisspeptin-GnRH pathway in human reproductive health and disease." Hum Reprod Update **20**(4): 485-500.

Slayden, O. D. and R. M. Brenner (1994). "RU 486 action after estrogen priming in the endometrium and oviducts of rhesus monkeys (Macaca mulatta)." J Clin Endocrinol Metab **78**(2): 440-448.

Slayden, O. D. and R. M. Brenner (2003). "Flutamide counteracts the antiproliferative effects of antiprogestins in the primate endometrium." J Clin Endocrinol Metab **88**(2): 946-949.

Slayden, O. D. and R. M. Brenner (2004). "Hormonal regulation and localization of estrogen, progestin and androgen receptors in the endometrium of nonhuman primates: effects of progesterone receptor antagonists." Arch Histol Cytol **67**(5): 393-409.

Slayden, O. D., J. J. Hirst and R. M. Brenner (1993). "Estrogen action in the reproductive tract of rhesus monkeys during antiprogestin treatment." Endocrinology **132**(4): 1845-1856.

Slayden, O. D., N. R. Nayak, K. A. Burton, K. Chwalisz, S. T. Cameron, H. O. Critchley, D. T. Baird and R. M. Brenner (2001). "Progesterone antagonists increase androgen receptor expression in the rhesus macaque and human endometrium." J Clin Endocrinol Metab **86**(6): 2668-2679.

Slayden, O. D., M. B. Zelinski-Wooten, K. Chwalisz, R. L. Stouffer and R. M. Brenner (1998). "Chronic treatment of cycling rhesus monkeys with low doses of the antiprogestin ZK 137 316: morphometric assessment of the uterus and oviduct." Hum Reprod **13**(2): 269-277.

Smith, C. L. and B. W. O'Malley (2004). "Coregulator function: a key to understanding tissue specificity of selective receptor modulators." Endocr Rev **25**(1): 45-71.

Smith, G. W. and R. Meidan (2014). "Ever-changing cell interactions during the life span of the corpus luteum: relevance to luteal regression." Reprod Biol **14**(2): 75-82.

Smith, K., R. Alnifaidy, Q. Wei and L. K. Nieman (2011). "Endometrial Indian hedgehog expression is decreased in women with endometriosis." Fertil Steril **95**(8): 2738-2741.e2731-2733.

Smyth, G. K. (2005). Limma: linear models for microarray data. Bioinformatics and Computational Biology Solutions using R and Bioconductor. R. Gentleman, V. Carey, S. Dudoit, R. Irizarry and W. Huber. New York, Springer**:** 397-420.

Snijders, M. P., A. F. de Goeij, M. J. Debets-Te Baerts, M. J. Rousch, J. Koudstaal and F. T. Bosman (1992). "Immunocytochemical analysis of oestrogen receptors and progesterone receptors in the human uterus throughout the menstrual cycle and after the menopause." J Reprod Fertil **94**(2): 363-371.

Spitz, I. M. (2003). "Progesterone antagonists and progesterone receptor modulators: An overview." Steroids **68**(10-13): 981-993.

Spitz, I. M. and K. Chwalisz (2000). "Progesterone receptor modulators and progesterone antagonists in women's health." Steroids **65**(10-11): 807-815.

Stewart, C. J. and M. L. Crook (2015). "PAX2 and cyclin D1 expression in the distinction between cervical microglandular hyperplasia and endometrial microglandular-like carcinoma: a comparison with p16, vimentin, and Ki67." Int J Gynecol Pathol **34**(1): 90-100.

Stewart, E. A., C. Cookson, R. A. Gandolfo and R. Schulze-Rath (2017). "Epidemiology of uterine fibroids: a systematic review." Bjog.

Stewart, E. A., S. K. Laughlin-Tommaso, W. H. Catherino, S. Lalitkumar, D. Gupta and B. Vollenhoven (2016). "Uterine fibroids." Nat Rev Dis Primers **2**: 16043.

Stewart, E. A. and R. A. Nowak (1996). "Leiomyoma-related bleeding: a classic hypothesis updated for the molecular era." Hum Reprod Update **2**(4): 295-306.

Stoeckemann, K., C. Hegele-Hartung and K. Chwalisz (1995). "Effects of the progesterone antagonists onapristone (ZK 98 299) and ZK 136 799 on surgically induced endometriosis in intact rats." Hum Reprod **10**(12): 3264-3271.

Strassmann, B. I. (1996). "The evolution of endometrial cycles and menstruation." Q Rev Biol **71**(2): 181-220.

Strowitzki, T., A. Germeyer, R. Popovici and M. von Wolff (2006). "The human endometrium as a fertility-determining factor." Hum Reprod Update **12**(5): 617-630.

Su, R. W., M. R. Strug, N. R. Joshi, J. W. Jeong, L. Miele, B. A. Lessey, S. L. Young and A. T. Fazleabas (2015). "Decreased Notch pathway signaling in the endometrium of women with endometriosis impairs decidualization." J Clin Endocrinol Metab **100**(3): E433-442.

Sudo, S., O. Avsian-Kretchmer, L. S. Wang and A. J. Hsueh (2004). "Protein related to DAN and cerberus is a bone morphogenetic protein antagonist that participates in ovarian paracrine regulation." J Biol Chem **279**(22): 23134-23141.

Sun, X., A. Christow, L. Marions and K. Gemzell-Danielsson (2003). "Progesterone receptor isoform B in the human fallopian tube and endometrium following mifepristone." Contraception **67**(4): 319-326.

Takamoto, N., B. Zhao, S. Y. Tsai and F. J. DeMayo (2002). "Identification of Indian hedgehog as a progesterone-responsive gene in the murine uterus." Mol Endocrinol **16**(10): 2338-2348.

Talbi, S., A. E. Hamilton, K. C. Vo, S. Tulac, M. T. Overgaard, C. Dosiou, N. Le Shay, C. N. Nezhat, R. Kempson, B. A. Lessey, N. R. Nayak and L. C. Giudice (2006). "Molecular

phenotyping of human endometrium distinguishes menstrual cycle phases and underlying biological processes in normo-ovulatory women." Endocrinology **147**(3): 1097-1121.

Tamm-Rosenstein, K., J. Simm, M. Suhorutshenko, A. Salumets and M. Metsis (2013). "Changes in the transcriptome of the human endometrial Ishikawa cancer cell line induced by estrogen, progesterone, tamoxifen, and mifepristone (RU486) as detected by RNA-sequencing." PLoS One **8**(7): e68907.

Tapia, A., C. Vilos, J. C. Marin, H. B. Croxatto and L. Devoto (2011). "Bioinformatic detection of E47, E2F1 and SREBP1 transcription factors as potential regulators of genes associated to acquisition of endometrial receptivity." Reprod Biol Endocrinol **9**: 14.

Tarantal, A. F., A. G. Hendrickx, S. A. Matlin, B. L. Lasley, Q. Q. Gu, C. A. Thomas, P. M. Vince and P. F. Van Look (1996). "Effects of two antiprogestins on early pregnancy in the long-tailed macaque (Macaca fascicularis)." Contraception **54**(2): 107-115.

Thiruchelvam, U., J. A. Maybin, G. M. Armstrong, E. Greaves, P. T. Saunders and H. O. Critchley (2016). "Cortisol regulates the paracrine action of macrophages by inducing vasoactive gene expression in endometrial cells." J Leukoc Biol **99**(6): 1165-1171.

Thomas, M. P. and B. V. Potter (2013). "The structural biology of oestrogen metabolism." J Steroid Biochem Mol Biol **137**: 27-49.

Trimble, C. L., M. Method, M. Leitao, K. Lu, O. Ioffe, M. Hampton, R. Higgins, R. Zaino and G. L. Mutter (2012). "Management of endometrial precancers." Obstet Gynecol **120**(5): 1160-1175.

Tsai, M. J. and B. W. O'Malley (1994). "Molecular mechanisms of action of steroid/thyroid receptor superfamily members." Annu Rev Biochem **63**: 451-486.

Tsubamoto, H., K. Sakata, R. Sakane, K. Inoue, H. Shibahara, H. Hao and S. Hirota (2016). "Gremlin 2 is Repressed in Invasive Endometrial Cancer and Inhibits Cell Growth In Vitro." Anticancer Res **36**(1): 199-203.

Ulmann, A. (2000). "The development of mifepristone: a pharmaceutical drama in three acts." J Am Med Womens Assoc (1972) **55**(3 Suppl): 117-120.

Ulmann, A. and L. Silvestre (1994). "RU486: the French experience." Hum Reprod **9 Suppl 1**: 126-130.

van der Kwast, T. H., H. B. Dommerholt, C. C. van Vroonhoven and S. Chadha (1994). "Androgen receptor expression in the cervix of androgen-treated female-to-male transsexuals: association with morphology and chain-specific keratin expression." Int J Gynecol Pathol **13**(2): 133-138.

Vanzulli, S., A. Efeyan, F. Benavides, L. A. Helguero, G. Peters, J. Shen, C. J. Conti, C. Lanari and A. Molinolo (2002). "p21, p27 and p53 in estrogen and antiprogestin-induced tumor regression of experimental mouse mammary ductal carcinomas." Carcinogenesis **23**(5): 749-758.

Vanzulli, S. I., R. Soldati, R. Meiss, L. Colombo, A. A. Molinolo and C. Lanari (2005). "Estrogen or antiprogestin treatment induces complete regression of pulmonary and axillary metastases in an experimental model of breast cancer progression." Carcinogenesis **26**(6): 1055-1063.

Vasquez, Y. M., E. C. Mazur, X. Li, R. Kommagani, L. Jiang, R. Chen, R. B. Lanz, E. Kovanci, W. E. Gibbons and F. J. DeMayo (2015). "FOXO1 is required for binding of PR on IRF4, novel transcriptional regulator of endometrial stromal decidualization." Mol Endocrinol **29**(3): 421-433.

Wagenfeld, A., W. Bone, W. Schwede, M. Fritsch, O. M. Fischer and C. Moeller (2013). "BAY 1002670: a novel, highly potent and selective progesterone receptor modulator for gynaecological therapies." Hum Reprod **28**(8): 2253-2264.

Wagenfeld, A., P. T. Saunders, L. Whitaker and H. O. Critchley (2016). "Selective progesterone receptor modulators (SPRMs): progesterone receptor action, mode of action on the endometrium and treatment options in gynecological therapies." Expert Opin Ther Targets.

Wang, H., H. O. Critchley, R. W. Kelly, D. Shen and D. T. Baird (1998). "Progesterone receptor subtype B is differentially regulated in human endometrial stroma." Mol Hum Reprod **4**(4): 407-412.

Wang, H. and S. K. Dey (2006). "Roadmap to embryo implantation: clues from mouse models." Nat Rev Genet **7**(3): 185-199.

Wegienka, G., D. D. Baird, T. Cooper, K. J. Woodcroft and S. Havstad (2013). "Cytokine patterns differ seasonally between women with and without uterine leiomyomata." Am J Reprod Immunol **70**(4): 327-335.

Wei, Q., E. D. Levens, L. Stefansson and L. K. Nieman (2010). "Indian Hedgehog and its targets in human endometrium: menstrual cycle expression and response to CDB-2914." J Clin Endocrinol Metab **95**(12): 5330-5337.

Wetendorf, M. and F. J. DeMayo (2012). "The progesterone receptor regulates implantation, decidualization, and glandular development via a complex paracrine signaling network." Mol Cell Endocrinol **357**(1-2): 108-118.

Whitaker, L. and H. O. Critchley (2016). "Abnormal uterine bleeding." Best Pract Res Clin Obstet Gynaecol **34**: 54-65.

Whitaker, L. H., A. A. Murray, R. Matthews, G. Shaw, A. R. Williams, P. T. Saunders and H. O. Critchley (2017). "Selective progesterone receptor modulator (SPRM) ulipristal acetate (UPA) and its effects on the human endometrium." Hum Reprod.

Whitaker, L. H., A. R. Williams and H. O. Critchley (2014). "Selective progesterone receptor modulators." Curr Opin Obstet Gynecol **26**(4): 237-242.

Wilkens, J., V. Male, P. Ghazal, T. Forster, D. A. Gibson, A. R. Williams, S. L. Brito-Mutunayagam, M. Craigon, P. Lourenco, I. T. Cameron, K. Chwalisz, A. Moffett and H. O. Critchley (2013). "Uterine NK cells regulate endometrial bleeding in women and are

suppressed by the progesterone receptor modulator asoprisnil." J Immunol **191**(5): 2226-2235.

Wilkens, J., A. R. Williams, K. Chwalisz, C. Han, I. T. Cameron and H. O. Critchley (2009). "Effect of asoprisnil on uterine proliferation markers and endometrial expression of the tumour suppressor gene, PTEN." Human Reproduction **24**(5): 1036-1044.

Williams, A. R., C. Bergeron, D. H. Barlow and A. Ferenczy (2012). "Endometrial morphology after treatment of uterine fibroids with the selective progesterone receptor modulator, ulipristal acetate." International Journal of Gynecological Pathology **31**(6): 556-569.

Williams, A. R., H. O. Critchley, J. Osei, S. Ingamells, I. T. Cameron, C. Han and K. Chwalisz (2007). "The effects of the selective progesterone receptor modulator asoprisnil on the morphology of uterine tissues after 3 months treatment in patients with symptomatic uterine leiomyomata." Human Reproduction **22**(6): 1696-1704.

Winkler, M., B. Kemp, I. Classen-Linke, D. C. Fischer, S. Zlatinsi, J. Neulen, H. M. Beier and W. Rath (2002). "Estrogen receptor alpha and progesterone receptor A and B concentration and localization in the lower uterine segment in term parturition." J Soc Gynecol Investig **9**(4): 226-232.

Wolf, J. P., J. G. Hsiu, T. L. Anderson, A. Ulmann, E. E. Baulieu and G. D. Hodgen (1989). "Noncompetitive antiestrogenic effect of RU 486 in blocking the estrogen-stimulated luteinizing hormone surge and the proliferative action of estradiol on endometrium in castrate monkeys." Fertil Steril **52**(6): 1055-1060.

Wu, Q., S. G. Tang and Z. M. Yuan (2015). "Gremlin 2 inhibits adipocyte differentiation through activation of Wnt/beta-catenin signaling." Mol Med Rep **12**(4): 5891-5896.

Wu, Y., E. Strawn, Z. Basir, Y. Wang, G. Halverson, P. Jailwala and S. W. Guo (2006). "Genomic alterations in ectopic and eutopic endometria of women with endometriosis." Gynecol Obstet Invest **62**(3): 148-159.

Xu, Q., S. Takekida, N. Ohara, W. Chen, R. Sitruk-Ware, E. D. Johansson and T. Maruo (2005). "Progesterone receptor modulator CDB-2914 down-regulates proliferative cell nuclear antigen and Bcl-2 protein expression and up-regulates caspase-3 and poly(adenosine 5'-diphosphate-ribose) polymerase expression in cultured human uterine leiomyoma cells." J Clin Endocrinol Metab **90**(2): 953-961.

Yamada, M., H. Masai and J. Bartek (2014). "Regulation and roles of Cdc7 kinase under replication stress." Cell Cycle **13**(12): 1859-1866.

Yang, H., Y. Zhou, B. Edelshain, F. Schatz, C. J. Lockwood and H. S. Taylor (2012). "FKBP4 is regulated by HOXA10 during decidualization and in endometriosis." Reproduction **143**(4): 531-538.

Yang, H. P., A. Meeker, R. Guido, M. J. Gunter, G. S. Huang, P. Luhn, L. d'Ambrosio, N. Wentzensen and M. E. Sherman (2015). "PTEN expression in benign human endometrial tissue and cancer in relation to endometrial cancer risk factors." Cancer Causes & Control **26**(12): 1729-1736.

Yellon, S. M., A. E. Dobyns, H. L. Beck, J. T. Kurtzman, R. E. Garfield and M. A. Kirby (2013). "Loss of progesterone receptor-mediated actions induce preterm cellular and structural remodeling of the cervix and premature birth." PLoS One **8**(12): e81340.

Yerushalmi, R., R. Woods, P. M. Ravdin, M. M. Hayes and K. A. Gelmon (2010). "Ki67 in breast cancer: prognostic and predictive potential." Lancet Oncol **11**(2): 174-183.

Yin, P., Z. Lin, S. Reierstad, J. Wu, H. Ishikawa, E. E. Marsh, J. Innes, Y. Cheng, K. Pearson, J. S. t. Coon, J. J. Kim, D. Chakravarti and S. E. Bulun (2010). "Transcription factor KLF11 integrates progesterone receptor signaling and proliferation in uterine leiomyoma cells." Cancer Res **70**(4): 1722-1730.

Yoshida, S., N. Ohara, Q. Xu, W. Chen, J. Wang, K. Nakabayashi, H. Sasaki, A. Morikawa and T. Maruo (2010). "Cell-type specific actions of progesterone receptor modulators in the regulation of uterine leiomyoma growth." Seminars in Reproductive Medicine **28**(3): 260-273.

Young, S. L. and B. A. Lessey (2010). "Progesterone function in human endometrium: clinical perspectives." Semin Reprod Med **28**(1): 5-16.

Yuan, J., W. Zhao, M. Yan, Q. Zhu, G. Qin, J. Qiu and J. Zhang (2015). "Ulipristal Acetate Antagonizes the Inhibitory Effect of Progesterone on Ciliary Beat Frequency and Upregulates Steroid Receptor Expression Levels in Human Fallopian Tubes." Reprod Sci.

Yun, B. S., S. J. Seong, D. H. Cha, J. Y. Kim, M. L. Kim, J. Y. Shim and J. E. Park (2015). "Changes in proliferating and apoptotic markers of leiomyoma following treatment with a selective progesterone receptor modulator or gonadotropin-releasing hormone agonist." Eur J Obstet Gynecol Reprod Biol **191**: 62-67.

Zhang, Y., W. Peng, J. Clarke and Z. Liu (2010). "Acupuncture for uterine fibroids." Cochrane Database Syst Rev(1): CD007221.

Zhao, S., W. P. Fung-Leung, A. Bittner, K. Ngo and X. Liu (2014). "Comparison of RNA-Seq and microarray in transcriptome profiling of activated T cells." PLoS One **9**(1): e78644.

Zhu, H. X., W. W. Zhang, Y. L. Zhuang and L. L. Huang (2009). "Mifepristone as an anti-implantation contraceptive drug: roles in regulation of uterine natural killer cells during implantation phase." Am J Reprod Immunol **61**(1): 68-74.

Zuniga, E., M. Rippen, C. Alexander, T. F. Schilling and J. G. Crump (2011). "Gremlin 2 regulates distinct roles of BMP and Endothelin 1 signaling in dorsoventral patterning of the facial skeleton." Development **138**(23): 5147-5156.

Appendices

Supplementary Table 1. Up-regulated transcripts following UPA Administration (FC >1.3, p <0.01)

Symbol	Description	logFC	FC	P.Value	adj.P.Val
SLC13A5	solute carrier family 13 member 5	2.781	6.874	5.69E-07	0.006861
RNF39	ring finger protein 39	2.687	6.441	5.44E-06	0.01555
MUC1	mucin 1, cell surface associated	1.643	3.122	5.50E-06	0.01555
MUC1	mucin 1, cell surface associated	1.895	3.72	5.81E-06	0.01555
EGLN3	egl-9 family hypoxia-inducible factor 3	2.51	5.695	8.03E-06	0.01759
MUC1	mucin 1, cell surface associated	2.538	5.807	1.26E-05	0.01992
ABCC3	ATP binding cassette subfamily C member 3	1.861	3.632	1.66E-05	0.02351
SOX9	SRY-box 9	3.148	8.862	3.46E-05	0.03879
HAMP	hepcidin antimicrobial peptide	1.922	3.789	5.81E-05	0.04632
TNFSF10	tumor necrosis factor superfamily member 10	1.298	2.459	7.66E-05	0.04632
LRRN2	leucine rich repeat neuronal 2	1.804	3.492	7.86E-05	0.04632
WDR72	WD repeat domain 72	1.208	2.31	8.23E-05	0.04632
SORL1	sortilin-related receptor, L(DLR class) A repeats containing	2.359	5.13	8.51E-05	0.04632
ABTB1	ankyrin repeat and BTB domain containing 1	1.127	2.183	8.57E-05	0.04632
SPINT1	serine peptidase inhibitor, Kunitz type 1	1.179	2.264	8.84E-05	0.04632
GIMAP5	GTPase, IMAP family member 5	1.192	2.285	9.77E-05	0.04902
CD86	CD86 molecule	1.218	2.326	0.0001082	0.05014
STMN2	stathmin 2	3.225	9.351	0.0001137	0.05167
ABLIM1	actin binding LIM protein 1	1.113	2.163	0.0001187	0.05202
METRNL	meteorin, glial cell differentiation regulator-like	1.056	2.08	0.0001242	0.05345
NA	NA	1.394	2.628	0.0001333	0.05432
DHRS3	dehydrogenase/reductase (SDR family) member 3	1.251	2.38	0.0001375	0.05432
ALPPL2	alkaline phosphatase, placental like 2	4.778	27.43	0.0001444	0.05614
BCL11A	B-cell CLL/lymphoma 11A	1.198	2.295	0.0001617	0.05905
NA	NA	3.973	15.7	0.0001687	0.06068
LMCD1	LIM and cysteine rich domains 1	1.499	2.826	0.0001787	0.06081
PCDH9	protocadherin 9	1.639	3.115	0.0001815	0.06081
PDGFB	platelet derived growth factor subunit B	1.016	2.022	0.0001845	0.06081
MYCN	v-myc avian myelocytomatosis viral oncogene neuroblastoma derived homolog	3.003	8.014	0.0001962	0.06195
ZSCAN31	zinc finger and SCAN domain containing 31	0.922	1.895	0.0002016	0.06224
SCNN1G	sodium channel epithelial 1 gamma subunit	1.353	2.555	0.0002092	0.06224
HPGD	hydroxyprostaglandin dehydrogenase 15-(NAD)	2.636	6.217	0.0002144	0.06224
CD68	CD68 molecule	1.815	3.519	0.0002151	0.06224
TNFRSF6B	tumor necrosis factor receptor superfamily member 6b	2.304	4.939	0.0002172	0.06224
RGS10	regulator of G-protein signaling 10	1.392	2.625	0.000228	0.06224
BCL2L15	BCL2 like 15	1.462	2.755	0.0002349	0.06224
LTC4S	leukotriene C4 synthase	1.509	2.846	0.0002353	0.06224
CFH	complement factor H	1.278	2.425	0.0002363	0.06224
TNIP1	TNFAIP3 interacting protein 1	0.9893	1.985	0.000248	0.06224
TNFRSF6B	tumor necrosis factor receptor superfamily member 6b	2.098	4.281	0.000251	0.06224
STMN2	stathmin 2	2.031	4.087	0.0002517	0.06224
TMEM108	transmembrane protein 108	1.886	3.696	0.0002552	0.06224
ELMO1	engulfment and cell motility 1	1.498	2.824	0.0002625	0.06262
DPP4	dipeptidyl peptidase 4	2.664	6.337	0.0002712	0.06307

BCL11A	B-cell CLL/lymphoma 11A	1.198	2.294	0.0002795	0.06307
VAV3	vav guanine nucleotide exchange factor 3	1.92	3.784	0.0002908	0.06309
FMOD	fibromodulin	0.8828	1.844	0.0002964	0.06309
SORL1	sortilin-related receptor, L(DLR class) A repeats containing	2.358	5.126	0.0003111	0.06464
FCGBP	Fc fragment of IgG binding protein	2.213	4.636	0.0003232	0.06656
CISH	cytokine inducible SH2-containing protein	1.139	2.202	0.0003506	0.07159
SCNN1G	sodium channel epithelial 1 gamma subunit	1.31	2.479	0.000371	0.07328
PLS1	plastin 1	1.049	2.069	0.0003833	0.07394
TMEM139	transmembrane protein 139	1.122	2.177	0.0003959	0.07394
NA	NA	3.112	8.645	0.0004019	0.07394
ZSCAN31	zinc finger and SCAN domain containing 31	0.9546	1.938	0.0004045	0.07394
NA	NA	1.339	2.531	0.0004056	0.07394
BHLHE41	basic helix-loop-helix family member e41	1.656	3.152	0.0004113	0.07394
C22orf24	chromosome 22 open reading frame 24	1.24	2.363	0.000417	0.07394
EVA1A	eva-1 homolog A, regulator of programmed cell death	0.8855	1.847	0.0004265	0.07394
CDKN2C	cyclin-dependent kinase inhibitor 2C	0.8917	1.855	0.000442	0.07525
ENTPD3	ectonucleoside triphosphate diphosphohydrolase 3	1.215	2.321	0.0004466	0.07525
MB21D2	Mab-21 domain containing 2	1.209	2.311	0.0004521	0.07565
SLC7A7	solute carrier family 7 member 7	1.159	2.234	0.0004601	0.07575
LPL	lipoprotein lipase	1.305	2.471	0.0004604	0.07575
CFH	complement factor H	1.323	2.503	0.0004668	0.07575
ABLIM1	actin binding LIM protein 1	1.24	2.363	0.0004721	0.07575
ADGRG5	adhesion G protein-coupled receptor G5	1.139	2.203	0.0004747	0.07575
C1QB	complement component 1, q subcomponent, B chain	0.8236	1.77	0.0004843	0.07621
TGFA	transforming growth factor alpha	1.451	2.734	0.0004878	0.07621
ARHGAP31	Rho GTPase activating protein 31	1.126	2.183	0.0005031	0.07621
GREM1	gremlin 1, DAN family BMP antagonist	2.516	5.721	0.000504	0.07621
EPHA1	EPH receptor A1	0.7881	1.727	0.0005154	0.07621
NA	NA	1.326	2.508	0.0005187	0.07621
UPK1B	uroplakin 1B	1.971	3.919	0.0005237	0.07648
PROSER2	proline and serine rich 2	1.303	2.468	0.0005401	0.07766
IER3	immediate early response 3	1.331	2.516	0.0005766	0.07961
KIAA0040	KIAA0040	1.003	2.005	0.0005798	0.07961
NA	NA	1.097	2.14	0.0005871	0.07961
APBB1IP	amyloid beta precursor protein binding family B member 1 interacting protein	0.9872	1.982	0.000611	0.07961
AHNAK	AHNAK nucleoprotein	0.7176	1.644	0.0006144	0.07961
KRT18	keratin 18	1.009	2.013	0.0006237	0.07961
CFH	complement factor H	1.314	2.487	0.0006265	0.07961
VAV3	vav guanine nucleotide exchange factor 3	2.137	4.398	0.000628	0.07961
MAP3K3	mitogen-activated protein kinase kinase kinase 3	1.061	2.086	0.0006282	0.07961
ALAS2	5'-aminolevulinate synthase 2	1.337	2.527	0.0006426	0.07961
NA	NA	1.184	2.273	0.0006447	0.07961
FCER1G	Fc fragment of IgE receptor Ig	1.124	2.18	0.000647	0.07961
SLC34A2	solute carrier family 34 member 2	1.688	3.222	0.0006475	0.07961
NA	NA	1.178	2.262	0.0006526	0.07961
CX3CR1	chemokine (C-X3-C motif) receptor 1	1.972	3.923	0.0006528	0.07961
NA	NA	0.785	1.723	0.0006574	0.07961
NA	NA	1.189	2.279	0.0007015	0.08274
SPINT1	serine peptidase inhibitor, Kunitz type 1	1.802	3.488	0.0007039	0.08274
ACY3	aminoacylase 3	2.018	4.05	0.0007126	0.08336

KBTBD11	kelch repeat and BTB domain containing 11	0.896	1.861	0.0007685	0.08694
SGK223	homolog of rat pragma of Rnd2	1.211	2.315	0.0007817	0.08773
NA	NA	1.296	2.456	0.0007905	0.08818
SLC9A1	solute carrier family 9 member A1	0.905	1.873	0.0008037	0.08891
CEBPA	CCAAT/enhancer binding protein alpha	1.567	2.963	0.0008043	0.08891
SPECC1	sperm antigen with calponin homology and coiled-coil domains 1	1.382	2.606	0.000831	0.09091
FOXC1	forkhead box C1	1.228	2.342	0.0008402	0.09091
MGAT3	mannosyl (beta-1,4-)-glycoprotein beta-1,4-N-acetylglucosaminyltransferase	1.299	2.461	0.0008413	0.09091
ERBB3	erb-b2 receptor tyrosine kinase 3	0.8359	1.785	0.0008649	0.09263
TLR7	toll like receptor 7	1.69	3.227	0.0008743	0.09264
SGF29	SAGA complex associated factor 29	0.8769	1.836	0.0008766	0.09264
TMPRSS3	transmembrane protease, serine 3	1.331	2.516	0.0008811	0.09272
NPRL3	NPR3-like, GATOR1 complex subunit	1.029	2.041	0.0008867	0.0929
STOX2	storkhead box 2	1.113	2.163	0.0009121	0.09379
VWA1	von Willebrand factor A domain containing 1	0.9984	1.998	0.0009146	0.09379
NA	NA	0.9545	1.938	0.0009186	0.0938
RUNX3	runt related transcription factor 3	1.358	2.564	0.0009324	0.0948
DHRS9	dehydrogenase/reductase (SDR family) member 9	1.087	2.124	0.000955	0.09511
C3AR1	complement component 3a receptor 1	1.148	2.216	0.0009898	0.09788
APOL3	apolipoprotein L3	0.7362	1.666	0.001026	0.1001
TOX3	TOX high mobility group box family member 3	2.316	4.98	0.001031	0.1002
MS4A7	membrane spanning 4-domains A7	0.9763	1.967	0.001037	0.1004
RNF150	ring finger protein 150	0.945	1.925	0.001046	0.1007
ABI3	ABI family member 3	1.191	2.282	0.001048	0.1007
GPR37	G protein-coupled receptor 37 (endothelin receptor type B-like)	1.486	2.801	0.001053	0.1007
SLC39A4	solute carrier family 39 member 4	0.6904	1.614	0.001064	0.1013
TBXAS1	thromboxane A synthase 1	1.025	2.036	0.001076	0.1021
NCF4	neutrophil cytosolic factor 4	1.173	2.255	0.001118	0.1048
PROSER2	proline and serine rich 2	1.758	3.381	0.001136	0.1055
UBD	ubiquitin D	2.336	5.048	0.001142	0.1055
SLC7A5	solute carrier family 7 member 5	1.432	2.699	0.001153	0.1061
NA	NA	1.04	2.056	0.001175	0.1063
NA	NA	0.9909	1.987	0.001178	0.1063
ANXA8L1	annexin A8-like 1	1.003	2.004	0.001194	0.1063
NA	NA	1.412	2.661	0.001197	0.1063
BTK	Bruton tyrosine kinase	1.564	2.958	0.001203	0.1063
CYBB	cytochrome b-245, beta polypeptide	1.276	2.422	0.001206	0.1063
NA	NA	1.488	2.806	0.001207	0.1063
ATP8B1	ATPase phospholipid transporting 8B1	1.616	3.066	0.001209	0.1063
SPI1	Spi-1 proto-oncogene	1.66	3.161	0.001212	0.1063
ABCG1	ATP binding cassette subfamily G member 1	1.508	2.844	0.001212	0.1063
RGS10	regulator of G-protein signaling 10	0.9213	1.894	0.001213	0.1063
NA	NA	1.085	2.121	0.001251	0.1073
NA	NA	1.221	2.33	0.001253	0.1073
LINC00452	long intergenic non-protein coding RNA 452	0.7319	1.661	0.001254	0.1073
THRA	thyroid hormone receptor, alpha	0.9966	1.995	0.001256	0.1073
USP25	ubiquitin specific peptidase 25	1.271	2.413	0.001265	0.1077
NA	NA	3.277	9.692	0.001273	0.108
NA	NA	1.654	3.147	0.001322	0.1111
SLC19A2	solute carrier family 19 member 2	0.8329	1.781	0.001329	0.1112

MARCO	macrophage receptor with collagenous structure	1.373	2.59	0.001333	0.1112
PROM1	prominin 1	1.38	2.602	0.00134	0.1114
SHOX2	short stature homeobox 2	1.566	2.962	0.001374	0.113
TNFRSF6B	tumor necrosis factor receptor superfamily member 6b	2.529	5.771	0.001401	0.113
NA	NA	1.005	2.007	0.001408	0.113
TNFRSF11B	tumor necrosis factor receptor superfamily member 11b	1.719	3.293	0.00141	0.113
DGCR11	DiGeorge syndrome critical region gene 11 (non-protein coding)	0.6954	1.619	0.001418	0.113
NA	NA	1.019	2.026	0.00142	0.113
GREM1	gremlin 1, DAN family BMP antagonist	2.65	6.278	0.001433	0.113
GPR183	G protein-coupled receptor 183	1.424	2.683	0.001451	0.113
MVP	major vault protein	0.8102	1.753	0.001456	0.113
LYPD6B	LY6/PLAUR domain containing 6B	1.758	3.383	0.001464	0.113
EVA1A	eva-1 homolog A, regulator of programmed cell death	0.8713	1.829	0.001465	0.113
ENTPD3	ectonucleoside triphosphate diphosphohydrolase 3	0.9926	1.99	0.001476	0.113
ATP1A1	ATPase Na+/K+ transporting subunit alpha 1	0.9172	1.888	0.001495	0.1136
LAMA3	laminin subunit alpha 3	1.182	2.268	0.001501	0.1136
KCNQ1	potassium voltage-gated channel subfamily Q member 1	1.015	2.021	0.001502	0.1136
CD160	CD160 molecule	1.285	2.436	0.001517	0.1136
LILRB4	leukocyte immunoglobulin like receptor B4	0.8568	1.811	0.001524	0.1136
KIZ	kizuna centrosomal protein	1.71	3.271	0.001535	0.1136
NA	NA	1.208	2.31	0.001536	0.1136
SPI1	Spi-1 proto-oncogene	1.441	2.714	0.001541	0.1136
ATP6V1B1	ATPase H+ transporting V1 subunit B1	1.582	2.994	0.001553	0.1136
CFH	complement factor H	1.55	2.928	0.00156	0.1136
ACVR2A	activin A receptor type 2A	0.7089	1.635	0.001593	0.1153
NA	NA	0.7671	1.702	0.001626	0.1163
NA	NA	0.6245	1.542	0.001627	0.1163
IFI30	interferon, gamma-inducible protein 30	0.9888	1.984	0.001631	0.1163
STARD10	StAR related lipid transfer domain containing 10	0.9202	1.892	0.001689	0.1174
TM7SF2	transmembrane 7 superfamily member 2	0.7031	1.628	0.001728	0.1174
SLAMF8	SLAM family member 8	1.207	2.308	0.001733	0.1174
NA	NA	1.315	2.488	0.001738	0.1174
KIT	KIT proto-oncogene receptor tyrosine kinase	0.743	1.674	0.001742	0.1174
METTL7B	methyltransferase like 7B	1.56	2.949	0.001749	0.1174
NA	NA	0.632	1.55	0.001762	0.1174
ARNT2	aryl hydrocarbon receptor nuclear translocator 2	0.7639	1.698	0.001783	0.1174
RBMS3	RNA binding motif, single stranded interacting protein 3	1.5	2.828	0.001784	0.1174
SIK2	salt inducible kinase 2	1.093	2.133	0.001805	0.1176
CD37	CD37 molecule	1.939	3.834	0.001812	0.1176
ABHD12	abhydrolase domain containing 12	0.7744	1.71	0.001816	0.1176
NA	NA	1.575	2.979	0.001867	0.1176
ABTB1	ankyrin repeat and BTB domain containing 1	0.734	1.663	0.001869	0.1176
RNASE4	ribonuclease A family member 4	0.6636	1.584	0.001876	0.1176
CD48	CD48 molecule	1.295	2.454	0.001893	0.1176
RHOF	ras homolog family member F (in filopodia)	1.07	2.1	0.001893	0.1176
SLC15A3	solute carrier family 15 member 3	0.7039	1.629	0.00191	0.1176

ALDH2	aldehyde dehydrogenase 2 family (mitochondrial)	0.796	1.736	0.001911	0.1176
AIF1	allograft inflammatory factor 1	0.9575	1.942	0.001916	0.1176
ARRDC1	arrestin domain containing 1	0.7442	1.675	0.001923	0.1176
SORCS2	sortilin related VPS10 domain containing receptor 2	1.993	3.982	0.001953	0.1182
JPH2	junctophilin 2	0.9371	1.915	0.001973	0.1182
FHIT	fragile histidine triad	1.17	2.25	0.001979	0.1182
SNX22	sorting nexin 22	0.6791	1.601	0.001985	0.1182
SFTA2	surfactant associated 2	1.297	2.457	0.002006	0.1182
HIPK2	homeodomain interacting protein kinase 2	0.9156	1.886	0.002022	0.1182
TYMP	thymidine phosphorylase	1.097	2.139	0.00203	0.1182
PLS1	plastin 1	0.8281	1.775	0.002034	0.1182
NRTN	neurturin	1.136	2.197	0.00205	0.1182
PRKD2	protein kinase D2	1.038	2.053	0.002055	0.1182
HAVCR2	hepatitis A virus cellular receptor 2	0.7539	1.686	0.002057	0.1182
NUAK2	NUAK family kinase 2	1.21	2.313	0.002058	0.1182
ANXA3	annexin A3	0.9444	1.924	0.002076	0.1182
NA	NA	0.6243	1.542	0.00208	0.1182
PPP1R13B	protein phosphatase 1 regulatory subunit 13B	0.584	1.499	0.002093	0.1182
IGF2BP2	insulin like growth factor 2 mRNA binding protein 2	0.7524	1.685	0.002095	0.1182
ABCG1	ATP binding cassette subfamily G member 1	1.032	2.045	0.002099	0.1182
CXCR3	chemokine (C-X-C motif) receptor 3	0.7691	1.704	0.002099	0.1182
NA	NA	1.013	2.018	0.00211	0.1185
GPRC5C	G protein-coupled receptor class C group 5 member C	1.102	2.147	0.002142	0.1189
CD68	CD68 molecule	0.7095	1.635	0.002147	0.1189
C1QC	complement component 1, q subcomponent, C chain	0.6496	1.569	0.002163	0.1189
TLR10	toll like receptor 10	0.7984	1.739	0.002167	0.1189
BEND5	BEN domain containing 5	0.8845	1.846	0.00217	0.1189
NA	NA	0.9816	1.975	0.002181	0.1189
NA	NA	0.6945	1.618	0.002191	0.1189
RNF39	ring finger protein 39	1.553	2.934	0.0022	0.1189
NA	NA	0.774	1.71	0.002224	0.119
C1orf162	chromosome 1 open reading frame 162	0.7064	1.632	0.002225	0.119
KLRF1	killer cell lectin like receptor F1	0.8163	1.761	0.002229	0.119
VASP	vasodilator-stimulated phosphoprotein	0.6774	1.599	0.002267	0.1195
KIT	KIT proto-oncogene receptor tyrosine kinase	0.702	1.627	0.002285	0.1198
RELN	reelin	2.299	4.921	0.002289	0.1198
MPPED2	metallophosphoesterase domain containing 2	1.129	2.186	0.002299	0.1198
NA	NA	0.9932	1.991	0.002302	0.1198
SLC2A12	solute carrier family 2 member 12	1.592	3.015	0.002303	0.1198
TRH	thyrotropin releasing hormone	2.919	7.561	0.002327	0.1204
CEBPD	CCAAT/enhancer binding protein delta	0.7986	1.739	0.002336	0.1204
CLUL1	clusterin like 1	1.348	2.545	0.002355	0.1205
PPP3CA	protein phosphatase 3 catalytic subunit alpha	1.06	2.085	0.002377	0.1208
ARG2	arginase 2	0.8437	1.795	0.002387	0.1208
SETD3	SET domain containing 3	0.8872	1.85	0.002433	0.1227
CCDC184	coiled-coil domain containing 184	1.131	2.19	0.00245	0.1232
AIF1	allograft inflammatory factor 1	0.9197	1.892	0.002464	0.1237
APOC1	apolipoprotein C-I	1.058	2.082	0.002482	0.1243
GPC4	glypican 4	1.018	2.026	0.002492	0.1243

CD33	CD33 molecule	1.145	2.211	0.002539	0.1248
FOS	FBJ murine osteosarcoma viral oncogene homolog	0.9808	1.974	0.002541	0.1248
TMPRSS3	transmembrane protease, serine 3	1.415	2.666	0.002547	0.1248
CD9	CD9 molecule	0.981	1.974	0.002561	0.1248
NA	NA	0.8763	1.836	0.002563	0.1248
HOXB5	homeobox B5	0.7398	1.67	0.002588	0.125
NA	NA	0.7799	1.717	0.002589	0.125
LAMP2	lysosomal associated membrane protein 2	1.096	2.138	0.002622	0.1254
SCRN1	secernin 1	0.6246	1.542	0.002627	0.1254
ROBO2	roundabout guidance receptor 2	2.014	4.038	0.002642	0.1254
SLC1A3	solute carrier family 1 member 3	1.584	2.998	0.002644	0.1254
FBLN1	fibulin 1	1.17	2.25	0.002713	0.1268
ZNF543	zinc finger protein 543	0.6165	1.533	0.002721	0.1268
PILRA	paired immunoglobin-like type 2 receptor alpha	1.685	3.215	0.002773	0.1277
CD1C	CD1c molecule	0.9087	1.877	0.002773	0.1277
RNF10	ring finger protein 10	0.742	1.673	0.002792	0.1277
ZNF540	zinc finger protein 540	1.511	2.851	0.002799	0.1277
CELSR2	cadherin EGF LAG seven-pass G-type receptor 2	0.9197	1.892	0.002801	0.1277
APOC2	apolipoprotein C-II	1.387	2.616	0.002839	0.1277
TTLL3	tubulin tyrosine ligase like 3	0.8753	1.834	0.002839	0.1277
HMGCS2	3-hydroxy-3-methylglutaryl-CoA synthase 2	4.07	16.8	0.00284	0.1277
FAM109A	family with sequence similarity 109 member A	0.6014	1.517	0.002855	0.1277
CD82	CD82 molecule	0.876	1.835	0.002859	0.1277
RBM47	RNA binding motif protein 47	0.7843	1.722	0.002875	0.1277
LAMTOR3	late endosomal/lysosomal adaptor, MAPK and MTOR activator 3	0.8845	1.846	0.002879	0.1277
MYCN	v-myc avian myelocytomatosis viral oncogene neuroblastoma derived homolog	2.178	4.525	0.002883	0.1277
RNASE2	ribonuclease A family member 2	1.556	2.94	0.002883	0.1277
OGDHL	oxoglutarate dehydrogenase-like	1.498	2.824	0.002901	0.128
NA	NA	1.312	2.482	0.002927	0.1287
FAM83F	family with sequence similarity 83 member F	0.7871	1.726	0.002928	0.1287
NA	NA	1.262	2.399	0.002966	0.1298
NA	NA	0.6561	1.576	0.002991	0.1298
FAM21A	family with sequence similarity 21 member A	1.119	2.172	0.002996	0.1298
GIMAP1	GTPase, IMAP family member 1	1.3	2.462	0.003012	0.1298
CD74	CD74 molecule	1.403	2.644	0.003013	0.1298
TMPRSS3	transmembrane protease, serine 3	1.22	2.33	0.00303	0.1298
HLA-DRB6	major histocompatibility complex, class II, DR beta 6 (pseudogene)	0.9642	1.951	0.003033	0.1298
RNLS	renalase, FAD-dependent amine oxidase	0.8675	1.824	0.003063	0.1298
MTUS1	microtubule associated tumor suppressor 1	0.7746	1.711	0.003078	0.1298
C1orf64	chromosome 1 open reading frame 64	2.447	5.453	0.003084	0.1298
LAIR2	leukocyte associated immunoglobulin like receptor 2	1.032	2.045	0.003088	0.1298
COL9A1	collagen type IX alpha 1	3.023	8.131	0.003095	0.1298
LY86	lymphocyte antigen 86	1.066	2.094	0.003103	0.1298
RASSF5	Ras association domain family member 5	0.6709	1.592	0.003138	0.1298
KRT7	keratin 7	1.607	3.047	0.003143	0.1298
RELB	v-rel avian reticuloendotheliosis viral oncogene homolog B	1.077	2.11	0.003143	0.1298

ACSF2	acyl-CoA synthetase family member 2	0.6423	1.561	0.003146	0.1298
SPHK1	sphingosine kinase 1	1.408	2.654	0.003151	0.1298
CDH3	cadherin 3	1.585	2.999	0.003175	0.1302
NA	NA	1.374	2.591	0.003182	0.1302
COL9A1	collagen type IX alpha 1	2.031	4.087	0.003187	0.1302
MMP9	matrix metallopeptidase 9	1.992	3.978	0.003188	0.1302
DPP7	dipeptidyl peptidase 7	0.7785	1.715	0.003195	0.1303
NA	NA	0.9924	1.989	0.003262	0.1315
SH3TC1	SH3 domain and tetratricopeptide repeats 1	0.956	1.94	0.00328	0.1315
CD163	CD163 molecule	0.7405	1.671	0.003295	0.1315
SUPT3H	SPT3 homolog, SAGA and STAGA complex component	0.7974	1.738	0.003309	0.1315
FGFRL1	fibroblast growth factor receptor-like 1	0.9466	1.927	0.003315	0.1315
SMPDL3A	sphingomyelin phosphodiesterase acid like 3A	1.34	2.531	0.003316	0.1315
LYZ	lysozyme	1.246	2.372	0.003349	0.1316
SP110	SP110 nuclear body protein	1.268	2.409	0.003368	0.1322
NA	NA	1.459	2.75	0.003384	0.1322
PRKCB	protein kinase C beta	1.32	2.497	0.003391	0.1322
LGALS8	lectin, galactoside-binding, soluble, 8	0.7031	1.628	0.003411	0.1323
FAM26F	family with sequence similarity 26 member F	1.136	2.197	0.003416	0.1323
LAMA3	laminin subunit alpha 3	1.129	2.186	0.00342	0.1323
WTIP	Wilms tumor 1 interacting protein	0.7678	1.703	0.003442	0.1327
NA	NA	0.8859	1.848	0.003497	0.1343
NA	NA	0.7454	1.676	0.003509	0.1343
NA	NA	0.8637	1.82	0.003515	0.1343
INPP5D	inositol polyphosphate-5-phosphatase D	0.9707	1.96	0.003517	0.1343
NA	NA	1.265	2.404	0.003518	0.1343
NOTCH2	notch 2	0.945	1.925	0.00357	0.1354
SEMA3F	semaphorin 3F	0.7713	1.707	0.003607	0.1354
NA	NA	1.013	2.018	0.003608	0.1354
HLA-DPB1	major histocompatibility complex, class II, DP beta 1	1.095	2.136	0.003609	0.1354
NXNL2	nucleoredoxin-like 2	1.383	2.608	0.003613	0.1354
NCF1C	neutrophil cytosolic factor 1C pseudogene	1.358	2.564	0.003614	0.1354
SLC28A2	solute carrier family 28 member 2	0.968	1.956	0.003616	0.1354
SLC45A3	solute carrier family 45 member 3	1.343	2.537	0.003617	0.1354
DHX8	DEAH-box helicase 8	0.555	1.469	0.003618	0.1354
ERBB3	erb-b2 receptor tyrosine kinase 3	0.7574	1.69	0.003636	0.1355
NA	NA	1.175	2.258	0.00364	0.1355
PLCG2	phospholipase C gamma 2	0.9817	1.975	0.003661	0.1359
RASSF9	Ras association domain family member 9	1.276	2.422	0.003666	0.1359
RCAN2	regulator of calcineurin 2	1.954	3.874	0.003694	0.1365
NUAK2	NUAK family kinase 2	1.228	2.342	0.003712	0.1368
TYMP	thymidine phosphorylase	1.171	2.251	0.003728	0.1371
SUSD6	sushi domain containing 6	0.663	1.583	0.003734	0.1372
PKP4	plakophilin 4	0.6689	1.59	0.003788	0.1379
PTP4A1	protein tyrosine phosphatase type IVA, member 1	0.8728	1.831	0.003792	0.1379
GBP1P1	guanylate binding protein 1 pseudogene 1	1.188	2.279	0.003814	0.1382
TNFRSF10C	tumor necrosis factor receptor superfamily member 10c	0.9577	1.942	0.003829	0.1384
CD14	CD14 molecule	1.048	2.068	0.0039	0.1399
GIMAP8	GTPase, IMAP family member 8	0.9323	1.908	0.003901	0.1399
TMEM176A	transmembrane protein 176A	0.9104	1.88	0.003906	0.1399

CX3CL1	C-X3-C motif chemokine ligand 1	1.297	2.457	0.003936	0.1401
DACH1	dachshund family transcription factor 1	0.8528	1.806	0.003936	0.1401
LGMN	legumain	0.6629	1.583	0.00396	0.1401
SOX11	SRY-box 11	1.158	2.232	0.003992	0.1407
FAM129B	family with sequence similarity 129 member B	0.8493	1.802	0.003996	0.1407
PPL	periplakin	1.498	2.825	0.004074	0.1425
SCNN1A	sodium channel epithelial 1 alpha subunit	0.7246	1.652	0.004096	0.1429
CXCL10	C-X-C motif chemokine ligand 10	1.504	2.836	0.00411	0.1431
ABLIM1	actin binding LIM protein 1	1.434	2.702	0.004122	0.1433
HLA-DRB4	major histocompatibility complex, class II, DR beta 4	1.303	2.468	0.004131	0.1433
ANKRD40	ankyrin repeat domain 40	0.5403	1.454	0.004138	0.1433
PLP1	proteolipid protein 1	0.9681	1.956	0.004153	0.1435
SLC40A1	solute carrier family 40 member 1	0.8954	1.86	0.00418	0.1435
PHC2	polyhomeotic homolog 2	0.6496	1.569	0.004192	0.1435
PRR5-ARHGAP8	PRR5-ARHGAP8 readthrough	1.002	2.002	0.004204	0.1435
CXCL9	C-X-C motif chemokine ligand 9	1.92	3.783	0.004249	0.1435
SLC27A6	solute carrier family 27 member 6	1.177	2.261	0.004261	0.1435
NA	NA	1.184	2.272	0.004263	0.1435
ARHGAP25	Rho GTPase activating protein 25	0.9182	1.89	0.004278	0.1435
HIST2H2BE	histone cluster 2, H2be	0.7469	1.678	0.004278	0.1435
FRZB	frizzled-related protein	1.164	2.24	0.004279	0.1435
WWC3	WWC family member 3	0.6425	1.561	0.004282	0.1435
KCTD6	potassium channel tetramerization domain containing 6	0.5015	1.416	0.004318	0.1441
BIK	BCL2-interacting killer	1.999	3.997	0.00433	0.1443
OPTN	optineurin	0.7782	1.715	0.004335	0.1443
MAPK8IP2	mitogen-activated protein kinase 8 interacting protein 2	0.8934	1.858	0.004361	0.1445
PTP4A1	protein tyrosine phosphatase type IVA, member 1	0.7483	1.68	0.004384	0.1446
FBLN1	fibulin 1	1.667	3.176	0.004387	0.1446
ADORA3	adenosine A3 receptor	1.412	2.662	0.004406	0.145
SKAP1	src kinase associated phosphoprotein 1	0.9839	1.978	0.004417	0.1452
NA	NA	1.075	2.107	0.004441	0.1458
B3GALT4	Beta-1,3-galactosyltransferase 4	0.9531	1.936	0.004457	0.1459
NA	NA	0.9771	1.968	0.00446	0.1459
HCK	HCK proto-oncogene, Src family tyrosine kinase	1.128	2.185	0.004468	0.1459
BAHD1	bromo adjacent homology domain containing 1	1.504	2.836	0.004477	0.146
P2RY8	purinergic receptor P2Y8	0.9666	1.954	0.004519	0.1465
NA	NA	1.364	2.574	0.004522	0.1465
LPAR5	lysophosphatidic acid receptor 5	1.593	3.016	0.004537	0.1468
TREM2	triggering receptor expressed on myeloid cells 2	1.097	2.139	0.004563	0.147
HERC5	HECT and RLD domain containing E3 ubiquitin protein ligase 5	0.8158	1.76	0.004589	0.1473
AVPR2	arginine vasopressin receptor 2	0.5359	1.45	0.004663	0.1474
NCKAP1L	NCK associated protein 1 like	1.215	2.322	0.004665	0.1474
SOD3	superoxide dismutase 3, extracellular	1.952	3.869	0.004668	0.1474
NA	NA	0.9588	1.944	0.004688	0.1477
SASH3	SAM and SH3 domain containing 3	0.7889	1.728	0.004699	0.1478
SLC40A1	solute carrier family 40 member 1	1.141	2.205	0.004713	0.1478
TAPBP	TAP binding protein (tapasin)	0.7925	1.732	0.004732	0.1478

BMP4	bone morphogenetic protein 4	0.64	1.558	0.004732	0.1478
EPN3	epsin 3	1.403	2.644	0.004742	0.1478
STK26	serine/threonine protein kinase 26	0.5967	1.512	0.004745	0.1478
NA	NA	0.6573	1.577	0.004765	0.1478
KAZN	kazrin, periplakin interacting protein	1.063	2.089	0.004789	0.1478
NECTIN2	nectin cell adhesion molecule 2	0.5588	1.473	0.004813	0.1479
MEGF8	multiple EGF like domains 8	0.7623	1.696	0.004828	0.1481
OSGIN1	oxidative stress induced growth inhibitor 1	1.037	2.052	0.004859	0.1481
TYROBP	TYRO protein tyrosine kinase binding protein	0.9236	1.897	0.004876	0.1481
PPID	peptidylprolyl isomerase D	1.258	2.392	0.004879	0.1481
PTPRO	protein tyrosine phosphatase, receptor type O	0.9793	1.972	0.004934	0.1488
GAPT	GRB2-binding adaptor protein, transmembrane	1.243	2.367	0.004941	0.1488
FOSL2	FOS like antigen 2	0.7217	1.649	0.004972	0.1495
NA	NA	0.6325	1.55	0.004977	0.1495
ABHD12	abhydrolase domain containing 12	0.6351	1.553	0.005028	0.1507
NA	NA	0.7831	1.721	0.005036	0.1507
SERTM1	serine rich and transmembrane domain containing 1	1.155	2.227	0.005074	0.1513
MATN3	matrilin 3	1.025	2.035	0.005074	0.1513
NA	NA	0.669	1.59	0.005117	0.1518
TPP1	tripeptidyl peptidase I	0.577	1.492	0.005125	0.1518
EVA1A	eva-1 homolog A, regulator of programmed cell death	0.87	1.828	0.005129	0.1518
NA	NA	0.7428	1.673	0.005161	0.1521
BEX2	brain expressed X-linked 2	0.7707	1.706	0.005176	0.1521
NA	NA	0.9313	1.907	0.005187	0.1521
FCN1	ficolin 1	1.432	2.697	0.005188	0.1521
IL25	interleukin 25	0.6597	1.58	0.005193	0.1521
CX3CR1	chemokine (C-X3-C motif) receptor 1	1.254	2.386	0.00521	0.1522
LEMD1	LEM domain containing 1	1.743	3.347	0.005224	0.1523
PSTPIP2	proline-serine-threonine phosphatase interacting protein 2	0.8123	1.756	0.005228	0.1523
PLEK	pleckstrin	0.9363	1.914	0.005237	0.1524
CASP7	caspase 7	1.102	2.146	0.005253	0.1526
LAPTM5	lysosomal protein transmembrane 5	0.9563	1.94	0.005303	0.1536
CITED4	Cbp/p300 interacting transactivator with Glu/Asp rich carboxy-terminal domain 4	0.9804	1.973	0.005345	0.1544
ZSWIM3	zinc finger SWIM-type containing 3	0.6035	1.519	0.005388	0.1555
NA	NA	1.079	2.113	0.005396	0.1555
CD37	CD37 molecule	1.682	3.209	0.005438	0.1561
PURA	purine-rich element binding protein A	0.6099	1.526	0.005442	0.1561
NINJ2	ninjurin 2	0.8424	1.793	0.005462	0.1565
SNTB1	syntrophin beta 1	0.7259	1.654	0.005472	0.1566
Sep-01	septin 1	0.6558	1.576	0.005497	0.1571
FCHO2	FCH domain only 2	0.7156	1.642	0.005523	0.1574
SYNGR1	synaptogyrin 1	1	2	0.005549	0.1577
NA	NA	0.7158	1.642	0.00556	0.1578
RTP4	receptor (chemosensory) transporter protein 4	0.6798	1.602	0.005573	0.1579
FCGR2B	Fc fragment of IgG receptor IIb	0.8681	1.825	0.0056	0.158
CD1E	CD1e molecule	0.9902	1.986	0.00561	0.158
TPBG	trophoblast glycoprotein	0.7555	1.688	0.005615	0.158
CALY	calcyon neuron specific vesicular protein	1.067	2.096	0.005623	0.158
INSIG1	insulin induced gene 1	0.6844	1.607	0.005626	0.158

ARHGAP30	Rho GTPase activating protein 30	0.6094	1.526	0.005632	0.158
TESC	tescalcin	1.046	2.065	0.005646	0.1581
BBC3	BCL2 binding component 3	0.6759	1.598	0.005649	0.1581
CD86	CD86 molecule	0.6192	1.536	0.005659	0.1582
KIAA0922	KIAA0922	0.525	1.439	0.005666	0.1582
MS4A6A	membrane spanning 4-domains A6A	0.638	1.556	0.005671	0.1582
HLA-DPA1	major histocompatibility complex, class II, DP alpha 1	1.057	2.081	0.005682	0.1583
NLRC3	NLR family, CARD domain containing 3	0.6622	1.582	0.005691	0.1583
DHCR7	7-dehydrocholesterol reductase	0.6111	1.527	0.005701	0.1583
ATP1A1	ATPase Na+/K+ transporting subunit alpha 1	0.9113	1.881	0.00571	0.1583
GNAI1	G protein subunit alpha i1	1.076	2.108	0.005715	0.1583
NA	NA	0.8065	1.749	0.005725	0.1584
RPS6KA3	ribosomal protein S6 kinase A3	0.7042	1.629	0.005744	0.1586
IL32	interleukin 32	0.9596	1.945	0.005747	0.1586
Mar-02	membrane associated ring-CH-type finger 2	0.5516	1.466	0.005757	0.1586
DUSP16	dual specificity phosphatase 16	0.5973	1.513	0.005783	0.1589
FOLR1	folate receptor 1 (adult)	2.066	4.188	0.00579	0.1589
PRR5	proline rich 5	0.6321	1.55	0.005791	0.1589
RAMP3	receptor (G protein-coupled) activity modifying protein 3	1.429	2.693	0.005836	0.1598
NA	NA	0.6705	1.592	0.005846	0.1598
ETNK2	ethanolamine kinase 2	0.8736	1.832	0.005853	0.1598
CYP51A1	cytochrome P450 family 51 subfamily A member 1	0.8016	1.743	0.005862	0.1598
OSBPL3	oxysterol binding protein like 3	0.7595	1.693	0.005883	0.16
NA	NA	0.6282	1.546	0.005899	0.1601
CRCP	CGRP receptor component	0.7279	1.656	0.005919	0.1603
GPR183	G protein-coupled receptor 183	1.259	2.394	0.005951	0.1603
TNF	tumor necrosis factor	1.094	2.135	0.005952	0.1603
NR3C2	nuclear receptor subfamily 3 group C member 2	1.103	2.149	0.005963	0.1603
RNF19B	ring finger protein 19B	0.8014	1.743	0.005992	0.1603
NA	NA	1.002	2.002	0.006	0.1603
NA	NA	2.184	4.546	0.006001	0.1603
RYR1	ryanodine receptor 1	0.8836	1.845	0.006015	0.1603
NA	NA	0.8506	1.803	0.006056	0.1607
NA	NA	1.002	2.003	0.006072	0.1607
SMOX	spermine oxidase	0.5011	1.415	0.006072	0.1607
TACSTD2	tumor-associated calcium signal transducer 2	0.8627	1.818	0.00613	0.1615
GPRC5C	G protein-coupled receptor class C group 5 member C	1.136	2.197	0.006145	0.1615
ERLIN2	ER lipid raft associated 2	0.6246	1.542	0.006174	0.1619
CD276	CD276 molecule	0.963	1.949	0.006194	0.162
TOP1P1	topoisomerase (DNA) I pseudogene 1	1.043	2.061	0.006198	0.162
PANX2	pannexin 2	0.8306	1.778	0.006244	0.1627
NELL1	neural EGFL like 1	4.057	16.65	0.0063	0.1638
ANXA11	annexin A11	0.7059	1.631	0.006326	0.1643
NA	NA	0.7838	1.722	0.006373	0.1651
EVI2A	ecotropic viral integration site 2A	0.9154	1.886	0.006378	0.1651
NA	NA	0.6043	1.52	0.006393	0.1651
ST8SIA4	ST8 alpha-N-acetylneuraminate alpha-2,8-sialyltransferase 4	1.367	2.579	0.006394	0.1651
KCTD1	potassium channel tetramerization domain containing 1	1.109	2.157	0.006437	0.1654
ARFGEF3	ARFGEF family member 3	1.323	2.501	0.006469	0.1654

RHPN2	rhophilin, Rho GTPase binding protein 2	0.719	1.646	0.006474	0.1654
NA	NA	1.287	2.44	0.006509	0.1655
ITGAM	integrin subunit alpha M	1.437	2.707	0.006536	0.1655
NA	NA	1.132	2.192	0.006536	0.1655
ELOVL7	ELOVL fatty acid elongase 7	0.8629	1.819	0.00657	0.1657
GAPT	GRB2-binding adaptor protein, transmembrane	0.8588	1.814	0.006581	0.1657
STK38L	serine/threonine kinase 38 like	0.6749	1.596	0.006604	0.1657
OR9A4	olfactory receptor family 9 subfamily A member 4	0.6581	1.578	0.006615	0.1657
EGR1	early growth response 1	0.8533	1.807	0.006616	0.1657
GADD45A	growth arrest and DNA damage inducible alpha	0.7826	1.72	0.006624	0.1657
GIMAP6	GTPase, IMAP family member 6	0.6881	1.611	0.006643	0.1657
KDM7A	lysine demethylase 7A	0.8711	1.829	0.006653	0.1657
NA	NA	0.8383	1.788	0.00667	0.1657
RBM47	RNA binding motif protein 47	0.8003	1.741	0.006678	0.1657
NA	NA	0.8947	1.859	0.006687	0.1657
NA	NA	0.7084	1.634	0.00669	0.1657
TMPRSS4	transmembrane protease, serine 4	0.8114	1.755	0.006707	0.1658
GABARAPL2	GABA(A) receptor-associated protein like 2	0.6088	1.525	0.006718	0.1659
SLC3A2	solute carrier family 3 member 2	0.5659	1.48	0.006731	0.1659
NA	NA	1.93	3.811	0.006732	0.1659
HYDIN	HYDIN, axonemal central pair apparatus protein	0.7732	1.709	0.006841	0.1675
BAIAP2	BAI1 associated protein 2	0.7542	1.687	0.006854	0.1675
PXN	paxillin	0.61	1.526	0.006861	0.1675
ADGRL2	adhesion G protein-coupled receptor L2	0.6675	1.588	0.006895	0.1676
LRP5	LDL receptor related protein 5	1.094	2.134	0.006908	0.1676
KIAA1522	KIAA1522	0.6426	1.561	0.00696	0.1683
CCL14	C-C motif chemokine ligand 14	1.523	2.873	0.006987	0.1683
LST1	leukocyte specific transcript 1	1.29	2.446	0.006994	0.1683
NA	NA	0.8064	1.749	0.007006	0.1683
ZBTB7A	zinc finger and BTB domain containing 7A	0.7212	1.649	0.007021	0.1685
SLCO2B1	solute carrier organic anion transporter family member 2B1	0.8762	1.836	0.007038	0.1686
B4GALT4	UDP-Gal:betaGlcNAc beta 1,4-galactosyltransferase, polypeptide 4	0.6306	1.548	0.007073	0.1688
NA	NA	1.267	2.407	0.007076	0.1688
FAXDC2	fatty acid hydroxylase domain containing 2	0.9597	1.945	0.007108	0.1688
RAI2	retinoic acid induced 2	0.987	1.982	0.007143	0.1688
CCL2	C-C motif chemokine ligand 2	1.2	2.298	0.007154	0.1688
RARB	retinoic acid receptor beta	1.242	2.365	0.00718	0.1688
FAM134A	family with sequence similarity 134 member A	0.6986	1.623	0.007187	0.1688
MAN2B1	mannosidase alpha class 2B member 1	0.6676	1.588	0.007191	0.1688
CD3D	CD3d molecule	1.121	2.175	0.007208	0.1688
NA	NA	0.9685	1.957	0.007208	0.1688
PCIF1	PDX1 C-terminal inhibiting factor 1	0.6655	1.586	0.007227	0.1688
RPL23AP32	ribosomal protein L23a pseudogene 32	0.5495	1.464	0.007242	0.1688
TSC22D4	TSC22 domain family member 4	1.138	2.201	0.007275	0.1688
FPR3	formyl peptide receptor 3	0.9664	1.954	0.007279	0.1688
NA	NA	0.557	1.471	0.007285	0.1688
DMRTA1	DMRT like family A1	0.5433	1.457	0.007294	0.1688
BCAM	basal cell adhesion molecule (Lutheran blood group)	1.039	2.055	0.007296	0.1688
TBC1D17	TBC1 domain family member 17	0.9786	1.971	0.007309	0.1688

NA	NA	0.8761	1.835	0.007329	0.1688
NA	NA	0.8082	1.751	0.007345	0.1688
KLRB1	killer cell lectin like receptor B1	0.7827	1.72	0.007346	0.1688
PATZ1	POZ/BTB and AT hook containing zinc finger 1	1.129	2.188	0.007347	0.1688
NA	NA	1.045	2.064	0.007351	0.1688
SERPINA1	serpin peptidase inhibitor, clade A (alpha-1 antiproteinase, antitrypsin), member 1	1.151	2.22	0.007353	0.1688
NA	NA	0.679	1.601	0.007358	0.1688
KLK10	kallikrein related peptidase 10	1.434	2.702	0.007388	0.1691
TNFSF13B	tumor necrosis factor superfamily member 13b	1.3	2.462	0.007394	0.1691
NA	NA	0.8583	1.813	0.007421	0.1692
CPAMD8	C3 and PZP like, alpha-2-macroglobulin domain containing 8	1.304	2.468	0.007422	0.1692
FUOM	fucose mutarotase	0.7906	1.73	0.007438	0.1692
LRBA	LPS responsive beige-like anchor protein	0.5477	1.462	0.007465	0.1694
NA	NA	0.9464	1.927	0.007492	0.1696
DPP10	dipeptidyl peptidase like 10	0.9001	1.866	0.007507	0.1696
CLIC6	chloride intracellular channel 6	1.885	3.693	0.007509	0.1696
NA	NA	1.144	2.21	0.007611	0.1707
LOC401052	uncharacterized LOC401052	0.6352	1.553	0.007614	0.1707
IGSF11	immunoglobulin superfamily member 11	0.9277	1.902	0.007618	0.1707
H1F0	H1 histone family member 0	0.5188	1.433	0.00767	0.1713
CCL3L3	C-C motif chemokine ligand 3 like 3	1.179	2.265	0.007695	0.1714
MICALL1	MICAL like 1	0.6245	1.542	0.007703	0.1714
ZNF33B	zinc finger protein 33B	1.061	2.086	0.007706	0.1714
LAMC2	laminin subunit gamma 2	1.233	2.351	0.007733	0.1717
SEMA3B	semaphorin 3B	0.6669	1.588	0.007745	0.1717
NA	NA	2.983	7.905	0.007754	0.1717
MIR657	microRNA 657	0.8715	1.83	0.007786	0.1718
CPTP	ceramide-1-phosphate transfer protein	0.6274	1.545	0.007838	0.1725
STAT3	signal transducer and activator of transcription 3 (acute-phase response factor)	0.5022	1.416	0.007839	0.1725
L3MBTL4	l(3)mbt-like 4 (Drosophila)	0.4496	1.366	0.007845	0.1725
BCAR3	breast cancer anti-estrogen resistance 3	0.8226	1.769	0.007862	0.1727
FAM46A	family with sequence similarity 46 member A	1.097	2.14	0.007878	0.1727
GAB2	GRB2 associated binding protein 2	0.5015	1.416	0.007882	0.1727
SHB	Src homology 2 domain containing adaptor protein B	0.6111	1.527	0.007939	0.1727
CCL15	C-C motif chemokine ligand 15	1.219	2.328	0.00795	0.1727
FCGR2A	Fc fragment of IgG receptor IIa	1.061	2.087	0.007951	0.1727
CPEB3	cytoplasmic polyadenylation element binding protein 3	0.8233	1.769	0.007953	0.1727
DIS3L2	DIS3 like 3'-5' exoribonuclease 2	1.122	2.177	0.008008	0.1731
SEMA3E	semaphorin 3E	1.57	2.969	0.008033	0.1731
NA	NA	0.8587	1.813	0.008033	0.1731
NA	NA	1.823	3.537	0.008034	0.1731
S1PR4	sphingosine-1-phosphate receptor 4	0.9547	1.938	0.008067	0.1731
MAFF	v-maf avian musculoaponeurotic fibrosarcoma oncogene homolog F	1.131	2.191	0.008087	0.1732
CD53	CD53 molecule	0.9508	1.933	0.008097	0.1732
MBNL3	muscleblind like splicing regulator 3	0.7191	1.646	0.008125	0.1732
RCAN1	regulator of calcineurin 1	0.6945	1.618	0.008128	0.1732

CMTM7	CKLF like MARVEL transmembrane domain containing 7	0.8919	1.856	0.008175	0.1737
COL26A1	collagen type XXVI alpha 1	1.08	2.114	0.008198	0.1737
GPR65	G protein-coupled receptor 65	0.9245	1.898	0.008214	0.1737
NA	NA	0.746	1.677	0.008233	0.1737
ARAP1	ArfGAP with RhoGAP domain, ankyrin repeat and PH domain 1	1.054	2.076	0.00824	0.1737
GBE1	glucan (1,4-alpha-), branching enzyme 1	1.053	2.075	0.008241	0.1737
NA	NA	0.658	1.578	0.008256	0.1738
CDKN2B	cyclin-dependent kinase inhibitor 2B	0.99	1.986	0.008263	0.1738
DUSP5	dual specificity phosphatase 5	0.6656	1.586	0.008264	0.1738
NA	NA	0.7359	1.665	0.008325	0.1744
CTF1	cardiotrophin 1	1.204	2.304	0.008329	0.1744
PLAUR	plasminogen activator, urokinase receptor	0.9034	1.87	0.008435	0.175
FURIN	furin, paired basic amino acid cleaving enzyme	0.9635	1.95	0.008444	0.175
CPVL	carboxypeptidase, vitellogenic like	0.8386	1.788	0.008454	0.175
ATP1A1	ATPase Na+/K+ transporting subunit alpha 1	0.6887	1.612	0.008511	0.1759
MAP2K3	mitogen-activated protein kinase kinase 3	0.8401	1.79	0.008549	0.1759
CALN1	calneuron 1	0.5786	1.493	0.008583	0.1759
LRP10	LDL receptor related protein 10	0.5315	1.445	0.00859	0.1759
MAGED4B	melanoma antigen family D4B	0.4584	1.374	0.00865	0.1764
CKMT1A	creatine kinase, mitochondrial 1A	0.8286	1.776	0.008667	0.1765
FCGR2A	Fc fragment of IgG receptor IIa	1.211	2.316	0.008702	0.1765
CORO1B	coronin 1B	0.7197	1.647	0.008704	0.1765
NA	NA	0.6231	1.54	0.008708	0.1765
NA	NA	0.4917	1.406	0.008716	0.1765
DOCK2	dedicator of cytokinesis 2	0.7797	1.717	0.008729	0.1766
NA	NA	0.5671	1.482	0.008742	0.1766
BST2	bone marrow stromal cell antigen 2	0.5737	1.488	0.008764	0.1766
P2RY6	pyrimidinergic receptor P2Y6	0.9395	1.918	0.008778	0.1766
ACSF2	acyl-CoA synthetase family member 2	0.9026	1.869	0.008779	0.1766
NA	NA	0.8846	1.846	0.008781	0.1766
SLC1A5	solute carrier family 1 member 5	1.024	2.034	0.00879	0.1766
MGLL	monoglyceride lipase	0.8846	1.846	0.00879	0.1766
ATG3	autophagy related 3	0.6636	1.584	0.008819	0.1766
DOCK8	dedicator of cytokinesis 8	1.053	2.075	0.008835	0.1767
NA	NA	1.219	2.327	0.008838	0.1767
CMKLR1	chemerin chemokine-like receptor 1	0.4598	1.375	0.008858	0.177
WWC1	WW and C2 domain containing 1	0.5631	1.477	0.0089	0.1774
Mar-01	membrane associated ring-CH-type finger 1	1.142	2.207	0.008908	0.1774
GBP2	guanylate binding protein 2	0.8141	1.758	0.008984	0.1782
MAX	MYC associated factor X	0.9206	1.893	0.009002	0.1782
NA	NA	1.348	2.546	0.00904	0.1782
RTF1	RTF1 homolog, Paf1/RNA polymerase II complex component	0.7127	1.639	0.009043	0.1782
DOCK3	dedicator of cytokinesis 3	0.9776	1.969	0.009064	0.1782
TNFSF13B	tumor necrosis factor superfamily member 13b	0.9206	1.893	0.009083	0.1782
METTL9	methyltransferase like 9	1.139	2.203	0.009096	0.1782
SEMA4A	semaphorin 4A	0.7294	1.658	0.009124	0.1782
NA	NA	0.5809	1.496	0.009129	0.1782
TSPAN7	tetraspanin 7	0.585	1.5	0.009146	0.1782
KRT23	keratin 23	0.821	1.767	0.009161	0.1782
MS4A6A	membrane spanning 4-domains A6A	0.6117	1.528	0.009205	0.1782
TRIB1	tribbles pseudokinase 1	0.7748	1.711	0.009208	0.1782

ITGB2	integrin subunit beta 2	0.8281	1.775	0.009219	0.1782
SPRY1	sprouty RTK signaling antagonist 1	0.5412	1.455	0.009251	0.1782
PRR5	proline rich 5	0.5066	1.421	0.00926	0.1782
NA	NA	0.8035	1.745	0.009263	0.1782
FAM49B	family with sequence similarity 49 member B	0.4379	1.355	0.009265	0.1782
LOC100288208	uncharacterized LOC100288208	1.028	2.04	0.009298	0.1782
ZNF764	zinc finger protein 764	0.768	1.703	0.009311	0.1782
FAM189B	family with sequence similarity 189 member B	1.448	2.729	0.009312	0.1782
RNLS	renalase, FAD-dependent amine oxidase	0.5861	1.501	0.009319	0.1782
PLA2G4C	phospholipase A2 group IVC	0.5534	1.468	0.009348	0.1783
NTNG1	netrin G1	1.433	2.699	0.009381	0.1784
PACS1	phosphofurin acidic cluster sorting protein 1	1.204	2.304	0.009416	0.1784
MMEL1	membrane metallo-endopeptidase-like 1	1.333	2.519	0.009419	0.1784
PBXIP1	pre-B-cell leukemia homeobox interacting protein 1	0.7975	1.738	0.009457	0.1784
GPX3	glutathione peroxidase 3	1.655	3.15	0.009486	0.1787
FKBP8	FK506 binding protein 8	1.066	2.093	0.009505	0.1787
NCF2	neutrophil cytosolic factor 2	1.107	2.153	0.009509	0.1787
CDK18	cyclin-dependent kinase 18	1.493	2.815	0.009524	0.1787
H2AFJ	H2A histone family member J	0.7098	1.636	0.009547	0.1788
SLC23A2	solute carrier family 23 member 2	0.6255	1.543	0.009568	0.179
GIMAP4	GTPase, IMAP family member 4	0.7587	1.692	0.009595	0.179
HDAC7	histone deacetylase 7	0.6505	1.57	0.009608	0.179
LDLR	low density lipoprotein receptor	0.8021	1.744	0.00967	0.1795
CTSD	cathepsin D	0.5263	1.44	0.009724	0.1801
CORO1A	coronin 1A	1.092	2.132	0.00976	0.1803
DIRAS2	DIRAS family GTP binding RAS like 2	0.8663	1.823	0.009787	0.1803
JDP2	Jun dimerization protein 2	0.8329	1.781	0.009812	0.1803
ERO1A	endoplasmic reticulum oxidoreductase alpha	0.6607	1.581	0.009881	0.1807
SC5D	sterol-C5-desaturase	0.6223	1.539	0.00989	0.1807
CD4	CD4 molecule	1.167	2.245	0.009891	0.1807
QSOX1	quiescin sulfhydryl oxidase 1	1.109	2.157	0.009901	0.1807
HCLS1	hematopoietic cell-specific Lyn substrate 1	0.8	1.741	0.009939	0.1807
NA	NA	0.9288	1.904	0.00994	0.1807
TRIM47	tripartite motif containing 47	0.748	1.679	0.00994	0.1807
CA12	carbonic anhydrase XII	1.107	2.154	0.00995	0.1807
IRX3	iroquois homeobox 3	0.893	1.857	0.009971	0.1807
EZR-AS1	EZR antisense RNA 1	0.8426	1.793	0.009978	0.1807
CMTM7	CKLF like MARVEL transmembrane domain containing 7	0.4965	1.411	0.009983	0.1807

Supplementary Table 2. Down-regulated transcripts following UPA Administration (FC >1.3, p <0.01)

GREM2	gremlin 2, DAN family BMP antagonist	-4.468	-22.13	8.51E-08	0.00205
GJB2	gap junction protein beta 2	-3.246	-9.485	1.65E-06	0.01225
GJA4	gap junction protein alpha 4	-2.178	-4.524	2.68E-06	0.01225
NA	NA	-3.077	-8.44	2.98E-06	0.01225
GPER1	G protein-coupled estrogen receptor 1	-2.787	-6.903	3.05E-06	0.01225
NA	NA	-2.178	-4.525	7.32E-06	0.01759
OPN3	opsin 3	-1.976	-3.934	1.13E-05	0.01992
LINC00461	long intergenic non-protein coding RNA 461	-1.762	-3.392	1.20E-05	0.01992
NA	NA	-2.195	-4.58	1.24E-05	0.01992
DIO3OS	DIO3 opposite strand/antisense RNA (head to head)	-2.126	-4.366	1.32E-05	0.01992
GLA	galactosidase alpha	-2.243	-4.732	2.23E-05	0.02982
PAPSS1	3'-phosphoadenosine 5'-phosphosulfate synthase 1	-1.517	-2.862	2.46E-05	0.03118
SGCD	sarcoglycan delta	-2.697	-6.484	2.70E-05	0.03252
FXYD4	FXYD domain containing ion transport regulator 4	-2.515	-5.716	3.54E-05	0.03879
PAPSS1	3'-phosphoadenosine 5'-phosphosulfate synthase 1	-1.329	-2.512	4.12E-05	0.04313
PAGE4	PAGE family member 4	-5.544	-46.65	4.33E-05	0.04352
ZCCHC12	zinc finger CCHC-type containing 12	-1.888	-3.702	4.63E-05	0.04462
KAZALD1	Kazal type serine peptidase inhibitor domain 1	-1.584	-2.998	5.02E-05	0.04563
GPER1	G protein-coupled estrogen receptor 1	-2.713	-6.555	5.11E-05	0.04563
TCF19	transcription factor 19	-1.488	-2.805	5.50E-05	0.04632
CEACAM21	carcinoembryonic antigen related cell adhesion molecule 21	-1.892	-3.711	6.16E-05	0.04632
SGK1	serum/glucocorticoid regulated kinase 1	-2.552	-5.866	6.55E-05	0.04632
HES6	hes family bHLH transcription factor 6	-0.9837	-1.977	7.03E-05	0.04632
RAB15	RAB15, member RAS oncogene family	-1.565	-2.959	7.29E-05	0.04632
TUBA3D	tubulin alpha 3d	-3.617	-12.27	7.89E-05	0.04632
FAM13C	family with sequence similarity 13 member C	-1.735	-3.329	7.93E-05	0.04632
NA	NA	-2.473	-5.552	8.01E-05	0.04632
HIST1H2BH	histone cluster 1, H2bh	-1.956	-3.879	8.19E-05	0.04632
SGK1	serum/glucocorticoid regulated kinase 1	-2.638	-6.226	8.25E-05	0.04632
ARSG	arylsulfatase G	-1.193	-2.286	8.46E-05	0.04632
COL17A1	collagen type XVII alpha 1	-1.421	-2.678	8.76E-05	0.04632
LRRC26	leucine rich repeat containing 26	-3.318	-9.976	9.60E-05	0.04902
EDN3	endothelin 3	-1.371	-2.586	1.00E-04	0.04918
SCGB1D4	secretoglobin family 1D member 4	-7.571	-190.1	0.000107	0.05014
EDN3	endothelin 3	-1.446	-2.725	0.000107	0.05014
SERPINA5	serpin peptidase inhibitor, clade A (alpha-1 antiproteinase, antitrypsin), member 5	-3.223	-9.336	0.000116	0.05167
SLC39A14	solute carrier family 39 member 14	-0.9807	-1.973	0.00013	0.05432
NA	NA	-1.392	-2.624	0.000137	0.05432
SGOL2	shugoshin-like 2 (S. pombe)	-1.733	-3.324	0.000137	0.05432
MSX2	msh homeobox 2	-3.03	-8.168	0.000149	0.05697
CDC25A	cell division cycle 25A	-1.569	-2.967	0.000158	0.05897
NA	NA	-2.069	-4.197	0.000159	0.05897
TUBGCP6	tubulin gamma complex associated protein 6	-1.377	-2.597	0.000173	0.06081
LRRC26	leucine rich repeat containing 26	-3.51	-11.39	0.00018	0.06081
SGK1	serum/glucocorticoid regulated kinase 1	-2.647	-6.262	0.000186	0.06081
FAM122B	family with sequence similarity 122B	-0.9426	-1.922	0.000187	0.06081
SPC25	SPC25, NDC80 kinetochore complex component	-1.305	-2.471	0.000195	0.06195
MKI67	marker of proliferation Ki-67	-1.231	-2.347	0.000198	0.06195
CST1	cystatin SN	-3.441	-10.86	0.000209	0.06224
AMD1	adenosylmethionine decarboxylase 1	-1.095	-2.136	0.000217	0.06224
GGT1	gamma-glutamyltransferase 1	-1.562	-2.954	0.000222	0.06224

SLC39A6	solute carrier family 39 member 6	-1.192	-2.284	0.000228	0.06224
PENK	proenkephalin	-3.4	-10.56	0.000232	0.06224
SGOL1	shugoshin-like 1 (S. pombe)	-1.638	-3.112	0.00024	0.06224
SOX7	SRY-box 7	-1.472	-2.774	0.000248	0.06224
SCGB1D2	secretoglobin, family 1D member 2	-4.226	-18.71	0.000253	0.06224
NA	NA	-1.065	-2.092	0.000256	0.06224
ATP8B3	ATPase phospholipid transporting 8B3	-1.819	-3.527	0.000259	0.06231
MOGAT1	monoacylglycerol O-acyltransferase 1	-2.365	-5.152	0.000272	0.06307
ERRFI1	ERBB receptor feedback inhibitor 1	-1.073	-2.103	0.000278	0.06307
GJB6	gap junction protein beta 6	-3.291	-9.789	0.000279	0.06307
EDNRA	endothelin receptor type A	-1.115	-2.165	0.00028	0.06307
ANXA9	annexin A9	-1.881	-3.682	0.000283	0.06309
GJB6	gap junction protein beta 6	-3.939	-15.33	0.000286	0.06309
NA	NA	-3.612	-12.23	0.000297	0.06309
SNORD14C	small nucleolar RNA, C/D box 14C	-1.445	-2.722	0.000298	0.06309
MT3	metallothionein 3	-2.846	-7.189	0.000299	0.06309
PCDH10	protocadherin 10	-2.086	-4.244	0.000302	0.06317
ACSL5	acyl-CoA synthetase long-chain family member 5	-1.39	-2.621	0.000357	0.07221
SRRM4	serine/arginine repetitive matrix 4	-2.37	-5.171	0.00036	0.07221
NA	NA	-1.443	-2.72	0.000364	0.07254
SGCD	sarcoglycan delta	-1.138	-2.2	0.000384	0.07394
E2F7	E2F transcription factor 7	-1.653	-3.145	0.000386	0.07394
ALDH1A2	aldehyde dehydrogenase 1 family member A2	-1.224	-2.336	0.00039	0.07394
ST3GAL5	ST3 beta-galactoside alpha-2,3-sialyltransferase 5	-1.197	-2.292	0.000394	0.07394
NA	NA	-1.404	-2.647	0.000402	0.07394
SYNDIG1	synapse differentiation inducing 1	-1.335	-2.523	0.000417	0.07394
ANGPTL2	angiopoietin like 2	-1.308	-2.476	0.000419	0.07394
TMEM132D	transmembrane protein 132D	-1.118	-2.17	0.000423	0.07394
NA	NA	-1.119	-2.172	0.000426	0.07394
NA	NA	-1.604	-3.04	0.000442	0.07525
UCHL1	ubiquitin C-terminal hydrolase L1	-2.212	-4.633	0.000446	0.07525
RNU11	RNA, U11 small nuclear	-1.755	-3.376	0.00047	0.07575
FAM124B	family with sequence similarity 124 member B	-2.48	-5.579	0.000474	0.07575
IGSF10	immunoglobulin superfamily member 10	-1.381	-2.604	0.00048	0.07604
ANAPC4	anaphase promoting complex subunit 4	-1.603	-3.037	0.000494	0.07621
DUSP2	dual specificity phosphatase 2	-1.321	-2.499	0.000495	0.07621
CCDC74A	coiled-coil domain containing 74A	-1.262	-2.399	0.000509	0.07621
SPINK8	serine peptidase inhibitor, Kazal type 8 (putative)	-2.406	-5.3	0.00051	0.07621
POU5F1B	POU class 5 homeobox 1B	-2.63	-6.189	0.000513	0.07621
PLCXD3	phosphatidylinositol specific phospholipase C X domain containing 3	-2.458	-5.493	0.000518	0.07621
MCOLN2	mucolipin 2	-0.7876	-1.726	0.000537	0.07766
ANKRD23	ankyrin repeat domain 23	-0.9233	-1.896	0.000541	0.07766
NA	NA	-1.295	-2.453	0.000545	0.07775
CCNA1	cyclin A1	-2.423	-5.364	0.000553	0.07834
POLQ	polymerase (DNA) theta	-1.252	-2.382	0.000581	0.07961
SYTL4	synaptotagmin like 4	-1.028	-2.039	0.000582	0.07961
GGA1	golgi-associated, gamma adaptin ear containing, ARF binding protein 1	-1.348	-2.545	0.000586	0.07961
SAPCD2	suppressor APC domain containing 2	-1.611	-3.056	0.000589	0.07961
LIMS1	LIM zinc finger domain containing 1	-1.16	-2.234	0.00059	0.07961
SERHL	serine hydrolase-like (pseudogene)	-1.387	-2.615	0.000608	0.07961
AMFR	autocrine motility factor receptor, E3 ubiquitin protein ligase	-1.282	-2.431	0.000622	0.07961
NAPSA	napsin A aspartic peptidase	-2.175	-4.517	0.000629	0.07961
OPN3	opsin 3	-0.9263	-1.9	0.000629	0.07961
C1orf186	chromosome 1 open reading frame 186	-2.244	-4.738	0.00064	0.07961

KMO	kynurenine 3-monooxygenase (kynurenine 3-hydroxylase)	-3.273	-9.668	0.000647	0.07961
MOGAT2	monoacylglycerol O-acyltransferase 2	-0.9805	-1.973	0.00065	0.07961
KIAA1210	KIAA1210	-0.9168	-1.888	0.000658	0.07961
SNORD14A	small nucleolar RNA, C/D box 14A	-1.903	-3.74	0.000669	0.08062
MCC	mutated in colorectal cancers	-1.2	-2.298	0.000675	0.08087
ALDH3B2	aldehyde dehydrogenase 3 family member B2	-2.312	-4.964	0.000678	0.08087
NDP	Norrie disease (pseudoglioma)	-2.235	-4.707	0.000697	0.08273
MYL10	myosin light chain 10	-1.41	-2.657	0.000722	0.08407
PAK7	p21 protein (Cdc42/Rac)-activated kinase 7	-2.028	-4.078	0.000731	0.08472
NA	NA	-0.7654	-1.7	0.000738	0.08511
PRKAR2A	protein kinase cAMP-dependent type II regulatory subunit alpha	-0.8314	-1.779	0.000747	0.08572
HSD11B2	hydroxysteroid (11-beta) dehydrogenase 2	-1.637	-3.109	0.000764	0.08694
MMP26	matrix metallopeptidase 26	-3.157	-8.92	0.000765	0.08694
ABCC5	ATP binding cassette subfamily C member 5	-1.504	-2.836	0.000783	0.08773
AMFR	autocrine motility factor receptor, E3 ubiquitin protein ligase	-0.7788	-1.716	0.00082	0.09021
CRYGS	crystallin gamma S	-1.831	-3.558	0.000841	0.09091
IGDCC3	immunoglobulin superfamily, DCC subclass, member 3	-1.535	-2.898	0.000855	0.09192
SCGB2A2	secretoglobin family 2A member 2	-2.737	-6.666	0.000869	0.09263
NA	NA	-1.258	-2.392	0.000894	0.0933
ZMIZ2	zinc finger MIZ-type containing 2	-0.9524	-1.935	0.000899	0.09335
CERKL	ceramide kinase like	-1.344	-2.538	0.000914	0.09379
DAPL1	death associated protein like 1	-1.651	-3.14	0.000945	0.09511
NA	NA	-1.264	-2.402	0.000946	0.09511
ORM2	orosomucoid 2	-2.506	-5.682	0.000951	0.09511
TMEM101	transmembrane protein 101	-1.4	-2.638	0.000955	0.09511
EFEMP1	EGF containing fibulin-like extracellular matrix protein 1	-0.8847	-1.846	0.000991	0.09788
NAPSB	napsin B aspartic peptidase, pseudogene	-1.429	-2.692	0.00101	0.09935
NA	NA	-0.7386	-1.669	0.001026	0.1001
BASP1	brain abundant membrane attached signal protein 1	-0.7256	-1.654	0.001105	0.1045
PDZD8	PDZ domain containing 8	-0.8621	-1.818	0.001114	0.1048
SULF2	sulfatase 2	-0.8939	-1.858	0.001128	0.1054
HACD1	3-hydroxyacyl-CoA dehydratase 1	-0.856	-1.81	0.001142	0.1055
DDIAS	DNA damage induced apoptosis suppressor	-1.186	-2.276	0.001161	0.1063
ALDH1A2	aldehyde dehydrogenase 1 family member A2	-1.154	-2.225	0.001191	0.1063
NA	NA	-0.9147	-1.885	0.001226	0.1069
NA	NA	-0.903	-1.87	0.001229	0.1069
CKAP2L	cytoskeleton associated protein 2 like	-1.621	-3.075	0.001239	0.1073
ALG3	ALG3, alpha-1,3- mannosyltransferase	-1.192	-2.285	0.001321	0.1111
KYNU	kynureninase	-1.496	-2.821	0.001323	0.1111
BCAN	brevican	-1.595	-3.022	0.001376	0.113
ENPP3	ectonucleotide pyrophosphatase/phosphodiesterase 3	-4.088	-17	0.001384	0.113
ESPL1	extra spindle pole bodies like 1, separase	-1.549	-2.926	0.001385	0.113
NAV2	neuron navigator 2	-1.398	-2.636	0.00139	0.113
RHBDL1	rhomboid, veinlet-like 1 (Drosophila)	-1.094	-2.135	0.001391	0.113
CCDC74B	coiled-coil domain containing 74B	-1.173	-2.254	0.001403	0.113
SLC39A6	solute carrier family 39 member 6	-1.086	-2.123	0.001441	0.113
SAPCD2	suppressor APC domain containing 2	-1.263	-2.4	0.001442	0.113
FAM234B	family with sequence similarity 234 member B	-1.753	-3.371	0.001458	0.113
ADAMTS8	ADAM metallopeptidase with thrombospondin type 1 motif 8	-2.373	-5.179	0.001463	0.113
PPP1R12C	protein phosphatase 1 regulatory subunit 12C	-1.09	-2.129	0.001468	0.113
DKK1	dickkopf WNT signaling pathway inhibitor 1	-1.826	-3.545	0.001476	0.113
DNAJC22	DnaJ heat shock protein family (Hsp40) member C22	-0.8233	-1.769	0.001477	0.113

GAL	galanin/GMAP prepropeptide	-1.748	-3.359	0.001518	0.1136
SULF2	sulfatase 2	-0.6941	-1.618	0.001523	0.1136
SPAG8	sperm associated antigen 8	-2.039	-4.111	0.001523	0.1136
CTAGE5	CTAGE family member 5	-1.192	-2.284	0.001541	0.1136
OLFM1	olfactomedin 1	-1.695	-3.237	0.001551	0.1136
MYC	v-myc avian myelocytomatosis viral oncogene homolog	-0.9049	-1.872	0.001556	0.1136
NA	NA	-0.7184	-1.645	0.001579	0.1146
CACYBP	calcyclin binding protein	-0.9221	-1.895	0.001604	0.1157
C6orf141	chromosome 6 open reading frame 141	-2.703	-6.51	0.001613	0.116
SMOC2	SPARC related modular calcium binding 2	-1.526	-2.88	0.001648	0.1171
NA	NA	-1.187	-2.276	0.001658	0.1174
FEN1	flap structure-specific endonuclease 1	-0.8501	-1.803	0.001662	0.1174
TCF12	transcription factor 12	-0.6735	-1.595	0.001668	0.1174
TUBA3E	tubulin alpha 3e	-2.856	-7.242	0.00168	0.1174
PSMC3IP	PSMC3 interacting protein	-1.064	-2.09	0.001685	0.1174
CCNO	cyclin O	-1.352	-2.553	0.001685	0.1174
SPEF2	sperm flagellar 2	-1.015	-2.021	0.001704	0.1174
BCAP29	B-cell receptor-associated protein 29	-0.7246	-1.652	0.001713	0.1174
RADIL	Ras association and DIL domains	-0.946	-1.927	0.001731	0.1174
TTF2	transcription termination factor, RNA polymerase II	-0.8072	-1.75	0.001738	0.1174
CHEK2	checkpoint kinase 2	-0.7159	-1.642	0.001744	0.1174
AUNIP	aurora kinase A and ninein interacting protein	-1.109	-2.157	0.001749	0.1174
ARMCX4	armadillo repeat containing, X-linked 4	-2.227	-4.682	0.001749	0.1174
SLC26A6	solute carrier family 26 member 6	-1.06	-2.086	0.001755	0.1174
NA	NA	-1.33	-2.514	0.001767	0.1174
SNORA26	small nucleolar RNA, H/ACA box 26	-1.618	-3.069	0.001781	0.1174
ALPL	alkaline phosphatase, liver/bone/kidney	-1.485	-2.8	0.001783	0.1174
NA	NA	-0.8658	-1.822	0.001787	0.1174
AMD1	adenosylmethionine decarboxylase 1	-0.8899	-1.853	0.001788	0.1174
GPM6B	glycoprotein M6B	-0.9018	-1.868	0.001796	0.1176
EEF1E1	eukaryotic translation elongation factor 1 epsilon 1	-0.6784	-1.6	0.001803	0.1176
NA	NA	-2.098	-4.281	0.001828	0.1176
SCN2B	sodium voltage-gated channel beta subunit 2	-1.291	-2.447	0.001837	0.1176
TEKT4	tektin 4	-1.22	-2.329	0.001847	0.1176
SMAD9	SMAD family member 9	-2.234	-4.704	0.001851	0.1176
SMAD9	SMAD family member 9	-1.711	-3.274	0.001882	0.1176
GREB1	growth regulation by estrogen in breast cancer 1	-0.6939	-1.618	0.001883	0.1176
ZNF589	zinc finger protein 589	-1.068	-2.096	0.001893	0.1176
FGF12	fibroblast growth factor 12	-1.183	-2.27	0.001897	0.1176
IL17RB	interleukin 17 receptor B	-1.069	-2.098	0.001902	0.1176
TUBA3D	tubulin alpha 3d	-0.6871	-1.61	0.001904	0.1176
CTNNA2	catenin alpha 2	-2.978	-7.877	0.001908	0.1176
IL17D	interleukin 17D	-1.253	-2.384	0.001916	0.1176
PLK4	polo like kinase 4	-1.259	-2.394	0.001923	0.1176
GLIS2	GLIS family zinc finger 2	-0.9945	-1.992	0.001961	0.1182
OIP5	Opa interacting protein 5	-1.328	-2.511	0.001969	0.1182
SULF2	sulfatase 2	-0.7477	-1.679	0.001972	0.1182
DLEC1	deleted in lung and esophageal cancer 1	-1.557	-2.942	0.00198	0.1182
NA	NA	-1.17	-2.251	0.001993	0.1182
RTN4	reticulon 4	-1.205	-2.306	0.002009	0.1182
NA	NA	-1.785	-3.447	0.002027	0.1182
ETNPPL	ethanolamine-phosphate phospho-lyase	-1.825	-3.543	0.002031	0.1182
PSMC3IP	PSMC3 interacting protein	-1.15	-2.22	0.00204	0.1182
NA	NA	-1.174	-2.256	0.002062	0.1182
FAM63A	family with sequence similarity 63 member A	-1.385	-2.611	0.002064	0.1182
RASSF2	Ras association domain family member 2	-0.988	-1.983	0.002068	0.1182
LRRC6	leucine rich repeat containing 6	-0.9267	-1.901	0.002087	0.1182

HOMER2	homer scaffolding protein 2	-1.562	-2.953	0.002088	0.1182
NA	NA	-1.439	-2.712	0.002092	0.1182
NGEF	neuronal guanine nucleotide exchange factor	-0.8481	-1.8	0.0021	0.1182
NA	NA	-0.6832	-1.606	0.002126	0.1189
TCAIM	T-cell activation inhibitor, mitochondrial	-0.8712	-1.829	0.002131	0.1189
RGS7BP	regulator of G-protein signaling 7 binding protein	-1.522	-2.871	0.002182	0.1189
TMEM132B	transmembrane protein 132B	-1.335	-2.522	0.002183	0.1189
TCF12	transcription factor 12	-0.6957	-1.62	0.002187	0.1189
NA	NA	-0.8489	-1.801	0.002188	0.1189
MRPS12	mitochondrial ribosomal protein S12	-0.6968	-1.621	0.002191	0.1189
COL9A2	collagen type IX alpha 2	-1.865	-3.643	0.002198	0.1189
BAIAP2L2	BAI1 associated protein 2 like 2	-1.002	-2.003	0.002199	0.1189
DYNC1I1	dynein cytoplasmic 1 intermediate chain 1	-1.444	-2.721	0.00222	0.119
PBK	PDZ binding kinase	-2.106	-4.306	0.00222	0.119
CNTNAP2	contactin associated protein-like 2	-1.921	-3.786	0.002236	0.119
BARD1	BRCA1 associated RING domain 1	-0.5967	-1.512	0.002238	0.119
KIF4A	kinesin family member 4A	-1.87	-3.655	0.002251	0.1195
EPB41L2	erythrocyte membrane protein band 4.1-like 2	-0.7377	-1.668	0.002265	0.1195
SLC46A2	solute carrier family 46 member 2	-2.99	-7.943	0.002267	0.1195
SGOL1	shugoshin-like 1 (S. pombe)	-1.619	-3.072	0.002271	0.1195
MMP16	matrix metallopeptidase 16	-1.125	-2.181	0.002308	0.1198
PIR	pirin	-1.129	-2.188	0.002335	0.1204
CCDC34	coiled-coil domain containing 34	-0.9194	-1.891	0.002338	0.1204
MIR503	microRNA 503	-2.016	-4.045	0.002343	0.1204
FANCL	Fanconi anemia complementation group L	-0.9485	-1.93	0.002348	0.1204
MFSD2A	major facilitator superfamily domain containing 2A	-1.644	-3.126	0.002375	0.1208
ANTXR1	anthrax toxin receptor 1	-0.953	-1.936	0.002382	0.1208
GTPBP3	GTP binding protein 3 (mitochondrial)	-0.8371	-1.786	0.002383	0.1208
SLC7A4	solute carrier family 7 member 4	-1.047	-2.067	0.002426	0.1226
NA	NA	-0.7917	-1.731	0.002487	0.1243
LRRC73	leucine rich repeat containing 73	-0.6712	-1.592	0.002508	0.1248
NA	NA	-1.022	-2.031	0.002516	0.1248
BHMT	betaine--homocysteine S-methyltransferase	-1.053	-2.075	0.002518	0.1248
P2RY14	purinergic receptor P2Y14	-1.675	-3.193	0.002551	0.1248
RECQL4	RecQ like helicase 4	-0.7944	-1.734	0.002552	0.1248
FAM65C	family with sequence similarity 65 member C	-1.5	-2.829	0.002559	0.1248
MYC	v-myc avian myelocytomatosis viral oncogene homolog	-0.9114	-1.881	0.00256	0.1248
RXFP1	relaxin/insulin-like family peptide receptor 1	-1.723	-3.301	0.002577	0.125
HELLS	helicase, lymphoid-specific	-1.522	-2.872	0.00258	0.125
MTPN	myotrophin	-0.7009	-1.626	0.002614	0.1254
LRRC75B	leucine rich repeat containing 75B	-1.22	-2.329	0.002626	0.1254
CDC20B	cell division cycle 20B	-1.821	-3.534	0.002626	0.1254
NA	NA	-1.049	-2.068	0.002637	0.1254
CCDC173	coiled-coil domain containing 173	-1.382	-2.605	0.002644	0.1254
ECI1	enoyl-CoA delta isomerase 1	-0.6746	-1.596	0.002676	0.1265
NA	NA	-1.079	-2.113	0.002676	0.1265
TYMSOS	TYMS opposite strand	-0.9022	-1.869	0.0027	0.1268
C17orf58	chromosome 17 open reading frame 58	-1.088	-2.125	0.0027	0.1268
BRICD5	BRICHOS domain containing 5	-2.237	-4.713	0.002712	0.1268
NA	NA	-0.6039	-1.52	0.002717	0.1268
MKS1	Meckel syndrome, type 1	-0.7035	-1.628	0.00272	0.1268
PAQR4	progestin and adipoQ receptor family member IV	-1.075	-2.107	0.002749	0.1277
PCDH20	protocadherin 20	-0.9733	-1.963	0.002767	0.1277
ACADL	acyl-CoA dehydrogenase, long chain	-1.057	-2.08	0.002777	0.1277
NA	NA	-1.426	-2.686	0.002779	0.1277
MMS22L	MMS22 like, DNA repair protein	-0.5925	-1.508	0.002781	0.1277
RAB7B	RAB7B, member RAS oncogene family	-1.604	-3.04	0.002813	0.1277

NA	NA	-1.762	-3.392	0.002818	0.1277
NUF2	NUF2, NDC80 kinetochore complex component	-1.699	-3.247	0.00282	0.1277
FANK1	fibronectin type III and ankyrin repeat domains 1	-1.382	-2.606	0.002832	0.1277
GPM6B	glycoprotein M6B	-0.8129	-1.757	0.002839	0.1277
NTN5	netrin 5	-0.8793	-1.839	0.00284	0.1277
MID1	midline 1	-0.7674	-1.702	0.002872	0.1277
CCDC74B	coiled-coil domain containing 74B	-1.458	-2.747	0.002882	0.1277
PDZK1	PDZ domain containing 1	-2.932	-7.629	0.002891	0.1278
ECI2	enoyl-CoA delta isomerase 2	-0.7238	-1.652	0.00298	0.1298
CEP152	centrosomal protein 152kDa	-1.484	-2.798	0.002994	0.1298
GNB4	G protein subunit beta 4	-0.7639	-1.698	0.002995	0.1298
ODF2L	outer dense fiber of sperm tails 2 like	-0.8544	-1.808	0.002996	0.1298
PKHD1L1	polycystic kidney and hepatic disease 1 (autosomal recessive)-like 1	-2.342	-5.072	0.003001	0.1298
CCDC146	coiled-coil domain containing 146	-2.081	-4.231	0.003028	0.1298
POU5F1B	POU class 5 homeobox 1B	-1.69	-3.227	0.003034	0.1298
HAGHL	hydroxyacylglutathione hydrolase-like	-0.9996	-1.999	0.003036	0.1298
ZNF432	zinc finger protein 432	-0.5796	-1.494	0.00304	0.1298
SLC46A1	solute carrier family 46 member 1	-0.8348	-1.784	0.003068	0.1298
ZDHHC23	zinc finger DHHC-type containing 23	-1.023	-2.032	0.003078	0.1298
SRL	sarcalumenin	-1.153	-2.223	0.003083	0.1298
PYCRL	pyrroline-5-carboxylate reductase-like	-0.725	-1.653	0.003121	0.1298
IGSF9	immunoglobulin superfamily member 9	-1.593	-3.018	0.003129	0.1298
CCDC189	coiled-coil domain containing 189	-0.9936	-1.991	0.00313	0.1298
ABCC8	ATP binding cassette subfamily C member 8	-1.569	-2.966	0.003142	0.1298
CDKN2A	cyclin-dependent kinase inhibitor 2A	-0.8345	-1.783	0.003143	0.1298
NA	NA	-1.354	-2.556	0.003147	0.1298
KIR2DL4	killer cell immunoglobulin like receptor, two Ig domains and long cytoplasmic tail 4	-0.8404	-1.791	0.003148	0.1298
OPN3	opsin 3	-0.6681	-1.589	0.003177	0.1302
ADAM28	ADAM metallopeptidase domain 28	-1.195	-2.289	0.003211	0.1304
TBRG1	transforming growth factor beta regulator 1	-1.419	-2.674	0.003215	0.1304
DONSON	downstream neighbor of SON	-1.467	-2.764	0.003215	0.1304
NA	NA	-0.9703	-1.959	0.003242	0.1313
TDP1	tyrosyl-DNA phosphodiesterase 1	-1.032	-2.045	0.003268	0.1315
E2F2	E2F transcription factor 2	-1.085	-2.121	0.003276	0.1315
KCTD8	potassium channel tetramerization domain containing 8	-1.837	-3.574	0.003278	0.1315
APOA1	apolipoprotein A-I	-1.421	-2.678	0.003287	0.1315
ARMCX6	armadillo repeat containing, X-linked 6	-0.7313	-1.66	0.003311	0.1315
ITPKA	inositol-trisphosphate 3-kinase A	-1.636	-3.108	0.003311	0.1315
KIF11	kinesin family member 11	-1.318	-2.493	0.003319	0.1315
ART3	ADP-ribosyltransferase 3	-1.578	-2.986	0.003326	0.1316
BHMT2	betaine--homocysteine S-methyltransferase 2	-1.348	-2.546	0.003331	0.1316
ARHGAP20	Rho GTPase activating protein 20	-1.687	-3.219	0.003337	0.1316
XPR1	xenotropic and polytropic retrovirus receptor 1	-0.5547	-1.469	0.003346	0.1316
ZNF692	zinc finger protein 692	-1.043	-2.06	0.003384	0.1322
NA	NA	-1.331	-2.515	0.003394	0.1322
MICB	MHC class I polypeptide-related sequence B	-1.147	-2.215	0.003398	0.1322
DOK6	docking protein 6	-0.7838	-1.722	0.003402	0.1322
STX2	syntaxin 2	-0.8474	-1.799	0.00344	0.1327
NA	NA	-1.017	-2.024	0.003517	0.1343
NEK2	NIMA related kinase 2	-1.568	-2.964	0.003592	0.1354
NA	NA	-1.364	-2.573	0.003608	0.1354
PDE8A	phosphodiesterase 8A	-1.037	-2.051	0.003609	0.1354
TMEM107	transmembrane protein 107	-1.108	-2.156	0.003619	0.1354
RAB36	RAB36, member RAS oncogene family	-0.723	-1.651	0.003641	0.1355
CEP120	centrosomal protein 120kDa	-1.097	-2.14	0.003643	0.1355

CEP57L1	centrosomal protein 57kDa-like 1	-0.7313	-1.66	0.003679	0.1362
SFI1	SFI1 centrin binding protein	-1.336	-2.524	0.003701	0.1366
SLC51B	solute carrier family 51 beta subunit	-2.244	-4.736	0.003765	0.1379
CEP55	centrosomal protein 55kDa	-1.399	-2.637	0.003775	0.1379
PCBP4	poly(rC) binding protein 4	-0.7471	-1.678	0.003783	0.1379
PTN	pleiotrophin	-1.505	-2.838	0.003783	0.1379
HIST1H2BC	histone cluster 1, H2bc	-1.321	-2.499	0.003793	0.1379
FGFR3	fibroblast growth factor receptor 3	-0.8195	-1.765	0.003813	0.1382
C7orf57	chromosome 7 open reading frame 57	-2.214	-4.639	0.003832	0.1384
NDC80	NDC80 kinetochore complex component	-1.192	-2.285	0.003861	0.1393
CHST3	carbohydrate (chondroitin 6) sulfotransferase 3	-0.6199	-1.537	0.003895	0.1399
NA	NA	-1.512	-2.851	0.003906	0.1399
ARL4D	ADP ribosylation factor like GTPase 4D	-1.655	-3.149	0.003941	0.1401
RCN2	reticulocalbin 2	-0.9515	-1.934	0.003944	0.1401
ST3GAL5	ST3 beta-galactoside alpha-2,3-sialyltransferase 5	-1.838	-3.575	0.003951	0.1401
OXCT1	3-oxoacid CoA-transferase 1	-1.243	-2.367	0.003961	0.1401
APOBEC4	apolipoprotein B mRNA editing enzyme catalytic polypeptide like 4	-0.8922	-1.856	0.003962	0.1401
OGFOD1	2-oxoglutarate and iron dependent oxygenase domain containing 1	-0.6969	-1.621	0.003965	0.1401
RDM1	RAD52 motif containing 1	-1.223	-2.334	0.003999	0.1407
ARHGEF19	Rho guanine nucleotide exchange factor 19	-0.8389	-1.789	0.004006	0.1407
CAPRIN2	caprin family member 2	-1.798	-3.478	0.004038	0.1416
ALDH3B2	aldehyde dehydrogenase 3 family member B2	-1.821	-3.533	0.004073	0.1425
IGHMBP2	immunoglobulin mu binding protein 2	-0.7298	-1.658	0.004096	0.1429
POC1B	POC1 centriolar protein B	-0.5508	-1.465	0.004136	0.1433
WIPI1	WD repeat domain, phosphoinositide interacting 1	-0.8721	-1.83	0.004181	0.1435
TSKU	tsukushi, small leucine rich proteoglycan	-0.9125	-1.882	0.004198	0.1435
SLC25A15	solute carrier family 25 member 15	-1.018	-2.025	0.004213	0.1435
KIF15	kinesin family member 15	-1.466	-2.763	0.004219	0.1435
NA	NA	-0.6884	-1.611	0.004221	0.1435
NA	NA	-0.7697	-1.705	0.004227	0.1435
ZNF93	zinc finger protein 93	-0.9974	-1.996	0.00423	0.1435
PSRC1	proline/serine-rich coiled-coil 1	-1.427	-2.689	0.004234	0.1435
SNORD96A	small nucleolar RNA, C/D box 96A	-1.025	-2.034	0.004244	0.1435
IKBIP	IKBKB interacting protein	-0.7914	-1.731	0.004264	0.1435
NA	NA	-0.7465	-1.678	0.00427	0.1435
ANKRD35	ankyrin repeat domain 35	-0.8591	-1.814	0.004274	0.1435
SLC45A1	solute carrier family 45 member 1	-1.621	-3.076	0.004309	0.1441
CHORDC1	cysteine and histidine rich domain containing 1	-0.6257	-1.543	0.004312	0.1441
CCDC24	coiled-coil domain containing 24	-0.8458	-1.797	0.004348	0.1445
C19orf48	chromosome 19 open reading frame 48	-0.6379	-1.556	0.004356	0.1445
KLRA1P	killer cell lectin like receptor A1, pseudogene	-0.7278	-1.656	0.004374	0.1446
RNU11	RNA, U11 small nuclear	-1.439	-2.711	0.00438	0.1446
UCN2	urocortin 2	-1.688	-3.223	0.004466	0.1459
PCDH10	protocadherin 10	-1.277	-2.423	0.004482	0.146
CLASRP	CLK4-associating serine/arginine rich protein	-0.9667	-1.954	0.004502	0.1463
CEP131	centrosomal protein 131kDa	-0.6626	-1.583	0.004504	0.1463
GDAP1	ganglioside induced differentiation associated protein 1	-0.773	-1.709	0.00455	0.147
COX15	COX15 cytochrome c oxidase assembly homolog	-0.8658	-1.822	0.00456	0.147
NA	NA	-1.058	-2.083	0.004583	0.1473
MEN1	menin 1	-0.9787	-1.971	0.00459	0.1473
NAA40	N(alpha)-acetyltransferase 40, NatD catalytic subunit	-1.131	-2.189	0.004603	0.1473
SNAP91	synaptosome associated protein 91kDa	-0.7163	-1.643	0.004605	0.1473

KIAA1524	KIAA1524	-1.369	-2.582	0.004615	0.1473
NA	NA	-1.283	-2.433	0.004616	0.1473
ITPR2	inositol 1,4,5-trisphosphate receptor type 2	-0.7363	-1.666	0.004639	0.1474
RGS22	regulator of G-protein signaling 22	-1.338	-2.528	0.004645	0.1474
CELF1	CUGBP, Elav-like family member 1	-0.7809	-1.718	0.004667	0.1474
USP35	ubiquitin specific peptidase 35	-0.8707	-1.829	0.004667	0.1474
SNHG15	small nucleolar RNA host gene 15	-0.5249	-1.439	0.004668	0.1474
ZNF662	zinc finger protein 662	-0.8987	-1.864	0.004688	0.1477
CCNE2	cyclin E2	-1.803	-3.489	0.00471	0.1478
SMC4	structural maintenance of chromosomes 4	-0.7561	-1.689	0.004735	0.1478
TMEM106C	transmembrane protein 106C	-0.6716	-1.593	0.004753	0.1478
OLFM1	olfactomedin 1	-1.528	-2.884	0.004757	0.1478
GGCT	gamma-glutamylcyclotransferase	-0.6011	-1.517	0.004761	0.1478
TRIP13	thyroid hormone receptor interactor 13	-0.8317	-1.78	0.004781	0.1478
FERMT1	fermitin family member 1	-0.9183	-1.89	0.004781	0.1478
TBC1D31	TBC1 domain family member 31	-1.178	-2.262	0.004787	0.1478
REV3L	REV3 like, DNA directed polymerase zeta catalytic subunit	-1.217	-2.324	0.00481	0.1479
AURKA	aurora kinase A	-1.284	-2.435	0.004811	0.1479
SAMD11	sterile alpha motif domain containing 11	-0.7804	-1.718	0.004833	0.1481
THBS3	thrombospondin 3	-0.7304	-1.659	0.004855	0.1481
KLK4	kallikrein related peptidase 4	-1.84	-3.58	0.004857	0.1481
BCAP29	B-cell receptor-associated protein 29	-0.6343	-1.552	0.004865	0.1481
TSPYL2	TSPY-like 2	-0.6123	-1.529	0.00487	0.1481
CCDC191	coiled-coil domain containing 191	-0.947	-1.928	0.004871	0.1481
MME	membrane metallo-endopeptidase	-1.247	-2.374	0.004903	0.1486
PIR	pirin	-1.306	-2.472	0.004917	0.1488
CNIH2	cornichon family AMPA receptor auxiliary protein 2	-1.681	-3.206	0.004924	0.1488
TRIOBP	TRIO and F-actin binding protein	-1.306	-2.473	0.004927	0.1488
ASPHD1	aspartate beta-hydroxylase domain containing 1	-1.01	-2.013	0.005015	0.1505
GAS2L3	growth arrest specific 2 like 3	-0.9647	-1.952	0.005072	0.1513
SMC4	structural maintenance of chromosomes 4	-1.117	-2.169	0.005083	0.1514
C2orf88	chromosome 2 open reading frame 88	-1.401	-2.641	0.005105	0.1518
NA	NA	-0.9333	-1.91	0.005107	0.1518
PIAS3	protein inhibitor of activated STAT 3	-0.7938	-1.734	0.005148	0.1521
ERI2	ERI1 exoribonuclease family member 2	-1.33	-2.514	0.005167	0.1521
HOMER2	homer scaffolding protein 2	-1.666	-3.173	0.005167	0.1521
CMAHP	cytidine monophospho-N-acetylneuraminic acid hydroxylase, pseudogene	-0.6514	-1.571	0.005185	0.1521
NA	NA	-1.024	-2.034	0.005211	0.1522
HPRT1	hypoxanthine phosphoribosyltransferase 1	-0.5219	-1.436	0.005255	0.1526
WDR73	WD repeat domain 73	-0.7533	-1.686	0.005284	0.1532
SEMA3C	semaphorin 3C	-0.9447	-1.925	0.005313	0.1537
RFC4	replication factor C subunit 4	-0.8234	-1.77	0.005414	0.1559
MAP9	microtubule associated protein 9	-1.172	-2.254	0.005423	0.156
AURKA	aurora kinase A	-1.053	-2.075	0.005512	0.1574
F3	coagulation factor III, tissue factor	-1.17	-2.25	0.005526	0.1574
SNORA67	small nucleolar RNA, H/ACA box 67	-1.689	-3.225	0.005532	0.1574
MND1	meiotic nuclear divisions 1	-1.157	-2.23	0.005577	0.1579
MAP6D1	MAP6 domain containing 1	-0.8417	-1.792	0.005617	0.158
OFD1	oral-facial-digital syndrome 1	-0.8271	-1.774	0.005632	0.158
LOC441268	uncharacterized LOC441268	-1.695	-3.237	0.005697	0.1583
KIF24	kinesin family member 24	-1.491	-2.811	0.00576	0.1586
GGT1	gamma-glutamyltransferase 1	-0.9276	-1.902	0.00583	0.1598
KNSTRN	kinetochore-localized astrin/SPAG5 binding protein	-0.8135	-1.757	0.005855	0.1598
NA	NA	-0.9639	-1.951	0.005888	0.16
FAM179A	family with sequence similarity 179 member A	-1.117	-2.169	0.005889	0.16
CORO2B	coronin 2B	-0.8396	-1.79	0.005925	0.1603

NA	NA	-2.489	-5.613	0.005949	0.1603
ARMCX6	armadillo repeat containing, X-linked 6	-0.5331	-1.447	0.005953	0.1603
ZSCAN29	zinc finger and SCAN domain containing 29	-0.9685	-1.957	0.005968	0.1603
NA	NA	-0.8604	-1.816	0.005971	0.1603
RNF144A	ring finger protein 144A	-0.5865	-1.502	0.005983	0.1603
KLRC1	killer cell lectin like receptor C1	-1.153	-2.224	0.005985	0.1603
ARHGEF39	Rho guanine nucleotide exchange factor 39	-1.307	-2.474	0.006005	0.1603
CNOT11	CCR4-NOT transcription complex subunit 11	-0.4775	-1.392	0.00606	0.1607
SIMC1	SUMO interacting motifs containing 1	-0.896	-1.861	0.006062	0.1607
NA	NA	-0.9149	-1.885	0.006069	0.1607
NA	NA	-0.8495	-1.802	0.006074	0.1607
CENPK	centromere protein K	-1.56	-2.948	0.006102	0.1612
ECM1	extracellular matrix protein 1	-0.5612	-1.476	0.006114	0.1614
GPR83	G protein-coupled receptor 83	-1.343	-2.536	0.006142	0.1615
DPY19L1	dpy-19 like 1 (C. elegans)	-0.8525	-1.806	0.006143	0.1615
FEN1	flap structure-specific endonuclease 1	-0.8893	-1.852	0.006176	0.1619
NPHP1	nephronophthisis 1 (juvenile)	-1.152	-2.222	0.006198	0.162
DLGAP5	discs large homolog associated protein 5	-1.589	-3.008	0.00621	0.1621
UBE2C	ubiquitin conjugating enzyme E2C	-1.302	-2.466	0.006239	0.1627
NA	NA	-1.246	-2.371	0.006254	0.1627
AEN	apoptosis enhancing nuclease	-0.6696	-1.591	0.006355	0.1648
PMP22	peripheral myelin protein 22	-0.8619	-1.817	0.006407	0.1652
ANKRD26	ankyrin repeat domain 26	-1.023	-2.031	0.006412	0.1652
SNORA33	small nucleolar RNA, H/ACA box 33	-1.089	-2.128	0.006437	0.1654
NA	NA	-1.606	-3.044	0.006441	0.1654
MITF	microphthalmia-associated transcription factor	-1.12	-2.173	0.006458	0.1654
TXN	thioredoxin	-0.5166	-1.431	0.006461	0.1654
FOXM1	forkhead box M1	-1.395	-2.629	0.006478	0.1654
LINC00926	long intergenic non-protein coding RNA 926	-1.224	-2.336	0.006482	0.1654
CCNA2	cyclin A2	-1.222	-2.333	0.006487	0.1654
NA	NA	-0.8333	-1.782	0.006509	0.1655
PCNA	proliferating cell nuclear antigen	-0.6453	-1.564	0.006523	0.1655
NSUN5P1	NOP2/Sun RNA methyltransferase family member 5 pseudogene 1	-1.365	-2.576	0.006526	0.1655
RTTN	rotatin	-0.7653	-1.7	0.006537	0.1655
ADCK5	aarF domain containing kinase 5	-0.7908	-1.73	0.006594	0.1657
GDF11	growth differentiation factor 11	-0.8359	-1.785	0.006599	0.1657
RAD54L	RAD54-like (S. cerevisiae)	-1.723	-3.301	0.006618	0.1657
GNLY	granulysin	-1.418	-2.671	0.00663	0.1657
NPEPPS	aminopeptidase puromycin sensitive	-0.7039	-1.629	0.006648	0.1657
CENPL	centromere protein L	-1.248	-2.376	0.006656	0.1657
FIGNL1	fidgetin like 1	-1.147	-2.215	0.006664	0.1657
ZNF280C	zinc finger protein 280C	-0.6937	-1.617	0.006683	0.1657
POLR1A	polymerase (RNA) I subunit A	-0.6053	-1.521	0.006685	0.1657
NA	NA	-0.7178	-1.645	0.006702	0.1658
C20orf27	chromosome 20 open reading frame 27	-0.6521	-1.571	0.006739	0.1659
CDC20	cell division cycle 20	-1.493	-2.814	0.006807	0.1673
NA	NA	-0.8066	-1.749	0.006813	0.1673
NA	NA	-0.9215	-1.894	0.006844	0.1675
MXD3	MAX dimerization protein 3	-2.004	-4.011	0.006846	0.1675
MNS1	meiosis specific nuclear structural 1	-0.919	-1.891	0.006852	0.1675
DEFB124	defensin beta 124	-2.586	-6.005	0.006875	0.1675
NA	NA	-0.8588	-1.814	0.006878	0.1675
GINS4	GINS complex subunit 4 (Sld5 homolog)	-1.225	-2.338	0.006883	0.1675
INPP5J	inositol polyphosphate-5-phosphatase J	-1.583	-2.996	0.006904	0.1676
NA	NA	-1.382	-2.605	0.006947	0.1683
NA	NA	-0.9065	-1.874	0.006955	0.1683
SLC17A9	solute carrier family 17 member 9	-1.305	-2.471	0.006969	0.1683
ZNF385B	zinc finger protein 385B	-2.252	-4.763	0.006988	0.1683
CCNB2	cyclin B2	-1.349	-2.547	0.006999	0.1683

KIF2C	kinesin family member 2C	-1.381	-2.604	0.007003	0.1683
ARVCF	armadillo repeat gene deleted in velocardiofacial syndrome	-1.057	-2.081	0.007039	0.1686
GMNN	geminin, DNA replication inhibitor	-0.6746	-1.596	0.007056	0.1688
BORA	bora, aurora kinase A activator	-0.8164	-1.761	0.007108	0.1688
SIRT5	sirtuin 5	-0.7995	-1.74	0.00711	0.1688
PHLDB1	pleckstrin homology like domain family B member 1	-0.6389	-1.557	0.007129	0.1688
GABBR1	gamma-aminobutyric acid type B receptor subunit 1	-1.239	-2.36	0.007142	0.1688
GJD3	gap junction protein delta 3	-1.066	-2.093	0.007154	0.1688
SNORD22	small nucleolar RNA, C/D box 22	-1.094	-2.135	0.007206	0.1688
TUBA3C	tubulin alpha 3c	-1.237	-2.356	0.007224	0.1688
NA	NA	-0.7169	-1.644	0.00725	0.1688
NA	NA	-1.147	-2.215	0.007267	0.1688
FAM13C	family with sequence similarity 13 member C	-1.406	-2.65	0.007284	0.1688
CKS2	CDC28 protein kinase regulatory subunit 2	-0.8584	-1.813	0.007304	0.1688
NA	NA	-1.135	-2.197	0.007306	0.1688
BRSK2	BR serine/threonine kinase 2	-1.047	-2.067	0.007317	0.1688
CENPA	centromere protein A	-1.451	-2.733	0.00732	0.1688
PTRH2	peptidyl-tRNA hydrolase 2	-1.159	-2.233	0.007323	0.1688
CFAP69	cilia and flagella associated protein 69	-1.068	-2.096	0.007327	0.1688
COL4A5	collagen type IV alpha 5	-0.6189	-1.536	0.007332	0.1688
CUX2	cut like homeobox 2	-1.485	-2.8	0.007358	0.1688
EZH2	enhancer of zeste 2 polycomb repressive complex 2 subunit	-1.792	-3.463	0.007363	0.1688
PXYLP1	2-phosphoxylose phosphatase 1	-0.815	-1.759	0.007396	0.1691
PLCL1	phospholipase C like 1	-0.9403	-1.919	0.007412	0.1692
NA	NA	-0.8936	-1.858	0.007432	0.1692
AKAP7	A-kinase anchoring protein 7	-0.7548	-1.687	0.007444	0.1692
ID2	inhibitor of DNA binding 2, HLH protein	-0.7414	-1.672	0.007462	0.1694
ATP6V0E2	ATPase H+ transporting V0 subunit e2	-0.5798	-1.495	0.007471	0.1694
TRIM6	tripartite motif containing 6	-0.9693	-1.958	0.007496	0.1696
CFAP157	cilia and flagella associated protein 157	-2.216	-4.647	0.007549	0.1703
CDK20	cyclin-dependent kinase 20	-0.6488	-1.568	0.007565	0.1704
HUS1	HUS1 checkpoint clamp component	-1.271	-2.413	0.007565	0.1704
QPRT	quinolinate phosphoribosyltransferase	-0.5329	-1.447	0.007602	0.1707
CDK1	cyclin-dependent kinase 1	-1.474	-2.777	0.00762	0.1707
NA	NA	-1.44	-2.714	0.007623	0.1707
CNNM1	cyclin and CBS domain divalent metal cation transport mediator 1	-1.119	-2.171	0.007647	0.1711
FAM159A	family with sequence similarity 159 member A	-1.218	-2.325	0.007653	0.1711
MOXD1	monooxygenase, DBH-like 1	-1.07	-2.099	0.007702	0.1714
CRABP2	cellular retinoic acid binding protein 2	-0.9861	-1.981	0.007734	0.1717
NA	NA	-0.513	-1.427	0.007752	0.1717
SNORD49A	small nucleolar RNA, C/D box 49A	-1.891	-3.71	0.007766	0.1718
ATRIP	ATR interacting protein	-0.7752	-1.711	0.00777	0.1718
SNORD52	small nucleolar RNA, C/D box 52	-1.674	-3.191	0.007779	0.1718
TACC3	transforming acidic coiled-coil containing protein 3	-0.7532	-1.686	0.007821	0.1724
DEPDC1	DEP domain containing 1	-0.9623	-1.948	0.007872	0.1727
HJURP	Holliday junction recognition protein	-2.053	-4.151	0.007895	0.1727
EMILIN3	elastin microfibril interfacer 3	-1.111	-2.159	0.0079	0.1727
CKS1B	CDC28 protein kinase regulatory subunit 1B	-0.641	-1.559	0.007908	0.1727
C5	complement component 5	-0.6039	-1.52	0.007931	0.1727
CCDC34	coiled-coil domain containing 34	-0.8109	-1.754	0.007933	0.1727
PTTG1	pituitary tumor-transforming 1	-1.258	-2.391	0.007952	0.1727
RACGAP1	Rac GTPase activating protein 1	-1.35	-2.548	0.007963	0.1727
NA	NA	-0.5737	-1.488	0.007975	0.1727
CCDC171	coiled-coil domain containing 171	-0.9955	-1.994	0.007979	0.1727
AKAP8	A-kinase anchoring protein 8	-0.5782	-1.493	0.008006	0.1731

NA	NA	-1.327	-2.508	0.008048	0.1731
CENPU	centromere protein U	-1.653	-3.145	0.008052	0.1731
PKD1L2	polycystin 1 like 2 (gene/pseudogene)	-1.692	-3.23	0.008067	0.1731
RUVBL1	RuvB like AAA ATPase 1	-0.4649	-1.38	0.008071	0.1731
PHF19	PHD finger protein 19	-0.6882	-1.611	0.008073	0.1731
CABP4	calcium binding protein 4	-1.14	-2.203	0.00813	0.1732
KLKP1	kallikrein pseudogene 1	-1.599	-3.029	0.008131	0.1732
NA	NA	-1.142	-2.207	0.008135	0.1732
PIDD1	p53-induced death domain protein 1	-1.444	-2.72	0.008138	0.1732
ZNF799	zinc finger protein 799	-0.7419	-1.672	0.008188	0.1737
SPC24	SPC24, NDC80 kinetochore complex component	-0.9091	-1.878	0.008209	0.1737
OGFOD1	2-oxoglutarate and iron dependent oxygenase domain containing 1	-0.6318	-1.55	0.008216	0.1737
NA	NA	-0.9195	-1.891	0.008217	0.1737
FBLN2	fibulin 2	-1.285	-2.437	0.008229	0.1737
DNMT3B	DNA (cytosine-5-)-methyltransferase 3 beta	-1.351	-2.55	0.0083	0.1742
RNF144A	ring finger protein 144A	-0.5621	-1.476	0.008301	0.1742
NA	NA	-1.562	-2.952	0.00831	0.1743
IL6R	interleukin 6 receptor	-1.071	-2.101	0.008347	0.1745
CCHCR1	coiled-coil alpha-helical rod protein 1	-1.114	-2.165	0.008352	0.1745
GPR180	G protein-coupled receptor 180	-0.5256	-1.439	0.008367	0.1745
STEAP1	six transmembrane epithelial antigen of the prostate 1	-0.973	-1.963	0.008369	0.1745
FANCC	Fanconi anemia complementation group C	-0.9718	-1.961	0.008372	0.1745
ADCY7	adenylate cyclase 7	-0.935	-1.912	0.008382	0.1746
EML1	echinoderm microtubule associated protein like 1	-0.7171	-1.644	0.008395	0.1747
NA	NA	-0.9786	-1.971	0.008428	0.175
ARFGAP1	ADP ribosylation factor GTPase activating protein 1	-0.5397	-1.454	0.008446	0.175
ARFGAP1	ADP ribosylation factor GTPase activating protein 1	-1.231	-2.347	0.008452	0.175
STX2	syntaxin 2	-0.8562	-1.81	0.008506	0.1759
NA	NA	-0.6299	-1.547	0.008519	0.1759
NLGN3	neuroligin 3	-1.124	-2.179	0.008526	0.1759
EBAG9	estrogen receptor binding site associated, antigen, 9	-1.422	-2.679	0.008535	0.1759
APOBEC3F	apolipoprotein B mRNA editing enzyme catalytic subunit 3F	-0.6056	-1.522	0.008551	0.1759
LONRF2	LON peptidase N-terminal domain and ring finger 2	-0.7587	-1.692	0.008565	0.1759
TMEM145	transmembrane protein 145	-0.8079	-1.751	0.008572	0.1759
BRINP1	BMP/retinoic acid inducible neural specific 1	-0.9691	-1.958	0.008576	0.1759
MAD2L1	MAD2 mitotic arrest deficient-like 1 (yeast)	-1.188	-2.278	0.008578	0.1759
NA	NA	-1.611	-3.055	0.008604	0.176
IGFBP5	insulin like growth factor binding protein 5	-1.384	-2.61	0.008637	0.1764
ZWINT	ZW10 interacting kinetochore protein	-1.533	-2.895	0.008644	0.1764
RLN2	relaxin 2	-0.7598	-1.693	0.008652	0.1764
XRRA1	X-ray radiation resistance associated 1	-0.9527	-1.935	0.008681	0.1765
UBE2C	ubiquitin conjugating enzyme E2C	-1.425	-2.685	0.008693	0.1765
NA	NA	-0.7301	-1.659	0.008694	0.1765
FAM72D	family with sequence similarity 72 member D	-1.659	-3.158	0.008787	0.1766
ASF1B	anti-silencing function 1B histone chaperone	-1.178	-2.263	0.008798	0.1766
ID1	inhibitor of DNA binding 1, HLH protein	-1.588	-3.006	0.008807	0.1766
SKA1	spindle and kinetochore associated complex subunit 1	-1.443	-2.719	0.008811	0.1766
NA	NA	-0.8566	-1.811	0.008871	0.1771
NA	NA	-0.8072	-1.75	0.008882	0.1772
KIFC1	kinesin family member C1	-1.274	-2.418	0.008931	0.1777
DDX17	DEAD-box helicase 17	-0.5734	-1.488	0.008987	0.1782

SNORA10	small nucleolar RNA, H/ACA box 10	-1.148	-2.216	0.009005	0.1782
PHF19	PHD finger protein 19	-0.8484	-1.8	0.009006	0.1782
XPR1	xenotropic and polytropic retrovirus receptor 1	-0.5045	-1.419	0.009033	0.1782
ATP6AP1L	ATPase H+ transporting accessory protein 1 like	-1.261	-2.397	0.009036	0.1782
ZIM3	zinc finger imprinted 3	-1.321	-2.498	0.009055	0.1782
CDCA8	cell division cycle associated 8	-1.409	-2.656	0.009069	0.1782
PPIEL	peptidylprolyl isomerase E like pseudogene	-1.279	-2.427	0.009072	0.1782
CEACAM1	carcinoembryonic antigen related cell adhesion molecule 1	-0.88	-1.84	0.009076	0.1782
CDC7	cell division cycle 7	-1.036	-2.051	0.009082	0.1782
N6AMT1	N-6 adenine-specific DNA methyltransferase 1 (putative)	-0.5185	-1.432	0.009086	0.1782
SUGP2	SURP and G-patch domain containing 2	-0.6241	-1.541	0.009095	0.1782
AGL	amylo-alpha-1, 6-glucosidase, 4-alpha-glucanotransferase	-0.8012	-1.743	0.009107	0.1782
RAD9A	RAD9 checkpoint clamp component A	-0.7601	-1.694	0.009129	0.1782
E4F1	E4F transcription factor 1	-0.5793	-1.494	0.009145	0.1782
FOXN4	forkhead box N4	-1.627	-3.088	0.009178	0.1782
NA	NA	-1.249	-2.377	0.009181	0.1782
NA	NA	-0.8875	-1.85	0.009183	0.1782
CCDC18	coiled-coil domain containing 18	-1.333	-2.52	0.009246	0.1782
MRI1	methylthioribose-1-phosphate isomerase 1	-0.7748	-1.711	0.00926	0.1782
NAAA	N-acylethanolamine acid amidase	-1.062	-2.087	0.009261	0.1782
POC1A	POC1 centriolar protein A	-0.8614	-1.817	0.009271	0.1782
CDCA5	cell division cycle associated 5	-1.328	-2.511	0.009274	0.1782
MID1	midline 1	-0.4811	-1.396	0.009281	0.1782
CEP85L	centrosomal protein 85kDa-like	-0.7564	-1.689	0.009283	0.1782
NA	NA	-0.9163	-1.887	0.00929	0.1782
KIAA0895L	KIAA0895-like	-1.994	-3.982	0.009292	0.1782
ARL17A	ADP ribosylation factor like GTPase 17A	-0.719	-1.646	0.009347	0.1783
ID2	inhibitor of DNA binding 2, HLH protein	-0.7549	-1.687	0.009348	0.1783
NA	NA	-1.652	-3.142	0.009376	0.1784
CCNB1	cyclin B1	-1.211	-2.314	0.009377	0.1784
CDKL2	cyclin dependent kinase like 2	-0.7326	-1.662	0.009391	0.1784
SSX2IP	synovial sarcoma, X breakpoint 2 interacting protein	-1.131	-2.19	0.009396	0.1784
USP4	ubiquitin specific peptidase 4 (proto-oncogene)	-0.8234	-1.77	0.009403	0.1784
NA	NA	-0.7034	-1.628	0.009411	0.1784
NA	NA	-0.906	-1.874	0.009434	0.1784
NXF3	nuclear RNA export factor 3	-0.9553	-1.939	0.009437	0.1784
PTTG3P	pituitary tumor-transforming 3, pseudogene	-1.334	-2.522	0.009442	0.1784
SCNN1D	sodium channel epithelial 1 delta subunit	-1.314	-2.486	0.009446	0.1784
PRC1	protein regulator of cytokinesis 1	-1.221	-2.331	0.009478	0.1787
HMGB2	high mobility group box 2	-0.7584	-1.692	0.009491	0.1787
F12	coagulation factor XII	-0.6995	-1.624	0.009516	0.1787
FANCI	Fanconi anemia complementation group I	-1.321	-2.499	0.009531	0.1787
ZEB1	zinc finger E-box binding homeobox 1	-1.176	-2.26	0.009551	0.1788
MOCOS	molybdenum cofactor sulfurase	-1.061	-2.086	0.009587	0.179
IDH1	isocitrate dehydrogenase 1 (NADP+)	-0.608	-1.524	0.009592	0.179
CCP110	centriolar coiled-coil protein 110kDa	-0.5664	-1.481	0.009598	0.179
TYMS	thymidylate synthetase	-1.331	-2.517	0.00961	0.179
TK1	thymidine kinase 1, soluble	-0.9221	-1.895	0.00962	0.179
FILIP1	filamin A interacting protein 1	-1.141	-2.206	0.009625	0.179
NA	NA	-0.6905	-1.614	0.009645	0.1792
ACOT7	acyl-CoA thioesterase 7	-0.6774	-1.599	0.00969	0.1798
GPR156	G protein-coupled receptor 156	-0.9671	-1.955	0.009725	0.1801
NT5DC3	5'-nucleotidase domain containing 3	-0.5341	-1.448	0.009742	0.1803
PGP	phosphoglycolate phosphatase	-0.4644	-1.38	0.009753	0.1803

DNAH12	dynein axonemal heavy chain 12	-0.9119	-1.882	0.00977	0.1803
C11orf70	chromosome 11 open reading frame 70	-1.424	-2.684	0.00978	0.1803
NAALAD2	N-acetylated alpha-linked acidic dipeptidase 2	-0.9759	-1.967	0.009804	0.1803
NA	NA	-0.8332	-1.782	0.00981	0.1803
NA	NA	-1.147	-2.214	0.009814	0.1803
FGFR3	fibroblast growth factor receptor 3	-1.072	-2.103	0.009821	0.1803
NA	NA	-0.6129	-1.529	0.009823	0.1803
PSRC1	proline/serine-rich coiled-coil 1	-1.254	-2.386	0.009849	0.1806
DLGAP5	discs large homolog associated protein 5	-1.908	-3.753	0.009853	0.1806
MPHOSPH6	M-phase phosphoprotein 6	-0.5895	-1.505	0.009941	0.1807
CENPM	centromere protein M	-1.013	-2.017	0.009943	0.1807
NA	NA	-0.8954	-1.86	0.00995	0.1807
GPR162	G protein-coupled receptor 162	-0.9158	-1.887	0.009967	0.1807
ANKRD16	ankyrin repeat domain 16	-0.7548	-1.687	0.009972	0.1807

Funding and awards

LHRW supported by MRC Developmental Clinical Studies Grant 'Reversing endometrial glucocorticoid deficiency in heavy menstrual bleeding' (MR/J003611/1);

Award for £3990 from the Barbour Watson Fund to fund microarray (2016)

Best platform poster presentation. RCOG Academic meeting 1-3rd March 2017

Short listed best oral presentation. Society of Endometriosis and Uterine Disorders (SEUD) Annual conference 12-14th May 2016

Oral presentations

- Impact of the selective progesterone receptor (SPRM) Ulipristal acetate (UPA) on progesterone-receptor (PR) response genes in the human endometrium World Congress on Endometriosis 17-20th May 2017
- Impact of the SPRM Ulipristal Acetate upon endometrial gene expression and cell proliferation. Society of Endometriosis and Uterine Disorders (SEUD) Annual conference 6-8th April 2017
- Uterine sex-steroid receptor expression and proliferation in women treated with selective progesterone receptor modulator (SPRM), ulipristal acetate RCOG Academic meeting 1-3rd March 2017 **Winner best platform presentation**
- Endometrial androgen receptor expression in women treated with selective progesterone receptor modulator (SPRM), ulipristal acetate. Edinburgh Obstetric Society 9th November 2016
- Uterine androgen receptor expression in women treated with selective progesterone receptor modulator, ulipristal acetate. Society of Endometriosis and Uterine Disorders (SEUD) Annual conference 12-14th May 2016 **Short listed best oral communication**
- Heavy menstrual bleeding South-East Scotland Practice Nurse Sexual Health Update NRIE 22nd January 2015

Posters

- **Whitaker LHR**, Murray AM, Walker C, Nicol MR, Williams ARW and Critchley HOD. Uterine sex-steroid receptor expression and proliferation in women treated with selective progesterone receptor modulator (SPRM), ulipristal acetate. RCOG Annual Academic meeting 1-3rd March 2017
- Leow H, Murray A, **Whitaker L**, Nicol M, Critchley H. Targeting progesterone receptors for the management of heavy menstrual bleeding (HMB). Fertility 5-7th 2017
- Matthews R, Murray A, **Whitaker L**, Millar M, Nicol M, Williams A and Critchley H. Impact of selective progesterone receptor modulator (SPRM), Ulipristal Acetate (UPA) administration upon cell proliferation markers within the human endometrium. Society for Reproduction and Fertility July 11-13th 2016

Published papers

Selective progesterone receptor modulator (SPRM) ulipristal acetate (UPA) and its effects on the human endometrium.
Whitaker LH, Murray AA, Matthews R, Shaw G, Williams AR, Saunders PT, Critchley HO.
Hum Reprod. 2017 Mar 1;32(3):531-543.
doi: 10.1093/humrep/dew359.
PMID: 28130434
Reproduced with permission (open access)

Abnormal uterine bleeding.
Whitaker L, Critchley HO.
Best Pract Res Clin Obstet Gynaecol. 2016 Jul;34:54-65.
doi: 10.1016/j.bpobgyn.2015.11.012. Epub 2015 Nov 25. Review.
PMID: 26803558
Open access: https://creativecommons.org/licenses/by/4.0

Selective progesterone receptor modulators (SPRMs): progesterone receptor action, mode of action on the endometrium and treatment options in gynecological therapies.
Wagenfeld A, Saunders PT, **Whitaker L**, Critchley HO.
Expert Opin Ther Targets. 2016 Sep;20(9):1045-54.
doi: 10.1080/14728222.2016.1180368. Epub 2016 May 14. Review.
PMID: 27138351
Open access: https://creativecommons.org/licenses/by/4.0

Selective progesterone receptor modulators (SPRMs) for uterine fibroids.
Murji A, **Whitaker L**, Chow TL, Sobel ML.
Cochrane Database Syst Rev. 2017 Apr 26;4:CD010770.
doi: 10.1002/14651858.CD010770.pub2. Review.
PMID: 28444736

JOHN WILEY AND SONS LICENSE
TERMS AND CONDITIONS

Jun 21, 2017

This Agreement between Lucy HR Whitaker ("You") and John Wiley and Sons ("John Wiley and Sons") consists of your license details and the terms and conditions provided by John Wiley and Sons and Copyright Clearance Center.

License Number	4118850509191
License date	May 30, 2017
Licensed Content Publisher	John Wiley and Sons
Licensed Content Publication	Cochrane Database of Systematic Reviews
Licensed Content Title	Selective progesterone receptor modulators (SPRMs) for uterine fibroids
Licensed Content Author	Ally Murji,Lucy Whitaker,Tiffany L Chow,Mara L Sobel
Licensed Content Date	Apr 26, 2017
Licensed Content Pages	1
Type of use	Dissertation/Thesis
Requestor type	Author of this Wiley article
Format	Print and electronic
Portion	Full article
Will you be translating?	No
Order reference number	CD010770
Title of your thesis / dissertation	Effect of administration of selective progesterone receptor modulators (SPRMs) on uterine and endometrial morphology
Expected completion date	Jun 2017
Expected size (number of pages)	300
Requestor Location	Lucy HR Whitaker MRC Centre for Reproductive Health Queen Medical Research Institute University of Edinburgh Edinburgh, EH16 4TJ United Kingdom Attn: Lucy HR Whitaker
Publisher Tax ID	EU826007151